論文 / 著書情報
Article / Book Information

題目(和文)	メタロセン触媒の特性を用いたオレフィンの重合
Title(English)	Olefin polymerizations related to the unique characteristics of metallocene catalysts
著者(和文)	永直文
Author(English)	
出典(和文)	学位:博士(工学), 学位授与機関:東京工業大学, 報告番号:乙第3303号, 授与年月日:1999年3月31日, 学位の種別:論文博士, 審査員:
Citation(English)	Degree:Doctor (Engineering), Conferring organization: Tokyo Institute of Technology, Report number:乙第3303号, Conferred date:1999/3/31, Degree Type:Thesis doctor, Examiner:
学位種別(和文)	博士論文
Type(English)	Doctoral Thesis

Olefin Polymerizations Related to the Unique Characteristics of Metallocene Catalysts

Naofumi NAGA

Tokyo Institute of Technology

1999

Contents

Abbreviations

Å	angstrom	m	meter(s), mili
$AlEt_3$	triethylaluminum	M	moles per liter
$Al\textit{i}Bu_3$	triisobutylaluminum	μ	micro
$AlMe_3$	trimethylaluminum	MAO	methylaluminoxane
AlR_3	trialkylaluminum	Me	methyl
atm	atmospheric pressure	min	minute(s)
℃	degrees Centigrade	M_n	number-average molecular weight
Cp	cyclopentadienyl	mol	mole(s)
DSC	differential scanning calorimetry	M_w	weight-average molecular wieght
E	ethene	MWD	molecular weight distribution
Et	ethyl, 1,2-ethene	NMR	nuclear magnetic resonance
EP	ethene/propene copolymer	*n*Pr	(normal)propyl
Flu	fluorenyl	P	propene
g	gram	PE	polyethene
GPC	gel permeation chromatography	Ph	phenyl
h	hour(s)	PP	polypropene
Hz	hertz	ppm	parts per million
*i*Bu	isobutyl	R	alkyl
Ind	indenyl	*rac*-	racemic
*i*Pr	isopropyl	s	second(s)
K	kelvin	*t*	time
kcal	kilo-calorie	*t*Bu	*tert*-butyl
kJ	kiro-joule	T_g	glass transition temperature
L	liter(s)	T_m	melting point

Metallocene catalysts

Cp_2TiCl_2	bis(cyclopentadienyl)titanium dichloride
Cp_2ZrCl_2	bis(cyclopentadienyl)zirconium dichloride
$Cp^*_2ZrCl_2$	bis(pentamethylcyclopentadienyl)zirconium dichloride
Ind_2ZrCl_2	bis(indenyl)zirconium dichloride
$Et(Ind)_2ZrCl_2$	ethenebis(indenyl)zirconium dichloride
$Et(Ind)_2HfCl_2$	ethenebis(indenyl)hafnium dichloride
$Me_2Si(Ind)_2ZrCl_2$	dimethylsilylenebis(indenyl)zirconium dichloride
$Me_2Si(Ind)_2HfCl_2$	dimethylsilylenebis(indenyl)zirconium dichloride
$Me_2Si(H_4Ind)_2ZrCl_2$	dimethylsilylenebis(tetrahydroindenyl)zirconium dichloride
$Me_2Si(2,3,5\text{-}MeCp)_2ZrCl_2$	dimethylsilylenebis(2,3,5-trimethylcyclopentadienyl)zirconium dichloride
$Me_2Si(2\text{-}MeInd)_2ZrCl_2$	dimethylsilylenebis(2-methylindenyl)zirconium dichloride
iPr(Cp)(Flu)$ZrCl_2$	isopropylidene(cyclopentadienyl)(9-fluorenyl)zirconium dichloride
$Ph_2C(Cp)(Flu)ZrCl_2$	diphenylmethylene(cyclopentadienyl)(9-fluorenyl)zirconium dichloride

Cation-forming reagents

$B(C_6F_5)_3$	tris(pentafluorophenyl)borane
$Ph_3CB(C_6F_5)_4$	triphenylcarbeniumtetrakis(pentafluorophenyl)borate

Chapter 1

General Introduction

1-1. Olefin Polymerization with Group 4 Metallocene Catalysts

1-1-1. Metallocene Catalysts for Olefin Polymerization

Group 4 metallocene complexes have long been known and were used for olefin polymerization catalysts. Groups of Natta and Breslow independently discovered the first homogeneous Ziegler–Natta catalyst of Cp_2TiCl_2 using dialkylaluminumchloride (R_2AlCl) as a cocatalyst.[1,2] The catalyst system showed very low activity for ethene polymerization and was used as a homogeneous system to define the active centers for olefin polymerizations. Subsequent studies were aimed at the identification of reaction mechanisms and the kinetic study of olefin polymerization with the catalyst system.[3]

Reichert and Mayer found that addition of a small amount of water enhanced the activity of olefin polymerization with Cp_2TiCl_2–ethylaluminumdichloride ($EtAlCl_2$) system.[4] Before this discovery, water was considered to be a poison for olefin polymerization catalysts. Subsequent studies were conducted by Long and Breslow on the effects of water in Cp_2TiCl_2–methylaluminumdichloride ($MeAlCl_2$) system.[5] In the catalyst system, $MeAlCl_2$ was partially hydrolyzed by the water to form dimeric aluminoxane (ClMeAl–O–AlClMe), and polymerization activity for ethene was observed.

A remarkable increase in activity for ethene polymerization was found by Sinn and Kaminsky when water was added to bis(cyclopentadienyl)zirconium dimethyl (Cp_2ZrMe_2)–$AlMe_3$ system which was inactive without water.[6,7] Formation of MAO by partial hydrolysis of $AlMe_3$ was supported by its direct synthesis and characterization. In 1980, Kaminsky and Sinn found the catalyst system, which was composed of group 4 metallocene catalysts and MAO, afforded to give high activity for ethene polymerization.[7] The discovery brought the way to expand possibilities of olefin polymerizations and properties of the resulting polyolefins. A considerable number of studies have been made on the group 4 metallocene catalysts and the olefin polymerizations from both the academic and industrial points of view.

1-1-2. Aluminoxane

Oligomeric alkylaluminoxanes have been known, for example, as initiators for polymerization of oxiranes.[8] The aluminoxanes are obtained through the reaction of alkylaluminums with water. The water should be present in a dilute or less accessible form such as in wet solvents or hydrated salts, since the reaction between water and alkylaluminums is extremely fast and highly exothermic. Several methods for synthesis of aluminoxanes have been reported in the literature.[9]

The type of aluminoxane affects the polymerization activity for olefins with metallocene-aluminoxane systems. MAO seems to be more effective as a cocatalyst than other aluminoxanes such as ethylaluminoxane (EAO) and isobutylaluminoxane (IBAO).[10] A modified form of methylaluminoxane (MMAO) containing isobutyl groups was synthesized to improve the solubility in aliphatic hydrocarbons.[11]

The structure of MAO has been investigated by IR (infrared), UV (ultraviolet), NMR spectroscopy, chromatography, and other means.[5,12] The exact structure of MAO is still a matter of controversy. There are different equilibria between residual $AlMe_3$ and/or MAO oligomers.[12b–g] The cyclic and linear structures of MAO with different oligomerization degree are considered as shown in Figure 1-1. Sinn *et al.* conducted phase separation of MAO solution in toluene and determined the cage structure.[12p]

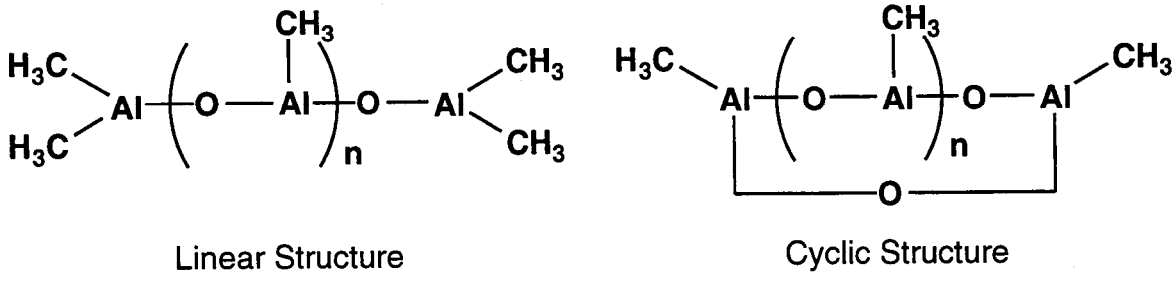

Figure 1-1. Plausible structures of MAO.

1-1-3. Metallocene–MAO Catalyst System

Many functions have been attributed to MAO. One function of MAO is alkylation of halogenated metallocene complex. The monomethyl compound is formed in the first step and excess MAO leads to the dialkylated species in the Cp_2ZrCl_2–MAO system.[10a,12f] It is at least necessary that one alkyl group is bonded to the metallocene for the activation.[13] MAO stabilizes the cationic metallocenealkyl by acting as counter-ion and prevents the catalyst from bimolecular reduction.[7,14,15] MAO also scavenges impurities such as water and oxygen from the reaction medium.[15] A large amount of MAO is required (Al:Zr ratios of about 1000:1 or higher) for the polymerization to reach its optimum activity.

It has been established that the active center in olefin polymerization is a cationic metallocene. The formation of cationic $[Cp_2ZrR]^+$ in Cp_2ZrMe_2–MAO system was confirmed by ^{91}Zr and ^{13}C NMR spectroscopy in the solution, and studied by XPS in the solid-state.[12n,16] The cation is stabilized by a weak coordinative contact with Al–O units or bridging CH_3 as shown in Figure 1-2.[9c,17,18] This information led to the discovery of highly-active cationic metallocene catalysts for olefin polymerizations.

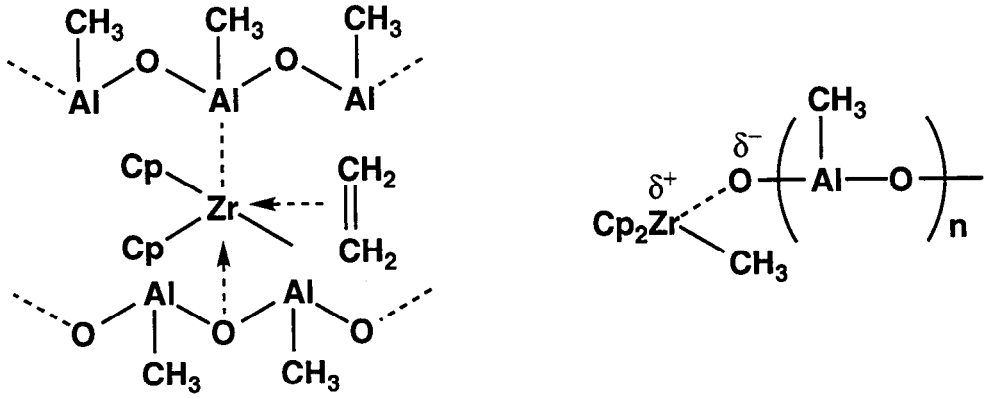

Figure 1-2. Plausible structures of active site in Cp_2ZrCl_2–MAO.

1-1-4. Cationic Metallocene Complexes with Cation-forming Reagent

Cationic metallocenes are prepared by combining at least two components. The first is a metallocene and the second is an ion exchange compound comprising a cation and a non-coordinating anion. Borane reagents such as tetraphenylborate ($B(C_6H_5)_4^-$) and carborane ($C_2B_9H_{12}^-$) were used for cation-forming reagents, while the resultant cation showed low

activity due to the strong interaction with the counter anions.[19] The use of fluorinated boranes, such as $Ph_3CB(C_6F_5)_4$ or dimethylanilinium-tetrakis(pentafluorophenyl)borate ($NHMe_2PhB(C_6F_5)_4$), for a cation-forming reagent led to highly active metallocene catalysts.[16d,19c,d,20] An ion pair $[L_2ZrMe]^+[B(C_6F_5)_4]^-$ (where L is substituted cyclopentadienyl or indenyl ligand) is formed through reactions of L_2ZrMe_2 with $Ph_3CB(C_6F_5)_4$ or $NHMe_2PhB(C_6F_5)_4$ as shown in Scheme 1-1(a). Cationic metallocene complexes can also be formed through a reaction with $B(C_6F_5)_3$ (Scheme 1-1(b)) and show highly activity for olefin polymerizations.[21]

(a)

$$L_2ZrMe_2 + [Ph_3C][B(C_6F_5)_4] \longrightarrow [L_2ZrMe]^+ + [B(C_6F_5)_4]^- + Ph_3CMe$$

$$L_2ZrMe_2 + [NHMe_2Ph][B(C_6F_5)_4] \longrightarrow [L_2ZrMe]^+ + [B(C_6F_5)_4]^- + NMe_2Ph + CH_4$$

(b)

$$L_2ZrMe_2 + B(C_6F_5)_3 \longrightarrow [L_2ZrMe]^+ + [MeB(C_6F_5)_3]^-$$

Scheme 1-1.

Crystalline structure of $(Me_2C_5H_3)ZrCH_3^+$ --- $H_3CB(C_6F_5)_3^-$ was obtained by Marks *et al.* using X-ray analysis.[21b] Partially coordinative contact still exists between the cationic Zr center and its counterion. The olefin coordinates to this compound by π-complexation then inserts into the Zr–Me bond.

Cationic metallocene complexes with cation-forming reagents show higher activity than those with MAO. A great advantage is that the molar ratio of borane reagent to Zr is about 1:1 enough for activation. On the other hand, these systems are easily deactivated by impurities. Addition of AlR_3, such as $AlEt_3$ or $Al\textit{i}Bu_3$, can stabilize these catalyst systems.[20a,d]

1-2. Stereospecific Polymerization of Propene with Metallocene Catalysts

1-2-1. Isospecific Polymerization of Propene with Metallocene Catalysts

Two types of stereochemical controls are considered in isospecific polymerization of propene. One is chain-end control derived from asymmetric configuration of the last inserted propene. The other is enantiomorphic-site control by chirality of the catalyst. Stereochemical structures of polypropene can be determined by ^{13}C NMR spectroscopy and the resonances from methyl groups have been assigned to the ten steric arrangements of five adjacent monomer units (pentad fraction) as shown in Figure 1-3. Only nine resonances are observed in the pentad fractions since the mmrm and rmrr pentads have the same chemical shift. Steric defect of --mmmrmmmm-- is predominantly observed in the chain-end controlled isotactic polypropene. While the defect of --mmmrrmmm-- is typically observed in the case of enantiomorphic-site control (Figure 1-4).

In 1984, Ewen reported the isospecific polymerization of propene with non-bridged (bis(cyclopentadienyl)titanium diphenyl, Cp_2TiPh_2) and C_2-symmetrical *ansa*-titanocene (ethenebis(indenyl)titanium dichloride, $Et(Ind)_2TiCl_2$) catalysts using MAO as a cocatalyst.[22] In the case of using Cp_2TiPh_2, polymerization should be conducted at low temperature (below –40 °C) to obtain the isotactic polymer although the isotacticity of the obtained polypropene was low ([mmmm] = 50%). The stereochemical structures of the polypropene indicated chain-end control model. On the other hand, isotactic polypropene ([mm] = 80% polymerized at –60 °C) derived from enantiomorphic-site control was obtained with $Et(Ind)_2TiCl_2$. Kaminsky and Brintzinger *et al.* synthesized *rac*-type *ansa*-zirconocenes, *rac*-$Et(Ind)_2ZrCl_2$ and *rac*-$Et(H_4Ind)_2ZrCl_2$, and conducted highly isospecific polymerization of propene activated by MAO (Figure 1-5).[9d]

Since the discovery of *rac*-bis(indenyl) type C_2-symmetrical metallocene catalysts for isospecific polymerization of propene, much effort has been expended in development of the

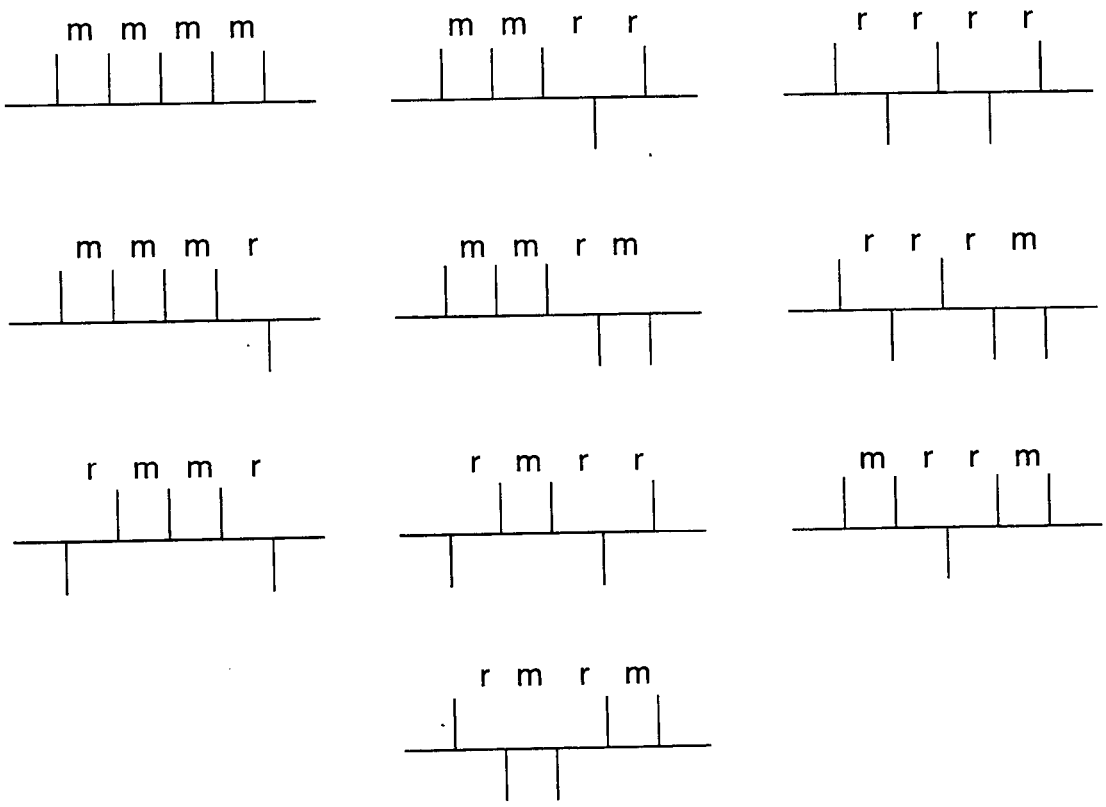

Figure 1-3. Pentad structures of polypropene.

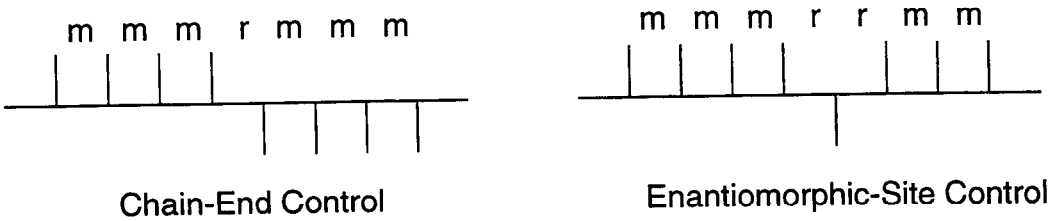

Figure 1-4. Steric defects of isotactic polypropene.

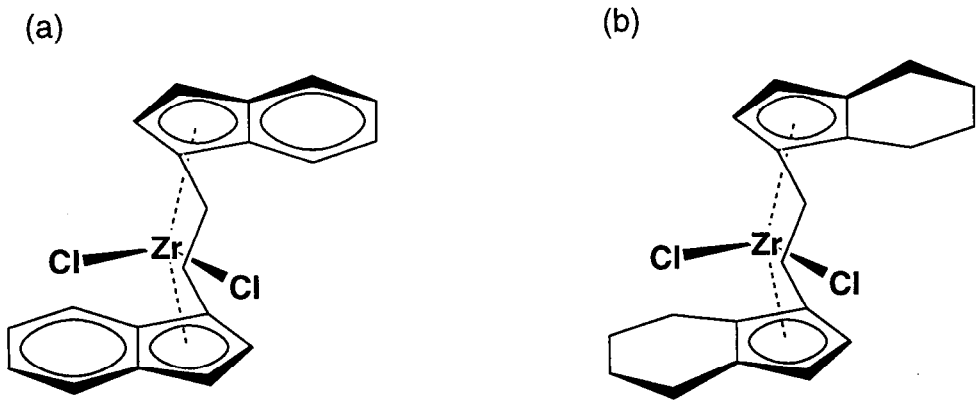

Figure 1-5. (a) *rac*-Et(Ind)$_2$ZrCl$_2$, (b) *rac*-Et(H$_4$Ind)$_2$ZrCl$_2$.

metallocene catalysts by modification of the bridge and the indenyl ligand. Yamazaki *et al.* reported isospecific polymerization of propene with *rac*-Me$_2$Si(2,3,5-Me$_3$Cp)(2',4',5'-Me$_3$Cp)ZrCl$_2$–MAO and obtained highly isotactic polypropene ([mmmm] = 97–98%).[23] Spaleck *et al.* synthesized *rac*-Me$_2$Si(2-Me-4-naphthyl Ind)$_2$ZrCl$_2$ and conducted highly isospecific polymerization of propene ([mmmm] = 91%) with high activity.[24] Kaminsky *et al.* developed *rac*-Et(2,4,7-Me$_3$Ind)$_2$ZrCl$_2$ and reported highly isospecific polymerization of propene with high molecular weight.[25,26]

A C_1-symmetrical metallocene, *i*Pr(3-*t*BuCp)(3-*t*BuInd)ZrCl$_2$, for highly isotactic polypropene has been developed by Showadenko Co., Ltd.[27] Ewen also reported the isospecific polymerization of propene with a C_1-symmetrical *i*Pr(3-*t*BuCp)(Flu)ZrCl$_2$.[28] In these catalysts, only one vacant site is available for propene coordination.

Propene insertion mainly proceeds with 1,2-regioselectivity in the isospecific polymerization with metallocene catalysts. However, a small amount of 2,1- and 1,3-inserted regioirregular units were observed in isotactic polypropene as shown in Figure 1-6.[29] Busico *et al.* reported that total fraction of regioirregular units was independent of polymerization temperature, while molar ratio of 1,3-inserted units to 2,1-inserted ones increased with an increase of polymerization temperature.[30] They also found the increase of 2,1-inserted units with an

increase of propene concentration. The 1,3-inserted units could be formed by isomerization of the 2,1-inserted propagating chain via β-H elimination followed by re-insertion. These regioirregular units affect properties of the isotactic polypropene. In general, melting point of the isotactic polypropene obtained with metallocene catalysts are lower than that obtained with conventional Ziegler–Natta catalysts. Improvement of regioselectivity should be one of the most important subjects for development in the metallocene catalysts.

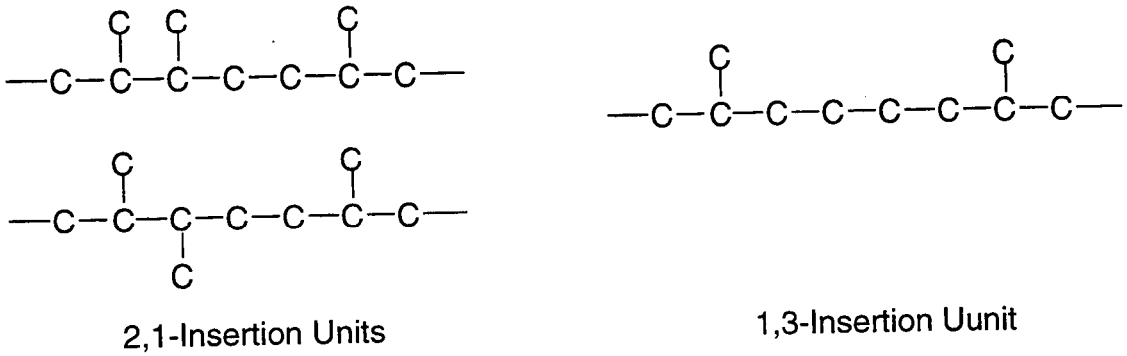

Figure 1-6. Formations of regioirregular units.

1-2-2. Syndiospecific Polymerization of Propene with Metallocene Catalysts

Two types of stereochemical controls can be considered also in syndiospecific polymerization of propene. One is the chain-end control and the other is enantiomorphic-site control. Steric defect of --rrrmrrr-- is predominantly observed in the chain-end controlled syndiotactic polypropene. While the defect of --rrrmmrr-- is typically observed in the case of enantiomorphic-site control (Figure 1-7).

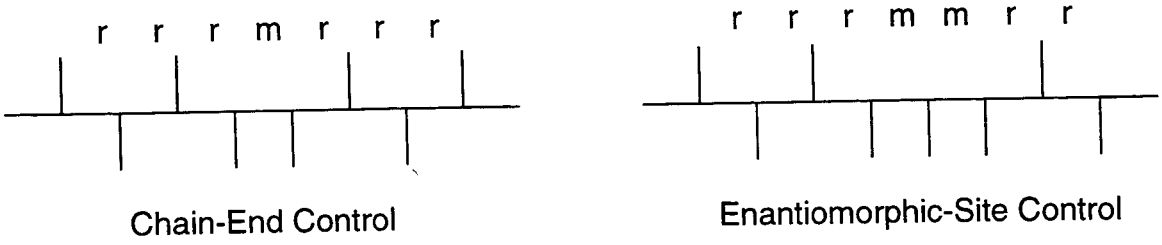

Figure 1-7. Steric defects of syndiotactic polypropene.

Ewen synthesized highly syndiotactic polypropene by using C_s-symmetrical metallocene, *i*Pr(Cp)(Flu)$ZrCl_2$–MAO (Figure 1-8).[31] The steric defect of [rmmr] was observed predominantly in this syndiotactic polypropene. The result indicated that syndiospecific polymerization of propene proceeded with alternating monomer insertions to the two different sites of C_s-symmetrical metallocene in the enantiomorphic-site control. On the other hands, the steric defect of [rmrr] was also detected. This steric defect originated from migration of the propagating polymer chain to the vacant site, and increased with a decrease of propene concentration.

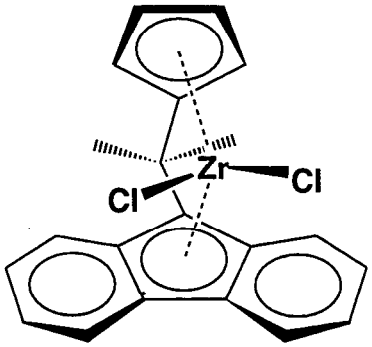

Figure 1-8. *i*Pr(Cp)(Flu)$ZrCl_2$.

Modifications of *i*Pr(Cp)(Flu)$ZrCl_2$ complex have been investigated.[32] Razavi *et al.* conducted propene polymerization with Ph_2C(Cp)(Flu)MCl_2 (M = Zr, Hf)–MAO and reported an increase of molecular weight of resulting syndiotactic polypropene.[32a] Asanuma *et al.* synthesized X(Cp)(2,7-*t*Bu_2Flu)$ZrCl_2$ (X = *i*Pr, Ph_2C), and reported an increase of syndiotacticity in propene polymerization using these catalysts.[32d]

1-2-3. Various Polypropenes Prepared by Metallocene Catalysts

Development of metallocene catalysts has enable us to synthesize new-type polypropenes. Ewen *et al.* reported that *i*Pr(3-MeCp)(Flu)$ZrCl_2$ –MAO produced hemiisotactic polypropene as shown in Figure 1-9.[33] The hemiisotactic polypropene is obtained because one of the two

coordination sites in the metallocene catalyst is less stereospecific than the other site due to the steric hindrance of Me substituent on the Cp ligand.

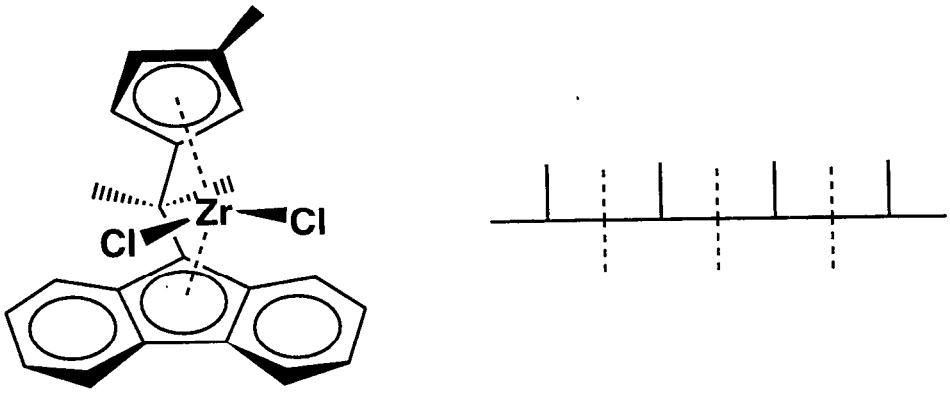

Figure 1-9. *i*Pr(3-MeCp)(Flu)$ZrCl_2$ and hemiisotactic polypropene.

Waymouth *et al.* reported synthesis of isotactic-atactic stereoblock polypropene with elastomeric properties using non-bridged (2-RInd)$_2ZrCl_2$ (R = Ph, 3,5-Me_2Ph, 3,5-$(CF_3)_2$Ph)–MAO as shown in Figure 1-10.[34] This catalyst appears to isomerize, by restricted rotation of its indenyl ligands, between chiral and achiral coordination geometry during chain growth. Collins *et al.* also reported the synthesis of elastomeric polypropene with $Me_2X(Cp)(Ind)MCl_2$ (X = C, Si; M = Ti, Zr, Hf)–MAO.[35]

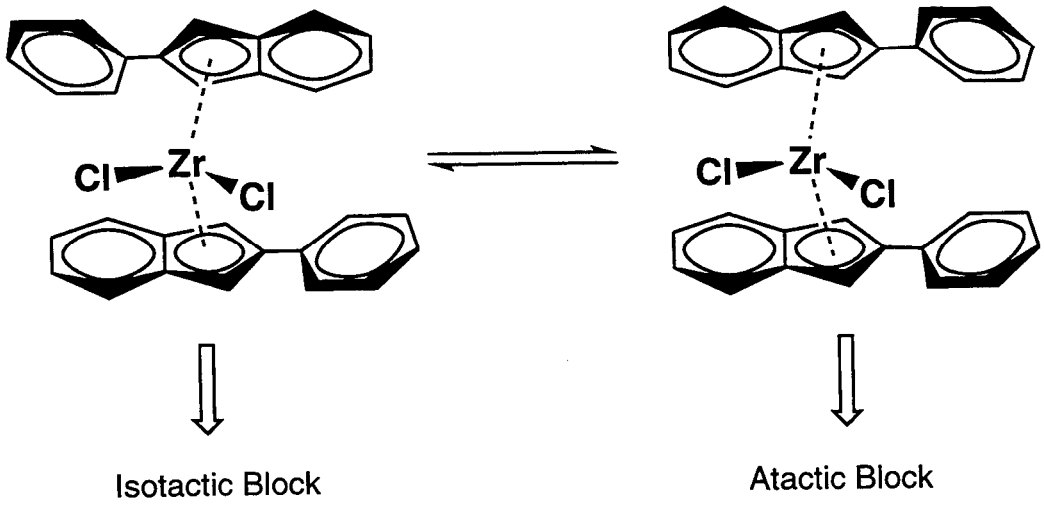

Figure 1-10. Propene polymerization with *i*Pr(2-phenyl Ind)$_2ZrCl_2$.

1-3. Copolymerization of Ethene or Propene with Other Olefins by Metallocene Catalysts

1-3-1. Copolymerization with α-Olefins

Copolymerization of ethene with α-olefin is an industrially important process. The length of side chain in the copolymer can be controlled by the introduced comonomer and that allows manufacture of liner low density polyethene (LLDPE). Metallocene catalysts show high activity for ethene/α-olefin copolymerization and have higher reactvities for α-olefins than conventional Ziegler–Natta catalysts. The copolymers produced are characterized by narrow molecular weight distribution and chemical composition with a random distribution of the comonomers.

Ethene/propene copolymerization has been carried out with a large number of metallocene catalysts and under various polymerization conditions.[36,37] Copolymerizations of ethene with conventional higher α-olefins, such as 1-butene, 1-hexene, and 1-octene, have been also conducted.[37,38] Monomer sequence distributions and monomer reactivity ratios were studied by ^{13}C NMR spectroscopy of the copolymers obtained. The monomer reactivity ratio was changed with the metallocene ligands, and reactivity ratios of α-olefins were decreased in the following order according to the chirality of metallocene catalysts: syndiospecific (C_s-symmetrical) > isospecific (C_2-symmetrical) > aspecific (C_{2v}-symmetrical).[38a] The LLDPEs obtained with metallocene catalysts have excellent physical properties due to the narrow composition distribution and the random distribution of comonomers. Further higher α-olefins such as 1-decene, 1-dodecene, 1-hexadecene, and 1-octadecene could be also copolymerized with ethene using metallocene catalysts.[37c,38o–s,39]

Recently, alternating copolymerizations of ethene/α-olefins were achieved. Soga *et al.* conducted ethene/1-octene copolymerization with *meso*-$Me_2Si(2\text{-MeInd})_2ZrCl_2$ and ethene/propene copolymerization with $Et(Ind)(Flu)ZrCl_2$ using MAO as cocatalyst, and succeeded in preparing the alternating copolymers.[40] Waymouth *et al.* carried out ethene/propene copolymerization with *i*Pr(3-MeCp)(Flu)$ZrCl_2$ (C_1-symmetrical) and *i*Pr(3,4-

$Me_2Cp)(Flu)ZrCl_2$ (C_s-symmetrical)–MAO, and observed highly-alternating monomer distributions in the copolymer.[41]

Copolymerizations of propene/other α-olefin with stereospecific metallocene catalysts have been reported.[42] Advantages of using metallocene catalysts are the high reactivity for α-olefins and homogeneous chemical structures of the resulting copolymers. Propene/α-olefin copolymers exhibit properties ranging form thermoplastic elastomers to typical rubbers. Decrease of T_m and T_g was observed with the increase of α-olefin content in the propene/higher α-olefin copolymers prepared by isospecific metallocene catalysts. The slight decrease of the T_m was observed with the increase of comonomer content in 1-butene copolymer, while the copolymers with higher α-olefins showed effective depression of the T_m independent of the side chain length. Although the T_g of propene/α-olefin copolymers decreased with increase of the length of α-olefins.[43c]

1-3-2. Copolymerization with Dienes or Cycloolefins

Copolymerizations of ethene/diene or cycloolefin, such as 4-vinyl-cyclohexene, norbornene, cyclopentene and so on have been conducted with metallocene catalysts.[43] Furthermore, terpolymerizations with ethene/propene/diene have been also carried out for the synthesis of EPDM (ethene-propene-diene terpolymer).[44] The EPDM is currently produced by vanadium catalysts, which are low in activity and limited in diene concentration due to side reactions. The metallocene catalyst technology was successfully employed in the copolymerization of cycloolefins. These cycloolefins are polymerized without ring opening. High incorporation of the cycloolefins in the terpolymer decreased crystallinity of the EPDM to amorphous elastomeric copolymers.

Copolymerizations of propene with cycloolefins have been conducted with isospecific metallocene catalysts. Kaminsky *et al.* conducted propene/cyclopentene copolymerization with *rac*-$Et(Ind)_2ZrCl_2$–MAO.[45a] Arnold, Henschke and Köller reported the copolymerization of propene/cyclopentene and propene/norbornene with isospecific metallocene catalysts.[45b,c]

The propene based copolymers with cyclic structures showed high T_g. The T_g value of copolymers could be controlled with the cycloolefin content in the copolymers.

Copolymerization with nonconjugated dienes involving intramolecular cyclization is one of the useful methods to obtain the polyolefins with cyclic structures. Waymouth *et al.* carried out polymerization of 1,5-hexadiene with metallocene catalysts and found that cycloaddition polymers were selectively obtained.[46] Marques *et al.*, Luft *et al.*, and Mülhaupt *et al.* applied the cycloaddition of 1,5-hexadiene to the copolymerization with ethene, and obtained polyethene with 1,3-cyclopentane structures.[47]

1-3-3. Copolymerization with Functionalized Vinyl Monomers

A large number of studies have been made on copolymerization of ethene, propene with various vinyl monomers with metallocene catalysts. Some metallocene catalysts proceed copolymerizations of ethene with styrene or substituted styrene in good yields.[48] Some attempts to copolymerize olefins with polar vinyl monomers have been made, and ethene- or propene-based copolymers including various functional groups have been synthesized.[49] These copolymers could be converted to graft copolymers and functionalized copolymers with various groups. Higher reactivity of metallocene catalysts for higher α-olefins has enable us to synthesize copolymers with polyolefin macromonomers.[50]

1-4. Aim of This Work

As described in the preceding section, not only the ligand and bridge structures but cocatalysts combined are important factors to control the activity, molecular weight and microstructures of resulting polymers in the polymerization of olefins with metallocene catalysts. However, most of the research works up to now have been concentrated on the structure of metallocenes. A variety of copolymerization is also one of the most excellent features in the olefin polymerization with metallocene catalysts. A great deal of effort has been

made on the synthesis of ethene-based copolymers such as LLDPE and EPDM with metallocene catalysts. What seems to be lacking , however, is synthesis and analysis of propene-based copolymers with various comonomers with metallocene catalysts.

In the present thesis, the author focused on two themes in olefin polymerization with metallocene catalysts as mentioned above. One is the effect of cocatalysts and the other is synthesis and structural analysis of propene-based copolymers.

In Chapter 2, ethene polymerization was conducted with *rac*-$Me_2Si(Ind)_2ZrCl_2$–MAO under various conditions and the molecular weight and MWD of resulting polyethenes were studied by GPC. The ethene polymerization was conducted also with zirconocenes, Cp_2ZrCl_2 and *rac*-$Me_2Si(Ind)_2ZrCl_2$, combined with AlR_3/borane compounds and the effect of cocatalysts on the polymerization activity and rate-time profile was studied.

In Chapter 3, propene, 1-butene, and 1-hexene polymerizations were carried out with *rac*- and *meso*-type *ansa*-zirconocene catalysts, $Me_2Si(2,3,5\text{-}Me_3Cp)_2ZrCl_2$ and $Me_2Si(2\text{-}MeInd)_2ZrCl_2$, using MAO and $AlR_3/Ph_3CB(C_6F_5)_4$. Effect of cocatalysts on the polymerization rate with *rac*-isomer and *meso*-isomer was studied. Furthermore, effect of the ligand structure of zirconocene catalysts on the olefin coordination was discussed.

In Chapter 4, propene polymerization was performed with isospecific and syndiospecific zirconocene catalysts using $AlR_3/Ph_3CB(C_6F_5)_4$ (R = Et, *i*Bu) to study the chain transfer reaction by AlR_3. Effect of R groups in AlR_3 and AlR_3 concentration was studied by the chain end structures and molecular weight of polypropenes obtained.

In Chapter 5, polypropenes were prepared by C_{2v}-, C_2-, and C_s-symmetrical zirconocene catalysts using MAO and $AlR_3/Ph_3CB(C_6F_5)_4$ as cocatalysts. Effect of cocatalysts on microstructures of the polypropenes was studied by ^{13}C NMR spectroscopy.

In Chapter 6, ethene/propene copolymerization was conducted with zirconocene and hafnocene catalysts and the molecular size (molecular weight) of resulting copolymers was studied by GPC. The profiles of molecular size were discussed in dependence of the propene content of the copolymer considering the chain propagation and chain transfer reactions.

In Chapter 7, copolymerizations of propene/nonconjugated dienes (1,5-hexadiene, 1,7-octadiene) were conducted with isospecific and syndiospecific zirconocene catalysts. Effect of

the stereospecificity of zirconocene catalysts on the insertion and intramolecular cyclization of dienes was discussed on the basis of structures of the resulting copolymers.

Highly syndiotactic polypropene could be synthesized by C_s-symmetrical metallocene catalysts. In Chapter 8, syndiotactic poly(propene-*co*-olefin)s (olefin = ethene, 1-butene, 1-pentene, 1-hexene, and 4-methyl-1-pentene) were prepared by a syndiospecific zirconocene catalyst. The crystalline structures and crystallization behaviors of the copolymers were studied.

In Chapter 9 is summarized the results obtained in the present work.

References

(1) Natta, G.; Pino, P.; Mazzanti, G.; Mazzanti, Giannini, G. *J. Am. Chem. Soc.* **1957**, *79*, 2957.

(2) Breslow, D. S.; Newburg, N. R. *J. Am. Chem. Soc.* **1957**, *79*, 5072.

(3) (a) Belov, G. P.; Kuznetsov, V. I.; Solovyeva, T. I.; Chirkov, N. M; Ivanchev, S. S. *Makromol. Chem.* **1970**, *140*, 213. (b) Dyachkovskii, F. S.; Shilova, A. K.; Shilov, A. E. *J. Polym. Sci.* **1967**, *16*, 2333. (c) Patat, F.; Sinn, H. *Angew. Chem.* **1958**, *70*, 469. (d) Clauss, K.; Bestian, H. *Justus Liebigs Ann. Chem.* **1962**, *654*, 8. (e) Henrici-Olivé, G.; Olivé, S. *J. Organomet. Chem.* **1969**, *16*, 339. (f) Reichert, K. H.; Schoetter, E. *Z. Physi. Chem.* **1968**, *57*, 74. (g) Fink, G. *Polym. Prepr. Am. Chem. Soc., Div. Polym. Sci.* **1972**, *13*, 443. (h) Bestian, H.; Clauss, K. *Angew. Chem., Int. Ed. Engl.* **1963**, *2*, 704. (i) Long, W. P.; Breslow, D. S. *J. Am. Chem. Soc.* **1960**, *81*, 1953. (j) Breslow, D. S.; Newburg, N. R. *J. Am. Chem. Soc.* **1959**, *81*, 81. (k) Henrici-Olivé, G.; Olivé, S. *Angew. Chem., Int. Ed. Engl.* **1967**, *6*, 790.

(4) Reichert, K. H.; Meyer, K. R. *Makromol. Chem.* **1973**, *169*, 163.

(5) Long, W. P., Breslow, D. S. *Justus Liebigs Ann. Chem.* **1975**, 463.

(6) Andresen, A.; Cordes, H. G.; Herwig, J.; Kaminsky, W.; Merck, A.; Mottweiler, R.; Pein, J.; Sinn, H.; Vollmer, H. J. *Angew. Chem., Int. Ed. Engl.* **1976**, *15*, 630.

(7) Sinn, H.; Kaminsky, W.; Vollmer, H. J.; Woldt, R. *Angew. Chem., Int. Ed. Engl.* **1980**, *19*, 369.

(8) Vandenberg, E. J. *J. Polym. Sci.* **1960**, *47*, 486.

(9) (a) Giannetti, E.; Nicoletti, G. M.; Mazzocchi, R. *J. Polym. Sci.: Polym. Chem. Ed.* **1985**, *23*, 2117. (b) Wild, F. R. W. P.; Zsolnai, L.; Huttner, G.; Brintzinger, H. H. *J. Organomet. Chem.* **1982**, *232*, 233. (c) Kaminsky, W.; Miri, M.; Sinn, H.; Wold, R. *Makromol. Chem., Rapid Commun.* **1983**, *4*, 417. (d) Kaminsky, W.; Külper, K.; Brintzinger, H. H.; Wild, F. R. W. P. *Angew. Chem., Int. Ed. Engl.* **1985**, *24*, 507.

(10) (a) Kaminsky, W.; Steiger, R. *Polyhedron* **1988**, *7*, 2375. (b) Charpentier, P. A.; Zhu, S.; Hamielec, A. E.; Brook, M. N. *Polymer* **1998**, *39*, 6501.

(11) Malpass, D. B.; Mirviss, S. B.; Catelli, A.; Tirendi, C. F.; Su, B. M.; Crapo, C. C.; Tran, N. H.; Rabbitt, C. S. *Proc. SPO '93*; Schotland Business Research, Inc.: 1993; p 185.

(12) (a) Sinn, H.; Bliemeister, J.; Clausnitzer, D.; Tikwe, L.; Winter, H.; Zarncke, O. In *Transition Metals and Organometallics as Catalysts for Olefin Polymerization*; Kaminsky, W., Sinn, H., Eds.; Springer: Berlin, 1988. (b) Piccolrovazzi, N.; Pino, P.; Cosiglio, G.; Sironi, A.; Moret, M. *Organometallics* **1990**, *9*, 3098. (c) Resconi, L.; Bossi, S.; Abis, L. *Macromolecules* **1990**, *23*, 4489. (d) Cam, D.; Albizzati, E.; Cinquina, P. *Makromol. Chem.* **1990**, *191*, 1641. (e) Cam, D.; Giannini, U. *Makromol. Chem.* **1992**, *193*, 1049. (f) Pasynkiewicz, S. *Polyhedron* **1990**, *9*, 429. (g) Giannetti, E.;

Nicoletti, G. M.; Mazzocchi, R. *J. Polym. Sci., Polym. Chem. Ed.* **1985**, *23*, 2117. (h) Mason, M. R.; Smith, J. M.; Bott, S. G.; Barron, A. R. *J. Am. Chem. Soc.* **1993**, *115*, 4971. (i) Harlan, C. J.; Mason, M. R.; Barron, A. R. *Organometallics* **1994**, *13*, 2957. (j) Harlan, C. J.; Bott, S. G.; Barron, A. R. *J. Am. Chem. Soc.* **1995**, *117*, 6465. (k) Nekhaeva, L. A.; Bondarenko, G. N.; Rykov, S. V.; Nekhaev, A. I.; Krentsel, B. A.; Mar'in, V. P.; Vyshinskaya, L. I.; Khrapova, I. M.; Polonskii, A. V.; Korneev, N. N. *J. Organomet. Chem.* **1991**, *406*, 139. (l) Siedle, A. R.; Newmark, R. A.; Lamanna, W. N.; Schroepfer, J. N. *Polyhedron* **1990**, *9*, 310. (m) Siedle, A. R.; Lamanna, W. N.; Newmark, R. A.; Stevens, J.; Richardson, D. E.; Ryan, M. *Makromol. Chem., Macrmol. Symp.* **1993**, *66*, 215. (n) Sugano, T.; Matsubara, K.; Fujita, T.; Takahashi, T. *J. Mol. Catal.* **1993**, *82*, 93. (o) Bliemeister, J.; Hagendorf, W.; Harder, A.;Heitmann, B.; Schimmel, I.; Schmedt, E.; Schnuchel, W.; Sinn, H.; Tikwe, L.; Thienen, N.; Urlass, K.; Winter, H.; Zaruke, O. In *Ziegler Catalysts*; Fink, G., Mülhaupt, R., Brintzinger, H. H., Eds.; Springer: Berlin, 1995; p 277.

(13) Tritto, I.; Li, S.; Sacchi, M. C.; Zannoni, G. *Macromolecules* **1993**, *26*, 7112.

(14) Chien, J. C. W.; Wang, B. P. *J. Polym. Sci., Part A: Polym. Chem.* **1990**, *28*, 15.

(15) Chien, J. C. W.; Sugimoto, R. *J. Polym. Sci., Part A: Polym. Chem.* **1991**, *29*, 459.

(16) (a) Gassman, P. G.; Callstrom, M. R. *J. Am. Chem. Soc.* **1987**, *109*, 7875. (b) Sishta, C.; Hathorn, R. M.; Marks, T. J. *J. Am. Chem. Soc.* **1992**, *114*, 1112. (c) Siedle, A. R.; Hanggi, B.; Newmark, R. A.; Mann, K. R.; Wilson, T. *Makromol. Chem., Macromol. Symp.* **1995**, *89*, 299. (d) Eisch, J. J.; Pombrick, S. I.; Zheng, G. X. *Organometallics* **1993**, *12*, 3856.

(17) Tait, P. J. T.; Watkins, N. D. In *Comprehensive Polymer Science*; Allen, G., Bevington, J. C., Eds.; Pergamon: Oxford, 1989; p 533.

(18) Chien, J. C. W.; Wang, B. P. *J. Polym. Sci., Part A: Polym. Chem.*, **1989**, *27*, 1539.

(19) (a) Hlatky, G. G.; Turner, H. W.; Eckman, R. R. *J. Am. Chem. Soc.* **1989**, *111*, 2728. (b) Hlatky, G. G.; Eckman, R. R.; Turner, H. W. *Organometallics* **1992**, *11*, 1413. (c) Yang, X.; Stern, C. L.; Marks, T. J. *Organometallics* **1991**, *10*, 840. (d) Horton, A. D.; Frijns, J. H. G. *Angew. Chem., Int. Ed. Engl.* **1991**, *30*, 1152. (e) Jordan, R. F.; LaPointe, R. E.; Bradley, P. K.; Baenziger, N. *Organometallics* **1989**, *8*, 2892. (f) Jordan, R. F.; Bradley, P. K.; LaPointe, R. E.; Taylor, D. F. *New J. Chem.* **1990**, *14*, 505. (g) Jordan, R. F.; *Adv. Organomet. Chem.* **1991**, *32*, 325. (h) Bochmann, M.; Wilson, L. M. *J. Chem. Soc., Chem. Commun.* **1986**, 1610. (i) Bochmann, M.; Wilson, L. M.; Hursthouse, M. B.; Short, R. L. *Organometallics* **1987**, *6*, 2556. (j) Bochmann, M.; Wilson, L. M.; Hursthouse, M. B.; Motevalli, M. *Organometallics* **1988**, *7*, 1148. (k) Bochmann, M.; Jaggar, A. J.; Nicholls, J. C. *Angew. Chem., Int. Ed. Engl.* **1990**, *29*, 780. (l) Bochmann, M.; Jaggar, A. J. *J. Organomet. Chem.* **1992**, *424*, C5. (m) Bochmann, M.; Lancaster, S. J. *J. Organomet. Chem.* **1992**, *434*, C1. (n) Eshuis, J. J. W.; Tan, Y. Y.; Teuben, J. H. *J. Mol. Catal.*

1990, *62*, 277. (o) Eshuis, J. J. W.; Tan, Y. Y.; Meetsma, A.; Teuben, J. H.; Renkema, J.; Evens, G. G. *Organometallics* **1992**, *11*, 362. (p) Taube, R.; Krukowka, L. *J. Organomet. Chem.* **1988**, *347*, C9.

(20) (a) Chien, J. C. W.; Tsai, W.; Rausch, M. D. *J. Am. Chem. Soc.* **1991**, *113*, 8570. (b) Bochmann, M.; Lancaster, S. J. *Organometallics* **1993**, *12*, 633. (c) Bochmann, M.; Lancaster, S. J.; Hursthouse, M. B.; Abdul Malik, K. I. M. *Organometallics* **1994**, *13*, 2235. (d) Bochmann, M.; Lancaster, S. J. *Angew. Chem., Int. Ed. Engl.* **1994**, *33*, 1634. (e) Horton, A. D.; Orpen, A. G. *Organometallics* **1991**, *10*, 3910. (f) Horton, A. D. *J. Chem. Soc. Chem. Commun.* **1992**, 185.

(21) (a) Yang, X.; Stern, C. L; Marks, T. J. *J. Am. Chem. Soc.* **1991**, *113*, 3623. (b) Yang, X.; Stern, C. L; Marks, T. J. *J. Am. Chem. Soc.* **1994**, *116*, 10015. (c) Yang, X.; Stern, C. L.; Marks, T. J. *Angew. Chem., Int. Ed. Engl.* **1992**, *31*, 1375.

(22) Ewen, J. A. *J. Am. Chem. Soc.* **1984**, *106*, 6355.

(23) Mise, T.; Miya, S.; Yamazaki, H. , *Chem. Lett.* **1989**, 1853.

(24) Spaleck, W.; Küber, F.; Winter, A.; Rohrman, J.; Bachmann, B.; Antberg, M.; Dolle, V.; Paulus, E. F. *Organometallics* **1994**, *13*, 954.

(25) Kaminsky, W.; Rage, O.; Schauwienold, A. M.; Schupfner, G. C.; Hanss, J.; Kopf, J. *J. Organomet. Chem.* **1995**, *497*, 181.

(26) Deng, H.; Winkelbach, H.; Taeji, K.; Kaminsky, W.; Soga, K. *Macromolecules* **1996**, *29*, 6371.

(27) Miyake, S.; Okumura, Y.; Inazawa, S. *Macromolecules* **1995**, *28*, 3074.

(28) (a) Ewen, J. A. *Makromol. Chem. Macromol. Symp.* **1995**, *89*, 181. (b) Razavi, A.; Atwood, J. L. *J. Organomet. Chem.* **1996**, *520*, 115.

(29) (a) Soga, K.; Shiono, T.; Takemura, S.; Kaminsky, W. *Makromol. Chem., Rapid Commun.* **1987**, *8*, 305. (b) Grassi, A.; Zambelli, A.; Resconi, L.; Albizzati, E.; Mazzocchi, R. *Macromolecules* **1988**, *21*, 617. (c) Cheng, H. N.; Ewen, J. A. *Makromol. Chem.* **1989**, *190*, 1931. (d) Hayashi, T.; Inoue, Y.; Cyujo, R.; Asanuma, T. *Macromolecules* **1988**, *21*, 2675. (e) Mizuno, A.; Abiru, T.; Motowoka, M.; Kioka, M.; Onda, M. *J. Appl. Polym. Sci., Appli. Polym. Symp.* **1993**, *52*, 159.

(30) Busico, V.; Cipullo, R.; Chadwick, J. C.; Modder, J. F.; Sudmeijer, O. *Macromolecules* **1994**, *27*, 7538.

(31) Ewen, J. A.; Jones, R. L.; Razavi, A.; Ferrara, J. D. *J. Am. Chem. Soc.* **1988**, *110*, 6255.

(32) (a) Razavi, A.; Atwood, J. L. *J. Organomet. Chem.* **1993**, *459*, 117. (b) Razavi, A.; Thewalt, U. *J. Organomet. Chem.* **1993**, *445*, 111. (c) Bochmann, M.; Lancaster, S. J. *Makromol. Chem., Rapid Commun.* **1993**, *14*, 807. (d) Asanuma, T.; Nishimori, Y.; Ito, M.; Shiomura, T. *Makromol. Chem., Rapid Commun.* **1993**, *14*, 315. (e) Asanuma, T.; Nishimori, Y.; Ito, M.; Shiomura, T. *Makromol. Chem., Rapid Commun.* **1994**, *15*, 723. (f) Fierro, R.; Yu, Z.; Rausch, M. D.; Dong, S.; Alvares, D.; Chien, J.

C. W. *J. Polym. Sci., Part A.: Polym. Chem.* **1994**, *32*, 661. (g) Yu, Z.; Chien, J. C. W. *J. Polym. Sci., Part A: Polym. Chem.* **1995**, *33*, 1085. (h) Rieger, B.; Repo, T.; Jany, G. *Polym. Bull.* **1995**, *35*, 87. (i) Alt, H. G.; Zenk, R.; Milius, W. *J. Organomet. Chem.* **1996**, *514*, 257. (j) Alt, H. G.; Zenk, R. *J. Organomet. Chem.* **1996**, *518*, 7. (k) Alt, H. G.; Zenk, R. *J. Organomet. Chem.* **1996**, *522*, 177. (l) Alt, H. G.; Zenk, R. *J. Organomet. Chem.* **1996**, *526*, 295.

(33) (a) Ewen, J. A.; Elder, M. J.; Jones, R. L.; Haspeslagh, L.; Atwood, J. L.; Bott, S. G.; Robinson, K. *Makromol. Chem., Macromol. Symp.* **1991**, *48/49*, 253. (b) Herfert, N.; Fink, G. *Makromol. Chem., Macromol. Symp.* **1993**, *66*, 157.

(34) (a) Coates, G. W.; Waymouth, R. M. *Science* **1995**, *267*, 217. (b) Hauptman, E.; Waymouth, R. M.; Ziller, J. M. *J. Am. Chem. Soc.* **1995**, *117*, 11586. (c) Kravchenko, R.; Masood, A.; Waymouth, R. M. *Organometallics* **1997**, *16*, 3635.

(35) (a) Gauthier, W. J.; Corrigan, J. F.; Taylor, N. J.; Collins, S. *Macromolecules* **1995**, *28*, 3771. (b) Gauthier, W. J.; Collins, S. *Macromolecules* **1995**, *28*, 3779.

(36) (a) Kaminsky, W.; Miri, M. *J. Polym. Sci., Polym. Chem. Ed.* **1985**, *23*, 2151. (b) Kaminsky, W.; Schlobohm, M. *Makromol. Chem., Macromol. Symp.* **1986**, *4*, 103. (c) Zambelli, A.; Grassi, A. *Makromol. Chem., Rapid Commun.* **1991**, *12*, 523. (d) Chien, J. C. W.; He, D. *J. Polym. Sci., Part A: Polym. Chem.* **1991**, *29*, 1595. (e) Tritto, I.; Fan, Z. Q.; Locatelli, P.; Sacchi, M. C.; Camurati, I.; Galimberti, M. *Macromolecules* **1995**, *28*, 3342. (f) Chien, J. C. W.; He, D. *J. Polym. Sci., Part A: Polym. Chem.* **1991**, *29*, 1585. (g) Lehtinen, C.; Löfgren, B. *Eur. Polym. J.* **1997**, *33*, 115. (h) Sugano, T.; Endo, J.; Takahama, T. In *Science and Technology in Catalysis 1994*; Kodansha: Tokyo, 1995; p 371. (i) Randall, J. C.; Rucker, S. P. *Macromolecules*, **1994**, *27*, 2120. (j) Shiono, T.; Uozumi, T.; Soga, K. *Kobunshi-ronbunsyu* **1994**, *51*, 663. (k) Banzi, V.; Angiolini, L.; Caretti, D.; Carlini, C. *Angew. Makromol. Chem.* **1995**, *229*, 113. (l) Herfert, N.; Fink, G. *Makromol. Chem.* **1992**, *193*, 1359. (m) Koivumäki, J.; Seppälä, J. V. *Polym. Bull.* **1993**, *31*, 441. (n) Koivumäki, J.; Seppälä, J. V. *Eur. Polym. J.* **1994**, *30*, 1111. (o) Tsai, W. M.; Chien, J. C. W. *J. Polym. Sci., Part A: Polym. Chem.* **1994**, *32*, 157. (p) Galimberti, M.; Martini, E.; Piemontesi, F.; Sartori, F.; Camurati, I.; Resconi, L.; Albizzzati, E. *Macromol. Symp.* **1995**, *89*, 259. (q) Pietikäinen, P.; Seppälä, J. V. *Macromolecules* **1994**, *27*, 1325. (r) Bergemann, C.; Cropp, R.; Luft, G. *J. Mol. Catal. A: Chem.* **1995**, *102*, 1. (s) Arndt, M.; Kaminsky, W.; Schauwienold, A. M.; Weingarten, U. *Macromol. Chem. Phys.* **1998**, *199*, 1135. (t) Galimberti, M.; Piemontesi, F.; Fusco, O.; Camurati, I.; Destro, M. *Macromolecules* **1998**, *31*, 3409. (u) Kravchenko, R.; Waymouth, R. M. *Macromolecules* **1998**, *31*, 2.

(37) (a) Uozumi, T.; Soga, K. *Makromol. Chem.* **1992**, *193*, 823. (b) Starck, P.; Lehtinene, C.; Löfgren, B. *Angew. Makromol. Chem.* **1997**, *249*, 115. (c) Lehtinen, C.; Starck, P.; Löfgren, B. *J. Polym. Sci., Part A: Polym. Chem.* **1997**, *35*, 307. (d)

Bergemann, C.; Cropp, R.; Luft, G. *J. Mol. Catal. A: Chem.* **1996**, *105*, 87. (e) Herfert, N.; Montag, P.; Fink, G. *Makromol. Chem.* **1993**, *194*, 3167.

(38) (a) Heiland, K.; Kaminsky, W. *Makromol. Chem.* **1992**, *193*, 601. (b) Rossi, A.; Zhang, J.; Odian, G. *Macromolecules* **1996**, *29*, 2331. (c) Mauler, R. S.; Galland, G. B.; Scipioni, R. B.; Quijada, R. *Polym. Bull.* **1996**, *37*, 469. (d) Koivumäki, J.; Lahti, H.; Seppälä, J. V. *Angew. Makromol. Chem.* **1994**, *221*, 117. (e) Soga, K.; Uozumi, T.; Arai, T.; Nakamura, S. *Macromol. Rapid Commun.* **1995**, *16*, 379. (f) Lahti, H.; Koivumäki, J.; Seppälä, J. V. *Angew. Makromol. Chem.* **1996**, *236*, 139. (g) Lahti, H.; Koivumäki, J.; Seppälä, J. V. *Angew. Makromol. Chem.* **1996**, *236*, 155. (h) Quijada, R.; Scipioni, R. B.; Mauler, R. S.; Galland, G. B.; Miranda, M. S. L. *Polym. Bull.* **1995**, *34*, 299. (i) Quijada, R.; Rojas, R.; Mauler, R. S.; Galland, G. B.; Scipioni, R. B. *J. Appl. Polym. Sci.* **1997**, *64*, 2567. (j) Galland, G. B.; Quijada, P.; Mauler, R. S.; Menezes, S. C. *Macromol. Rapid Commun.* **1996**, *17*, 607. (k) Quijada, R.; Dupont, J.; Miranda, M. S. L.; Scipioni, R. B.; Galland, G. B. *Macromol. Chem. Phys.* **1995**, *196*, 3991. (l) Soga, K.; Uozumi, T.; Nakamura, S.; Toneri, T.; Teranishi, T.; Sano, T.; Arai, T. *Macromol. Chem. Phys.* **1996**, *197*, 4237. (m) Suhm, J.; Schneider, M. J.; Mülhaupt, R. *J. Polym. Sci., Part A: Polym. Chem.* **1997**, *35*, 735. (n) Xu, G.; Ruckenstein, E. *Macromolecules* **1998**, *31*, 4724. (o) Koivumäki, J. *Polym. Bull.* **1996**, *36*, 7. (p) Seppälä, J. V.; Koivumäki, J.; Liu, X. *J. Polym. Sci., Part A: Polym. Chem.* **1993**, *31*, 3447. (q) Quijada, R.; Galland, G. B.; Mauler, R. S. *Macromol. Chem. Phys.* **1996**, *197*, 3091. (r) Möhring, P. C.; Coville, N. J. *J. Mol. Catal. A: Chem.* **1995**, *96*, 181. (s) Lehmus, P.; Härkki, O.; Leino, R.; Luttikhedde, H. J. G.; Näsman, J. H.; Seppälä, J. V. *Macromol. Chem. Phys.* **1998**, *199*, 1965.

(39) (a) Koivumäki, J. *Polym. Bull.* **1995**, *34*, 413. (b) Koivumäki, J.; Fink, G.; Seppälä, J. V. *Macromolecules* **1994**, *27*, 6254. (c) Koivumäki, J.; Seppälä, J. V. *Polym. Commun.* **1993**, *34*, 1958.

(40) (a) Uozumi, T.; Miyazawa, K.; Sano, T.; Soga, K. *Macromol. Rapid Commun.* **1997**, *18*, 883. (b) Jin, J.; Uozumi, T.; Sano, T.; Teranishi, T.; Soga, K.; Shiono, T. *Macromol. Rapid Commun.* **1998**, *19*, 337.

(41) Leclerc, M. K.; Waymouth, R. M. *Angew. Chem., Int. Ed.* **1998**, *37*, 922.

(42) (a) Jüngling, S.; Mülhaupt, R.; Langhauser, F. *Angew. Makromol. Chem.* **1995**, *229*, 93. (b) Schneider, M.; Mülhaupt, R. *J. Mol. Catal. A: Chem.* **1995**, *101*, 11. (c) Arnold, M.; Henschke, O.; Knorr, J. *Macromol. Chem. Phys.* **1996**, *197*, 563. (d) Forlini, F.; Fan, Z. Q.; Tritto, I.; Locatelli, P.; Sacchi, M. C. *Macromol. Chem. Phys.* **1997**, *198*, 2397. (e) Kim, I. *Macromol. Rapid Commun.* **1998**, *19*, 299.

(43) (a) Kaminsky, W.; Spiehl, R. *Makromol. Chem.* **1989**, *190*, 515. (b) Rische, T.; Waddo, A. J.; Dickinson, L. C.; MacKnight, W. J. *Macromolecules* **1998**, *31*, 1871. (c) Wang, Q.; Weng, J.; Fan, Z.; Feng, L. *Macromol. Rapid Commun.* **1997**, *18*,

1101. (d) Kaminsky, W.; Noll, A. *Polym. Bull.* **1993**, *31*, 175. (e) Bergström, C. H.; Seppälä, J. V. *J. Appl. Polym. Sci.* **1997**, *63*, 1063. (f) Bergström, C. H.; Vnnen, T. L. J.; Seppälä, J. V. *J. Appl. Polym. Sci.* **1997**, *63*, 1071. (g) Lasarov, H.; Mönkkönen, K.; Pakkanen, T. T. *Macromol. Chem. Phys.* **1998**, *199*, 1939. (h) Arndt, M.; Beulich, I. *Macromol. Chem. Phys.* **1998**, *199*, 1221. (i) Ruchatz, D.; Fink, G. *Macromolecules* **1998**, *31*, 4669. (j) *ibid.* **1998**, *31*, 4674. (k) *ibid.* **1998**, *31*, 4681. (l) *ibid.* **1998**, *31*, 4684. (m) Bergström, C. H.; Starck, P. G.; Seppälä, J. V. *J. Appl. Polym. Sci.* **1998**, *67*, 385. (n) Kaminsky, W.; Arrowmith, D.; Winkelbach, H. R. *Polym. Bull.* **1996**, *36*, 577. (o) Mani, R.; Burns, C. M. *Polymer* **1993**, *34*, 1941. (p) Sivaram, S.; Marathe, S. *Macromolecules* **1994**, *27*, 1083. (q) Marathe, S.; Mohandas, T. P.; Sivaram, S. *Macromolecules* **1995**, *28*, 7318.

(44) (a) Chien, J. C. W.; Xu, B. *Makromol. Chem., Rapid Commun.* **1993**, *14*, 109. (b) Chien, J. C. W.; Yu, Z.; Marques, M. M.; Flores, J. C.; Rausch, M. D. *J. Polym. Sci., Part A: Polym. Chem.* **1998**, *36*, 319. (c) Lee, D. H.; Yoon, K. B.; Park, J. R.; Lee, B. H. *Eur. Polym. J.* **1997**, *33*, 447. (d) Marques, M.; Yu, Z.; Rausch, M. D.; Chien, J. C. W. *J. Polym. Sci., Part A: Polym. Chem.* **1995**, *33*, 2787. (e) Chien, J. C. W.; He, D. *J. Polym. Sci., Part A: Polym. Chem.* **1991**, *29*, 1609. (f) Yu, Z.; Marques, M.; Rausch, M. D.; Chien, J. C. W. *J. Polym. Sci., Part A: Polym. Chem.* **1995**, *33*, 2795. (g) Malmberg, A.; Löfgren, B. *J. Appl. Polym. Sci.* **1997**, *66*, 35. (h) Yu, Z.; Marques, M.; Rausch, M. D.; Chien, J. C. W. *J. Polym. Sci., Part A: Polym. Chem.* **1995**, *33*, 979. (i) Kaminsky, W.; Drgemller, H. *Makromol. Chem., Rapid Commun.* **1990**, *11*, 89.

(45) (a) Kaminsky, W.; Bark, A.; Arndt, M. *Makromol. Chem., Macromol. Symp.* **1991**, *47*, 83. (b) Arnold, M.; Henschke, O.; Köller, F. *Macromol. Reports* **1996**, *A33* (Suppl. 3–4) 219. (c) Henschke, O.; Köller, F.; Arnold, M. *Macromol. Rapid Commun.* **1997**, *18*, 617.

(46) (a) Resconi, L.; Waymouth, R. M. *J. Am. Chem. Soc.* **1990**, *112*, 4953. (b) Mogstad, A.; Waymouth, R. M. *Macromolecules* **1992**, *25*, 2282. (c) Kesti, M. R.; Waymouth, R. M. *J. Am. Chem. Soc.* **1992**, *114*, 3565. (d) Cavallo, L.; Guerra, G.; Corradini, P.; Resconi, L.; Waymouth, R. M. *Macromolecules* **1993**, *26*, 260.

(47) (a) Coutinho, F. M. B.; Marques, M. F. V. *Polim. Cienc. Technol.* **1993**, *3* (1), 20. (b) Bergemann, C.; Cropp, R.; Luft, G. *J. Mol. Catal. A: Chem.* **1997**, *116*, 317. (c) Sernetz, F. G.; Mülhaupt, R.; Waymouth, R. M. *Polym. Bull.* **1997**, *38*, 141.

(48) (a) Lu, H. L.; Chung, T. C. *Macromolecules* **1998**, *31*, 2028. (b) Xu, G.; Lin, S. *Macromolecules* **1997**, *30*, 685. (c) Chung, T. C.; Lu, H. L. *J. Polym. Sci., Part A: Polym. Chem.* **1997**, *35*, 575. (d) Oliva, L.; Mazza, S.; Longo, P. *Macromol. Chem. Phys.* **1996**, *197*, 3115. (e) Oliva, L.; Izzo, L.; Longo, P. *Macromol. Rapid Commun.* **1996**, *17*, 745. (f) Sernetz, F. G.; Mülhaupt, R.; Waymouth, R. M. *Macromol. Chem. Phys.* **1996**, *197*, 1071. (g) Xu, G. *Macromolecules* **1998**, *31*, 2395. (h) Pellecchia,

C.; Pappalardo, D.; D'Arco, M.; Zambelli, A. *Macromolecules* **1996**, *29*, 1158. (i) Aaltonen, P.; Seppälä, J. *Eur. Polym. J.* **1994**, *30*, 683. (j) Lee, D. H.; Yoon, K. B.; Kim, H. J.; Woo, S. S.; Noh, S. K. *J. Appl. Polym. Sci.* **1998**, *67*, 2187. (k) Oliva, L.; Longo, P.; Izo, L.; Serio, M. D. *Macromolecules* **1997**, *30*, 5616. (l) Sernetz, F. G.; Mülhaupt, R.; Amor, F.; Eberle, T.; Okuda, J. *J. Polym. Sci., Part A: Polym. Chem.* **1997**, *35*, 1571. (m) Wu, Q.; Ye, Z.; Gao, Q.; Lin, S. *Macromol. Chem. Phys.* **1998**, *199*, 1715. (n) Chung, T. C.; Lu, H. L. *J. Polym. Sci., Part A: Polym. Chem.* **1998**, *36*, 1017. (o) Chung, T. C.; Lu, H. L.; Ding, R. D. *Macromolecules* **1997**, *30*, 1272. (p) Arai, T.; Ohtsu, T.; Suzuki, S. *Macromol. Rapid Commun.* **1998**, *19*, 327. (q) Venditto, V.; De Tullio, G.; Izzo, L.; Oliva, L. *Macromolecules* **1998**, *31*, 4027. (r) Sernetz, F. G.; Mülhaupt, R. *J. Polym. Sci., Part A: Polym. Chem.* **1997**, *35*, 2549.

(49) (a) Wilén, C. E.; Näsman, J. H. *Macromolecules* **1994**, *27*, 4051. (b) Mudalige, D. C.; Rempel, G. L. *Pure Appl. Chem.* **1997**, *A34*, 361. (c) Aaltonen, P.; Löfgren, B. *Eur. Polym. J.* **1997**, *33*, 1187. (d) Wilén, C. E.; Luttikhedde, H.; Hjertberg, T.; Näsman, J. H. *Macromolecules* **1996**, *29*, 8569. (e) Stehling, U. M.; Malmstrm, E. E.; Waymouth, R. M.; Hawker, C. J. *Macromolecules* **1998**, *31*, 4396. (f) Tsuchida, A.; Bolln, C.; Sernetz, F. G.; Frey, H.; Mülhaupt, R. *Macromolecules* **1997**, *30*, 2818. (g) Bruzaud, S.; Cramail, H.; Duvignac, L.; Deffieux, A. *Macromol. Chem. Phys.* **1997**, *198*, 291. (h) Aaltonen, P.; Löfgren B. *Macromolecules* **1995**, *28*, 5353. (i) Hakala, K.; Löfgren, B.; Helaja, T. *Eur. Polym. J.* **1998**, *34*, 1093.

(50) (a) Shiono, T.; Moriki, Y.; Ikeda, T. *Macromol. Chem. Phys.* **1997**, *198*, 3229. (b) Henschke, O.; Neubauer, A.; Arnold, M. *Macromolecules* **1997**, *30*, 8097.

Chapter 2

Effect of Cocatalysts on Ethene Polymerization with Zirconocene Catalysts

2-1. Introduction

Since the discovery of metallocene–MAO catalyst system developed by Kaminsky and Sinn,[1] a great number of olefin polymerizations have been carried out with metallocene catalysts.

The active species in metallocene catalysts with MAO have been analyzed by various techniques. Cam *et al.* analyzed Cp_2ZrCl_2–MAO catalyst system by an electron paramagnetic spectroscopy and observed reduction of Zr(IV) to Zr(III) in the presence of ethene.[2] Decrease of polymerization activity along with the polymerization time was thus assumed to result from the reduction of the Zr species. Analyses of the metallocene–MAO systems by UV (ultraviolet) absorption spectroscopy also have been investigated.[3–9] For example, Tol *et al.* analyzed the *rac*-$Et(Ind)_2ZrCl_2$–MAO system and observed hypsochromic and bathochromic shifts of the ligand-to-metal charge transfer band, which were explained to be derived from the methylation of zirconocene and the formation of cationic complex, respectively.[8] Recently, Tritto *et al.* have examined Cp_2TiCH_3Cl–MAO and $Cp_2Zr(^{13}CH_3)_2$–MAO by ^{13}C NMR spectroscopy under various molar ratios of (MAO)Al/M (M = Ti, Zr) with different concentrations of metallocene as well as at various reaction temperatures.[10] They have detected two kinds of ionpairs, *i.e.*, monomeric and bimeric ones and discussed the polymerization activity in relation to these ionpairs.

The active species for olefin polymerization derived from the group 4 metallocene catalysts have been considered to be metallocenium cation M^+(IV) (M = metal in group 4). Jordan *et al.* found that a cationic zirconocene complex, $[Cp_2ZrCH_3(THF)]^+[BPh_4]^-$ (THF = tetrahydrofuran), was active for ethene polymerization in a polar solvent without any cocatalysts.[11] After that finding, much effort has been focused on the development of cocatalysts and the investigation of active species for olefin polymerization with metallocene catalysts.

Marks *et al.* synthesized a cationic zirconocene catalyst, $[Cp_2ZrCH_3]^+[CH_3B(C_6F_5)_3]^-$, through a reaction of zirconocenedimethyl ($Cp_2Zr(CH_3)_2$) with $B(C_6F_5)_3$, and studied the structure, solution dynamic, and catalytic activity for olefin polymerization.[12–15] Bochmann *et al.* isolated binuclear and heterobinuclear zirconocene and hafnocene complexes through a

reaction of dialkylmetallocene and $Ph_3CB(C_6F_5)_4$, and applied them for propene polymerization.[16] On the basis of the activity in propene polymerization with $AlMe_3/Ph_3CB(C_6F_5)_4$ at various molar ratios of Al/Zr, they proposed dormant states of the active sites for olefin polymerization. Brintzinger *et al.* studied binuclear zirconocene cations by solution ^1H NMR spectroscopy.[17,18] They found the equilibrium between solvent-separated ion pairs and associated ion pairs of the $[Cp_2ZrCH_3]^+[CH_3B(C_6F_5)_3]^-$ complex in benzene-d_6 solution. Tritto *et al.* studied the structures of cation-like and binuclear zirconocene complexes by means of ^{13}C NMR spectroscopy using ^{13}C-enriched $Cp_2Zr(^{13}CH_3)_2$ in toluene-d_8 solution.[10d] Fink *et al.* and Brintzinger *et al.* hypothesized that the binuclear ion pairs were active for ethene polymerization.[17,18,19] However, there is room for argument on this point.

Chien *et al.* reported effect of counter-ions for isospecific polymerization of propene catalyzed by *rac*-$Et(Ind)_2Zr(CH_3)_2$ or *rac*-$Et(Ind)_2ZrCl_2$–$AlEt_3$ combined with $Ph_3CB(C_6F_5)_4$ or $B(C_6F_5)_3$, and found that $Ph_3CB(C_6F_5)_4$ showed much higher activity than $B(C_6F_5)_3$.[21] They suggested the existence of free Zr cations which enhanced the activity for propene polymerization.

The metallocene catalysts are known to possess uniform active species and therefore give polyolefins with narrow molecular weight distributions and narrow composition distributions. Whereas, Soga *et al.* recently found that the poly(ethene-*co*-1-hexene) obtained with a typical metallocene showed a bimodal molecular weight distribution when the copolymerization was conducted for a short period.[21]

Rate-time profile of polymerization gives important information for the formation of active species and decay process. A large number of attempts have been made on the polymerization profiles with metallocene–MAO to study the effect of polymerization temperature, concentration or molar ratio of metallocene to MAO and aging condition of metallocene and MAO.[16,20c,22–28] Some investigations have been reported to study the effect of AlR_3 and/or borane compound on the activity for the olefin polymerization with metallocene catalysts.[16,20a,c,27] Although, few data have been reported about the polymerization profile with the metallocene–AlR_3/borane compound systems.

In this chapter, the author has conducted polymerization of ethene by zirconocene catalysts combined with MAO or AlR_3/borane compounds to study the effect of cocatalyst system on the polymerization profile, molecular weight and molecular weight distribution of resulting polyethene. The mechanisms of active-site formation were discussed on the basis of molecular weight and molecular weight distribution of the polyethenes obtained and the rate-time profiles.

2-2. Experimental Part

Materials

Cp_2ZrCl_2 and *rac*-$Me_2Si(Ind)_2ZrCl_2$ were commercially obtained from Aldrich Co., Ltd., and Witco Co., Ltd., respectively, and used without further purification. Elemental analysis of *rac*-$Me_2Si(Ind)_2ZrCl_2$ was conducted, and the compound was found to contain a small quantity of aluminum (0.16 wt %) but no other transition metals. $AlMe_3$, $AlEt_3$, and Al*i*Bu_3 were donated from Tosoh Akzo Co., Ltd. and used without further purification. Toluene solution of MAO was purchased from Tosoh Akzo Co., Ltd. and used without further purification. $Ph_3CB(C_6F_5)_4$ and $B(C_6F_5)_3$ were donated from Asahi glass Co., Ltd. and used without further purification. Toluene was commercially obtained and dried over molecular sieves 3A and/or CaH_2. CH_2Cl_2 (dehydrated grade) was also commercially obtained and used without further purification. Ethene and propene were purified by passing it through a column of molecular sieves 3A.

Polymerization

Polymerizations of ethene and propene with MAO were conducted in a 1 L glass flask. After the reactor was replaced with argon, 300 mL of solvent was injected, followed by introducing the monomer at an atmospheric pressure to saturate the solvent. A zirconocene catalyst was contacted to MAO in toluene for 5 min at 25 °C prior to use. Polymerization was started by adding the premixed catalyst solution into the reactor. Polymerization was

terminated by addition of isobutyl alcohol. The polymer produced was adequately washed with methanol and dried in vacuo at 60 °C for 6 h.

Polymerization of ethene with AlR_3/borane reagent was conducted at 40 °C in a 300 mL glass reactor equipped with a magnetic stirrer. After 190 mL of toluene was added to the reactor, the solvent was saturated with an atmospheric pressure of ethene. Toluene (10 mL), metallocene catalyst (1.0 μmol) and AlR_3 (0.5 mmol) were premixed in a 100 mL glass flask at 25 °C for 5 min. Polymerization was started by introducing the catalyst solution and borane reagent (1.0 μmol in 1.0 mL of toluene solution). Consumption of ethene was monitored by a gas flow meter. Reaction medium was sampled through an equipped seal septum with a syringe and quenched in methanol. During the polymerization, temperature was kept at 40 °C. Polymerization was terminated by adding dilute hydrochloric acid solution in methanol. The polyethene obtained was adequately washed with plenty of methanol and dried in vacuo at 60 °C for 6 h.

Analytical procedure

M_n and MWD (M_w/M_n) of polymers were measured at 140–145 °C by GPC (Waters 150CV) using *o*-dichlorobenzene as a solvent. Calibration was made with standard polystyrene samples. The M_n values of polyethene and polypropene were converted using the Q-factor by the following equations: $M_n = M_n(PS)\cdot Q_{PE}/Q_{PS}$ and $M_n = M_n(PS)\cdot Q_{PP}/Q_{PS}$, respectively ($M_n(PS)$, M_n calibrated by polystyrene standards; Q_{PE}, Q-factor of polyethene = 17.7; Q_{PP}, Q-factor of polypropene = 26.4; Q_{PS}, Q-factor of polystyrene = 41.3).[29,30]

2-3. Results and Discussion

2-3A. Ethene Polymerization with *rac*-$Me_2Si(Ind)_2ZrCl_2$–MAO

2-3A-1. Effect of Polymerization Time

Polymerizations of ethene and propene (for a reference) were conducted under the standard conditions, [Zr] = 2.5 μmol, molar ratio of Al/Zr = 1000, in 500 mL of toluene at 40 °C. The

results of polymerizations and the plots of polymer yield against polymerization time are shown in Table 2-1 and Figure 2-1, respectively. In the case of propene polymerization, the polymer yield increased roughly in proportion to the polymerization time, while the activity for ethene polymerization markedly decreased after 10 min. The decrease in the activity for ethene polymerization could be explained in terms of the monomer diffusion through the crystalline polyethene.[31] The GPC curves of polyethenes are shown in Figure 2-2, which displays shoulders at a low molecular weight region. The two fractions were separated by a simple curve fitting method. As illustrated in Figure 2-2, the relative area of the low molecular weight fraction decreased with an increase in the polymerization time, which tendency suggested that the fraction was produced at the initial stage of polymerization. On the contrary, the M_w/M_n values of polypropenes were found to be approximately 2, which indicated that propene polymerization proceeded with a single active species according to the Schultz–Flory statistics.[32]

Table 2-1. Results of ethene and propene polymerizations with *rac*-$Me_2Si(Ind)_2ZrCl_2$–MAO[a]

Run	Monomer	t[b] (min)	Yield (g)	Activity (kgPE,PP/ mol Zr·h)	M_n[c] ($\times 10^{-4}$)	M_w/M_n[c]	Low M_w fraction		High M_w fraction
							(g)[d]	(wt %)[d]	(g)[d]
1	ethene	5	4.2	20200	17.1	3.8	1.3	31.0	2.9
2		10	7.1	17000	20.7	3.5	1.8	25.4	5.3
3		20	9.0	11000	18.4	3.4	1.9	21.1	7.1
4		40	12.6	7600	18.8	3.6	2.6	20.6	10.0
5	propene	5	3.9	18700	2.77	2.0			
6		10	7.5	18000	2.56	2.0			
7		20	14.3	17200	2.50	1.9			
8		40	27.2	16300	2.64	2.0			
9		60	37.2	14900	2.66	2.0			

[a] Polymerization conditions: polymerization temperature = 40 ℃, toluene = 500 mL, feed rate of ethene and propene = 760 mL/min, *rac*-$Me_2Si(Ind)_2ZrCl_2$ = 0.25 μmol, molar ratio of (MAO)Al/Zr = 1000. [b] Polymerization time. [c] Determined by GPC using polystyrene standards. [d] Calculated from GPC curves.

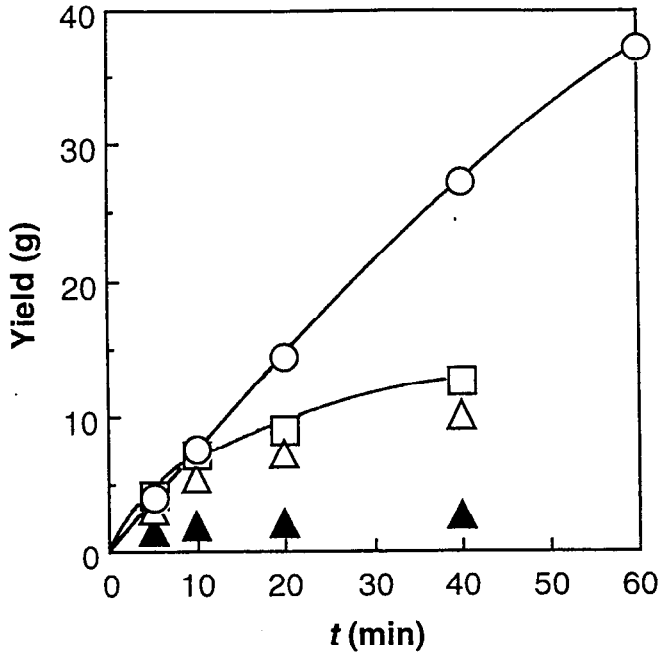

Figure 2-1. Plots of the polymer yield against polymerization time: (□) polyethene (whole); (△) high M_w fraction; (▲) low M_w fraction, (○) polypropene.

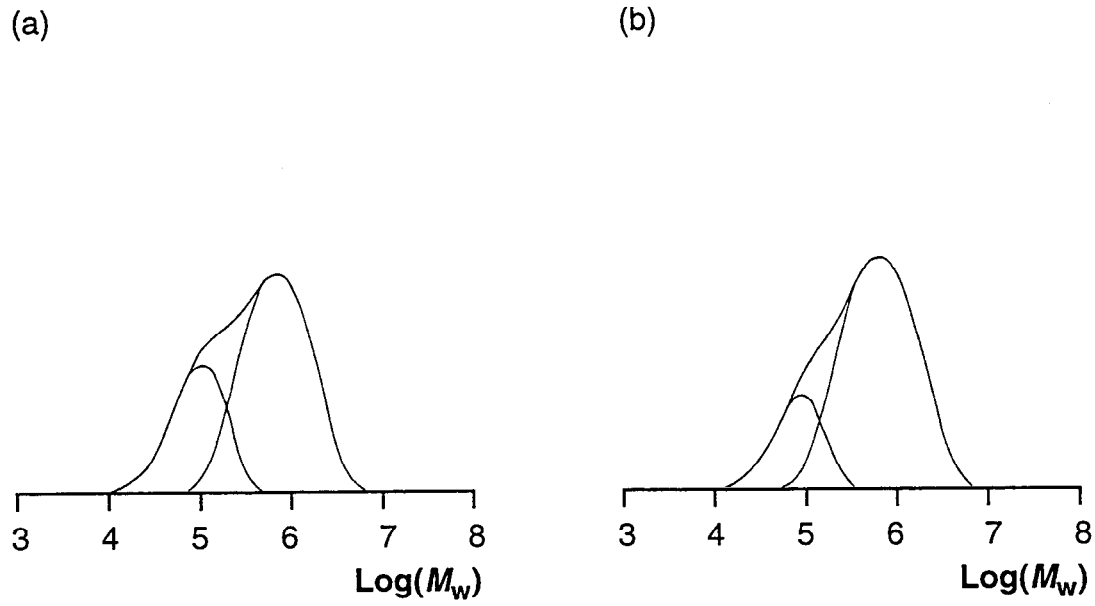

Figure 2-2. GPC elution curves of polyethenes obtained with *rac*-$Me_2Si(Ind)_2ZrCl_2$–MAO: (a) t = 5 min, (b) t = 30 min.

2-3A-2. Effect of [Al]/[Zr] Ratio, and [Zr] Concentration

Polymerization of ethene was then conducted with the *rac*-$Me_2Si(Ind)_2ZrCl_2$–MAO system at 40 °C in toluene with various molar ratios of Al/Zr and the [Zr] concentrations. The results are shown in Table 2-2. The GPC curves of all the polyethene samples displayed shoulders at low molecular weight region. The content of the shoulder fraction was plotted against the polymerization time in Figure 2-3. It may be roughly said that the content of low molecular region does not depend upon the molar ratio of Al/Zr and the [Zr] concentration.

Polymerization of propene was also examined under the same conditions of ethene polymerization (Table 2-3). None of the polypropene sample displayed such a shoulder fraction in the GPC curve.

Table 2-2. Results of ethene polymerization with *rac*-$Me_2Si(Ind)_2ZrCl_2$–MAO[a]

Run	[Zr] (μmol)	Molar ratio Al/Zr	t[b] (min)	Yield (g)	Activity (kgPE/ mol Zr·h)	M_n[c] ($\times 10^{-4}$)	M_w/M_n[c]	Low M_w fraction[d] (wt %)
10	0.625	1000	30	8.4	26900	13.9	2.9	21.5
11		4000	20	7.9	37900	16.3	3.0	20.5
12	2.50	250	20	9.0	10800	17.1	3.1	20.8
2		1000	10	7.1	17000	20.7	3.5	25.4
13		4000	10	6.6	15800	20.7	3.7	27.7
14	10.0	250	10	7.2	4320	19.0	3.5	24.7
15		1000	10	8.2	4920	18.7	3.6	25.5

[a] Polymerization conditions: polymerization temperature = 40 ℃, toluene = 500 mL, feed rate of ethene = 760 mL/min. [b] Polymerization time. [c] Determined by GPC using polystyrene standards. [d] Calculated from GPC curves.

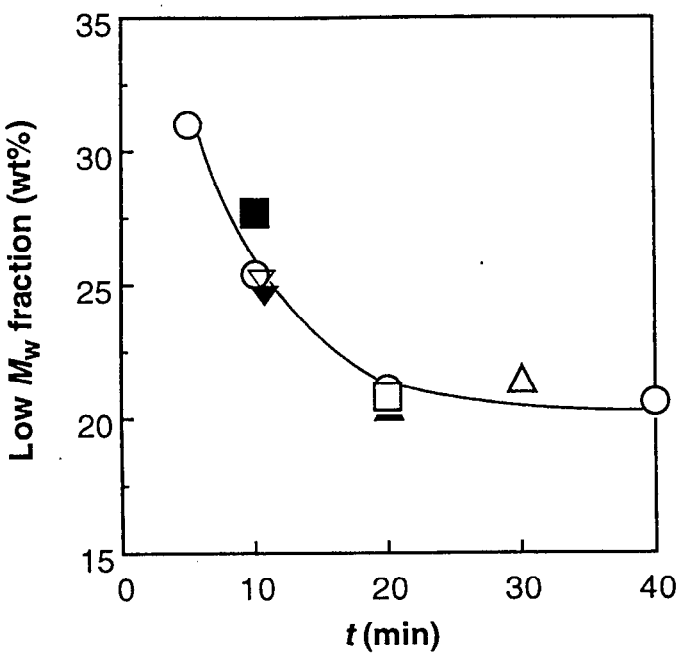

Figure 2-3. Plots of low M_w fraction against polymerization time: (○) run 1–4, (△) run 10, (▲) run 11, (□) run 12, (■) run 13, (▽) run 14, (▼) run 15.

Table 2-3. Results of propene polymerization with *rac*-$Me_2Si(Ind)_2ZrCl_2$–MAO[a]

Run	[Zr] (μmol)	Molar ratio Al/Zr	t[b] (min)	Yield (g)	Activity (kgPP/ mol Zr·h)	M_n[c] ($\times 10^{-4}$)	M_w/M_n[c]
16	0.625	1000	60	1.3	2080	2.88	2.0
17		4000	60	4.7	7520	2.81	2.0
18	2.50	250	60	21.2	8480	2.72	2.0
9		1000	60	37.2	14880	2.66	2.0
19		4000	60	24.0	9600	2.70	2.0
20	10.0	250	60	40.7	4070	2.10	2.0
21		1000	60	66.6	6660	1.88	2.1

[a] Polymerization conditions: polymerization temperature = 40 ℃, toluene = 500 mL, feed rate of propene = 760 mL/min. [b] Polymerization time. [c] Determined by GPC using polystyrene standards.

2-3A-3. Effect of Polymerization Temperature, Cocatalyst and Solvent

Polymerization of ethene was conducted with the same catalyst with the different polymerization temperatures (T_p), cocatalysts as well as solvents. The results of polymerization and the GPC curves of typical polyethenes are shown in Table 2-4 and Figure 2-4, respectively. Since the different lot of MAO was used in the examinations from that of in Table 2-1, polymerization of ethene was first re-examined under the same conditions as conducted before in Table 2-1. In comparison with the results of runs 1–4 in Table 2-1, one may notice that both the value of M_n and the low molecular weight fraction are different to some extent. The profiles of those values along with the polymerization time, however, seem to be very similar. When polymerization was carried out at 0 °C (runs 27–29), the GPC curves of produced polyethenes displayed a single peak, and the high molecular fraction was completely disappeared as illustrated in Figure 2-4 (2).

Then the effect of cocatalysts was studied. A dry MAO was prepared from toluene solution of conventional MAO by removing the toluene and the free $AlMe_3$ in vacuo at room temperature for 6 h.[1,33,34] The use of the dry MAO as a cocatalyst (runs 30–34) also caused to decrease the high molecular fraction to a great extent (Figure 2-4 (3)). It is reasonable to consider that the lowering in polymerization temperature and/or the removing of free $AlMe_3$ suppress the chain transfer reactions to yield polyethene with a higher molecular weight. The present unexpected results might be explained in terms of an equilibrium between the two kinds of active species which give low and high molecular weight fractions of polyethenes. The equilibrium may shift toward the species giving the low molecular weight fraction at low temperature and with dry MAO.

The GPC curves of polyethenes obtained with the use of the mixture of MAO and $AlMe_3$ (runs 35–39) are shown in Figure 2-4 (4). It is clear from Figure 2-4 (4) that addition of $AlMe_3$ to MAO affords polyethene with a much of low molecular weight shoulder at the initial stage of polymerization. The decrease of the shoulder fraction along with the polymerization time (Figure 2-4 (4) b) was observed as discussed above. Several authors have studied the effect of additional AlR_3 on polymerization activity of olefins with metallocene catalysts,[5,35–37] but no result has ever been reported about the effect on MWD of produced polyolefins. From

Table 2-4. Results of ethene polymerization with *rac*-$Me_2Si(Ind)ZrCl_2$ under various conditions[a]

Run	Cocatalyst	Solvent	T_p[b] (℃)	t[c] (min)	M_n[d] ($\times 10^{-4}$)	M_w/M_n[d]	Low M_w fraction[e] (wt %)	High M_w fraction[e] (wt %)	Yield (g)
22	MAO	toluene	40	5	18.8	3.6	56.0	44.0	
23				10	21.0	3.7	50.9	49.1	
24				15	24.3	3.3	48.5	51.5	
25				20	23.0	3.5	46.6	53.4	
26				30	22.3	3.3	45.9	54.1	9.9
27	MAO	toluene	0	30	16.5	2.2			
28				60	18.9	2.3			
29				120	20.1	2.3			2.5
30	Dry-MAO[f]	toluene	40	5	11.9	2.4			
31				10	12.2	2.5			
32				20	12.9	2.5			
33				40	12.2	2.5			
34				60	11.3	2.3			4.9
35	MAO+TMA[g]	toluene	40	5	14.2	3.3	64.6	35.4	
36				10	16.5	3.2	39.7	60.3	
37				15	17.2	3.2	38.1	61.9	
38				20	17.7	3.2	35.4	64.6	
39				30	18.0	3.1	30.8	69.2	8.8
40	MAO	Tol./CM[h]	40	5	15.3	3.3	50.6	49.4	
41				10	16.9	3.4	48.7	51.3	
42				20	16.8	3.4	46.8	53.2	
43				40	16.6	3.3	43.1	56.9	3.2

[a] Polymerization conditions: solvent = 500 mL, feed rate of ethene = 760 mL/min, *rac*-$Me_2Si(Ind)_2ZrCl_2$ = 2.5 μmol, molar ratio of Al/Zr = 1000. [b] Polymerization temperature. [c] Polymerization time. [d] Determined by GPC using polystyrene standards. [e] Calculated from GPC curves. [f] MAO was dried up in vacuo at room temperature for 6 h. [g] MAO (Al: 2.0 mmol) + $AlMe_3$ (0.5 mmol). [h] Toluene (250 mL) + CH_2Cl_2 (250 mL).

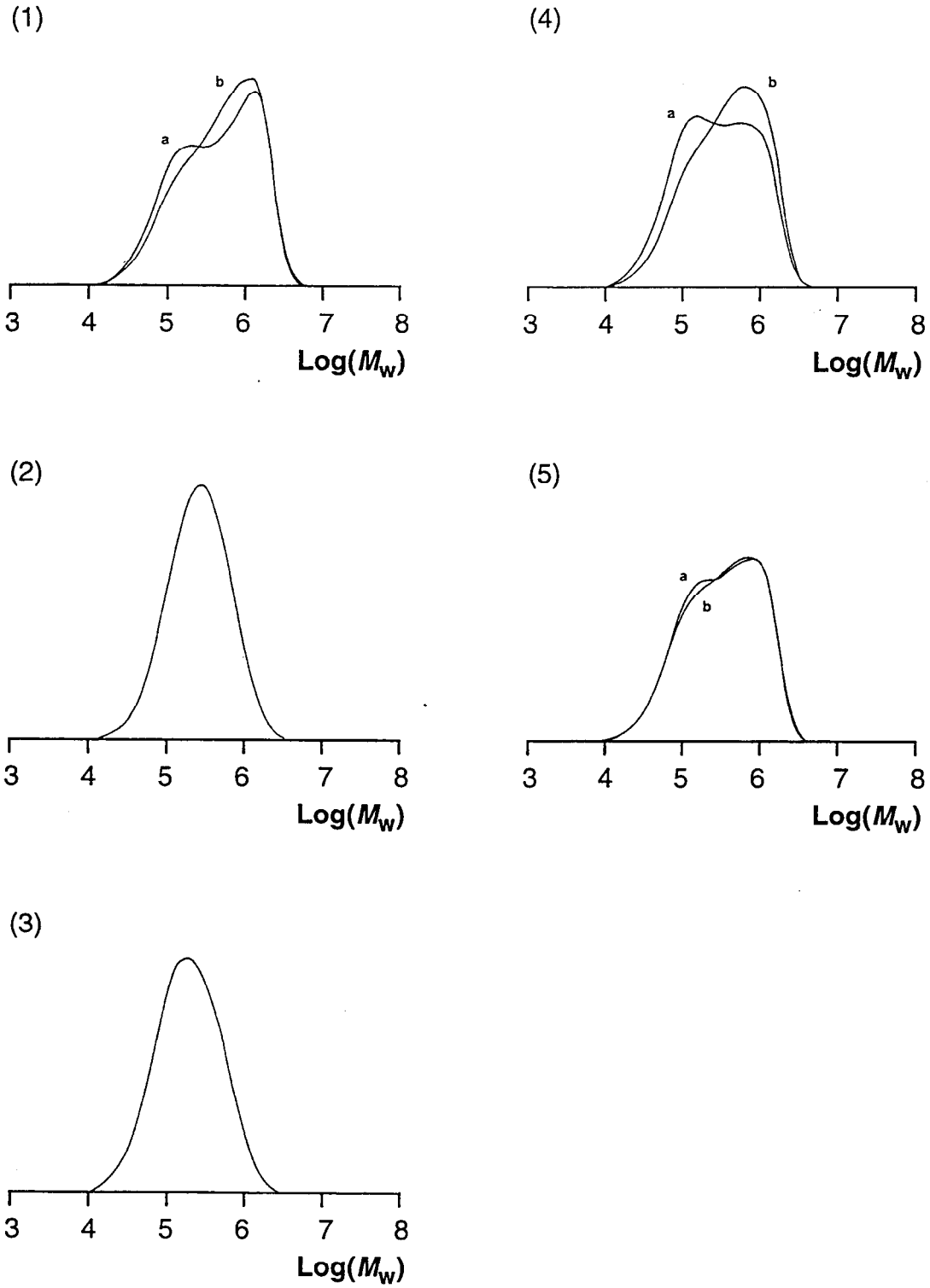

Figure 2-4. GPC elution curves of polyethenes obtained with *rac*-$Me_2Si(Ind)_2ZrCl_2$: (1) MAO at 40 °C in toluene, a = 5 min, b = 30 min; (2) MAO at 0 °C in toluene, 30min; (3) dry MAO at 40 °C in toluene, 5min; (4) MAO + $AlMe_3$ at 40 °C in toluene, a = 5 min, b = 30 min; (5) MAO at 40 °C in toluene + CH_2Cl_2, a = 5 min,, b = 40 min.

a detail analysis of MAO–$AlMe_3$ system by ^1H and ^{13}C NMR spectroscopy at low temperatures, Tritto *et al.* have proposed two kinds of active species, one is a common one and the other is a bimetallic active species associated with $AlMe_3$.[38] The above results could be well explained by their model.

It is well known that polarity of CH_2Cl_2 ($\varepsilon = 9.1$) is higher than that of toluene ($\varepsilon = 2.4$). From such a viewpoint, polymerization of ethene was conducted by using the mixture of CH_2Cl_2 and toluene as solvent (runs 40–43). The addition of CH_2Cl_2 to toluene caused to increase the low molecular weight fraction through the polymerization (Figure 2-4 (5)).

2-3B. Rate-Time Profiles of Ethene Polymerization with Zirconocene–AlR_3/ Borane Compound

2-3B-1. Polymerization with Cp_2ZrCl_2

Polymerization of ethene was performed at 40 °C under an atmospheric pressure with Cp_2ZrCl_2 using AlR_3 (R = Me, Et, *i*Bu)/$Ph_3CB(C_6F_5)_4$ or $B(C_6F_5)_3$ as cocatalysts. The results are summarized in Tables 2-5 and 2-6, respectively.

In the case of using $Ph_3CB(C_6F_5)_4$ as cation-forming reagent, the order of average polymerization activity for 1 h decreased in the following order: Al*i*Bu_3 > $AlEt_3$ > $AlMe_3$. In the polymerization with $AlEt_3$, Cp_2ZrCl_2 showed moderate activity after a remarkably long induction time (about 30 min). The molecular weight of polyethene obtained with Al*i*Bu_3 was higher than that with $AlEt_3$. When $B(C_6F_5)_3$ was used as a cation-forming reagent, the polymerization proceeded with Al*i*Bu_3, however, no activity was observed with $AlMe_3$ and $AlEt_3$.

Polymerization rate (R_p) at polymerization time t ($t = (t_1 + t_2)/2$) was determined according to the following equation:

$$R_p = (Y_2 - Y_1)/(t_2 - t_1)$$

Table 2-5. Results of ethene polymerization with Cp_2ZrCl_2–$AlR_3/Ph_3CB(C_6F_5)_4$[a]

Run	AlR_3	t[b] (min)	Yield (kgPE/ mol Zr)	M_n[c] ($\times10^{-4}$)	M_w/M_n[c]	N[d] (mol PE/ mol Zr)
1	$AlMe_3$	60	22.0	2.1	2.8	
2(a)	$AlEt_3$	5	0.0			
2(b)		10	0.0			
2(c)		20	0.0			
2(d)		30	3.5			
2(e)		45	29.2	3.3	2.4	0.89
2(f)		60	126	3.4	2.4	3.7
2(g)		75	153	3.3	2.5	4.6
2(h)		90	157	3.3	2.5	4.7
3(a)	$Al\textit{i}Bu_3$	5	46.6	13.0	2.7	0.36
3(b)		10	95.5	13.8	2.6	0.69
3(c)		20	198	13.8	2.6	1.4
3(d)		30	298	14.8	2.5	2.0
3(e)		45	432	13.5	2.6	3.2
3(f)		60	553	15.4	2.3	3.6

[a] Polymerization conditions: Cp_2ZrCl_2 = 1.0 μmol, AlR_3 = 0.5 mmol, $Ph_3CB(C_6F_5)_4$ = 1.0 μmol, polymerization temperature = 40 ℃, ethene = 1 atm. [b] Polymerization time. [c] Determined by GPC using polystyrene standards. [d] Number of polymer chains.

Table 2-6. Results of ethene polymerization with Cp_2ZrCl_2–$AlR_3/B(C_6F_5)_3$[a]

Run	AlR_3	t[b] (min)	Yield (kgPE/ mol Zr)	M_n[c] ($\times10^{-4}$)	M_w/M_n[c]	N[d] (mol PE/ mol Zr)
4	$AlMe_3$	60	0			
5	$AlEt_3$	60	0			
6(a)	$Al\textit{i}Bu_3$	5	255	8.9	3.0	2.5
6(b)		10	362	8.7	3.5	4.2
6(c)		20	455	8.4	3.3	5.4
6(d)		30	529	9.1	3.6	5.8
6(e)		45	631	9.7	3.5	6.5
6(f)		60	714	10.4	3.5	6.8

[a] Polymerization conditions: Cp_2ZrCl_2 = 1.0 μmol, AlR_3 = 0.5 mmol, $B(C_6F_5)_3$ = 1.0 μmol, polymerization temperature = 40 ℃, ethene = 1 atm. [b] Polymerization time. [c] Determined by GPC using polystyrene standards. [d] Number of polymer chains.

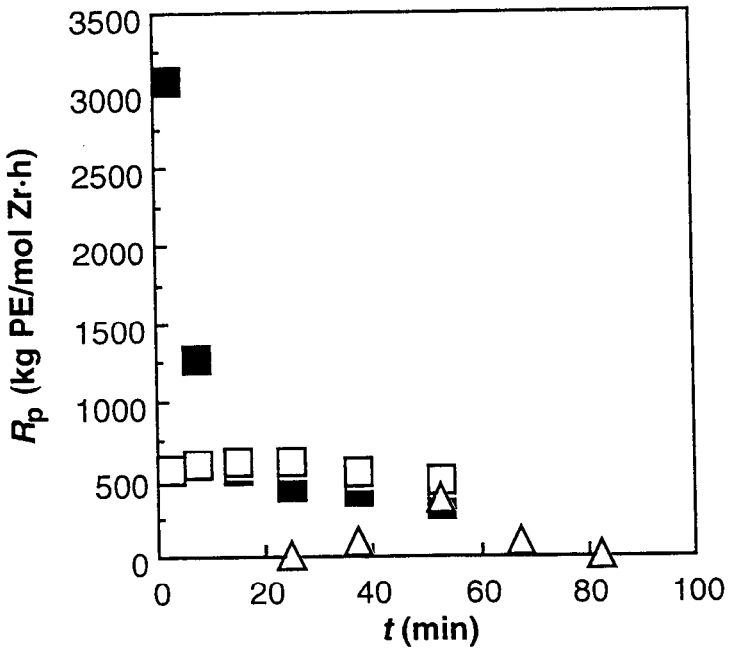

Figure 2-5. Plots of polymerization rate (R_p) against polymerization time with Cp_2ZrCl_2: (△) $AlEt_3/Ph_3CB(C_6F_5)_4$; (□) $Al\textit{i}Bu_3/Ph_3CB(C_6F_5)_4$; (■) $Al\textit{i}Bu_3/B(C_6F_5)_3$.

where Y_1 and Y_2 are yields of polyethene at polymerization time t_2 and t_1 determined by the consumption of ethene, respectively. The R_p values with Cp_2ZrCl_2 against the polymerization time are displayed in Figure 2-5. In the case of using $Ph_3CB(C_6F_5)_4$ as a cation-forming reagent, induction time to reach the maximum R_p was observed with both $AlEt_3$ and AliBu$_3$. When $B(C_6F_5)_3$ was used with AliBu$_3$, R_p showed maximum value at the beginning of polymerization, and then rapidly dropped.

R_p can be expressed by the following equation:

$$R_p = k_p[M]^a[C^*]$$

where k_p, [M], a, and [C*] are, respectively, the rate constant of propagation, monomer concentration, reaction order and number of active centers. The [M] value is constant during the polymerization. Therefore, the time dependence of R_p should derive from the change of k_p and/or [C*] during the polymerization. The number of polymer chains (N: mol polyethene/mol Zr) and the polymer yield show almost the same profile with the increase in polymerization time. Furthermore, the decrease of molecular weight of resulting polyethenes could not be observed in spite of the decrease of R_p. These results suggest that the decrease of R_p with the increase of polymerization time is not caused by the decrease of k_p but the decrease of [C*].

2-3B-2. Polymerization with *rac*-$Me_2Si(Ind)_2ZrCl_2$

Polymerization of ethene was conducted at 40 °C under an atmospheric pressure with *rac*-$Me_2Si(Ind)_2ZrCl_2$ using AlR_3 (R = Me, Et, *i*Bu)/$Ph_3CB(C_6F_5)_4$ or $B(C_6F_5)_3$ as cocatalysts. The results are summarized in Tables 2-7 and 2-8, respectively. The order of average activity for 1 h polymerization decreased in the following order in the case of using $Ph_3CB(C_6F_5)_4$: AliBu$_3$ > $AlEt_3$ > $AlMe_3$. When $B(C_6F_5)_3$ was used, the order of activity was the same with that using $Ph_3CB(C_6F_5)_4$, however, the activity with $AlEt_3$ was very low and no activity was observed with $AlMe_3$.

Table 2-7. Results of ethene polymerization with *rac*-$Me_2Si(Ind)_2ZrCl_2$–$AlR_3/Ph_3CB(C_6F_5)_4$[a]

Run	AlR_3	t[b] (min)	Yield (kgPE/ mol Zr)	M_n[c] ($\times10^{-4}$)	M_w/M_n[c]	N[d] (mol PE/ mol Zr)
7	$AlMe_3$	60	56.3	1.8	2.8	
8(a)	$AlEt_3$	2	301	1.6	3.2	18.8
8(b)		5	525	1.5	3.0	35.3
8(c)		10	841	1.5	3.1	56.1
8(d)		15	1121	1.7	2.8	66.5
8(e)		20	1275	1.7	3.2	76.5
8(f)		30	1454	1.8	3.0	81.3
9(a)	$Al\textit{i}Bu_3$	2	405	6.4	4.2	6.3
9(b)		5	904	6.6	4.3	13.7
9(c)		10	1193	7.1	4.6	16.9
9(d)		15	1475	7.5	4.4	19.7
9(e)		20	1670	7.7	4.0	21.7
9(f)		30	1867	8.1	4.7	23.1

[a] Polymerization conditions: *rac*-$Me_2Si(Ind)_2ZrCl_2$ = 1.0 μmol, AlR_3 = 0.5 mmol, $Ph_3CB(C_6F_5)_4$ = 1.0 μmol, polymerization temperature = 40 ℃, ethene = 1 atm. [b] Polymerization time. [c] Determined by GPC using polystyrene standards. [d] Number of polymer chains.

Table 2-8. Results of ethene polymerization with *rac*-$Me_2Si(Ind)_2ZrCl_2$–$AlR_3/B(C_6F_5)_3$[a]

Run	AlR_3	t [b] (min)	Yield (kgPE/ mol Zr)	M_n [c] ($\times10^{-4}$)	M_w/M_n [c]	N [d] (mol PE/ mol Zr)
10	$AlMe_3$	60	0			
11(a)	$AlEt_3$	5	40.8	1.9	2.3	2.1
11(b)		10	48.1	1.9	2.7	2.6
11(c)		20	55.9	1.9	2.8	2.9
11(d)		30	58.7	1.9	2.5	3.1
11(e)		45	58.7			
12(a)	$Al\textit{i}Bu_3$	2	290	3.0	6.8	9.7
12(b)		5	669	4.5	6.4	14.9
12(c)		10	1245	7.0	5.3	17.7
12(d)		15	1802	7.0	5.3	25.7
12(e)		20	2253	6.9	5.3	32.8
12(f)		30	2919	8.2	5.7	35.8

[a] Polymerization conditions: *rac*-$Me_2Si(Ind)_2ZrCl_2$ = 1.0 μmol, AlR_3 = 0.5 mmol, $B(C_6F_5)_3$ = 1.0 μmol, polymerization temperature = 40℃, ethene = 1 atm. [b] Polymerization time. [c] Determined by GPC using polystyrene standards. [d] Number of polymer chains.

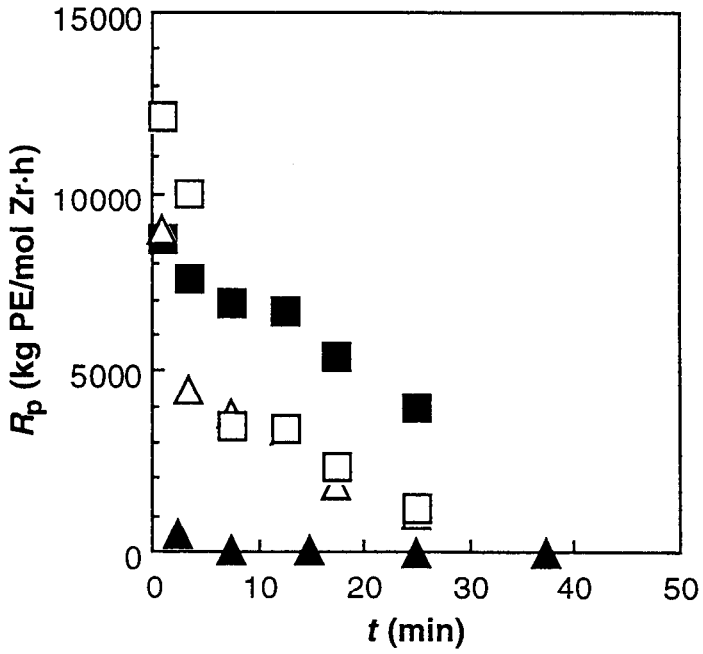

Figure 2-6. Plots of polymerization rate (R_p) against polymerization time with *rac*-$Me_2Si(Ind)_2ZrCl_2$: (△) $AlEt_3/Ph_3CB(C_6F_5)_4$; (□) $Al\textit{i}Bu_3/Ph_3CB(C_6F_5)_4$; (▲) $AlEt_3/B(C_6F_5)_3$; (■) $Al\textit{i}Bu_3/B(C_6F_5)_3$.

The R_p values with *rac*-$Me_2Si(Ind)_2ZrCl_2$ against the polymerization time are displayed in Figure 2-6. R_p showed maximum value at the beginning of polymerization and decayed regardless of AlR_3 and cation-forming reagents used. The R_p value with $B(C_6F_5)_3$ decayed slower than that with $Ph_3B(C_6F_5)_4$. The decrease of R_p would derive from the decrease of [C*] for the same reason in the polymerization with Cp_2ZrCl_2.

2-3B-3. Mechanistic Study in Formation of Active Species

As described above, the activity and rate-time profiles of ethylene polymerization were strongly depended on the combination of zirconocene, trialkylaluminum, and borane compound. The summary of ethene polymerizations with zirconocene–AlR_3/borane compound systems are listed in Table 2-9. Schemes 2-1 and 2-2 show the proposed reaction mechanisms using $Ph_3CB(C_6F_5)_4$ and $B(C_6F_5)_3$ as cation-forming reagents, respectively. In

Table 2-9. Summary of ethene polymerization with zirconocene–AlR_3/borane compound systems

Zirconocene catalyst	AlR_3	Borane compound	Induction time[a] (min)	$R_p$max[b]	Activity[c]	M_n[d] ($\times10^{-4}$)	MWD[e]
Cp_2ZrCl_2	$AlMe_3$	$Ph_3CB(C_6F_5)_4$	---	---	22	2.1	2.8
		$B(C_6F_5)_3$			0	---	---
	$AlEt_3$	$Ph_3CB(C_6F_5)_4$	52.5	387	153	3.3	2.5
		$B(C_6F_5)_3$			0	---	---
	Al*i*Bu_3	$Ph_3CB(C_6F_5)_4$	15	615	553	14.1	2.6
		$B(C_6F_5)_3$	---	3060	714	9.2	5.2
rac-$Me_2Si(Ind)_2ZrCl_2$	$AlMe_3$	$Ph_3CB(C_6F_5)_4$	---	---	56	1.8	2.8
		$B(C_6F_5)_3$			0	---	---
	$AlEt_3$	$Ph_3CB(C_6F_5)_4$	---	9030	2900	1.6	3.1
		$B(C_6F_5)_3$	---	490	117	1.9	2.7
	Al*i*Bu_3	$Ph_3CB(C_6F_5)_4$	---	12200	3730	7.2	4.4
		$B(C_6F_5)_3$	---	8700	5840	6.1	5.8

[a] Induction time to reach the maximum R_p value. [b] Maximum R_p (kg PE/mol Zr·h). [c] Average value of polymerization activity for 1 h (kg PE/mol Zr·h). [d] Average value of M_n. [e] Average value of MWD (M_w/M_n).

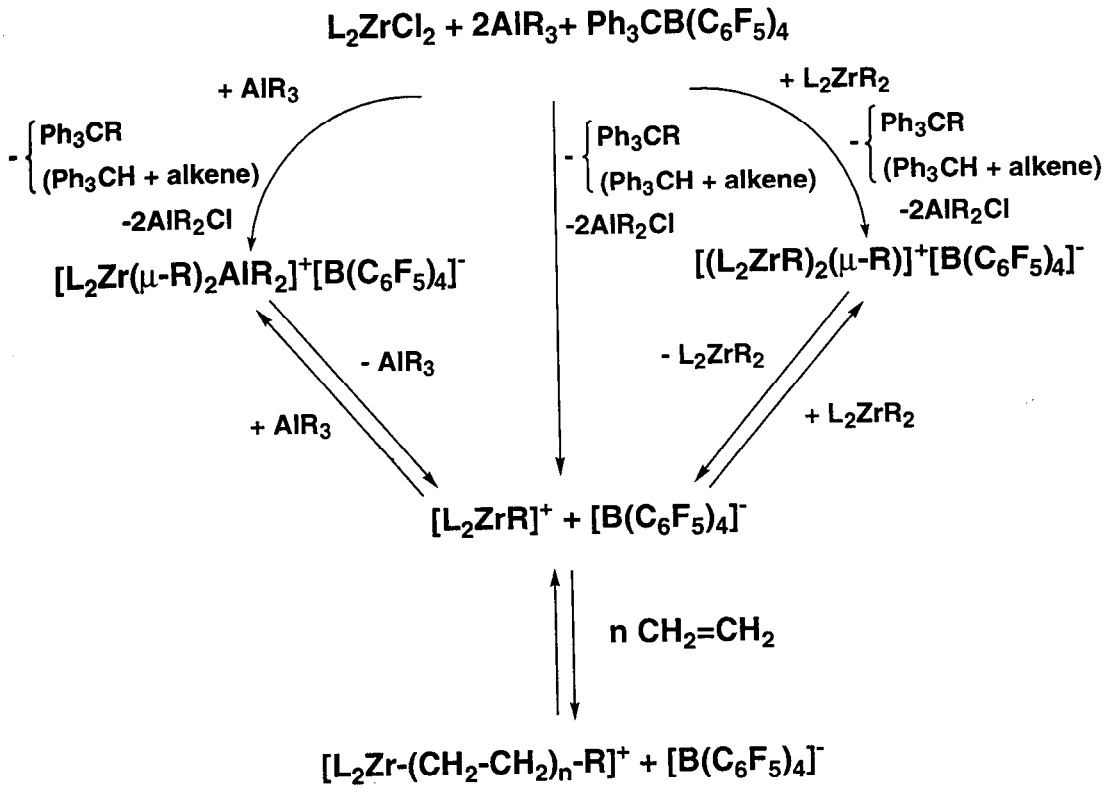

Scheme 2-1. Proposed reaction mechanism of active-site formation in zirconocene–$AlR_3/Ph_3CB(C_6F_5)_4$.

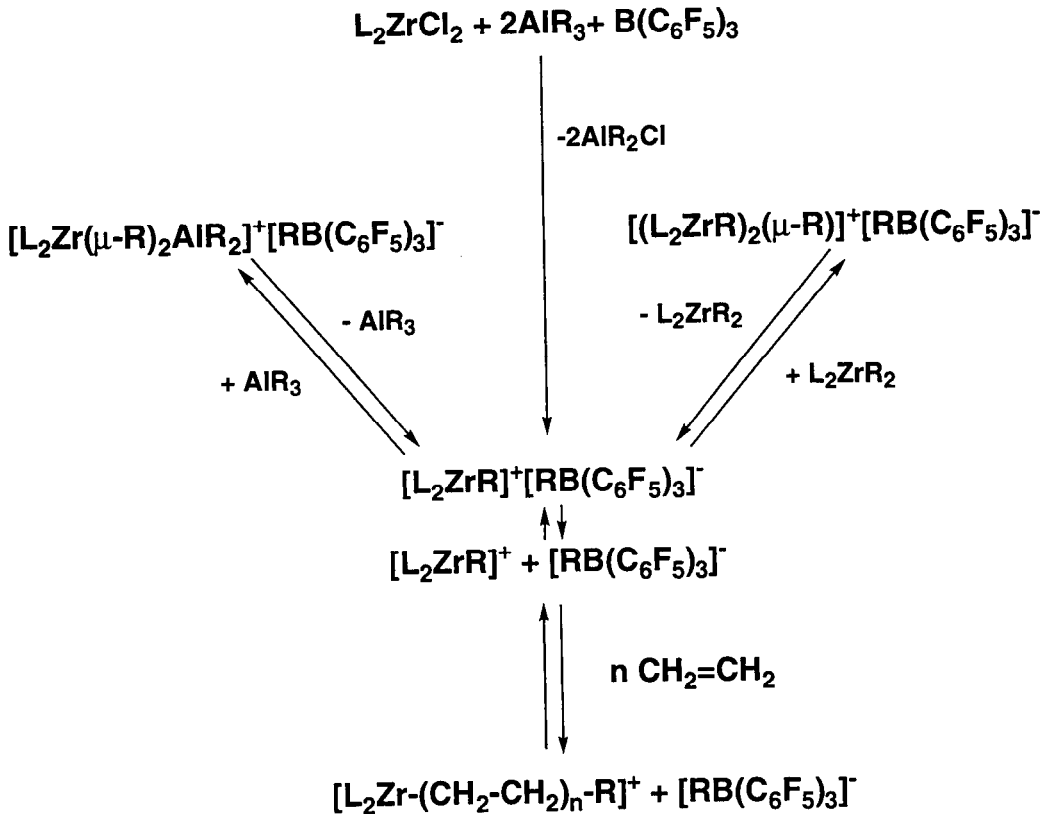

Scheme 2-2. Proposed reaction mechanism of active-site formation in zirconocene–$AlR_3/B(C_6F_5)_3$.

the polymerization with $AlMe_3$, no activity or very low activity was found in each zirconocene catalyst by using any kinds of cation-forming reagents. This result could be due to the stability of $[L_2Zr(\mu\text{-}Me)_2AlMe_2]^+[B(C_6F_5)_4]^-$ and $[L_2Zr(\mu\text{-}Me)_2AlMe_2]^+[MeB(C_6F_5)_3]^-$ (L_2 = ligand; Cp_2 for Cp_2ZrCl_2 and $Me_2Si(Ind)_2$ for *rac*-$Me_2Si(Ind)_2ZrCl_2$) which formed by the zirconocene, $AlMe_3$ and counter-ion.

The induction time before the maximum R_p with Cp_2ZrCl_2–AlR_3 (R = Et, *i*Bu)/$Ph_3CB(C_6F_5)_4$, especially in the case of using $AlEt_3$, could be explained by the formation of dormant complexes, $[Cp_2Zr(\mu\text{-}R)_2AlR_2]^+[B(C_6F_5)_4]^-$ or binuclear $[(Cp_2ZrR)_2(\mu\text{-}R)]^+[B(C_6F_5)_4]^-$ (R = Et, *i*Bu), similarly to the case of $AlMe_3$. When $AlEt_3$ was applied, these complexes should be so stable that it took considerably long time to form the activated free ion. While in the polymerization with *rac*-$Me_2Si(Ind)_2ZrCl_2$–AlR_3 (R = Et, *i*Bu)/$Ph_3CB(C_6F_5)_4$, almost no induction time was observed. Active species were formed without staying the dormant complexes probably due to the steric hindrance of bridged bis(indenyl) ligand and the alkyl group.

In the case of using $B(C_6F_5)_3$ as cation-forming reagent, high activity was observed with $Al\textit{i}Bu_3$, while no activity or very low activity was found with $AlEt_3$ in the polymerization with both Cp_2ZrCl_2 and *rac*-$Me_2Si(Ind)_2ZrCl_2$. Two reasons could be considered to explain this tendency. One is the stability of dormant site as $[L_2Zr(\mu\text{-}Et)_2AlEt_2]^+[EtB(C_6F_5)_3]^-$ or binuclear $[(L_2ZrEt)_2(\mu\text{-}Et)]^+[EtB(C_6F_5)_3]^-$. The other is the stability of ion pair $[L_2ZrR]^+[RB(C_6F_5)_3]^-$ which might have very small k_p in ethene polymerization. In these case, the alkyl group of AlR_3 should significantly affect the nature of these species. Chien *et al.* suggested dissociation of the ion pair to free ion in the *rac*-$Et(Ind)_2ZrMe_2$–$B(C_6F_5)_3$ system which has very large k_p for polymerization.[20c] Brintzinger *et al.* reported existence of solvent-separated ion pairs and associated ion pairs in both Cp_2ZrMe_2–$B(C_6F_5)_3$ and *rac*-$Me_2Si(Ind)_2ZrMe_2$–$B(C_6F_5)_3$.[17,18] High activity with $Al\textit{i}Bu_3/B(C_6F_5)_3$ could be explained by the formation of free ion or solvent-separated ion pairs due to the isobutyl groups which enhance separation of dormant complexes and/or $[L_2ZrR]^+[RB(C_6F_5)_3]^-$ ion pair.

2-4. Summary

In summary, it was suggested that there were two kinds of active species for ethene polymerization with *rac*-$Me_2Si(Ind)_2ZrCl_2$–MAO system, one produced high molecular weight fraction and the other produced low molecular weight fraction. The low molecular weight fraction was produced at the initial stage of the polymerization. Polymerization temperature, kind of MAO and polymerization solvent also affected the molecular weight and MWD of obtained polyethenes.

Activity and rate-time profiles of ethene polymerization with zirconocene–AlR_3/borane compound were also studied. In summary, not only AlR_3 but the borane compound used as a cation-forming reagent affected the induction time and activity if ethene polymerization. Very low activity or no activity was observed with $AlMe_3$ independent of borane compound used. In the case of using $Ph_3CB(C_6F_5)_4$, high activity was observed with both $AlEt_3$ and $Al\textit{i}Bu_3$. On the other hand, when $B(C_6F_5)_3$ was used, high activity was observed only with $Al\textit{i}Bu_3$.

References

(1) Sinn, H.; Kaminsky, W. *Adv. Organomet. Chem.* **1980**, *18*, 99.

(2) Cam, D.; Sartori, F.; Maldotti, A. *Macromol. Chem. Phys.* **1994**, *195*, 2817.

(3) Andresen, A.; Cordes, H-G.; Herwig, J.; Kaminsky, W.; Merck, A.; Mottweiler, R.; Pein, J.; Sinn, H.; Vollmer, H-J. *Angew. Chem., Int. Ed. Engl.* **1976**, *15*, 630.

(4) Giannetti, E.; Nicoletti, G. M.; Mazzocchi, R. *J. Polym. Sci.: Polym. Chem.* **1985**, *23*, 2117.

(5) Reddy, S. S.; Shashidhar, G.; Sivaram, S. *Macromolecules* **1993**, *26*, 1180.

(6) Siedle, A. R.; Hanggi, B.; Newmark, R. A.; Mann, K. R.; Wilson, T. *Makromol. Chem., Macromol. Symp.* **1995**, *89*, 299.

(7) Kaminsky, W. *Makromol. Chem., Macromol. Symp.* **1995**, *97*, 79.

(8) Pieters, P. J. J.; Beek, J. A. M.; Tol, M. F. H. *Macromol. Rapid Commun.* **1995**, *16*, 463.

(9) (a) Coevoet, D.; Caramail, H.; Deffieux, A. *Macromol. Chem. Phys.* **1998**, *199*, 1451. (b) Coevoet, D.; Caramail, H.; Deffieux, A. *Macromol. Chem. Phys.* **1998**, *199*, 1459.

(10) (a) Tritto, I.; Li, S.; Sacchi, M. C.; Zannoni, G. *Macromolecules* **1993**, *26*, 7111. (b) Tritto, I.; Sacchi, M. C.; Li, S. X. *Macromol. Rapid Commun.* **1994**, *15*, 217. (c) Tritto, I.; Li, S. X.; Sacchi, M. C.; Locatelli, P.; Zannoti, G. *Macromolecules* **1995**, *28*, 5358. (d) Tritto, I.; Donetti, R.; Sacchi, M. C.; Locatelli, P.; Zannoni, G. *Macromolecules* **1997**, *30*, 1247.

(11) Jordan, R. F.; Bajgur, C. S.; Willett, R.; Scotto, B. *J. Am. Chem. Soc.* **1986**, *108*, 7410.

(12) Yang, X.; Stern, C. L.; Marks, T. J. *J. Am. Chem. Soc.* **1991**, *113*, 3623.

(13) Yang, X.; Stern, C. L.; Marks, T. J. *J. Am. Chem. Soc.* **1994**, *116*, 10015.

(14) Deck, P. D.; Marks, T. J. *J. Am. Chem. Soc.* **1995**, *117*, 6128.

(15) Jia, L.; Yang, X.; Stern, C. L.; Marks, T. J. *Organometallics* **1997**, *16*, 842.

(16) (a) Bochmann, M.; Lancaster, S. J. *Angew. Chem., Int. Ed. Engl.* **1994**, *33*, 1634. (b) Bochmann, M.; Lancaster, S. J. *J. Organomet. Chem.* **1995**, *497*, 55.

(17) Beck, S.; Prosenc, M. H.; Brintzinger, H. H.; Goretzki, R.; Herfert, N.; Fink, G. *J. Mol. Catal. A: Chem.* **1996**, *111*, 67.

(18) Haselwander, T.; Beck, S.; Brintzinger, H. H. In *Ziegler Catalysts*; Fink, G., Mülhaupt, R., Brintzinger, H. H., Eds.; Springer: Berlin, 1995; p 182.

(19) Herfert, N.; Fink, G. *Makromol. Chem., Rapid Commun.* **1993**, *14*, 91.

(20) (a) Chien, J. C. W.; Tsai, W. M.; Rausch, M. D. *J. Am. Chem. Soc.*, **1991** *113*, 8570. (b) Chien, J. C. W.; Song, W.; Rausch, M. D. *Macromolecules* **1993**, *26*, 3239. (c) Chien, J. C. W.; Song, W.; Rausch, M. D. *J. Polym. Sci., Part A: Polym. Chem.* **1994**, *32*, 2387.

(21) Soga, K.; Uozumi, T.; Arai, T.; Nakamura, S. *Macromol. Rapid Commun.* **1995**, *16*, 379.

(22) (a) Chien, J. C. W.; Razavi, A. *J. Polym. Sci., Part A: Polym. Chem.* **1988**, *26*, 2369. (b) Chien, J. C. W.; Wang, B. P. *J. Polym. Sci., Part A: Polym. Chem.* **1990**, *28*, 15.(c) Chien, J. C. W.; Llinas, G. H.; Rausch, M. D.; Lin, Y. G.; Winter, H. H.; Atwood, J. L.; Bott, S. G. *J. Polym. Sci., Part A: Polym. Chem.* **1992**, *30*, 2601.

(23) Fischer, D.; Mülhaupt, R. *J. Organomet. Chem.* **1991**, *417*, C7.

(24) Stehling, U.; Diebold, J.; Kirsten, R.; Röll, W.; Brintzinger, H. H.; Jüngling, S.; Mülhaupt, R.; Langhauser, F. *Organometallics* **1994**, *13*, 964.

(25) (a) Jüngling, S.; Mülhaupt, R.; Stehling, U.; Brintzinger, H. H.; Fischer, D.; Langhauser, F. *J. Polym. Sci., Part A: Polym. Chem.* **1995**, *33*, 1305. (b) Jüngling, S.; Mülhaupt, R. *J. Organomet. Chem.* **1995**, *497*, 27. (c) Jüngling, S.; Mülhaupt, R. *Makromol. Chem., Macromol. Symp.* **1995**, *97*, 205.

(26) (a) Han, T. K.; Woo, B. W.; Park, J. T.; Do, Y.; Ko, Y. S.; Woo, S. I.; *Macromolecules* **1995**, *28*, 4801. (b) Han, T. K.; Ko, Y. S.; Park, J. W.; Woo, S. I. *Macromolecules* **1996**, *29*, 7305.

(27) Uchida, O.; Takeuchi, K.; Sugimoto, R. In *Science and Technology in Catalysis 1994*; Kodansha: Tokyo, 1995; p 367.

(28) Wester, T. S.; Johnsen, H.; Kittilsen, P.; Rytter, E. *Macromol. Chem. Phys.* **1998**, *199*, 1989.

(29) Dawkins, J. V.; Maddock, J. W. *Eur. Polym. J.* **1971**, *7*, 1537.

(30) Ouano, A. C.; Mereier, P. L. *J. Polym. Sci.* **1968**, *C21*, 309.

(31) Soga, K.; Ohgizawa, M.; Shiono, T.; Lee, D.H. *Macromolecules* **1991**, *24*, 1699.

(32) Flory, P. J. In *Principle of Polymer Chemistry*; Cornell University Press: Ithaca, 1986; p 317.

(33) Sinn, H.; Bliemeister, J.; Clausnitzer, D.; Tikwe, L.; Winter, H.; Zarnke, O. In *Transition Metals and Organometallics as Catalysts for Olefin Polymerization*; Kaminsky, W., Sinn, H., Eds.; Springer: Berlin, 1998; p 257.

(34) Barron, A. *Organometallics* **1995**, *14*, 3581.

(35) Resconi, L.; Bossi, S.; Abis, L. *Macromolecules* **1990**, *23*, 4489.

(36) Michiels, W.; Escalona, A. M. *Makromol. Chem., Macromol. Symp.* **1995**, *97*, 171.

(37) Reddy, S. S.; Radhakrishnan, K.; Sivaram, S. *Polym. Bull.* **1996**, *37*, 165.

(38) Tritto, I.; Sacchi, M. C.; Locatelli, P.; Li, S. X. *Macromol. Chem. Phys.* **1996**, *197*, 1537.

Chapter 3

Effect of Cocatalysts on α-Olefin Polymerization with Zirconocene Catalysts

3-1. Introduction

MAO is an excellent cocatalyst for olefin polymerization with metallocene catalysts. A considerable number of studies have been made on the structure of MAO and the mechanism of olefin polymerization with MAO. On the other hand, Jordan *et al.* found that a cationic zirconocene complex, $[Cp_2ZrCH_3(THF)]^+[BPh_4]^-$, was active for ethene polymerization in a polar solvent without any cocatalysts.[1] The result clearly indicates that MAO is not necessary for olefin polymerization with metallocene catalysts.[2] Chien *et al.* reported the isospecific polymerization of propene catalyzed by *rac*-$Et(Ind)_2Zr(CH_3)_2$ and *rac*-$Et(Ind)_2ZrCl_2$–$AlEt_3$ combined with $Ph_3CB(C_6F_5)_4$, which systems exhibited higher activity than that with MAO.[3] After that, a large number of studies have been made on stereospecific polymerizations of propene with cationic metallocene catalysts combined with various cation-forming reagents, especially borane compounds.[4]

Since the discovery of isospecific polymerization of propene with *rac*-type *ansa*-metallocene by Brintzinger *et al.*,[5] a great deal of effort has been made on development of highly stereospecific metallocenes by modification of the ligand structure from both industrial and scientific points of view. Yamazaki *et al.* reported highly isospecific polymerization of propene with *rac*-bis(cyclopentadienyl) type metallocene catalysts.[6] Spaleck *et al.* and Kaminsky *et al.* synthesized *rac*-bis(indenyl) type metallocenes which could produce highly isotactic polypropene.[7,8]

On the other hand, the achiral *meso*-type metallocene catalysts afford atactic polymers, and only few attentions have so far been paid on polymerization of olefins with these catalysts.[9] In recent years there have been renewal of interests in synthesis of *meso*-type *ansa*-metallocene catalysts[10] and polymerization of olefins with those catalysts. Kaminsky *et al.* reported photoinduced *rac-/meso-* interconversion of *ansa*-metallocene and investigated α-olefin polymerization with *rac-* and *meso-* type *ansa*-zirconocenes–MAO.[11] Waymouth *et al.* conducted propene polymerization with *rac-* and *meso*-dimethylsilylenebis(2-phenyindenyl)zirconium dichloride–MAO to model the polymerization behavior with unbridged bis(2-phenylindenyl)zirconium dichloride, which produces isotactic-atactic stereoblock

polypropene.[12] There is another thing that is important in polymerization of olefin with *meso*-type *ansa*-metallocene catalyst. Soga *et al.* recently reported that alternating copolymerization of ethene and 1-octene with *meso*-$Me_2Si(2\text{-}MeInd)_2ZrCl_2$–MAO.[13]

As described in Chapter 2, cocatalyst plays important roll to control the profile, activity and molecular weight of resulting polymer in the polymerization of ethene with zirconocene catalysts. In this chapter, the author has studied the effect of cocatalysts on α-olefin (propene, 1-butene and 1-hexene) polymerizations by mixtures of *rac*-, *meso*-$Me_2Si(2,3,5\text{-}Me_3Cp)_2ZrCl_2$ and $Me_2Si(2\text{-}MeInd)_2ZrCl_2$ (Scheme 3-1). There are several reasons for applying the mixture of *rac*- and *meso*-zirconocene to the polymerization. One is that the purification of *meso*-isomer is difficult. Another reason is that there must be errors between polymerization batches with *rac*-isomer and *meso*-isomer, and it can be reduced by the method. Furthermore, effect of metallocene ligand was discussed in comparison with the results of corresponding polymerization with $Me_2Si(2,3,5\text{-}Me_3Cp)_2ZrCl_2$ and with $Me_2Si(2\text{-}MeInd)_2ZrCl_2$.

3-2. Experimental Part

Materials

$Me_2Si(2,3,5\text{-}Me_3Cp)_2ZrCl_2$ was prepared according to the literature as a mixture of diastereomers.[6] A composition of the isomers (*rac*-isomer ≈ 57%, *meso*-isomer = 43%) was determined by ^1H NMR spectroscopy. $Me_2Si(2\text{-}MeInd)_2ZrCl_2$ was prepared according to the literature and a part of *rac*-isomer was separated by recrystallization.[14] A composition of the isomers was determined as follows, *rac*-isomer = 16.7%, *meso*-isomer = 83.3%. Toluene solutions of MAO, $AlEt_3$ and $Al\textit{i}Bu_3$ were donated from Tosoh Akzo Co., Ltd. and used without further purification. $Ph_3CB(C_6F_5)_4$ was donated from Tosoh Akzo Co., Ltd. and Asahi glass Co., Ltd., and used without further purification. Propene and 1-butene were purified by passing it through a column of molecular sieves 3A. Toluene and 1-hexene were commercially obtained and dried over molecular sieves 3A and CaH_2.

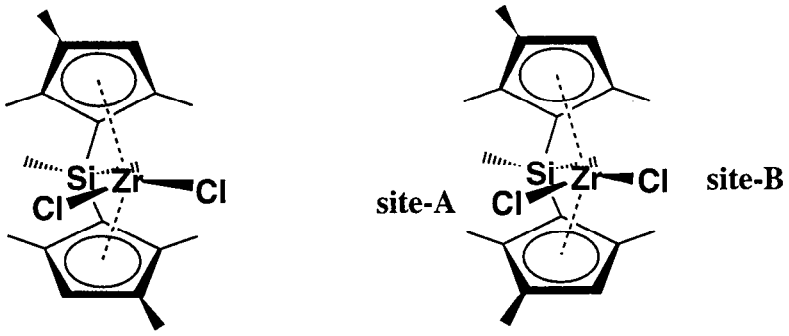

rac- (57 %) *meso*- (43 %)

$Me_2Si(2,3,5\text{-}Me_3Cp)_2ZrCl_2$

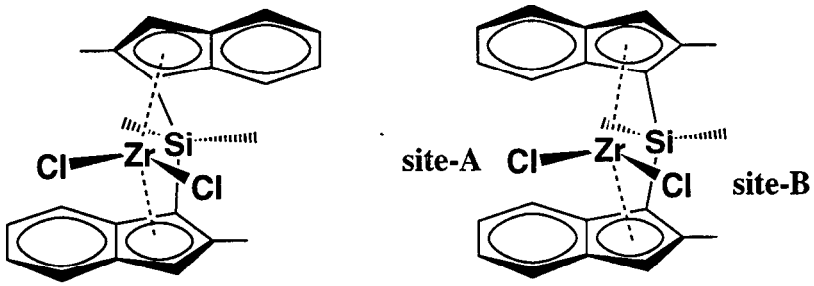

rac- (16.7 %) *meso*- (83.3 %)

$Me_2Si(2\text{-}MeInd)_2ZrCl_2$

Scheme 3-1. *rac*- and *meso*-type *ansa*-zirconocenes.

Polymerization of α-olefins

A. Polymerization with $Me_2Si(2,3,5\text{-}Me_3Cp)_2ZrCl_2$

Polymerization of propene was carried out in an agitated 1 L autoclave at 40 °C. 280 g (6.7 mol) of liquid propene was fed to the autoclave. Toluene (10 mL), MAO or AlR_3 ($AlEt_3$ or $Al\textit{i}Bu_3$) and $Me_2Si(2,3,5\text{-}Me_3Cp)_2ZrCl_2$ were pre-mixed in a 100 mL glass flask at 25 °C for 5 min. The polymerization was started by adding the catalyst solution to the autoclave. In the

case of using AlR_3 (R = Et, *i*Bu), toluene solution of $Ph_3CB(C_6F_5)_4$ was added furthermore. During the polymerization, temperature was kept at 40 °C. The polymerization was terminated by adding isobutyl alcohol. The polymer obtained (mixture of isotactic and atactic polypropene) was adequately washed with plenty of methanol and dried in vacuo at 60 °C for 6 h.

Polymerizations of 1-butene and 1-hexene were carried out in the same method of the propene polymerization, except feed of 1-butene was 140 g (2.5 mol) and 1-hexene was 84 g (1.0 mol).

B. Polymerization with $Me_2Si(2\text{-}MeInd)_2ZrCl_2$

Polymerization of propene was conducted in a 300 mL three necked glass reactor equipped with a seal septum and a magnetic stirrer. Toluene (190 mL) was added to the reactor followed by introduction of propene under an atmospheric pressure at 40 °C until the solvent was saturated with propene. The other experimental procedures were the same with those described in the polymerization with $Me_2Si(2,3,5\text{-}Me_3Cp)_2ZrCl_2$. Consumption of propene was monitored by a gas flow meter. Reaction medium was sampled through the seal septum with a syringe and quenched in methanol.

Polymerization of 1-butene was carried out in a 200 mL autoclave equipped with a magnetic stirrer. Toluene (100 mL) was added to the reactor and 1-butene (0.2 mol) was introduced at −10 °C. Catalyst solution was prepared with the same procedure in the polymerization of propene. The polymerization was started by adding the catalyst solution with aluminum compound (and toluene solution of $Ph_3CB(C_6F_5)_4$, in the case of using AlR_3) to the reactor at −10 °C and heated the reactor quickly to 40 °C. The polymerization was terminated by purging the monomer remained and adding methanol. The resulting polymer was collected by the same method in the propene polymerization.

Polymerization of 1-hexene was carried out in a 200 mL glass reactor equipped with a magnetic stirrer. Toluene (90 mL) and 1-hexene (0.08 mol) were added to the reactor. The reaction medium was heated to 40 °C, then the polymerization was started by adding the catalyst solution with aluminum compound (and toluene solution of $Ph_3CB(C_6F_5)_4$, in the case of using

AlR_3) to the reactor. The polymerization was terminated by adding methanol. The resulting polymer was collected according to the same manner in the propene polymerization.

Separation of isotactic and atactic polymers

The mixture of isotactic and atactic polypropenes was dissolved in xylene or toluene and refluxed for 1 h. After cooling the solution to room temperature and keeping it at 25 °C for 2 h, the isotactic polypropene was separated by filtration. The atactic polypropene, which was solved in xylene and toluene, was obtained by evaporation. Both isotactic and atactic polypropenes were dried in vacuo at 60 °C for 6 h.

The mixture of isotactic and atactic poly(1-butene) was extracted with methylenedichloride (CH_2Cl_2) for 6 h: atactic poly(1-butene) is soluble in CH_2Cl_2.[15]

Analytical procedure

M_n and MWD (M_w/M_n) of the polymers were measured at 140 °C by means of GPC (Waters 150CV) using *o*-dichlorobenzene as a solvent using polystyrene standards. M_n of polypropenes could be converted using the Q-factor by the equation: $M_n = M_n(PS)\cdot Q_{PP}/Q_{PS}$ ($M_n(PS)$, M_n calibrated by polystyrene standards; Q_{PP}, Q-factor of polypropene = 26.4; Q_{PS}, Q-factor of polystyrene = 41.3).[16] ^{13}C NMR spectrum of poly(1-hexene) was recorded at 135 °C using a JEOL GX-270 NMR spectrometer or at 130 °C using a JEOL EX-400 NMR spectrometer. Polymers were dissolved in *o*-dichlorobenzene/benzene-d_6 (vol. ratio = 9/1) or in 1,1,2,2-tetrachloroethane-d_2 up to 5 wt%. DSC measurements were made using a Perkin-elmer DSC-I at a heating rate of 5 °C/min.

3-3. Results and Discussion

3-3A. Polymerization with $Me_2Si(2,3,5\text{-}Me_3Cp)_2ZrCl_2$

3-3A-1. Polymerization of Propene with $Me_2Si(2,3,5\text{-}Me_3Cp)_2ZrCl_2$

Table 3-1. Results of propene polymerization with *rac*- and *meso*-$Me_2Si(2,3,5\text{-}Me_3Cp)_2ZrCl_2$[a]

Run	Catalyst (μmol)	Cocatalyst[b]	t[c] (min)	Yield (g)	R_p[d]	R_p(*rac*)[e]	R_p(*meso*)[e]	R_p(*rac*)/ R_p(*meso*)	W_a[f]	M_{ni}[g] (×10^{-4})	M_{wi}/M_{ni}[g]	M_{na}[h] (×10^{-4})	M_{wa}/M_{na}[h]
1	7.6	MAO	15	10.3	5400	7540	2560	2.95	0.20	8.9	1.9	1.3	2.2
2	9.9		30	22.4	4510	6460	1920	3.36	0.18	8.1	2.0	1.0	2.3
3	4.1		60	31.9	3370	4870	1370	3.55	0.18	7.8	1.9	1.2	2.1
4	10.8	$AlEt_3$/TB	15	2.3	830	840	840	1.00	0.44	1.7	2.0	0.6	1.9
5	8.6		30	3.4	780	660	940	0.70	0.52	1.7	2.0	0.6	1.9
6	10.9		60	7.7	700	480	990	0.48	0.61	1.7	2.0	0.7	1.8
7	1.6	Al*i*Bu_3/TB	10	9.5	36300	21600	56000	0.39	0.66	3.8	1.9	1.0	1.9
8	1.2		30	13.5	22500	13800	34000	0.41	0.65	3.5	2.0	0.9	2.0

[a] *rac*-isomer = 57%, *meso*-isomer = 43%. [b] Molar ratio of (MAO)Al/Zr = 1000, molar ratio of ($AlEt_3$, Al*i*Bu_3)Al/Zr = 250, TB = $Ph_3CB(C_6F_5)_4$, molar ratio of B/Zr = 1.0. [c] Polymerization time. [d] Rate of polymerization (kg polypropene/mol Zr·h). [e] Rate of polymerization with *rac*-isomer and *meso*-isomer (kg polypropene/mol Zr·h). [f] Weight fraction of atactic polymer. [g,h] Number-average molecular weight (converted by Q-factor) and molecular weight distribution of isotactic and atactic polymer determined by GPC.

Propene polymerizations with a mixture of *rac*- and *meso*-$Me_2Si(2,3,5\text{-}Me_3Cp)_2ZrCl_2$ combined with three cocatalysts were conducted at 40 °C. The results are summarized in Table 3-1. Isotactic and atactic polypropenes were obtained from *rac*-isomer and *meso*-isomer, respectively. The polymerization activity was changed with the cocatalyst combined, and the order of activities are Al*i*$Bu_3/Ph_3CB(C_6F_5)_4$ > MAO > $AlEt_3/Ph_3CB(C_6F_5)_4$ in both isospecific and aspecific polymerization. The ratios of $R_p(rac)$ (rate of polymerization with *rac*-isomer) to $R_p(meso)$ (rate of polymerization with *meso*-isomer), $R_p(rac)/R_p(meso)$, are compared. The average values of the $R_p(rac)/R_p(meso)$ ratio were 3.4 with MAO, 0.71 with $AlEt_3/Ph_3CB(C_6F_5)_4$, and 0.38 with Al*i*$Bu_3/Ph_3CB(C_6F_5)_4$. To put it plainly, the activity of *meso*-isomer is higher than that of *rac*-isomer in the case of using $AlR_3/Ph_3CB(C_6F_5)_4$ as cocatalysts, especially using Al*i*Bu_3. Collins *et al.* reported results of propene polymerization with *rac*- and *meso*-$Et(3\text{-}RCp)_2ZrCl_2$ (R = Me, *i*Pr, *t*Bu) and $Et(H_4Ind)_2ZrCl_2$ combined with MAO at 40 °C in toluene, and the $R_p(rac)/R_p(meso)$ values were 4.8, 4.1, 12.8, and 10.7, respectively.[9a] Kaminsky *et al.* reported a result of propene polymerization with *rac*- and *meso*-$Me_2Si(2\text{-}Me\text{-}4,6\text{-}iPr_2Ind)_2ZrCl_2$–MAO at 30 °C in toluene, and the $R_p(rac)/R_p(meso)$ value was 15.6.[11] Judging from these results, $R_p(rac)$ is higher than $R_p(meso)$ in propene polymerization with *ansa*-zirconocene–MAO. The tendency, $R_p(rac)$ was lower than $R_p(meso)$ in the case of using $AlR_3/Ph_3CB(C_6F_5)_4$, could be attributed to the nature of cocatalysts. In the case of using MAO as a cocatalyst, the $R_p(rac)/R_p(meso)$ value increased with polymerization time, while decrease of the $R_p(rac)/R_p(meso)$ value was observed in the case of using $AlEt_3/Ph_3CB(C_6F_5)_4$. These tendencies could be explained by the difference of the polymerization profiles between with *rac*-isomer and with *meso*-isomer.

3-3A-2. Polymerization of 1-Butene and 1-Hexene with $Me_2Si(2,3,5\text{-}Me_3Cp)_2ZrCl_2$

1-Butene and 1-hexene polymerizations with the mixture of *rac*- and *meso*-$Me_2Si(2,3,5\text{-}Me_3Cp)_2ZrCl_2$ combined with three cocatalysts were conducted at 40 °C. The results are summarized in Tables 3-2 and 3-3, respectively. Atactic and isotactic poly(1-butene)s could be separated according to the procedures described in the Experimental Part. Weight fraction

Table 3-2. Results of 1-butene polymerization with *rac*- and *meso*-$Me_2Si(2,3,5\text{-}Me_3Cp)_2ZrCl_2$[a]

Run	Catalyst (μmol)	Cocatalyst[b]	t[c] (min)	Yield (g)	Rp[d]	$Rp(rac)$[e]	$Rp(meso)$[e]	$Rp(rac)/Rp(meso)$	W_a[f]	M_{ni}[g] (×10^{-4})	M_{wi}/M_{ni}[g]	M_{na}[h] (×10^{-4})	M_{wa}/M_{na}[h]
9	1.6	MAO	60	0.79	490	640	280	2.29	0.25	5.6	1.9	0.6	2.4
10	3.7	$AlEt_3$/TB	120	1.56	210	260	150	1.73	0.31	2.1	2.0	0.4	1.8
11	2.1	Al*i*Bu_3/TB	60	5.77	3060	3760	2140	1.76	0.30	3.8	1.7	0.5	1.9

[a] *rac*-isomer = 57%, *meso*-isomer = 43%. [b] Molar ratio of (MAO)Al/Zr = 1000, molar ratio of ($AlEt_3$, Al*i*Bu_3)Al/Zr = 250, TB = $Ph_3CB(C_6F_5)_4$, molar ratio of B/Zr = 1.0. [c] Polymerization time. [d] Rate of polymerization (kg poly(1-butene)/mol Zr·h). [e] Rate of polymerization with *rac*-isomer and *meso*-isomer (kg poly(1-butene)/mol Zr·h). [f] Weight fraction of atactic polymer. [g,h] Number-average molecular weight and molecular weight distribution of isotactic and atactic polymer determined by GPC.

Table 3-3. Results of 1-hexene polymerization with *rac*- and *meso*-$Me_2Si(2,3,5\text{-}Me_3Cp)_2ZrCl_2$[a]

Run	Catalyst (μmol)	Cocatalyst[b]	t[c] (min)	Yield (g)	R_p[d]	$R_p(rac)$[e]	$R_p(meso)$[e]	$R_p(rac)/R_p(meso)$	W_a[f]	M_n[g] (×10^{-4})	M_w/M_n[g]
12	1.4	MAO	60	11.6	8390	12100	3420	3.54	0.18	6.1	2.2
13	8.8	$AlEt_3$/TB	180	1.27	48	47	50	0.94	0.45	0.9	2.7
14	3.0	Al*i*Bu_3/TB	60	10.6	3530	3680	3310	1.11	0.40	1.8	3.3

[a] *rac*-isomer = 57%, *meso*-isomer = 43%. [b] Molar ratio of (MAO)Al/Zr = 1000, molar ratio of ($AlEt_3$, Al*i*Bu_3)Al/Zr = 250, TB = $Ph_3CB(C_6F_5)_4$, molar ratio of B/Zr = 1.0. [c] Polymerization time. [d] Rate of polymerization (kg poly(1-hexene)/mol Zr·h). [e] Rate of polymerization with *rac*-isomer and *meso*-isomer (kg poly(1-hexene)/mol Zr·h). [f] Weight fraction of atactic polymer determined by ^{13}C NMR spectroscopy. [g] Number-average molecular weight and molecular weight distribution determined by GPC.

of atactic poly(1-hexene) was determined by ^{13}C NMR spectrum of whole polymer[17] assuming that the fraction of [*mmrm*]+[*rmrr*] is derived from the atactic polymer and the atactic polymer is almost perfectly atactic in statistics ([*mm*] = 25%, [*mr*] = 50%, and [*rr*] = 25%). The $R_p(rac)/R_p(meso)$ values of 1-butene and 1-hexene with MAO were, respectively, 2.29 and 3.54 ($R_p(rac) > R_p(meso)$). Kaminsky *et al.* investigated 1-pentene, 1-hexene and 1-octene polymerization with *rac*- and *meso*-Me_2Si(2-Me-4,6-*i*Pr_2Ind)$_2ZrCl_2$–MAO at 30 °C in toluene and reported the $R_p(rac)/R_p(meso)$ values were 0.23, 0.18, and 0.17 ($R_p(rac) < R_p(meso)$), respectively.[11] It seems reasonable to suppose that these contrary results are derived from the difference of ligand (in steric effect) between (2,3,5-Me_3Cp) and (2-Me-4,6-*i*Pr_2Ind). The $R_p(rac)/R_p(meso)$ values with $AlR_3/Ph_3CB(C_6F_5)_4$ in both 1-butene and 1-hexene polymerizations are smaller than those with MAO. This tendency is the same with the propene polymerization. In the 1-butene polymerization, the $R_p(rac)$ is almost equal to the $R_p(meso)$, and the $R_p(meso)$ is slightly higher than the $R_p(rac)$ in the 1-hexene polymerization with $AlR_3/Ph_3CB(C_6F_5)_4$. Although, the $R_p(rac)$ is much lower than the $R_p(meso)$ in the propene polymerization with $AlR_3/Ph_3CB(C_6F_5)_4$ (Table 3-1). These results would be caused by the difference of side chain length in monomers.

As reported by Soga *et al.*, helical conformation is formed when the polymer chains grow to a critical number of monomer units in the isospecific polymerization of α-olefins.[18] This argument makes sense that rate constant of propagation (k_p) of isospecific active site is more than that of aspecific site. The R_p can be expressed by the following equation:

$$R_p = k_p[M]^a[C^*]$$

where [M], a, and [C*] are, respectively, monomer concentration, reaction order, and number of active centers. Assuming that the k_p of isospecific *rac*-isomer is larger than that of aspecific *meso*-isomer, the results, of which the $R_p(rac)/R_p(meso)$ values are less than 1 in the polymerization of propene with $AlR_3/Ph_3CB(C_6F_5)_4$, can not be explained by the difference of the k_p values. There is considerable validity in the difference of the $R_p(rac)/R_p(meso)$ values

between the cocatalysts used, which is probably derived from difference of [C*] in *rac*-zirconocene and [C*] in *meso*-zirconocene.

3-3B. Polymerization with $Me_2Si(2\text{-}MeInd)_2ZrCl_2$

3-3B-1. Polymerization of Propene with $Me_2Si(2\text{-}MeInd)_2ZrCl_2$

Propene polymerization with mixture of *rac*- and *meso*-$Me_2Si(2\text{-}MeInd)_2ZrCl_2$ was conducted at 40 °C using three cocatalysts, MAO and $Ph_3CB(C_6F_5)_4$ combined with AlR_3 (R = Et, *i*Bu). The results are summarized in Tables 3-4, 3-5 and 3-6, respectively. The polymerization activity and M_n of the polymers (M_{ni} and M_{na} denote number-average molecular weight of the isotactic and the atactic polymers) depended on the combined cocatalysts and decreased in the following order: $Al\textit{i}Bu_3/Ph_3CB(C_6F_5)_4$ > MAO > $AlEt_3/Ph_3CB(C_6F_5)_4$.

Table 3-4. Results of propene polymerization with *rac*- and *meso*-$Me_2Si(2\text{-}MeInd)_2ZrCl_2$–MAO[a] (Run 15)

t[b] (min)	Y[c]	M_n[d] ($\times10^{-4}$)	M_w/M_n[d]	W_a[e]	Y_i[f]	N_i[g]	Y_a[f]	N_a[g]
5	22.1	1.51	4.5	0.29	93.7	2.5	7.8	1.3
10	119	1.48	4.7	0.30	496	13.4	43.2	7.0
15	226	1.44	4.9	0.32	926	25.0	85.8	13.8
20	311	1.41	5.0	0.33	1250	33.7	122	19.7
30	485	1.34	5.3	0.36	1870	50.4	207	33.3
45	698	1.30	5.2	0.37	2620	70.6	314	50.8
60[h]	902			0.38	3380	91.0	406	65.5

[a] *rac*-isomer = 16.7%, *meso*-isomer = 83.3%. [b] Polymerization (sampling) time. [c] Yield of whole polymer (kg polypropene/mol Zr). [d] Number-average molecular weight and molecular weight distribution of whole polymer determined by GPC. [e] Weight fraction of atactic polymer. [f] Yield of isotactic polymer (Y_i) and atactic polymer (Y_a) (kg polypropene/mol Zr). [g] Number of isotactic (N_i) and atactic (N_a) polymer chains (mol polypropene/mol Zr). [h] Isotactic polypropene: M_{ni} = 37100, M_{wi}/M_{ni} = 2.6; atactic polypropene: M_{na} = 6200, M_{wa}/M_{na} = 2.4.

Table 3-5. Results of propene polymerization with *rac*- and *meso*-$Me_2Si(2\text{-}MeInd)_2ZrCl_2$–$AlEt_3/Ph_3CB(C_6F_5)_4$[a] (Run 16)

t[b] (min)	Y[c]	M_n[d] ($\times10^{-4}$)	M_w/M_n[d]	W_a[e]	Y_i[f]	N_i[g]	Y_a[f]	N_a[g]
5	71.3	0.64	2.3	0.12	374	53.7	10.5	2.7
10	114	0.65	2.3	0.10	613	87.9	13.5	3.5
15	151	0.65	2.3	0.09	829	119	15.6	4.0
20	186	0.66	2.4	0.08	1020	147	17.4	4.5
30	247	0.66	2.4	0.07	1380	197	20.8	5.4
45[h]	262	0.66	2.4	0.07	1460	209	22.3	5.8

[a] *rac*-isomer = 16.7%, *meso*-isomer = 83.3%. [b] Polymerization (sampling) time. [c] Yield of whole polymer (kg polypropene/mol Zr). [d] Number-average molecular weight and molecular weight distribution of whole polymer determined by GPC. [e] Weight fraction of atactic polymer. [f] Yield of isotactic polymer (Y_i) and atactic polymer (Y_a) (kg polypropene/mol Zr). [g] Number of isotactic (N_i) and atactic (N_a) polymer chains (mol polypropene/mol Zr). [h] Isotactic polypropene: M_{ni} = 7000, M_{wi}/M_{ni} = 2.3; atactic polypropene: M_{na} = 3900, M_{wa}/M_{na} = 2.6.

Table 3-6. Results of propene polymerization with *rac*- and *meso*-$Me_2Si(2\text{-}MeInd)_2ZrCl_2$–$Al\textit{i}Bu_3/Ph_3CB(C_6F_5)_4$[a] (Run 17)

t[b] (min)	Y[c]	M_n[d] ($\times10^{-4}$)	M_w/M_n[d]	W_a[e]	Y_i[f]	N_i[g]	Y_a[f]	N_a[g]
2	321	4.32	4.7	0.42	1120	16.5	161	10.6
5	1470	3.82	3.3	0.22	6870	102	391	25.9
10	3210	3.91	3.6	0.21	15200	225	810	53.6
15	4930	3.97	4.0	0.20	23600	348	1200	79.2
20	6390	4.18	3.8	0.18	31400	465	1370	90.4
30[h]	8650			0.15	43900	649	1590	105

[a] *rac*-isomer = 16.7%, *meso*-isomer = 83.3%. [b] Polymerization (sampling) time. [c] Yield of whole polymer (kg polypropene/mol Zr). [d] Number-average molecular weight and molecular weight distribution of whole polymer determined by GPC. [e] Weight fraction of atactic polymer. [f] Yield of isotactic polymer (Y_i) and atactic polymer (Y_a) (kg polypropene/mol Zr). [g] Number of isotactic (N_i) and atactic (N_a)polymer chains (mol polypropene/mol Zr). [h] Isotactic polypropene: M_{ni} = 67700, M_{wi}/M_{ni} = 2.9; atactic polypropene: M_{na} = 15100, M_{wa}/M_{na} = 2.7.

The amounts of polymers sampled during the polymerization were too small to be fractionated. GPC curves of polypropenes obtained using MAO as cocatalyst are displayed in Figure 3-1. The GPC curves of the sampled polypropenes showed bimodal distribution, which corresponded to isotactic and atactic fractions produced by *rac*- and *meso*-isomer, respectively. The increase of atactic fraction was observed with the increase of polymerization time as shown in Figure 3-1. However, the elution time of each peak top did not change during the polymerization and agreed well with the curves of fractionated polymers finally obtained. Therefore, weight fraction of the atactic polymer (W_a) can be calculated from the GPC curves as follows on the assumption that M_n and M_w/M_n of the each fraction do not change during the polymerization.

$$M_n = \sum_{j=0}^{\infty} M_j N_j / \sum_{j=0}^{\infty} N_j = \sum_{j=0}^{\infty} (M_j N_{ij} + M_j N_{aj}) / \sum_{j=0}^{\infty} (N_{ij} + N_{aj})$$

$$= \left(\sum_{j=0}^{\infty} M_j N_{ij} / \sum_{j=0}^{\infty} N_{ij}\right) \cdot \left[\sum_{j=0}^{\infty} N_{ij} / \sum_{j=0}^{\infty} (N_{ij} + N_{aj})\right] + \left(\sum_{j=0}^{\infty} M_j N_{aj} / \sum_{j=0}^{\infty} N_{aj}\right) \cdot \left[\sum_{j=0}^{\infty} N_{aj} / \sum_{j=0}^{\infty} (N_{ij} + N_{aj})\right] \quad (1)$$

where M_n, M_j, N_j, N_{ij}, and N_{aj} are number-average molecular weight of whole polymer, molecular weight of fraction j in the whole polymer, a total number of polymer chains in fraction j, a number of isotactic and atactic polymer chains in fraction j, respectively. The equation (1) can be further developed to equation (2).

$$M_n = M_{ni} \cdot N_i/(N_i + N_a) + M_{na} \cdot N_a/(N_i + N_a) \quad (2)$$

where N_i and N_a are, respectively, numbers of isotactic and atactic polymer chains. The values of M_{ni} and M_{na} were determined from the finally quenched polymer in the series of polymerizations, and could be constant through the polymerization as described above. The weight fraction of the atactic polymer (W_a), yield of isotactic polymer (Y_i) and atactic polymer (Y_a) are determined by the following equations:

$$W_a = M_{na} \cdot N_a/(M_{ni} \cdot N_i + M_{na} \cdot N_a) \quad (3)$$

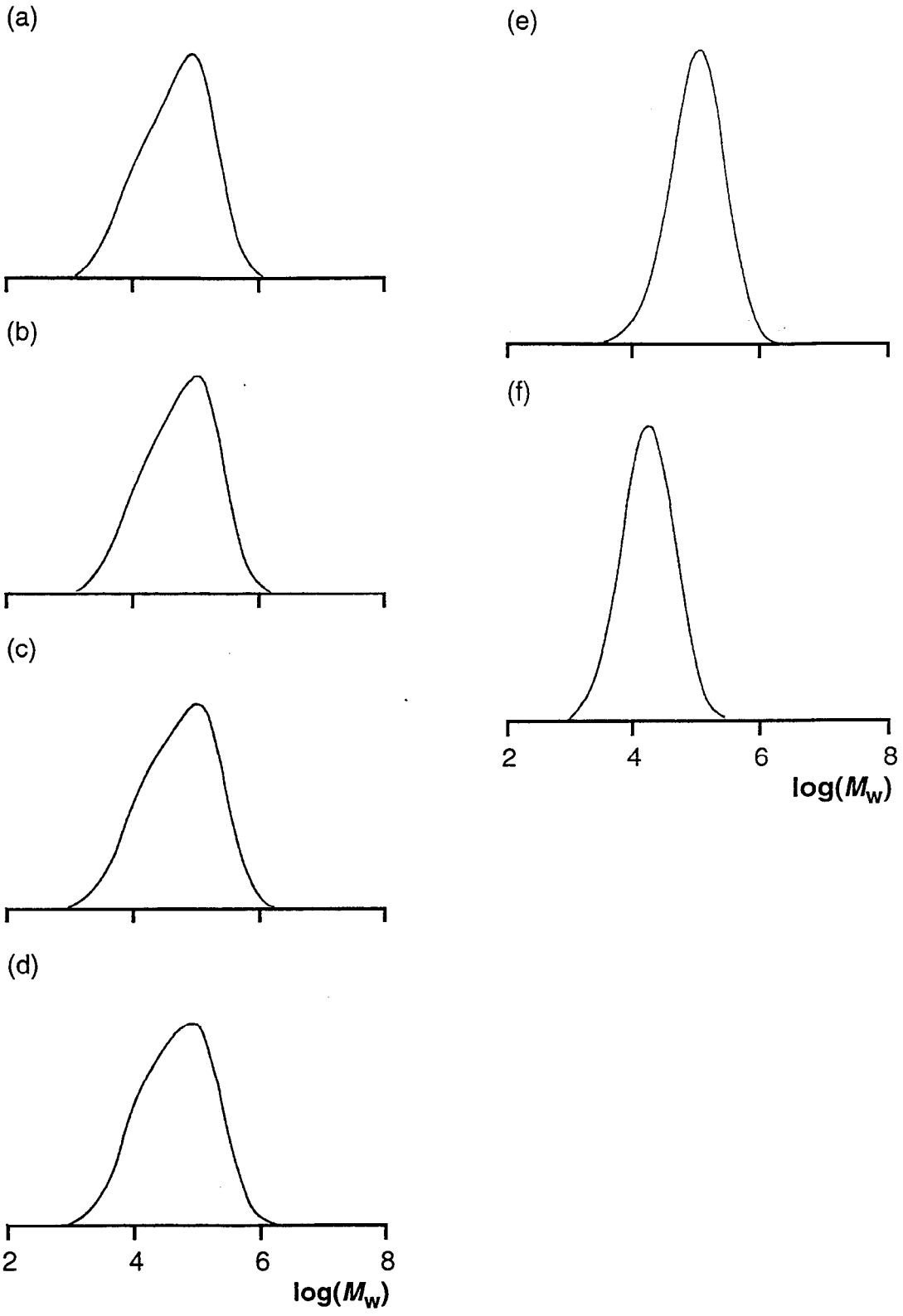

Figure 3-1. GPC curves of polypropenes obtained with mixture of *rac*- and *meso*-$Me_2Si(2\text{-}MeInd)_2ZrCl_2$–MAO: (a) 5 min, (b) 10 min, (c) 30 min, (d) 45 min, (e) isotactic fraction, (f) atactic fraction.

$$Y_i = Y(1\text{-}W_a)/0.167 \quad (4)$$

$$Y_a = YW_a/0.833 \quad (5)$$

where Y is yield of whole polymer calculated from the amount of propene consumed during the polymerization.

Polymerization rate at polymerization time t ($t = (t_1 + t_2)/2$) is determined by the following equation:

$$R_p = (Y_{t2} - Y_{t1})/(t_2 - t_1) \quad (6)$$

where Y_{t1} and Y_{t2} are yield of polypropene at polymerization time of t_1 and t_2. The R_p values thus obtained are summarized in Table 3-7, and the plots of R_p against polymerization time with MAO, $AlEt_3/Ph_3CB(C_6F_5)_4$, and $Al\textit{i}Bu_3/Ph_3CB(C_6F_5)_4$ are displayed in Figures 3-2, 3-3 and 3-4, respectively. It took about 10 min to reach the maximum R_p, and then R_p gradually decreased in the case of using MAO with both *rac*-isomer and *meso*-isomer (Figure 3-2 (a), (b)). The R_p of *rac*-isomer and *meso*-isomer with $AlEt_3/Ph_3CB(C_6F_5)_4$ reached to the maximum value within 5 min and dropped rapidly (Figure 3-3 (a), (b)). In the case of using $Al\textit{i}Bu_3/Ph_3CB(C_6F_5)_4$, short induction time was observed to reach the maximum R_p with *rac*-isomer followed by gradual decay of R_p (Figure 3-3 (a)). On the other hand, R_p showed the maximum value at the initial stage for about 10 min, and then rapidly decreased in the polymerization profile with *meso*-isomer (Figure 3-3 (b)).

$R_p(rac)$ and $R_p(meso)$ can be expressed by the following equations:

$$R_p(rac) = k_p(rac)[M]^a[C^*]_{rac} \quad (7)$$

$$R_p(meso) = k_p(meso)[M]^a[C^*]_{meso} \quad (8)$$

where $k_p(rac)$, $k_p(meso)$, [M], a, $[C^*]_{rac}$, and $[C^*]_{meso}$ are, respectively, rate constants of propagation in *rac*-isomer and *meso*-isomer, monomer concentration, reaction order, number of active centers in *rac*-isomer and *meso*-isomer. There are two possibilities for the change of R_p

Table 3-7. Data of R_p values in propene polymerization with *rac*- and *meso*-$Me_2Si(2\text{-}MeInd)_2ZrCl_2$[a]

	MAO			$AlEt_3/Ph_3CB(C_6F_5)_4$			$Ali Bu_3/Ph_3CB(C_6F_5)_4$		
t (min)	$R_p(rac)$	$R_p(meso)$	$R_p(rac)/R_p(meso)$	$R_p(rac)$	$R_p(meso)$	$R_p(rac)/R_p(meso)$	$R_p(rac)$	$R_p(meso)$	$R_p(rac)/R_p(meso)$
1.0							33600	4820	7.0
2.5	1120	93.4	12.0	4490	126	35.7			
3.5							115000	4600	17.6
7.5	4830	425	11.4	2860	36.0	79.4	99900	5030	19.9
12.5	5160	511	10.1	2590	25.1	103	100000	4630	21.6
17.5	3900	439	9.0	2330	21.6	108	78700	2030	38.8
25.0	3720	505	7.4	2090	20.0	105	74700	1350	55.3
37.5	2990	428	7.0	504	6.3	79.7			
52.5	3030	370	8.2						

[a] $R_p(rac)$, $R_p(meso)$: rate of polymerization with *rac*-isomer and *meso*-isomer (kg polypropene/mol Zr·h).

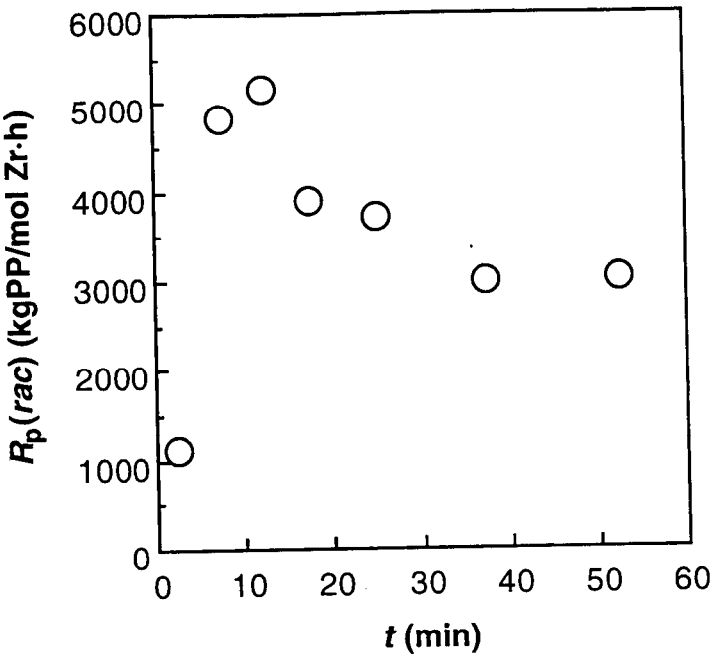

Figure 3-2(a). Polymerization profile of propene with *rac*-$Me_2Si(2\text{-}MeInd)_2ZrCl_2$–MAO.

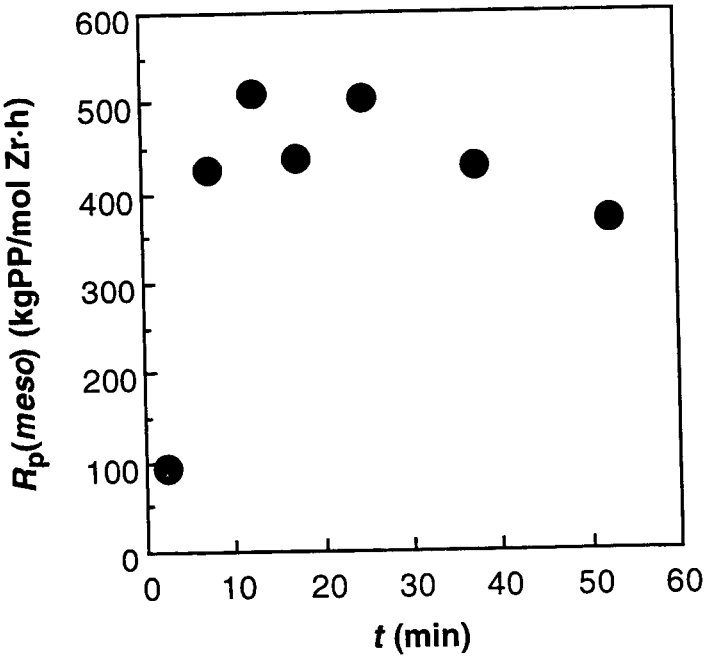

Figure 3-2(b). Polymerization profile of propene with *meso*-$Me_2Si(2\text{-}MeInd)_2ZrCl_2$–MAO.

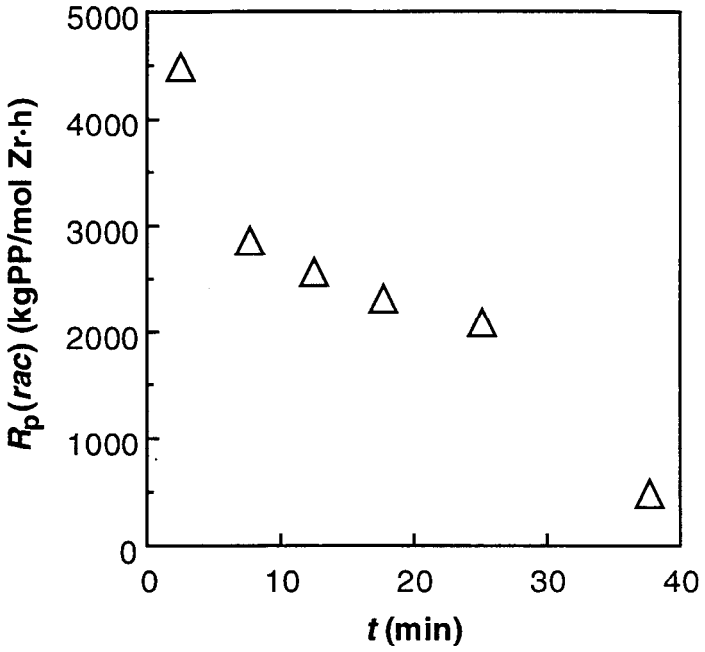

Figure 3-3(a). Polymerization profile of propene with *rac*-$Me_2Si(2\text{-}MeInd)_2ZrCl_2$–$AlEt_3/Ph_3CB(C_6F_5)_4$.

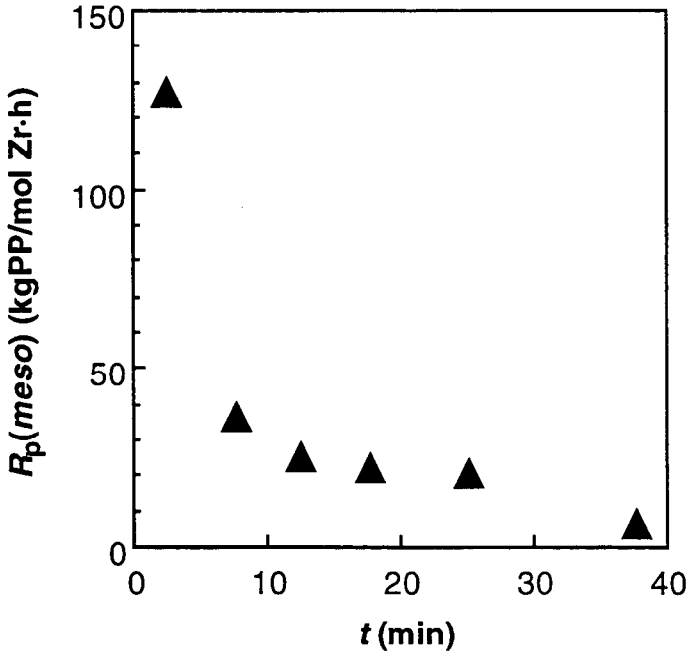

Figure 3-3(b). Polymerization profile of propene with *meso*-$Me_2Si(2\text{-}MeInd)_2ZrCl_2$–$AlEt_3/Ph_3CB(C_6F_5)_4$.

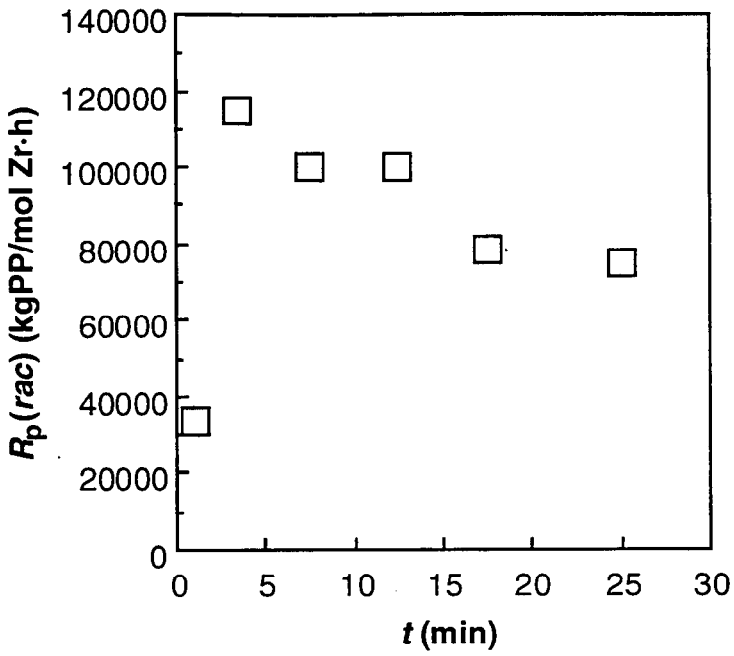

Figure 3-4(a). Polymerization profile of propene with *rac*$Me_2Si(2\text{-}MeInd)_2ZrCl_2$–Al*i*$Bu_3/Ph_3CB(C_6F_5)_4$.

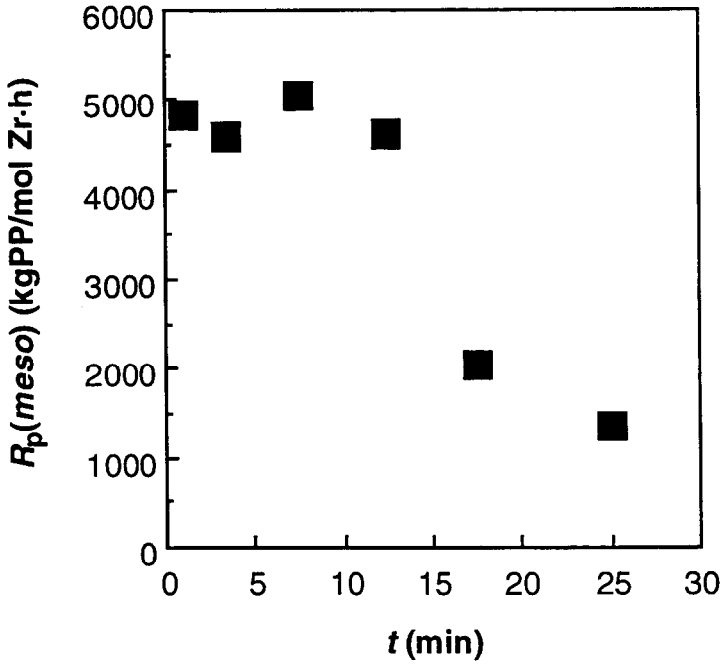

Figure 3-4(b). Polymerization profile of propene with *meso*-$Me_2Si(2\text{-}MeInd)_2ZrCl_2$–Al*i*$Bu_3/Ph_3CB(C_6F_5)_4$.

during the polymerization. One is the change of k_p value and the other is the change of [C*] value. If the k_p value could change, it is plausible that the M_n value also changes during the polymerization. As mentioned above, the M_n values were almost independent of the polymerization time in the present polymerizations. Therefore, it seems reasonable to suppose that the change of R_p is due to the change of [C*].

Several methods have been applied to determine the [C*] value in olefin polymerization with metallocene catalysts.[19] In this study, the author roughly estimated the [C*] by a typical kinetic method with the following equations[20]:

before the maximum R_p

$$M_n = \int k_p[M][C^*]_t dt / \{[C^*]_t + \int (k_{tr} + k_{trA}[Al] + k_{trM}[M])[C^*]_t dt\} \quad (9)$$

$$1/M_n = [C^*]_t/Y + (k_{tr} + k_{trA}[Al] + k_{trM}[M])/k_p[M] \quad (10)$$

$$N = Y/M_n = [C^*]_t + (k_{tr} + k_{trA}[Al] + k_{trM}[M]) \cdot Y/k_p[M] \quad (11)$$

after the maximum R_p

$$M_n = \int k_p[M][C^*]_t dt / \{[C^*]_{max} + \int (k_{tr} + k_{trA}[Al] + k_{trM}[M])[C^*]_t dt\} \quad (12)$$

$$1/M_n = [C^*]_{max}/Y + (k_{tr} + k_{trA}[Al] + k_{trM}[M])/k_p[M] \quad (13)$$

$$N = Y/M_n + (k_{tr} + k_{trA}[Al] + k_{trM}[M]) \cdot Y/k_p[M] \quad (14)$$

where $[C^*]_t$ and $[C^*]_{max}$ are numbers of active centers at polymerization time = t and maximum R_p, k_{tr}, k_{trA}, and k_{trM} are rate constants of chain transfer by β-hydrogen elimination, alkylaluminum, and propene monomer, [Al] is concentration of AlR_3, Y is yield of polypropene, respectively. From the plots of N against Y, [C*] values of *rac*-$Me_2Si(2\text{-}MeInd)_2ZrCl_2$ could be determined at maximum R_p with MAO and Al*i*$Bu_3/Ph_3CB(C_6F_5)_4$ by the equation (11), and at $Y = 0$ ($t = 0$) with $AlEt_3/Ph_3CB(C_6F_5)_4$ by the equation (14). The [C*] values are 0.086 mol/mol with MAO, 0.54 mol/mol with $AlEt_3/Ph_3CB(C_6F_5)_4$, and 0.24 mol/mol with Al*i*$Bu_3/Ph_3CB(C_6F_5)_4$, respectively. These values are lower than the [C*] values previously reported in propene polymerization determined by another method.[19b,d] This difference may be due to the induction time to produce the maximum [C*]. The [C*]

values of *meso*-$Me_2Si(2\text{-}MeInd)_2ZrCl_2$ could not be determined because the [C*] value was too small.

It was found that $R_p(rac)/R_p(meso)$ values with *rac*- and *meso*-$Me_2Si(2\text{-}MeInd)_2ZrCl_2$ decreased in the following order according to the combined cocatalysts: $AlEt_3/Ph_3CB(C_6F_5)_4$ (36–108) > $Al\textit{i}Bu_3/Ph_3CB(C_6F_5)_4$ (7.0–55) > MAO (8.2–12). In the results with *rac*- and *meso*-$Me_2Si(2,3,5\text{-}Me_3Cp)_2ZrCl_2$, the $R_p(rac)/R_p(meso)$ values decreased in the following order: MAO (3.0–3.6) > $AlEt_3/Ph_3CB(C_6F_5)_4$ (0.5–1.0) > $Al\textit{i}Bu_3/Ph_3CB(C_6F_5)_4$ (0.4) (Table 3-1). Although the polymerization conditions are slightly different among these polymerizations with $Me_2Si(2\text{-}MeInd)_2ZrCl_2$ and $Me_2Si(2,3,5\text{-}Me_3Cp)_2ZrCl_2$, the comparison would make sense. Therefore, the results of propene polymerization with these catalysts are discussed in more detail. The difference among these catalysts could be found especially when MAO was used. In the polymerization with $Me_2Si(2\text{-}MeInd)_2ZrCl_2$, the lower values of $R_p(rac)/R_p(meso)$ were observed using MAO than using $AlR_3/Ph_3CB(C_6F_5)_4$. On the other hand, the opposite tendency was observed in the polymerization with $Me_2Si(2,3,5\text{-}Me_3Cp)_2ZrCl_2$. Furthermore, the $R_p(rac)/R_p(meso)$ values with $Me_2Si(2\text{-}MeInd)_2ZrCl_2$ were higher than those with $Me_2Si(2,3,5\text{-}Me_3Cp)_2ZrCl_2$ combined with any kinds of cocatalysts. These differences may be derived from the steric effect between (2-MeInd) and (2,3,5-Me_3Cp) ligands. It seems hard to activate the *meso*-bis(indenyl) type *ansa*-zirconocene, especially by MAO, due to the steric hindrance of site-A in Scheme 3-1.

3-3B-2. Polymerization of 1-Butene and 1-Hexene with $Me_2Si(2\text{-}MeInd)_2ZrCl_2$

Polymerization of 1-butene with the mixture of *rac*- and *meso*-$Me_2Si(2\text{-}MeInd)_2ZrCl_2$ was conducted using three cocatalysts at 40 °C in a 200 mL autoclave. The results are summarized in Table 3-8. Atactic and isotactic poly(1-butene)s were separated according to the Experimental Part. The polymerization activity and M_n of the polymer obtained with combined cocatalysts showed the same tendency observed in the propene polymerization, and decreased in the following order: $Al\textit{i}Bu_3/Ph_3CB(C_6F_5)_4$ > MAO > $AlEt_3/Ph_3CB(C_6F_5)_4$. The $R_p(rac)/R_p(meso)$ values decreased in the same order of the propene polymerization:

Table 3-8. Results of 1-butene polymerization with *rac*- and *meso*-$Me_2Si(2\text{-}MeInd)_2ZrCl_2$[a]

Run	Catalyst (μmol)	Co-catalyst[b]	t[c] (min)	Yield (g)	R_p[d]	W_a[e]	$R_p(rac)$[f]	$R_p(meso)$[f]	$R_p(rac)/R_p(meso)$	M_{ni}[g] ($\times10^{-4}$)	M_{wi}/M_{ni}[g]	M_{na}[h] ($\times10^{-4}$)	M_{wa}/M_{na}[h]
18	2.0	MAO	60	1.94	970	0.46	3140	534	5.9	7.2	2.6	1.2	2.4
19	2.0	$AlEt_3$/TB	180	0.36	59.4	0.15	301	10.9	27.6	3.9	2.4	1.3	1.9
20	1.0	Al*i*Bu_3/TB	60	2.34	2340	0.22	10100	603	18.2	25.1	2.9	2.4	2.4

[a] *rac*-isomer = 16.7%, *meso*-isomer = 83.3%. [b] Molar ratio of (MAO)Al/Zr = 1000, molar ratio of ($AlEt_3$, Al*i*Bu_3)Al/Zr = 500, TB = $Ph_3CB(C_6F_5)_4$, molar ratio of B/Zr = 1.0. [c] Polymerization time. [d] Rate of polymerization (kg poly(1-butene)/mol Zr·h). [e] Weight fraction of atactic polymer. [f] Rate of polymerization with *rac*-isomer ($R_p(rac)$) and *meso*-isomer ($R_p(meso)$) (kg poly(1-butene)/mol Zr·h). [g,h] Number-average molecular weight and molecular weight distribution of isotactic and atactic polymer determined by GPC.

Table 3-9. Results of 1-hexene polymerization with *rac*- and *meso*-$Me_2Si(2\text{-}MeInd)_2ZrCl_2$[a]

Run	Catalyst (μmol)	Co-catalyst[b]	t[c] (min)	Yield (g)	R_p[d]	W_a[e]	$R_p(rac)$[f]	$R_p(meso)$[f]	$R_p(rac)/R_p(meso)$	M_n[g] ($\times10^{-4}$)	M_w/M_n[g]
21	2.0	MAO	60	0.96	480	0.06	2700	33.6	80.5	1.3	4.2
22	2.0	$AlEt_3$/TB	180	0.09	14.3	0.05	81.7	0.8	98.9	0.9	3.2
23	2.0	Al*i*Bu_3/TB	60	0.62	311	0.03	1810	11.2	161	3.6	7.3

[a] *rac*-isomer = 16.7%, *meso*-isomer = 83.3%. [b] Molar ratio of (MAO)Al/Zr = 1000, molar ratio of ($AlEt_3$, Al*i*Bu_3)Al/Zr = 500, TB = $Ph_3CB(C_6F_5)_4$, molar ratio of B/Zr = 1.0. [c] Polymerization time. [d] Rate of polymerization (kg poly(1-hexene)/mol Zr·h). [e] Weight fraction of atactic polymer determined by ^{13}C NMR spectroscopy. [f] Rate of polymerization with *rac*-isomer ($R_p(rac)$) and *meso*-isomer ($R_p(meso)$) (kg poly(1-hexene)/mol Zr·h). [g] Number-average molecular weight and molecular weight distribution of whole polymer determined by GPC.

$AlEt_3/Ph_3CB(C_6F_5)_4$ > $Al\textit{i}Bu_3/Ph_3CB(C_6F_5)_4$ > MAO. It seems reasonable to suppose that alkyl groups of propene and 1-butene, methyl and ethyl, do not affect the polymerization behaviors with *rac*- and *meso*-$Me_2Si(2\text{-}MeInd)_2ZrCl_2$.

Polymerization of 1-hexene with the mixture of *rac*- and *meso*-$Me_2Si(2\text{-}MeInd)_2ZrCl_2$ combined with three cocatalysts were also conducted at 40 °C in a 200 mL glass reactor. The results are summarized in Table 3-9. Higher activity was observed with MAO than with $Al\textit{i}Bu_3/Ph_3CB(C_6F_5)_4$. The same tendency was observed in the 1-hexene polymerization with $Me_2Si(2,3,5\text{-}Me_3Cp)_2ZrCl_2$. Weight fraction of atactic poly(1-hexene) was determined from a ^{13}C NMR spectrum of the whole polymer as mentioned in the Experimental Part. The point about the polymerization of 1-hexene is remarkably higher values of $R_p(rac)/R_p(meso)$ (about 80–160) than those of propene and 1-butene polymerizations independent of cocatalysts used. This result might indicate that the site-A of *meso*-$Me_2Si(2\text{-}MeInd)_2ZrCl_2$ is too sterically hindered for 1-hexene to coordinate it (Scheme 3-2). This result supports the mechanism of alternating copolymerization of ethene and 1-octene with *meso*-$Me_2Si(2\text{-}MeInd)_2ZrCl_2$, which was proposed by Soga *et al.*[13] On the other hand, remarkable difference in $R_p(rac)/R_p(meso)$ values among the α-olefins (propene, 1-butene, and 1-hexene) could not be observed in the polymerization with the mixture of *rac*- and *meso*-$Me_2Si(2,3,5\text{-}Me_3Cp)_2ZrCl_2$.

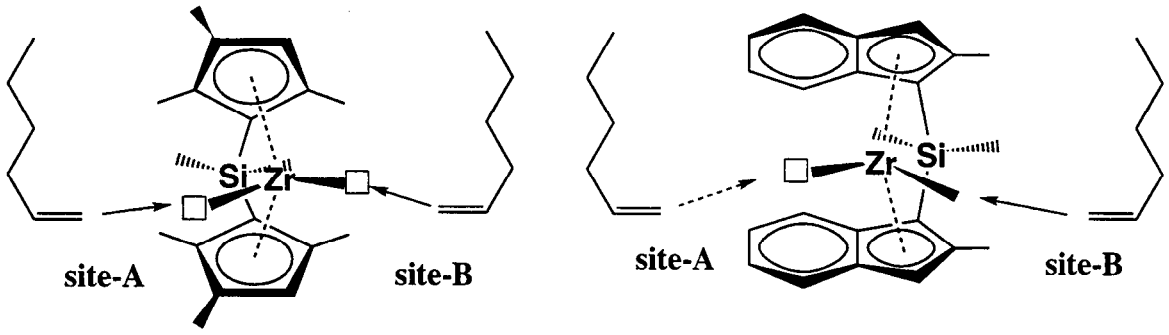

***meso*-$Me_2Si(2,3,5\text{-}Me_3Cp)_2ZrCl_2$** ***meso*-$Me_2Si(2\text{-}MeInd)_2ZrCl_2$**

Scheme 3-2. Proposed models of 1-hexene coordination to *meso*-type *ansa*-zirconocenes.

3-4. Summary

Effect of cocatalysts on α-olefin polymerization with *rac*- and *meso*-isomers of *ansa*-zirconocene catalysts was studied. When the polymerizations were conducted with $Me_2Si(2,3,5\text{-}Me_3Cp)_2ZrCl_2$, higher $R_p(rac)/R_p(meso)$ values were observed using MAO than using $AlR_3/Ph_3CB(C_6F_5)_4$. On the other hand, the opposite result was observed in the polymerization with $Me_2Si(2\text{-}MeInd)_2ZrCl_2$. This result could be derived from the difference in the bulkiness of zirconocene ligands. Remarkably high $R_p(rac)/R_p(meso)$ values in the 1-hexene polymerization with $Me_2Si(2\text{-}MeInd)_2ZrCl_2$ indicated that coordination of 1-hexene to the *meso*-isomer was disturbed due to the steric hindrance in the Site-A.

References

(1) (a) Jordan, R. F.; Bajgur, C. S.; Willett, R.; Scotto, B. *J. Am. Chem. Soc.* **1986**, *108*, 7410. (b) Jordan, R. F.; LaPointe, R. E.; Bajgur, C. S.; Echols, S. F.; Willett, R. *J. Am. Chem. Soc.* **1987**, *109*, 4111. (c) Jordan, R. F.; LaPointe, R. E.; Bradley, P. K.; Baenziger, N. *Organometallics* **1989**, *8*, 2892. (d) Jordan, R. F.; Bradley, P. K.; LaPointe, R. E. *J. Am. Chem. Soc.* **1990**, *112*, 1289. (e) Jordan, R. F.; LaPointe, R. E.; Baenziger, N. C.; Hinch, G. D. *Organometallics* **1990**, *9*, 1539. (f) Borkowsky, S. L.; Jordan, R. F.; Hinch, G. D. *Organometallics* **1989**, *10*, 1268.

(2) (a) Hlatky, G. G.; Turner, H. W.; Eckman, R. R. *J. Am. Chem. Soc.* **1989**, *111*, 2357. (b) Zambelli, A.; Longo, P.; Grassi, A. *Macromolecules* **1989**, *22*, 2186. (c) Longo, P.; Oliva, L.; Grassi, A.; Pellecchia, C. *Makromol. Chem.* **1989**, *190*, 2357. (d) Hlatky, G. G.; Eckman, R. R.; Turner, H. W. *Organometallics* **1992**, *11*, 1413. (e) Yang, X.; Stern, C. L.; Marks, T. J. *Angew. Chem., Int. Ed. Engl.* **1992**, *31*, 1375. (f) Eshuis, J. J. W.; Tan, Y. Y.; Meetsma, A.; Teuben, J. H. *Organometallics* **1992**, *11*, 362. (g) Yang, X.; Stern, C. L.; Marks, T. J. *J. Am. Chem. Soc.* **1994**, *116*, 10015. (h) Guo, Z.; Swenson, D. C.; Jordan, R. F. *Organometallics* **1994**, *13*, 1424.

(3) (a) Chien, J. C. W.; Tsai, W. M.; Rausch, M. D. *J. Am. Chem. Soc.* **1991**, *113*, 8570. (b) Chien, J. C. W.; Song, W.; Rausch, M. D. *Macromolecules* **1993**, *26*, 3239. (c) Tsai, M. W.; Rausch, M. D.; Chien, J. C. W. *Appl. Organomet. Chem.* **1993**, *7*, 71.

(4) (a) Horton, A. D.; Frijns, J. H. G. *Angew. Chem., Int. Ed. Engl.* **1991**, *30*, 1152. (b) Herfert, N.; Fink, G. *Makromol. Chem., Rapid Commun.* **1993**, *14*, 91. (c) Chien, J. C. W.; Song, W.; Rausch, M. D. *J. Polym. Sci., Part A: Polym. Chem.* **1994**, *32*, 2387. (d) Bochmann, M.; Lancaster, S. J. *Angew. Chem., Int. Ed. Engl.* **1994**, *33*, 1634. (e) Uchida, O.; Takeuchi, K.; Sugimoto, R. In *Science and Technology in Catalysis 1994*; Kodansha Ltd: Tokyo, 1995; p 367. (f) Bochmann, M.; Lancaster, S. J. *J. Organomet. Chem.* **1995**, *497*, 55. (g) Dagorne, S.; Rodewald, S.; Jordan, R. F. *Organometallics* **1997**, *16*, 5541. (h) Hahn, S.; Fink, G. *Macromol. Rapid Commun.* **1997**, *18*, 117. (i) Beck, S.; Brintzinger, H. H.; Suhm, J.; Mülhaupt, R. *Macromol. Rapid Commun.* **1998**, *19*, 235.

(5) Kaminsky, W.; Külper, K.; Brintzinger, H. H.; Wild, F. R. W. P. *Angew. Chem., Int. Ed. Engl.* **1985**, *24*, 507.

(6) Mise, T.; Miya, S.; Yamazaki, H. *Chem. Lett.* **1989**, 1853.

(7) Spaleck, W.; Küber, F.; Winter, A.; Rohrmann, J.; Bachmann, B.; Antberg, M.; Dolle, V.; Paulus, E. F. *Organometallics* **1994**, *13*, 954.

(8) Kaminsky, W.; Rabe, O.; Schauwienold, A. M.; Schupfner, G. C.; Hanss, J.; Kopf, J. *J. Organomet. Chem.* **1995**, *497*, 181.

(9) (a) Collins, S.; Gauthier, W. J.; Holden, D. A.; Kuntz, B. A.; Taylor, N. J.; Ward, D. G. *Organometallics* **1991**, *10*, 2061. (b) Piemontesi, F.; Camurati, I.; Resconi, L.; Balboni, D.; Moret, M.; Zeigler, R.; Piccolrazavi, N. *Organometallics* **1995**, 14, 1256.

(10) (a) Resconi, L.; Piemontesi, F.; Camurati, I.; Balboni, D.; Sironi, A.; Moret, M.; Rychlicki, H.; Zeigler, R. *Organometallics* **1996**, *15*, 5046. (b) Könemann, M.; Erker, G.; Fröhlich, R.; Kotila, S. *Organometallics* **1997**, *16*, 2900. (c) Luttikhedde, H. J. G.; Leino, R.; Ahlgén, M. J.; Pakkanen, T. A.; Nsman, J. H. *J. Organomet. Chem.* **1998**, *557*, 227.

(11) Kaminsky, W.; Schauwienold, A. M.; Freidanck, F. *J. Mol. Catal. A: Chem.* **1996**, *112*, 37.

(12) Petoff, J. L. M.; Agoston, T.; Lal, T. K.; Waymouth, R. M. *J. Am. Chem. Soc.* **1998**, *120*, 11316.

(13) Uozumi, T.; Miyazawa, K.; Sano, T.; Soga, K. *Macromol. Rapid Commun.* **1997**, *18*, 883.

(14) Spaleck, W.; Antberg, M.; Rohrmann, J.; Winter, A.; Bachmann, B.; Kiprof, P.; Behm, J.; Herrmann, W. A. *Angew. Chem., Int. Ed. Engl.* **1992**, *31*, 1347.

(15) Mauzac, M.; Vairon, J. P.; Sigwalt, P. *Polymer* **1977**, *18*, 1193.

(16) Ouano, A. C.; Mereier, P. L. *J. Polym. Sci., Part C* **1968**, *21*, 309.

(17) Asakura, T.; Demura, M.; Nishiyama; Y. *Macromolecules* **1991**, *24*, 2334.

(18) Soga, K.; Lee, D. H.; Morikawa, Y. *Polymer* **1992**, *33*, 2408.

(19) (a) Tait, P. J. T.; Booth, B. L.; Jejelowo, M. O. *Macromol. Rapid Commun.* **1998**, *9*, 393. (b) Chien, J. C. W.; Wang, B. P. *J. Polym. Sci., Part A: Polym. Chem.* **1990**, *28*, 15. (c) Chien, J. C. W.; Sugimoto, R. *J. Polym. Sci., Part A: Polym. Chem.* **1991**, *29*, 459. (d) Chien, J. C. W.; Tsai, W. M. *Makromol. Chem., Macromol. Symp.* **1993**, *66*, 141. (e) Shiono, T.; Ohgizawa, M.; Soga, K. *Polymer* **1994**, *35*, 187. (f) Han, T. K.; Ko, Y. S.; Park, J. W.; Woo, S. I. *Macromolecules* **1996**, *29*, 7305.

(20) Tsutsui, T.; Kashiwa, N. *Polymer* **1988**, *29*, 180.

Chapter 4

Chain Transfer Reaction by Trialkylaluminum in Stereospecific Polymerization of Propene with Zirconocene Catalysts

4-1. Introduction

End group analysis of polymer provides important insight into the chain transfer reaction in Ziegler–Natta polymerization. Four kinds of chain transfer reactions have been observed in propene polymerization with metallocene catalysts (Scheme 4-1). The first chain transfer reaction is β-hydrogen transfer to the metal.[1–9] This reaction produces vinylidene groups at the terminated chain end and *n*Pr groups at the initiated chain end. The second chain transfer reaction is β-hydrogen transfer to the monomer.[4,6,8,10] The same chain end groups derived from β-hydrogen transfer to the metal are formed through this reaction. The chain end structure of the 2-butenyl group, which was derived from the β-hydrogen transfer after secondary insertion, was also observed.[11,12] The third chain transfer reaction is β-methyl elimination.[13–23] The chain end structure of a vinyl group is formed through the β-methyl elimination. The fourth chain transfer reaction is chain transfer to aluminum.[7,17,24–26] In the case of using MAO, this chain transfer reaction occurred at lower polymerization temperature or lower propene concentration. In the case of using AlR_3 (without MAO), chain transfer to the aluminum was determined by the chain end analysis of resulting polypropenes. Zambelli *et al.* carried out the polymerization of propene with *rac*-$Et(Ind)_2ZrCl_2$–$Al(CH_3)_2F$/$AlMe_3$ and observed a chain transfer process to $AlMe_3$ by the chain end structures of resulting polypropene.[24] Soga *et al.* investigated the polymerization of propene with supported metallocene catalysts (for example *rac*-$Et(Ind)_2ZrCl_2/Al_2O_3$) activated by common AlR_3 and reported the chain transfer to AlR_3.[26] Only a few investigations have been reported about the effect of AlR_3 concentration on the stereospecific polymerization of propene. Bochmann *et al.* studied the effect of $AlMe_3$ concentration on the propene polymerization with *rac*-$[Me_2Si(Ind)_2Zr(\mu\text{-}Me)_2AlMe_2]$–$B(C_6F_5)_4$/$AlMe_3$, *rac*-$Me_2Si(Ind)_2ZrMe_2$–$Ph_3CB(C_6F_5)_4$/$AlEt_3$, and observed decrease of molecular weight of the resulting polypropene with an increase in the AlR_3 concentration.[27,28] Uchida *et al.* also reported the stereospecific polymerization of propene with zirconocene catalysts combined with $AlR_3/Ph_3CB(C_6F_5)_4$ and a great deal of effort was made to determine the effect of AlR_3 concentration on the catalytic activity.[29]

1. β-Hydrogen transfer to the metal

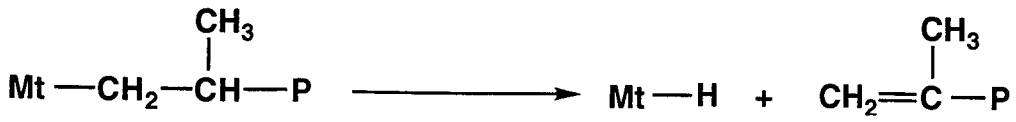

2. β-Hydrogen transfer to the monomer

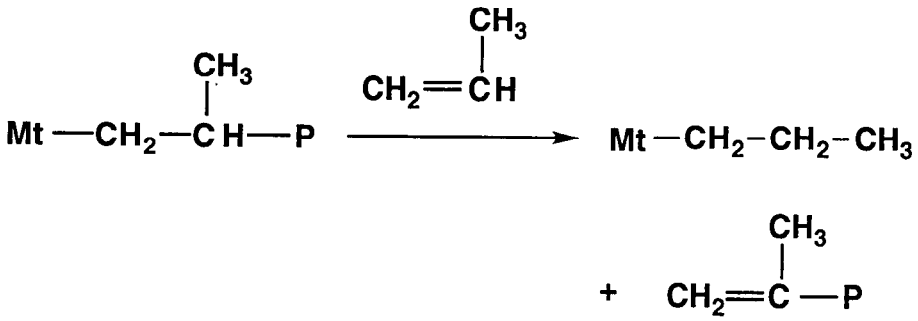

3. β-Methyl elimination

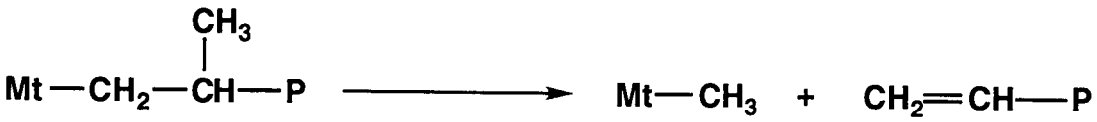

4. Chain transfer to AlR_3

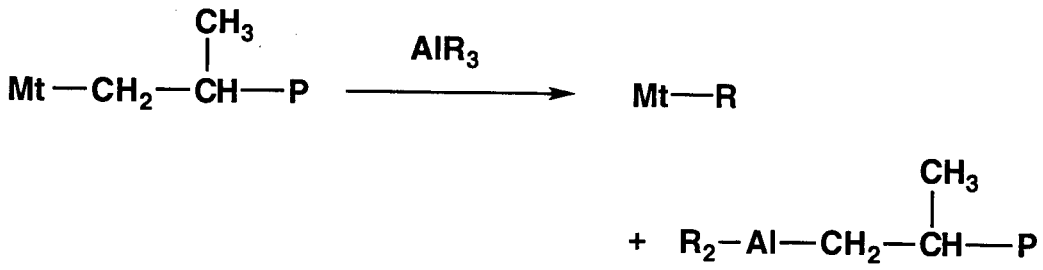

Scheme 4-1. Chain transfer reactions in propene polymerization: Mt = metal, P = polymer chain.

In this work, the author studied the effect of AlR_3 concentration on the molecular weight and the chain end structures of obtained polypropene to characterize the process of chain transfer to AlR_3 ($AlEt_3$ and $Al\textit{i}Bu_3$) in stereospecific (isospecific and syndiospecific) polymerizations of propene with zirconocene–AlR_3/$Ph_3CB(C_6F_5)_4$ catalyst systems.

4-2. Experimental Part

Materials

rac-$Et(Ind)_2ZrCl_2$ and *rac*-$Me_2Si(Ind)_2ZrCl_2$ were commercially obtained from Witco Co., Ltd. and used without further purification. $\textit{i}Pr(Cp)(Flu)ZrCl_2$ was prepared according to the literature.[30] $AlEt_3$, $Al\textit{i}Bu_3$, and MAO were commercially obtained from Tosoh Akzo Co., Ltd. and used without further purification. $Ph_3CB(C_6F_5)_4$ was commercially obtained from Tosoh Akzo Co., Ltd. and used without further purification. Toluene was commercially obtained and dried over molecular sieves 3A.

Polymerization of propene

Polymerizations were conducted in an agitated 1 L autoclave. The autoclave was back-flushed with argon several times, then 300 mL of toluene was injected and the system was warmed to 40 °C. The argon was replaced with 4 kg/cm^{2}G of propene, and the toluene was stirred until the monomer saturation was achieved. A 100 mL glass flask was charged with 10 mL of toluene, AlR_3 and a zirconocene catalyst, and the mixture was stirred for 5 min at room temperature in advance. The catalyst solution and toluene solution of $Ph_3CB(C_6F_5)_4$ were added to start the polymerization. In the polymerization with MAO, MAO was used instead of AlR_3 and the polymerization was started without $Ph_3CB(C_6F_5)_4$. Termination was carried out by the addition of isobutyl alcohol. After the polymerization, the unreacted monomer was vented and the mixture was quenched with plenty of methanol. The polymer was filtered, washed with methanol and dried in vacuo at 60 °C for 6 h.

Analytical procedure

Molecular weight and MWD of polymers were measured at 145 °C by GPC (Waters 150CV) using *o*-dichlorobenzene as a solvent. M_n was determined by the equation: $M_n = A_n \cdot Q$ (A_n and Q are, respectively, weight-average molecular size (Å) and Q-factor = 26.4 for polypropene).[31] ^{13}C NMR spectra were recorded at 135 °C on a JEOL EX-270 NMR spectrometer operating at 67.8 MHz. Polymers were dissolved in *o*-dichlorobenzene/benzene-d_6 (vol. ratio = 9/1) up to 5 wt %. T_m of polymers were determined by DSC (Perkin-elmer DSC-VII) from the melting endotherm at a heating rate of 5 °C/min after previous heating to 180 °C and cooling to 50 °C by 5 °C/min.

Propene/toluene vapor–liquid equilibrium in the polymerization conditions, at 40 °C and 4 kg/cm^{2}G of propene, was estimated from Soave–Redich–Kwong equation[32] using the ASPEN-PLUS™ program.

4-3. Results and Discussion

4-3-1. Propene Polymerization with Isospecific Catalysts

Isospecific polymerization of propene was conducted with *rac*-Et(Ind)$_2$ZrCl$_2$ and *rac*-Me$_2$Si(Ind)$_2$ZrCl$_2$ combined with AlEt$_3$/Ph$_3$CB(C$_6$F$_5$)$_4$ and Al*i*Bu$_3$/Ph$_3$CB(C$_6$F$_5$)$_4$. The polymerizations using MAO as a cocatalyst were also conducted for references. The polymerization results, together with the molecular weight of polypropenes, are summarized in Tables 4-1 and 4-2. Increase in the molar ratio of AlEt$_3$/Zr resulted in marked decrease of the molecular weight. On the other hand, the molecular weights of polypropenes were independent of the molar ratio of Al*i*Bu$_3$/Zr. These results indicate that chain transfer to AlEt$_3$ occurs frequently, whereas, Al*i*Bu$_3$ does not participate in the chain transfer reaction.

Chain end groups of the polypropenes were detected by ^{13}C NMR spectroscopy to study the chain transfer reaction in more detail. The typical polymer end groups, found in low molecular polypropene produced by ordinary metallocene catalysts, are the vinylidene group resulting from β-hydrogen transfer and the *n*Pr group formed through an insertion of propene into the resulting metal–hydride bond as shown in Scheme 4-2 (a). When the chain transfer to

Table 4-1. Results of propene polymerization with *rac*-Et(Ind)$_2$ZrCl$_2$–AlR$_3$/Ph$_3$CB(C$_6$F$_5$)$_4$ and MAO[a]

Run	Cat.[b] (μmol)	AlR_3	Al/Zr[c]	t[d] (min)	Yield (g)	Activity (kgPP/ mol Zr·h)	M_n[e] (×10^{-4})	M_w/M_n[e]	End group[f] R/*n*Pr
1	3.6	$AlEt_3$	150	60	26.4	7300	3.2	1.9	0.56
2	3.1		250	60	44.7	14400	2.7	2.0	
3	2.9		500	60	25.6	9000	2.7	1.9	
4	3.6		1000	60	11.5	3200	1.8	2.0	1.76
5	1.6	Al*i*Bu$_3$	150	30	44.3	56100	3.8	1.9	
6	1.2		250	30	63.5	102000	3.6	1.9	
7	1.3		500	30	61.0	94400	3.4	2.0	
8	1.1		1000	30	50.0	92900	3.7	1.9	0.00
9	7.4	(MAO)	1000	10	29.2	23600	2.2	2.2	

[a] Polymerization conditions: polymerization temperature = 40 ℃, toluene = 300 mL, propene = 4 kg/cm^{2}G, molar ratio of B/Zr = 1.0. [b] Amount of catalyst. [c] Molar ration of Al/Zr. [d] Polymerization time. [e] Determined by GPC. [f] Molar ratio of R end groups to *n*Pr end groups; R is alkyl group of AlR_3.

Table 4-2. Results of propene polymerization with *rac*-Me$_2$Si(Ind)$_2$ZrCl$_2$–AlR$_3$/Ph$_3$CB(C$_6$F$_5$)$_4$ and MAO[a]

Run	Cat.[b] (μmol)	AlR_3	Al/Zr[c]	t[d] (min)	Yield (g)	Activity (kgPP/ mol Zr·h)	M_n[e] (×10^{-4})	M_w/M_n[e]	End group[f] R/*n*Pr
10	4.7	$AlEt_3$	150	60	20.2	4300	3.4	1.9	0.62
11	4.6		250	60	22.9	4900	2.9	1.9	
12	4.2		500	60	9.3	2200	2.4	2.0	
13	5.1		1000	60	36.0	7000	1.8	2.0	1.25
14	1.7	Al*i*Bu$_3$	250	10	59.3	213000	2.9	1.9	
15	0.71		500	10	46.3	389000	3.2	2.0	
16	0.67		1000	10	40.2	361000	3.2	1.9	0.00
17	0.60	(MAO)	1000	60	4.0	6600	3.9	1.9	

[a] Polymerization conditions: polymerization temperature = 40 ℃, toluene = 300 mL, propene = 4 kg/cm^{2}G, molar ratio of B/Zr = 1.0. [b] Amount of catalyst. [c] Molar ratio of Al/Zr. [d] Polymerization time. [e] Determined by GPC. [f] Molar ratio of R end groups to *n*Pr end groups; R is alkyl group of AlR_3.

(a) β-Hydrogen transfer

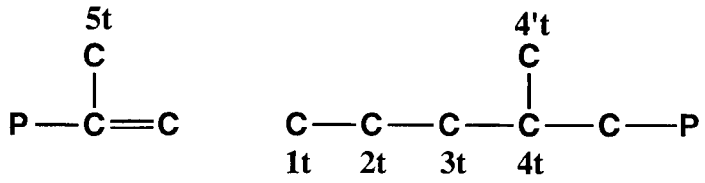

(b) Transfer to $AlEt_3$

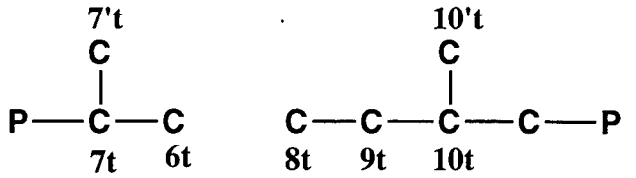

(c) Transfer to $Ali Bu_3$

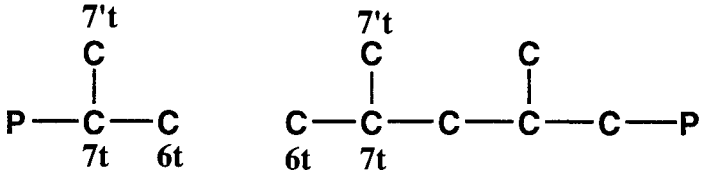

Scheme 4-2. Chain end structures of polypropene: P = polymer chain.

(a) 2,1-Insertion

2,1-(m)

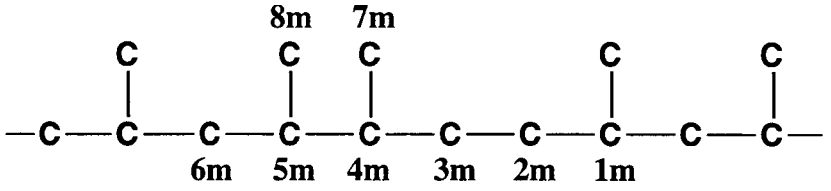

2,1-(r)

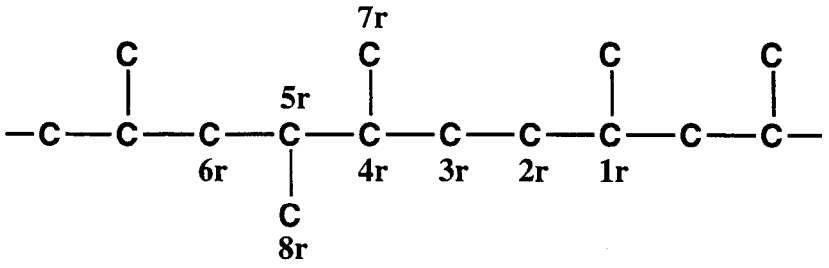

(b) 1,3-Insertion

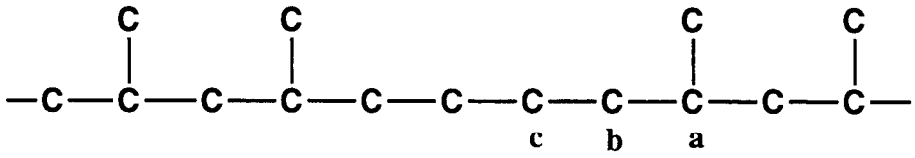

Scheme 4-3. Regio-irregular structures of isotactic polypropene obtained with metallocene catalyst.

$AlEt_3$ occurs, the polymer end groups are *i*Pr group resulting from Al–polymer connection and Et group formed through an insertion of propene into the resulting metal–Et bond as shown in Scheme 4-2 (b). The chain transfer to $AlEt_3$ was detected by Soga *et al.* in the propene polymerization with *rac*-Et(H_4Ind)$_2ZrCl_2$/Al_2O_3–$AlEt_3$ without MAO, and the assignment of the chemical shifts in ^{13}C NMR spectra could be made according to the report.[26] The chain transfer to Al*i*Bu_3 in the propene polymerization produces only an *i*Pr end group resulting from Al–polymer connection and insertion of propene into the metal–*i*Bu bond as shown in Scheme 4-2 (c). The same *i*Pr end group could be formed by the chain transfer to $AlMe_3$. Busico *et al.* reported the chain transfer to $AlMe_3$ (in equilibrium with MAO) in the isospecific polymerization of propene with *rac*-Et(Ind)$_2ZrCl_2$–MAO, and the assignment of chemical shifts in ^{13}C NMR spectrum could be made according to the report.[8] Figure 4-1, (a), (b), and (c), illustrates the ^{13}C NMR spectra of isotactic polypropenes obtained with *rac*-Et(Ind)$_2ZrCl_2$ combined with different cocatalysts. The assignments of chain end structures and

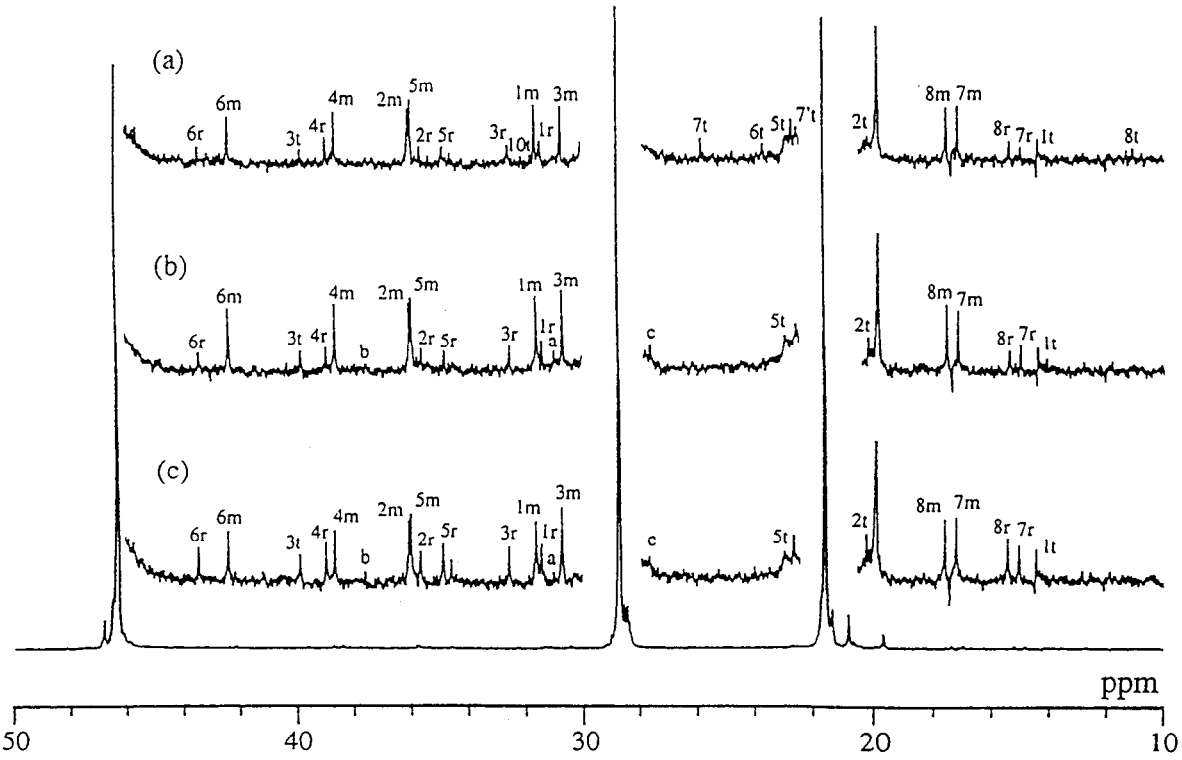

Figure 4-1. ^{13}C NMR spectra of isotactic polypropenes obtained with *rac*-Et(Ind)$_2ZrCl_2$: (a) $AlEt_3/Ph_3CB(C_6F_5)_4$, (b) Al*i*$Bu_3/Ph_3CB(C_6F_5)_4$, (c) MAO.

regioirregular units are shown in Schemes 4-2 and 4-3, respectively. The ^{13}C NMR spectrum of isotactic polypropene obtained with $AlEt_3/Ph_3CB(C_6F_5)_4$ (Figure 4-1 (a)) displays not only the peaks attributable to *n*Pr end groups at *ca.* 14.3 (1t), 20.2 (2t), 39.8 (3t), 22.8 (5t) ppm, but also strong peaks at *ca.* 23.6 (6t), 25.7 (7t) ppm attributable to *i*Pr end groups and at *ca.* 11.1 (8t), 32.8 (10t) ppm attributable to Et end groups derived from the chain transfer to $AlEt_3$. The molar ratio of (Et end groups)/(*n*Pr end groups) was determined from the intensities of corresponding peaks in the ^{13}C NMR spectra . The content of Et end groups was higher than that of *n*Pr end groups in the polypropenes obtained with both *rac*-$Et(Ind)_2ZrCl_2$ and *rac*-$Me_2Si(Ind)_2ZrCl_2$ at the molar ratio of $AlEt_3/Zr = 150$. Higher concentration of Et end groups in comparison with *n*Pr end groups was detected in the polymers obtained at the molar ratio of $AlEt_3/Zr = 1000$. On the other hand, only the peaks attributable to *n*Pr end groups, which were derived from β-hydrogen transfer, were detected in the ^{13}C NMR spectrum of polypropene using Al*i*Bu_3 (Figure 4-1 (b)).

4-3-2. Propene Polymerization with a Syndiospecific Catalyst

Syndiospecific polymerization of propene was carried out with *i*Pr(Cp)(Flu)$ZrCl_2$ combined with $AlR_3/Ph_3CB(C_6F_5)_4$. The results are listed in Table 4-3. Decrease of the molecular weight of polypropenes was observed with an increase in the molar ratio of $AlEt_3/Zr$ and Al*i*Bu_3/Zr. The polypropenes of higher molecular weight were obtained with Al*i*Bu_3 than with $AlEt_3$.

Figure 4-2, (a), (b), and (c), illustrates the ^{13}C NMR spectra of the syndiotactic polypropenes obtained with different cocatalysts. The ^{13}C NMR spectrum of the syndiotactic polypropene obtained with $AlEt_3/Ph_3CB(C_6F_5)_4$ (Figure 4-2 (a)) displays not only the peaks attributable to *n*Pr end groups (1t, 2t, 3t, 5t) but also the strong peaks attributable to Et end groups (8t, 10t) and *i*Pr end groups (6t, 7t) derived from the chain transfer reaction by $AlEt_3$. Furthermore, the ^{13}C NMR spectrum of the syndiotactic polypropene obtained with Al*i*$Bu_3/Ph_3CB(C_6F_5)_4$ (Figure 4-2 (b)) displays not only the peaks attributable to *n*Pr end groups (1t, 2t, 3t, 5t), but also weak peaks attributable to *i*Pr (*i*Bu) end groups derived from the

Table 4-3. Results of propene polymerization with *i*Pr(Cp)(Flu)$ZrCl_2$–$AlR_3/Ph_3CB(C_6F_5)_4$ and MAO[a]

Run	Cat.[b] (μmol)	AlR_3	Al/Zr[c]	t[d] (min)	Yield (g)	Activity (kgPP/ mol Zr·h)	M_n[e] ($\times10^{-4}$)	M_w/M_n[e]	End group[f] R/*n*Pr
18	7.9	$AlEt_3$	250	120	3.5	220	3.3	1.9	
19	7.2		500	120	2.5	170	2.7	2.1	
20	6.9		1000	120	2.5	180	1.7	2.2	2.80
21	7.2	Al*i*Bu_3	250	120	12.5	870	6.2	2.2	
22	7.2		500	120	11.7	810	5.2	2.5	
23	5.3		1000	120	8.8	630	4.6	2.3	0.87
24	6.9	(MAO)	1000	30	35.8	10400	8.3	1.9	

[a] Polymerization conditions: polymerization temperature = 40 ℃, toluene = 300 mL, propene = 4.0 kg/cm^2G, molar ratio of B/Zr = 1.0. [b] Amount of catalyst. [c] Molar ratio of Al/Zr. [d] Polymerization time. [e] Determined by GPC. [f] Molar ratio of R end groups to *n*Pr end groups; R is alkyl group of AlR_3.

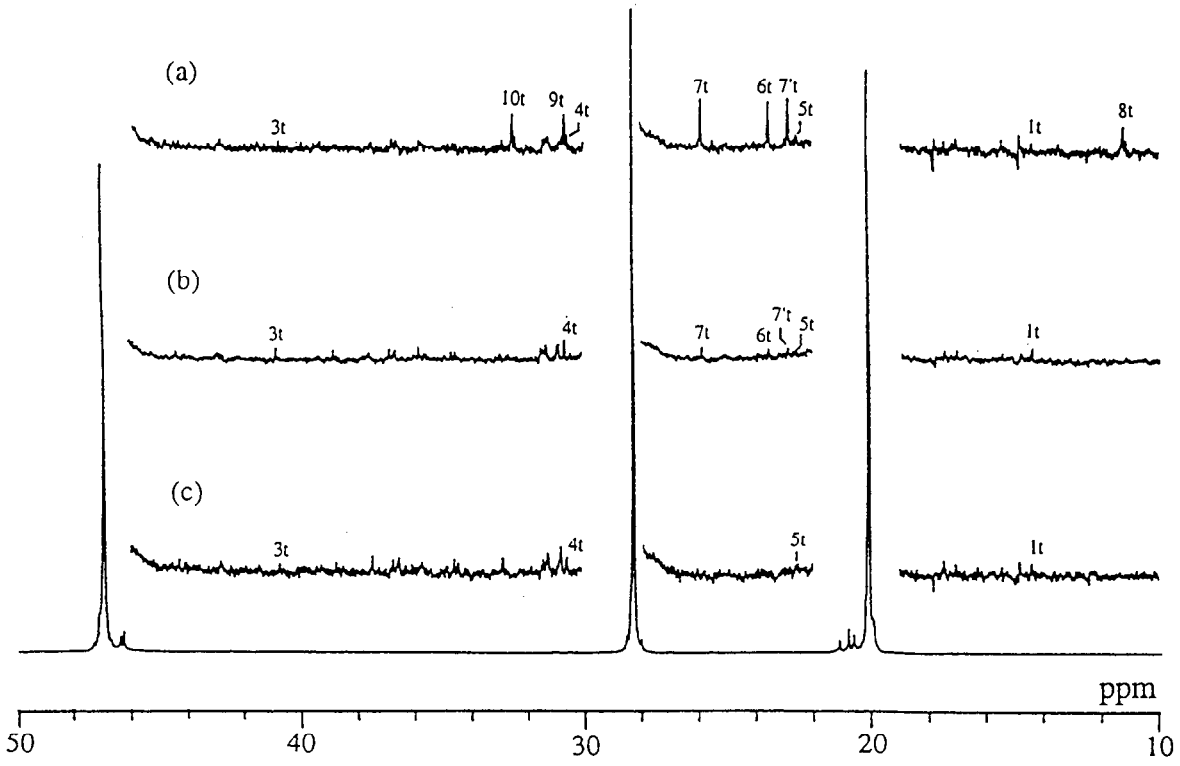

Figure 4-2. ^{13}C NMR spectra of syndiotactic polypropenes obtained with *i*Pr(Cp)(Flu)$ZrCl_2$– (a) $AlEt_3/Ph_3CB(C_6F_5)_4$, (b) Al*i*$Bu_3/Ph_3CB(C_6F_5)_4$, (c) MAO.

chain transfer reaction by Al*i*Bu$_3$. These results indicate that chain transfers not only to AlEt$_3$ but also to Al*i*Bu$_3$ occur in the syndiospecific polymerization of propene with *i*Pr(Cp)(Flu)ZrCl$_2$. The molar ratio of (Et or *i*Pr end groups)/(*n*Pr end groups) was determined. It was very difficult to determine the end groups of the syndiotactic polypropenes obtained at the low molar ratio of AlR$_3$/Zr because the molecular weights of polymers are too high. At the molar ratio of AlR$_3$/Zr = 1000, the end groups of syndiotactic polypropenes were detectable in ^{13}C NMR spectra. Since the *i*Pr end groups are formed at both the initiated and terminated chain ends through the chain transfer reaction by Al*i*Bu$_3$, half of the peaks intensity of *i*Pr end groups is applied to the intensity of initiated *i*Pr end groups. At the molar ratio of AlEt$_3$/Zr = 1000, high concentration of Et end groups was detected. On the other hand, the content of *i*Pr end groups derived from the chain transfer reaction by Al*i*Bu$_3$ was less than that of *n*Pr end groups even at the molar ratio of Al*i*Bu$_3$/Zr = 1000. These results suggest that the chain transfer reaction occurred more frequently by AlEt$_3$ than by Al*i*Bu$_3$.

4-3-2. Kinetic Study of Chain Transfer to AlR$_3$

The effect of AlR$_3$ concentration ([Al]) on the molecular weight of polypropene was investigated to characterize the chain transfer reactions by AlEt$_3$ and Al*i*Bu$_3$. Degree of polymerization (P_n) can be described by the following equations[34]:

$$P_n = \int k_p[M_p]^a[C^*]dt \,/\, \{[C^*] + \int (k_{tr} + k_{trA}[Al]^b + k_{trM}[M_p]^c)[C^*]dt\}$$

$$1/P_n = (k_{tr} + k_{trM}[M_p]^c)/k_p[M_p]^a + k_{trA}[Al]^b/k_p[M_p]^a$$

where k_p, [M$_p$], [C*], [Al], k_{tr}, k_{trA}, and k_{trM} are, respectively, rate constant of propagation, propene concentration, number of active centers, AlR$_3$ concentration, rate constant of β-hydrogen transfer to the metal, transfer to AlR$_3$ and β-hydrogen transfer to the propene monomer; [M$_p$] at the polymerization condition, propene/toluene equilibrium at 40 °C of 4 kg/cm^{2}G, was calculated by Soave–Redich–Kwong equation[33] and total volume = 389 mL, [M$_p$] = 2.9 mol/L were applied to the condition; a, b, and c are the reaction orders.

According to previous reports, polymerization activity of propene increased in proportion to the concentration of propene monomer. The relationship between polymerization rate and monomer concentration has been studied by Fink *et al.* for metallocene–MAO catalysts, and reaction orders in the propene concentration of 1.2–1.4 for *rac*-$Me_2Si(Ind)_2ZrCl_2$–MAO and *i*Pr(Cp)(Flu)$ZrCl_2$–MAO systems have been reported.[35] Although, higher value (1.7) of reaction order for the polymerization rate with respect to the propene concentration was reported with *rac*-Me_2Si(benz[e]indenyl)$_2ZrCl_2$ and *rac*-Me_2Si(2-Me benz[e]indenyl)$_2ZrCl_2$–MAO by Mülhaupt *et al.*[12] In this study, the author assumes that only one propene molecule is involved in the propagation step, and apply a = 1 for the reaction order.

The value of $1/P_n$ increases in proportion to the concentration of AlR_3 ([Al]) as shown in Figure 4-3, and the reaction order of b = 1 is applied for the chain transfer rate with respect to AlR_3 concentration. The relative constants k_{trA}/k_p were calculated from the plots in Figure 4-3. The results are summarized in Table 4-4. The values of relative constants of k_{trA}/k_p with

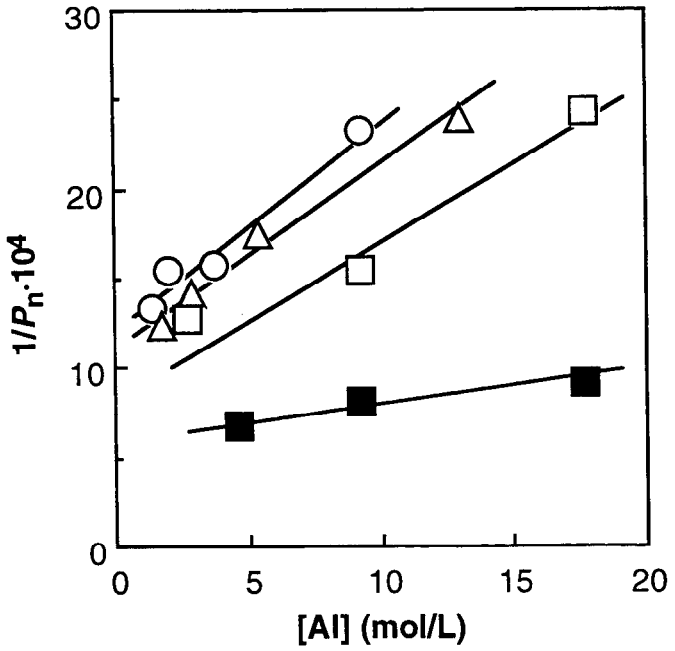

Figure 4-3. Plots of $1/P_n$ against trialkylaluminum concentration: (○) *rac*-Et(Ind)$_2ZrCl_2$–$AlEt_3$; (△) *rac*-$Me_2Si(Ind)_2ZrCl_2$–$AlEt_3$; (□) *i*Pr(Cp)(Flu)$ZrCl_2$–$AlEt_3$; (■) *i*Pr(Cp)(Flu)$ZrCl_2$–Al*i*Bu_3.

Table 4-4. Kinetic study of chain transfer reaction by AlR_3 in stereospecific polymerization of propene with zirconocene catalysts[a]

Run	Zirconocene catalyst	AlR_3	[Al] (mol/L)	$1/P_n$ ($\times 10^4$)	k_{trA}/k_p ($\times 10^4$)
1	*rac*-Et(Ind)$_2$ZrCl$_2$	$AlEt_3$	1.39	13.3	
2			1.99	15.5	3.54
3			3.72	15.7	
4			9.25	23.3	
10	*rac*-Me$_2$Si(Ind)$_2$ZrCl$_2$	$AlEt_3$	1.81	12.5	
11			2.95	14.2	2.88
12			5.40	17.5	
13			13.1	24.0	
18	*i*Pr(Cp)(Flu)ZrCl$_2$	$AlEt_3$	2.76	12.7	
19			9.25	15.5	2.29
20			17.7	24.3	
21	*i*Pr(Cp)(Flu)ZrCl$_2$	Al*i*Bu_3	4.63	6.80	
22			9.25	8.15	0.49
23			17.7	9.11	

[a] Propene monomer concentration [M] = 2.9 (mol/L). [b] P_n = degree of polymerization. [c] k_{trA} and k_p are, respectively, rate constant of chain transfer to AlR_3 and rate constant of propagation.

$AlEt_3/Ph_3CB(C_6F_5)_4$ ranged from 2.3×10^{-4} to 3.5×10^{-4} in the polymerization with *rac*-Et(Ind)$_2$ZrCl$_2$, *rac*-Me$_2$Si(Ind)$_2$ZrCl$_2$, and *i*Pr(Cp)(Flu)ZrCl$_2$ under the polymerization condition. The k_{trA}/k_p values with $AlEt_3/Ph_3CB(C_6F_5)_4$ decrease in the following order: *rac*-Et(Ind)$_2$ZrCl$_2$ > *rac*-Me$_2$Si(Ind)$_2$ZrCl$_2$ > *i*Pr(Cp)(Flu)ZrCl$_2$. The k_{trA}/k_p value with *i*Pr(Cp)(Flu)ZrCl$_2$ combined with Al*i*$Bu_3/Ph_3CB(C_6F_5)_4$ is 0.49×10^{-4} about one fifth of that combined with $AlEt_3/Ph_3CB(C_6F_5)_4$.

4-4. Summary

In the stereospecific polymerization of propene with zirconocene catalysts combined with $AlR_3/Ph_3CB(C_6F_5)_4$, chain transfer to AlR_3 plays an important role in determining the molecular weight of polypropene. The chain transfer reactions by $AlEt_3$ and $Al\textit{i}Bu_3$ were studied by the analysis of molecular weight, chain end structures of obtained polymers, and kinetic study.

In isospecific polymerization with *rac*-$Et(Ind)_2ZrCl_2$ and *rac*-$Me_2Si(Ind)_2ZrCl_2$ combined with $AlR_3/Ph_3CB(C_6F_5)_4$, the molecular weight of resulting polymers decreased with an increase in the molar ratio of $AlEt_3/Zr$, and the chain end groups resulting from the chain transfer to $AlEt_3$ were detected. On the other hand, the molecular weight of polymers was independent of the molar ratio of $Al\textit{i}Bu_3/Zr$ and the chain end groups resulting from the chain transfer to $Al\textit{i}Bu_3$ could not be observed by ^{13}C NMR spectroscopy. The syndiospecific polymerization of propene was also conducted with $\textit{i}Pr(Cp)(Flu)ZrCl_2$ combined with $AlR_3/Ph_3CB(C_6F_5)_4$ and the chain transfer reactions by both $AlEt_3$ and $Al\textit{i}Bu_3$ were observed. The chain transfer to $AlEt_3$ occurs more frequently than to $Al\textit{i}Bu_3$.

The relative constants of k_{trA}/k_p with zirconocene catalysts were calculated from the plots of $1/P_n$ against [Al]. The k_{trA}/k_p value with $\textit{i}Pr(Cp)(Flu)ZrCl_2$ combined with $Al\textit{i}Bu_3/Ph_3CB(C_6F_5)_4$ is about one fifth of that combined with $AlEt_3/Ph_3CB(C_6F_5)_4$.

References

(1) Soga, K.; Shiono, T.; Takemura, S.; Kaminsky, W. *Makromol.Chem., Rapid Commun.* **1987**, *8*, 305.

(2) Grassi, A.; Zambelli, A.; Resconi, L.; Albizzati, E.; Mazzocchi, R. *Macromolecules* **1988**, *21*, 617.

(3) Cheng, H. N.; Ewen, J. A. *Makromol. Chem.* **1989**, *190*, 1931.

(4) Tsutsui, T.; Mizuno, A.; Kashiwa, N. *Polymer* **1989**, *30*, 428.

(5) Rieger, B.; Mu, X.; Mallin, D. T.; Rausch, M. D.; Chien, J. C. W. *Macromolecules* **1990**, *23*, 3559.

(6) Ewen, J. A.; Elder, M.;Jones, R.;Haspeslagh, L.; Atwood, J.; Bott, S.; Robinson, K. *Macromol. Chem., Macromol. Symp.* **1991**, *48/49*, 253.

(7) Rieger, B.; Reinmuth, W.; Röll, W.; Brintzinger, H. H. *J. Mol. Catal.* **1993**, *82*, 67.

(8) Busico, V.; Cipullo, R.; Chadwick, J. C.; Modder, J. F.; Sudmeijer, O. *Macromolecules* **1994**, *27*, 7538.

(9) Giardello, M. A.; Eisen, M. S.; Stern, C. L.; Marks, T. J. *J. Am. Chem. Soc.* **1995**, *117*, 12114.

(10) Stehling, U.; Diebold, J.; Kirsten, R.; Röll, W.; Brintzinger, H. H.; Jüngling, S.; Mülhaupt, R.; Langhauser, F. *Organometallics* **1994**, *13*, 964.

(11) Resconi, L.; Fait, A.; Piemontesi, F.; Colonnesi, M.; Rychlicki, H.; Zeigler, R. *Macromolecules* **1995**, *28*, 6667.

(12) Jüngling, S.; Mülhaupt, R.; Stehling, U.; Brintzinger, H. H.; Fischer, D.; Langhauser, F. *J. Polym. Sci., Part A: Polym. Chem.* **1995**, *33*, 1305.

(13) Eshuis, J.; Tan, Y.; Teuben, J. H.; Renkema, J. *J. Mol. Catal.* **1990**, *62*, 277.

(14) Eshuis, J.; Tan, Y.; Meetsma, A.; Teuben, J. H. *Organometallics* **1992**, *11*, 362.

(15) Yang, X.; Stern, C. L.; Marks, T. J. *Angew. Chem., Int. Ed. Engl.* **1992**, *31*, 1375.

(16) Mise, T.; Kageyama, A., Miya, S., Yamazaki, H. *Chem. Lett.* **1991**, 1525.

(17) Resconi, L.;Piemontesi, F.; Franciscono, G.; Abis, L.; Fiorani, T. *J. Am. Chem. Soc.* **1992**, *114*, 1025.

(18) Guo, Z.; Swenson, D.; Jordan, R. *Organometallics* **1994**, *13*, 1424.

(19) Hajela, S.; Bercaw, J. E. *Organometallics* **1994**, *13*, 1147.

(20) Yang, X.; Stern, C. L.; Marks, T. J. *J. Am. Chem. Soc.* **1994**, *116*, 10015.

(21) Sini, G.; Macgregor, S.A.; Eisenstein, O.; Tauben, J. H. *Organometallics* **1994**, *13*, 1049.

(22) Resconi, L.; Jones, R. L.; Rheingold, A. L.; Yap, G. P. A. *Organometallics* **1996**, *15*, 998.

(23) Resconi, L.; Piemontesi, F.; Camurati, I.; Balboni, D.; Sironi, A.; Moret, M.; Rychlicki, H.; Zeigler, R. *Organometallics* **1996**, *15*, 5046.

(24) Zambelli, A.; Longo, P.; Grassi, A. *Macromolecules* **1989**, *22*, 2186.

(25) Mogstad, A. L.; Resconi, L.; Waymouth, R. M. *Polym. Prepr.* **1991**, *32*, 160.

(26) Soga, K.; Kaminaka, M. *Makromol. Chem.* **1993**, *194*, 1745.

(27) Bochmann, M.; Lancaster, S. J. *Angew. Chem., Int. Ed. Engl.* **1994**, *33*, 1634.

(28) Bochmann, M.; Lancaster, S. J. *J. Organomet. Chem.* **1995**, *497*, 55.

(29) Uchida, O.; Takeuchi, K.; Sugimoto, R. In *Science and Technology in Catalysis 1994*; Kodansha Ltd: Tokyo, 1995; p 367.

(30) Ewen, J. A.; Jones, R. L.; Razavi, A.; Ferrara, J. D. *J. Am. Chem. Soc.* **1988**, *110*, 6255.

(31) Ouano, A. C.; Mercier, P. L. *J. Polym. Sci., Part C* **1968**, *21*, 309.

(32) Soave, G. *Chem. Eng. Sci.* **1972**, *27*, 1197.

(33) Shiono, T.; Uozumi, T.; Soga, K. *Kobunshi Ronbunshu* **1994**, *51*, 663.

(34) Herfert, N.; Fink, G. *Makromol. Chem.* **1992**, *193*, 1359.

Chapter 5

Effect of Cocatalysts on Microstructures of Polypropene Obtained with Zirconocene Catalysts

5-1. Introduction

Comparison in microstructures of polypropenes obtained with cationic and MAO-activated metallocene catalysts has been reported. Ewen performed stereospecific polymerizations of propene with *rac*-Et(Ind)$_2$ZrCl$_2$ and *i*Pr(Cp)(Flu)ZrCl$_2$ combined with MAO, AlEt$_3$/Ph$_3$CB(C$_6$F$_5$)$_4$ and AlEt$_3$/Ph$_3$CAl(C$_6$F$_5$)$_4$.[1] Judging from the results, the isotacticities of polypropenes obtained with *rac*-Et(Ind)$_2$ZrCl$_2$ were almost the same regardless of the cocatalysts used. In contrast, the syndiotacticities of polypropenes obtained with *i*Pr(Cp)(Flu)ZrCl$_2$ were dependent on the cocatalysts used, and AlEt$_3$/cation-forming reagents gave lower syndiotactic polymer than MAO. Fink *et al.* carried out propene polymerization with *rac*-Me$_2$Si(Ind)$_2$ZrMe$_2$–(C$_4$H$_9$)$_3$NHB(C$_6$F$_5$)$_4$ and *rac*-Me$_2$Si(Ind)$_2$ZrCl$_2$–MAO, and concluded that no difference in stereoregularity was observed in the polypropenes obtained with each catalyst system.[2,3] Chien *et al.* discussed differences between coordinating and non-coordinating counterions in propene polymerization with metallocene catalysts on the rate constant of propagation, isospecificity and molecular weight of polypropenes obtained.[4]

On the other hand, drastic changes in stereoregularity of polypropenes obtained with some metallocene catalysts were reported by varying the cocatalyst. Shiomura *et al.* reported the change of stereospecificity in propene polymerization with Me$_2$Si(Flu)(N-*t*Bu)ZrCl$_2$ from syndiospecific to isospecific by changing the cocatalyst from MAO (with Al*i*Bu$_3$) to Al*i*Bu$_3$/Ph$_3$CB(C$_6$F$_5$)$_4$.[5] Shiono *et al.* investigated the polymerization of propene with Cp$_2$TiMe$_2$ in toluene at –50 °C, and reported that MAO and B(C$_6$F$_5$)$_3$ gave isotactic polymer in chain-end control mechanism, while Ph$_3$CB(C$_6$F$_5$)$_4$ gave statistically atactic polymer.[6]

The effect of cocatalyst has not been reported on the stereoregularity of polypropene obtained with non-bridged zirconocene and *meso*-type *ansa*-zirconocene catalysts, and regioregularity of isotactic polypropene obtained with *rac*-type *ansa*-zirconocene catalysts. In this chapter, the effect of cocatalyst on the microstructures of polypropenes prepared by non-bridged zirconocenes, *rac*- and *meso*-zirconocene was investigated by ^{13}C NMR spectroscopy. In addition, microstructures of syndiotactic polypropene were studied to clear the reason for the

lowering of syndiotacticity in the polypropene prepared by cationic C_s-symmetrical zirconocene catalyst.

5-2. Experimental Part

Materials

Cp_2ZrCl_2, $Cp^*_2ZrCl_2$, and Ind_2ZrCl_2 were commercially obtained from Aldrich Co., Ltd. and Boulder Science Co., Ltd., and used without further purification. Toluene solution of MAO and Al*i*Bu$_3$ were donated from Tosoh Akzo Co., Ltd. and used without further purification. $Ph_3CB(C_6F_5)_4$ was donated from Asahi glass Co., Ltd. and used without further purification.

Propene polymerization with non-bridged zirconocenes

Polymerization of propene with MAO was carried out in a 1 L autoclave, and 280 g (6.7 mol) of liquid propene was introduced to the autoclave. Toluene (10 mL), MAO, and catalyst were mixed in a 100 mL glass flask at 25 °C for 5 min in advance. The molar ratio of Al/Zr was adjusted to 1000. The polymerization was started by adding the catalyst solution to the autoclave. Temperature was kept at a fixed temperature during the polymerization. The polymerization was terminated by adding isobutyl alcohol. The obtained polymer was precipitated in excess methanol and dried *i. vac.* at 60 °C for 6 h.

Polymerization of propene with Al*i*Bu$_3$/$Ph_3CB(C_6F_5)_4$ was carried out in a 100 mL autoclave and 21 g (0.5 mol) of propene was introduced to the autoclave. Toluene (10 mL), Al*i*Bu$_3$ (2.0 mmol), and catalyst (4.0 μmol) were mixed in a 100 mL glass flask at 25 °C for 5 min in advance. The polymerization was started by adding the catalyst solution and toluene solution of $Ph_3CB(C_6F_5)_4$ (4.0 μmol, 1.0 M solution) to the autoclave. The other experimental procedures were the same with those described in the polymerization with MAO.

Propene polymerization with ansa-zirconocenes

Polypropenes obtained with *rac*- and *meso*- $Me_2Si(2,3,5\text{-}Me_3Cp)_2ZrCl_2$ at 40 °C were prepared in Chapter 3 at 40 °C. Isotactic and syndiotactic polypropenes were prepared by *rac*-$Et(Ind)_2ZrCl_2$, *rac*-$Me_2Si(Ind)_2ZrCl_2$, and *i*$Pr(Cp)(Flu)ZrCl_2$ as described in Chapter 4.

Analytical procedure

^{13}C NMR spectra were recorded at 135 °C on a JEOL EX-270 NMR or at 130 °C on a JEOL EX-400 spectrometer. Polymers were dissolved in *o*-dichlorobenzene/benzene-d_6 (vol. ratio = 9/1) up to 5 wt%. Pentad assignment was determined according to the literature.[7–10]

5-3. Results and Discussion

5-3-1. Microstructures of Atactic Polypropenes Obtained with Non-Bridged Zirconocene Catalysts

Polymerization of propene was conducted with non-bridged zirconocene catalysts (Cp_2ZrCl_2, $Cp^*_2ZrCl_2$, Ind_2ZrCl_2) using MAO and Al*i*$Bu_3/Ph_3CB(C_6F_5)_4$ as cocatalysts at 40, 0, and –20 °C. The microstructures of polypropenes obtained are summarized in Tables 5-1 and 5-2. Clear difference in stereochemistry of the polypropenes could not be observed among the cocatalysts used.

Portion of *meso*-sequences ([m]) increased with lowering of the polymerization temperature. $Cp^*_2ZrCl_2$ produced syndiotactic-rich polypropenes. This result is the same with the result of 1-butene polymerization previously reported.[11] Judging from the triad sequence, chain-end control is predominant for producing the isotactic portion (2[rr]/[mr] = 1 for site control, $4[mm][rr]/[mr]^2 = 1$ for chain-end control).[12] According to the previous report, (2-PhInd)$_2ZrCl_2$ produced isotactic-atactic stereoblock polypropene, and increase of [mm] value was observed with the decrease of polymerization temperature.[13] The proposed mechanism is that rotation of ligands made equilibrium of *rac-meso* conformation, which lead to isotactic and atactic sequences, respectively. In the case of polymerization with Ind_2ZrCl_2, triad tests of polypropenes fit to the chain-end control, and one can conclude that the isospecific

Table 5-1. Microstructures of polypropenes obtained with non-bridged zirconocene–MAO[a]

Run	Catalysyt	T_p[b] (℃)	[mmmm] (%)	[mmmr]	[rmmr]	[mmrr]	[mmrm] + [rmrr]	[rmrm]	[rrrr]	[mrrr]	[mrrm]	[mm] (%)	[mr]	[rr]	triad tests 2[rr] /[mr]	triad tests 4[mm][rr] /[mr]^2
1	Cp_2ZrCl_2	40	5.1	11.1	7.1	9.7	24.2	17.6	5.5	9.5	10.2	23.3	51.5	25.2	0.98	0.86
2		0	7.8	13.2	7.6	10.2	25.6	14.4	4.0	8.6	8.7	28.6	50.2	21.3	0.85	0.97
3		–20	10.2	17.2	7.5	11.5	27.4	12.6	2.2	5.5	5.9	34.9	51.5	13.6	0.53	0.72
4	$Cp^*_2ZrCl_2$	40	2.0	5.3	6.4	9.8	22.2	15.0	15.8	16.9	6.5	13.7	47.0	39.2	1.67	0.97
5		0	4.0	8.4	7.1	12.6	23.9	11.2	12.3	14.0	6.5	19.5	47.7	32.8	1.38	1.12
6		–20	4.3	9.2	6.8	13.1	23.9	10.7	11.2	15.8	5.0	20.3	47.7	32.0	1.34	1.14
7	Ind_2ZrCl_2	40	9.0	14.4	6.9	12.4	23.9	12.7	4.7	9.1	7.0	30.3	49.0	20.8	0.85	1.05
8		0	8.4	14.8	7.3	13.1	24.3	12.6	4.3	8.9	6.3	30.5	50.0	19.5	0.78	0.95
9		–20	10.7	15.8	7.2	12.3	24.4	12.1	3.4	8.0	6.1	33.7	48.8	17.5	0.72	0.99

[a] Polymerization conditions: 1 L autoclave, propene = 280 g (6.7 mol), molar ratio of (MAO)Al/Zr = 1000. [b] Polymerization temperature.

Table 5-2. Microstructures of polypropenes obtained with non-bridged zirconocene–Al*i*Bu$_3$/Ph$_3$CB(C$_6$F$_5$)$_4$[a]

Run	Catalysyt	T_p[b] (℃)	[mmmm] (%)	[mmmr]	[rmmr]	[mmrr]	[mmrm] + [rmrr]	[rmrm]	[rrrr]	[mrrr]	[mrrm]	[mm] (%)	[mr]	[rr]	triad tests 2[rr] /[mr]	triad tests 4[mm][rr] /[mr]^2
10	Cp_2ZrCl_2	40	6.2	14.0	7.0	12.9	27.4	13.4	3.2	9.9	6.0	27.2	53.7	19.1	0.71	0.72
11		0	9.8	16.2	6.8	12.6	26.2	12.9	2.9	6.9	5.7	32.8	51.7	15.5	0.60	0.76
12		–20	13.9	16.8	6.4	12.7	27.2	10.8	2.2	6.0	4.1	37.1	50.7	12.3	0.49	0.71
13	$Cp^*_2ZrCl_2$	40										11.2	45.3	43.5	1.92	0.95
14		0	4.2	9.4	6.3	13.5	23.9	12.7	9.7	14.2	6.1	19.9	50.1	30.0	1.20	0.95
15		–20	6.1	9.9	5.7	13.4	23.7	12.1	6.5	14.3	8.4	21.7	49.2	29.2	1.19	1.05
16	Ind_2ZrCl_2	40	8.5	14.6	7.3	13.5	24.9	12.5	3.1	9.4	6.2	30.4	50.9	18.7	0.73	0.88
17		0										35.5	45.8	18.7	0.82	1.27
18		–20										37.9	46.7	15.4	0.66	1.07

[a] Polymerization conditions: 100 mL autoclave, propene = 21 g (0.5 mol), Zr = 4.0 μmol, molar ratio of Al/Zr = 500, molar ratio of $Ph_3CB(C_6F_5)_4$/Zr = 1.0. [b] Polymerization temperature.

polymerization mechanism is different from that of with (2-PhInd)$_2$ZrCl$_2$. The substituent of 2-position in the indenyl ligand is essential in determining the stereochemistry of propene polymerization with non-bridged bis(indenyl)-type zirconocenes.

Stereoregulation energies were determined on the basis of Arrhenius plot according to the equations:

$$[m]/[r] = P_m/P_r$$

$$\ln ([m]/[r]) = \ln a_m/a_r + (E_r - E_m)/RT$$

where P_m and P_r are probabilities of isotactic and syndiotactic placements, a_m and a_r are Arrhenius preexponential coefficients, E_m and E_r are activation energies for the formation of isotactic and syndiotactic dyads in propagation process.[3,9,11] The Arrhenius plots are shown in Figures 5-1 and 5-2. The plots show almost the same profiles in each zirconocene with both MAO and Al*i*Bu$_3$/Ph$_3$CB(C$_6$F$_5$)$_4$ cocatalyst systems. The stereoregulation energies were calculated from the slope of the plots. The values of $E_r - E_m$ are 1.19, 0.79, and 0.33 kcal/mol with Cp$_2$ZrCl$_2$, Cp*$_2$ZrCl$_2$, and Ind$_2$ZrCl$_2$ using MAO, respectively, and 0.89, 1.42, and 0.56 kcal/mol with Cp$_2$ZrCl$_2$, Cp*$_2$ZrCl$_2$, and Ind$_2$ZrCl$_2$ using Al*i*Bu$_3$/Ph$_3$CB(C$_6$F$_5$)$_4$, respectively.

5-3-2. Microstructures of Atactic Polypropenes Obtained with A *meso*-Type *ansa*-Zirconocene Catalyst

Microstructures of polypropenes obtained with *meso*-Me$_2$Si(2,3,5-Me$_3$Cp)$_2$ZrCl$_2$ at 40 °C are summarized in Table 5-3. The microstructures of resulting polypropenes are almost the same regardless of the cocatalysts used. It is clear that cocatalyst does not affected the microstructures of polypropene obtained with *meso*-Me$_2$Si(2,3,5-Me$_3$Cp)$_2$ZrCl$_2$.

5-3-3. Microstructures of Isotactic Polypropenes Obtained with C_2-Symmetrical Zirconocene Catalysts

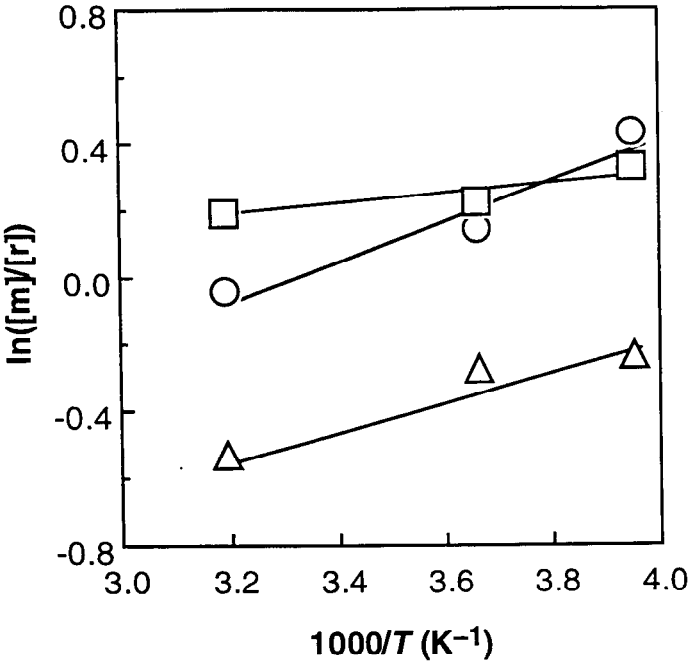

Figure 5-1. Arrhenius plots of ln([m]/[r]) versus $1/T$ for polypropenes prepared by zirconocenes–MAO: (○) Cp_2ZrCl_2; (△) $Cp^*_2ZrCl_2$; (□) Ind_2ZrCl_2.

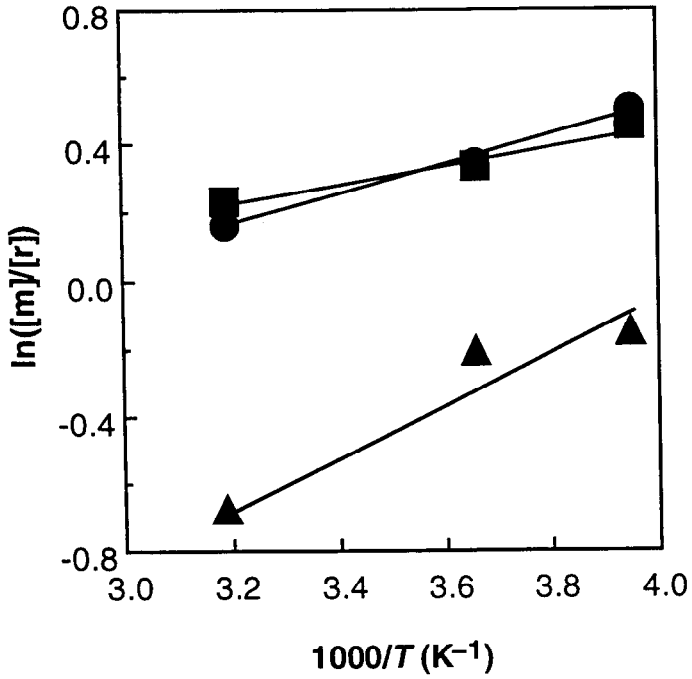

Figure 5-2. Arrhenius plots of ln([m]/[r]) versus $1/T$ for polypropenes prepared by zirconocense–Al*i*Bu_3/$Ph_3CB(C_6F_5)_4$: (●) Cp_2ZrCl_2; (▲) $Cp^*_2ZrCl_2$; (■) Ind_2ZrCl_2.

Table 5-3. Microstructures of polypropenes obtained with *meso*-$Me_2Si(2,3,5\text{-}Me_3Cp)_2ZrCl_2$[a]

Run	Cocatalyst[b]	[mmmm] (%)	[mmmr]	[rmmr]	[mmrr]	[mmrm] + [rmrr]	[rmrm]	[rrrr]	[mrrr]	[mrrm]	[mm] (%)	[mr]	[rr]	triad tests 2[rr] /[mr]	triad tests 4[mm][rr] /[mr]^2
19	MAO	4.3	10.7	8.2	11.8	26.9	15.3	5.3	10.8	6.7	23.2	54.0	22.8	0.84	0.73
20	$AlEt_3$/TB	4.3	10.9	8.2	12.1	26.3	14.2	6.0	11.6	6.2	23.4	52.6	23.8	0.90	0.81
21	Al*i*Bu_3/TB	4.2	10.4	8.3	12.1	26.3	14.6	6.3	11.2	6.6	22.9	53.0	24.1	0.91	0.79

[a] Polymerization conditions: 1 L autoclave, propene = 280 g (6.7 mol), polymerization temperature = 40 °C. [b] Molar ratio of (MAO)Al/Zr = 1000, molar ratio of AlR_3/Zr = 250, TB = $Ph_3CB(C_6F_5)_4$, molar ratio of B/Zr = 1.0.

Table 5-4. Microstructiures of isotactic polypropenes obtained with C_2-symmetrical zirconocene catalysts[a]

Run	Catalyst	Cocatalyst[b]	Molar ratio Al/Zr	[mmmm] (%)	[mmrr] (%)	[mrrm] (%)	2,1-(m) (%)	2,1-(r) (%)	1,3- (%)	T_m[c] (℃)
22	*rac*-$Me_2Si(2,3,5\text{-}Me_3Cp)_2ZrCl_2$	MAO	1000	98.8	0.47	0.54				162.1
23		$AlEt_3$/TB	250	98.9	0.44	0.61				159.8
24		Al*i*Bu_3/TB	250	98.1	0.75	0.87				162.2
25	*rac*-$Et(Ind)_2ZrCl_2$	MAO	1000	87.4	5.6	2.1	0.53	0.26	0.08	136.9
26		$AlEt_3$/TB	150	88.9	4.9	1.9	0.60	0.19	0.19	141.0
27			1000	88.2	5.2	2.0	0.65	0.21	0.14	141.0
28		Al*i*Bu_3/TB	1000	89.6	4.3	2.0	0.58	0.22	0.17	138.7
29	*rac*-$Me_2Si(Ind)_2ZrCl_2$	MAO	1000	93.3	3.0	1.1	0.40	0.20		145.1
30		$AlEt_3$/TB	150	92.4	3.3	1.3	0.53	0.16	0.04	145.6
31			1000	92.8	3.0	1.3	0.58	0.30	0.07	146.0
32		Al*i*Bu_3/TB	1000	91.8	3.4	1.5	0.64	0.23	0.17	142.3

[a] Polymerization conditions: 1 L autoclave, polymerization temperature = 40 ℃, propene = 280 g (6.7 mol) (run 22–24), propene = 4 kg/cm^2 with toluene = 300 mL (run 25–32). [b] TB = $Ph_3CB(C_6F_5)_4$, molar ratio of B/Zr = 1.0, [c] Melting temperature.

Microstructures of isotactic polypropenes prepared by *rac*-$Me_2Si(2,3,5\text{-}Me_3Cp)_2ZrCl_2$, *rac*-$Et(Ind)_2ZrCl_2$ and *rac*-$Me_2Si(Ind)_2ZrCl_2$ are also studied by ^{13}C NMR spectroscopy. The assignments of the chemical shifts of 2,1-insertion and 1,3-insertion (Scheme 4-3 in Chapter 4) were made according to the literature,[14–18] and the results are summarized in Table 5-4. The difference of isotacticity and regio specificity was not clearly observed among the polypropenes obtained with different cocatalysts and at the different molar ratios of $AlEt_3$/Zr.

5-3-4. Microstructures of Syndiotactic Polypropenes Obtained with A C_s-Symmetrical Zirconocene Catalyst

Microstructures of syndiotactic polypropenes obtained with *i*Pr(Cp)(Flu)$ZrCl_2$ are summarized in Table 5-5. The [rrrr] pentad fraction of syndiotactic polypropene using MAO as a cocatalyst is higher than that with AlR_3 (R = Et, *i*Bu)/$Ph_3CB(C_6F_5)_4$, as reported by Ewen previously.[1] Two types of stereo-irregular sequences are found in syndiospecific polymerization of propene with *i*Pr(Cp)(Flu)$ZrCl_2$ as shown in Scheme 5-1.[19] One is [rmmr] that originated from reversed diastereoface selectivity (miss-insertion of propene), the other is [rmrr] sequence originated from migration of the propagating polymer chain to the vacant site. The stereo-irregular fraction of [rmmr] was almost the same in any syndiotactic polypropenes, but higher [rmrr] was found in the polypropenes obtained with $AlR_3/Ph_3CB(C_6F_5)_4$. These results suggest that the migration of propagating polymer chain to the vacant site occurs more frequently in syndiospecific polymerization with $AlR_3/Ph_3CB(C_6F_5)_4$ than with MAO.

Table 5-5. Microstructures of syndiotactic polypropenes obtained with *i*Pr(Cp)(Flu)$ZrCl_2$[a]

Run	Cocatalyst	Molar ratio Al/Zr	[rrrr] (%)	[rmrr] (%)	[rmmr] (%)
33	MAO	1000	88.4	2.0	1.5
34	$AlEt_3/Ph_3CB(C_6F_5)_4$	1000	86.6	2.7	1.6
35	Al*i*$Bu_3/Ph_3CB(C_6F_5)_4$	1000	84.4	3.3	1.6

[a] Polymerization conditions: 1 L autoclave, toluene = 300 mL, propene = 4 kg/cm^2, molar ratio of B/Zr = 1.0.

1. Syndiotactic propagation.

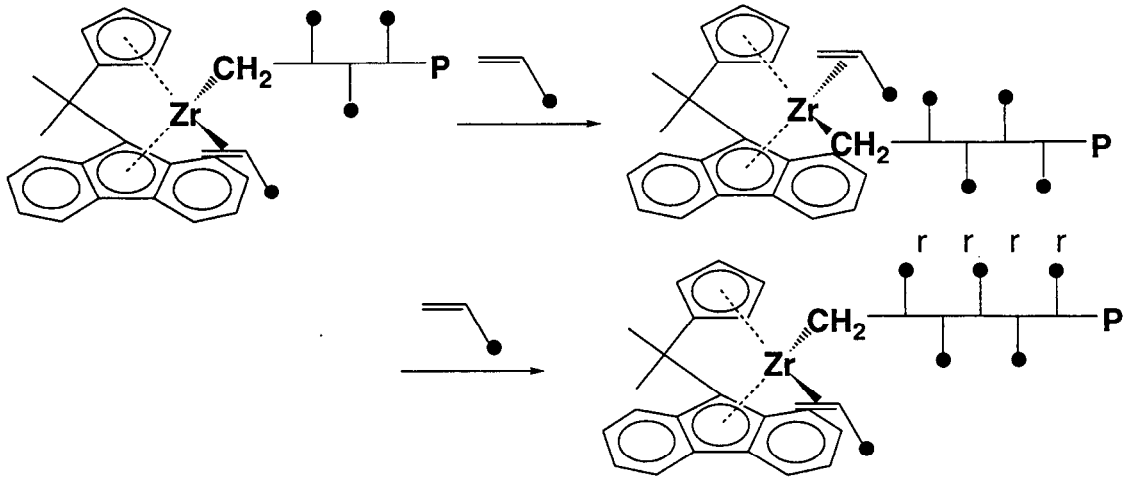

2. Reversed diastereoface selectivty.

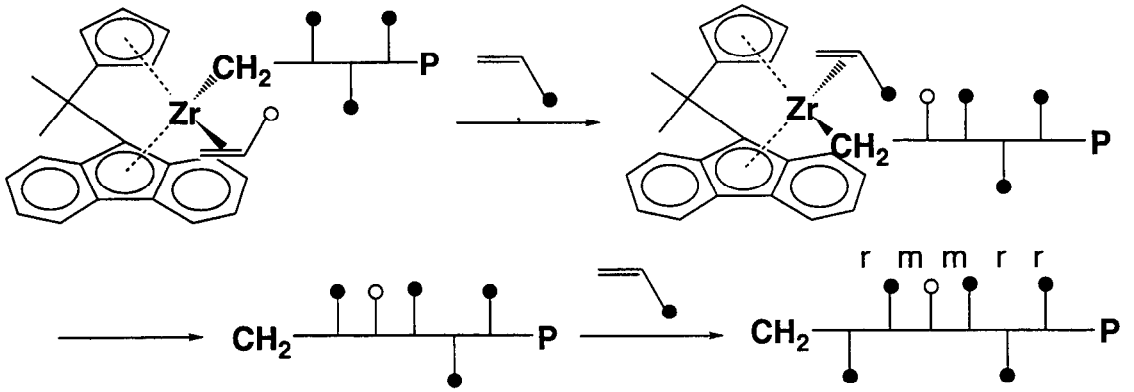

3. Chain migration to vacant site.

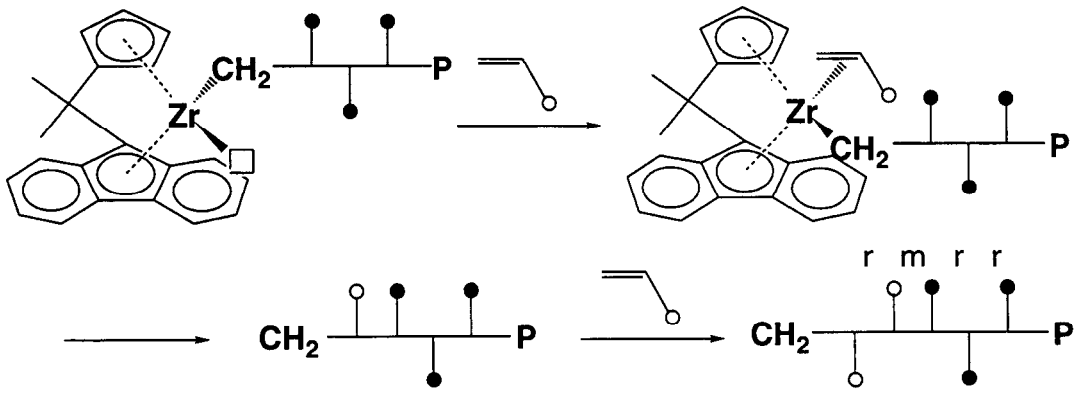

Scheme 5-1. Mechanisms of syndiospecific polymerization of propene with *i*Pr(Cp)(Flu)$ZrCl_2$: P = polymer chain.

5-4. Summary

Propene polymerization was conducted with non-bridged zirconocenes, *meso*-type *ansa*-zirconocene, C_2-symmetrical zirconocenes and C_s-symmetrical zirconocene using MAO and $AlR_3/Ph_3CB(C_6F_5)_4$ as cocatalysts. The cocatalyst did not affect the microstructures of resulting polypropenes in the aspecific and the isospecific polymerizations. In the syndiospecific polymerization, the decrease of [rrrr] fraction derived from the migration of the propagating polymer chain to the vacant site was observed when $AlR_3/Ph_3CB(C_6F_5)_4$ was used.

References

(1) Ewen, J. A. In *Catalyst Design for Tailor-made Polyolefins*; Soga, K., Terano, M., Eds.; Elsevier: Amsterdam, Oxford, New York, Tokyo, 1994; p 405.

(2) Herfert, N.; Fink, G. *Makromol. Chem., Rapid Commun.* **1993**, *14*, 91.

(3) Beck, S.; Prosec, M. H.; Brintzinger, H. H.; Goretzki, R.; Herfert, N.; Fink, G. *J. Mol. Catal. A: Chem.* **1996**, *111*, 67.

(4) Chien, J. C. W.; Song, W.; Rausch, M. D. *J. Polym. Sci., Part A: Polym. Chem.* **1994**, *32*, 2387.

(5) Shiomura, T.; Asanuma, T.; Inoue, N. *Macromol. Rapid Commun.* **1996**, *17*, 9.

(6) Hagihara, H.; Shiono, T.; Ikeda, T. *Macromol. Chem. Phys.* **1998**, *199*, 2439.

(7) Stehling, F. C.; Knox, J. R. *Macromolecules* **1975**, *8*, 595.

(8) Zambelli, A.; Locatelli, P.; Bajo, G.; Bovey, F. A. *Macromolecules* **1975**, *8*, 687.

(9) Zambelli, A.; Locatelli, P.; Zannoni, G.; Bovey, F. A. *Macromolecules* **1978**, *11*, 923.

(10) Zambelli, A.; Locatelli, P.; Provasoli, A.; Ferro, D. R. *Macromolecules* **1980**, *13*, 267.

(11) Resconi, L.; Abis, L.; Franciscono, G. *Macromolecules* **1992**, *25*, 6814.

(12) Ewen, J. A. *J. Am. Chem. Soc.* **1984**, *106*, 6355.

(13) Coates, G. W.; Waymouth, R. M. *Science* **1995**, *267*, 217.

(14) Soga, K.; Shiono, T.; Takemura, S.; Kàminsky, W. *Makromol. Chem., Rapid Commun.* **1987**, *8*, 305.

(15) Grassi, A.; Zambelli, A.; Resconi, L.; Albizzati, E.; Mazzocchi, R. *Macromolecules* **1988**, *21*, 617.

(16) Cheng, H. N.; Ewen, J. A. *Makromol. Chem.* **1989**, *190*, 1931.

(17) Hayashi, T.; Inoue, Y.; Cyujo, R.; Asanuma, T. *Macromolecules* **1988**, *21*, 2675.

(18) Mizuno, A.; Abiru, T.; Motowoka, M.; Kioka, M.; Onda, M. *J. Appli. Polym. Sci., Appli. Polym. Symp.* **1993**, *52*, 159.

(19) Ewen, J. A., Jones, R. L.; Razavi, A., Ferrara, J. D. *J. Am. Chem. Soc.* **1988**, *110*, 6255.

Chapter 6

Molecular Size of Poly(ethene-*co*-propene) Obtained with Zirconocene and Hafnocene Catalysts

6-1. Introduction

From both industrial and scientific points of view, ethene/propene copolymerization has been carried out with various metallocene catalysts.[1–16] Zambelli *et al.* determined the monomer reactivity ratios in the copolymerization, r_E and r_P (E = ethene, P = propene), with various metallocene catalysts.[3] Soga *et al.* carried out the ethene/propene copolymerization with Cp_2ZrCl_2, *rac*-Et(H_4Ind)$ZrCl_2$ and *i*Pr(Cp)(Flu)$ZrCl_2$.[4] These reports concluded that reactivity of propene (r_P) depended on the symmetry of zirconocene catalysts and decreased in the following order; syndiospecific (C_s-symmetrical) > isospecific (C_2-symmetrical) > aspecific (C_{2v}-symmetrical). The same results were reported by Fink *et al.*, and they explained the tendency by the size difference in the coordination gap aperture of the π-ligands.[5] Chien *et al.* and Lehtinen *et al.* compared bridged and non-bridged metallocenes in the ethene/propene copolymerization and discussed about the polymerization behavior and the microstructures of copolymers obtained.[6,7] In these two reports, the molecular weight of copolymer decreased with the increase of propene in the feed. On the other hand, Sugano *et al.* carried out the ethene/propene copolymerization with *rac*-$Me_2Si(H_4Ind)_2ZrCl_2$ and observed the minimum molecular weight at about 80 mol% of propene in the copolymer.[8]

The author compared zirconocene and hafnocene catalysts for ethene/propene copolymerization, and found a remarkable decrease in molecular size at about 50 mol % of propene content in the copolymer obtained with *ansa*-hafnocene catalysts. The profile of the molecular size was discussed with the chain propagation and chain transfer reaction.

6-2. Experimental Part

Materials

Cp_2MCl_2, *rac*-Et$(Ind)_2MCl_2$, *rac*-$Me_2Si(Ind)_2MCl_2$ (M = Zr, Hf), and *rac*-$Me_2Si(H_4Ind)_2ZrCl_2$ were purchased from Boulder Science Co., Ltd. and Witco Co., Ltd., and used without further purification. MAO was purchased from Tosoh Akzo Co., Ltd., and

used without further purification. Toluene was commercially obtained and dried over molecular sieves 3A.

Ethene/propene copolymerization

Ethene/propene copolymerization was carried out in an agitated 1 L glass flask. The gaseous mixture of ethene and propene was fed to the reactor containing 500 mL of toluene at 40 °C in the feed rate of 760 mL/min. Toluene (10 mL), MAO and a catalyst were mixed in a 100 mL glass flask at 25 °C for 5 min in advance. The molar ratio of (MAO)Al/M (M = Zr, Hf) was adjusted to 1000. After the toluene was saturated with the gaseous mixture, the polymerization was started by adding the catalyst solution to the reactor. Polymerization temperature and monomer feed rate were kept constant during the polymerization. The polymerization was terminated by adding isobutyl alcohol. The obtained polymer was precipitated in large excess of methanol and dried in vacuo at 60 °C for 4 h.

Analytical procedure

^{13}C NMR spectra of ethene/propene copolymers were measured at 67.8 MHz in *o*-dichlorobenzene at 135 °C with a JEOL EX-270 spectrometer. The weight-average molecular size (extended chain length) (A_w (Å)) and MWD (M_w/M_n) of produced polymers were measured at 145 °C by means of GPC (Waters 150CV) using *o*-dichlorobenzene as a solvent and calibrated with standard polystyrene samples. The molecular size was defined as projected chain length on the chain axis of extended chain.

Concentrations of ethene and propene monomers at the polymerization conditions were detected by gas-chromatography.

6-3. Results and Discussion

6-3-1. Ethene/Propene Copolymerization with Cp_2MCl_2 (M = Zr, Hf)

Results of ethene/propene copolymerization with Cp_2MCl_2 are shown in Tables 6-1 and 6-2. Decrease of polymerization activities was observed with an increase of propene in the feed on the whole. Exceptionally, Cp_2ZrCl_2 showed the highest activity at 20 mol % of propene in the feed. In the case of copolymerization with Cp_2HfCl_2, the activity monotonously and drastically decreased with the addition of propene. Plots of weight-average molecular size (A_w) against propene content of the copolymer with Cp_2ZrCl_2 and Cp_2HfCl_2 are shown in Figure 6-1. The molecular size of the copolymers decreased with the increase of propene content. Considering the decrease of polymerization activity with the increase of propene and the feasibility of chain transfer at propene inserted state,[9,10] the decrease of molecular size with the increase of propene content in the copolymer is entirely reasonable. The copolymerization diagrams of ethene/propene with Cp_2MCl_2 are shown in Figure 6-2. Slightly higher

Table 6-1. Results of ethene/propene (EP) copolymerization with Cp_2MCl_2–MAO

Run	M	Cat.[a] (μmol)	P in feed (mol %)	P in medium[b] (mol %)	t[c] (min)	Yield (g)	Activity (kg EP/ molM·h)	P in polymer[d] (mol %)	A_w[e] (Å)	M_w/M_n[e]
1	Zr	9.6	0	0	5	6.2	7800	0	10200	4.5
2		5.8	20	54.9	10	8.6	8900	11.2	2150	7.8
3		7.2	50	82.3	60	29.3	4100	40.4	345	4.6
4		9.2	80	94.7	60	19.9	2200	51.7	86	2.2
5		12.3	100	100	60	6.5	530	100	23	1.6
6	Hf	12.4	0	0	10	8.0	3900	0	13700	2.1
7		15.3	20	54.9	60	16.8	1100	9.7	6740	1.9
8		17.3	50	82.3	60	10.2	560	34.2	1880	2.0
9		17.9	80	94.7	60	3.4	190	74.4	264	2.1
									362[f]	2.8[f]
10		14.2	100	100	60	2.8	200	100	148	1.8
									587[f]	6.7[f]

[a] Amount of catalyst. [b] Determined by gas-chromatography. [c] Polymerization time. [d] Determined by ^{13}C NMR spectroscopy. [e] Determined by GPC. [f] Including the higher molecular weight fraction.

Table 6-2. Monomer sequence distributions of poly(ethene-*co*-propene) and copolymerization profiles with Cp_2MCl_2

Run	[PP] %	[EP]+ [PE] %	[EE] %	[PPP] %	[PPE]+ [EPP] %	[PEP] %	[EPE] %	[PEE]+ [EEP] %	[EEE] %	r_E[a]	r_P[b]	$r_E \cdot r_P$	A_E[c] ($\times 10^{-4}$)	A_P[d] ($\times 10^{-4}$)	A_E/A_P
1			100						100				315	---	
2	1.1	20.2	78.7	---	1.7	2.1	9.5	17.7	69.0	9.49	0.0895	0.85	592	61.5	9.64
3	10.3	60.2	29.5	4.6	9.1	16.2	25.0	27.5	17.6	4.56	0.0736	0.34	225	32.8	6.85
4	20.3	62.6	17.1	9.2	19.8	20.1	22.5	20.7	7.6	9.76	0.0365	0.36	222	12.1	17.5
5	100			100									---	3.91	
										9.27[e]	0.109[e]				
6			100						100				236	---	
7	---	19.4	80.6	---	1.7	1.9	9.4	16.6	70.4	10.1	---	---	74.9	6.60	11.3
8	6.1	56.2	37.7	2.8	9.0	13.2	23.1	27.7	24.2	6.24	0.0467	0.21	36.9	4.13	8.83
9	53.4	42.0	4.6	39.2	18.0	9.2	9.2	6.6	1.5	3.91	0.142	0.56	8.98	1.47	6.12
10	100			100									---	1.46	
										13.3[e]	0.222[e]				

[a] $r_E = 2[EE]/([EP] \cdot X)$: $X = [M_E]/[M_P]$ ($[M_E]$, $[M_P]$ = concentration of ethene and propene (mol/L), respectively). [b] $r_P = 2[PP] \cdot X/[EP]$.

[c] A_E = mol of polymerized ethene/mol M·h $[M_E]$. [d] A_P = mol of polymerized propene/mol M·h $[M_P]$. [e] Calculated from Fineman–Ross plot.

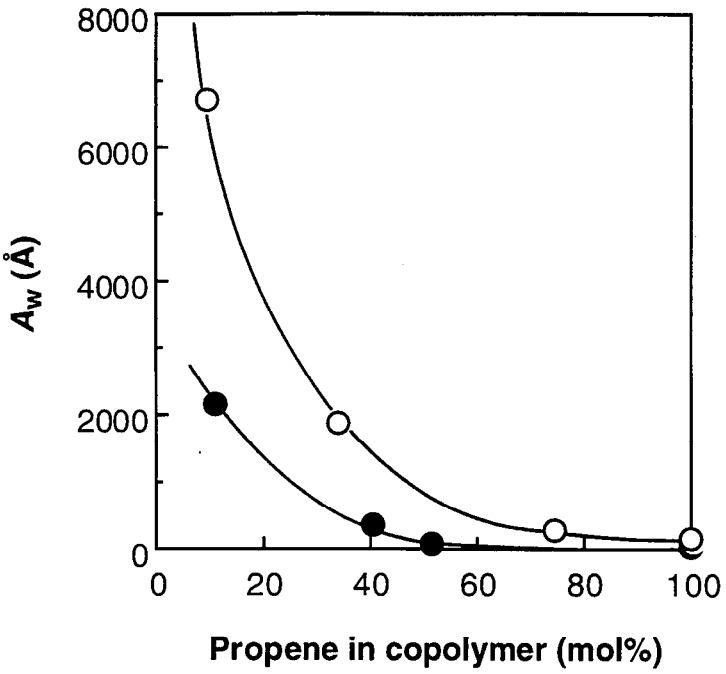

Figure 6-1. Weight-average molecular size (A_w) in dependence on the propene content in EP-copolymer obtained with zirconocene catalysts: (●) Cp_2ZrCl_2; (○) Cp_2HfCl_2.

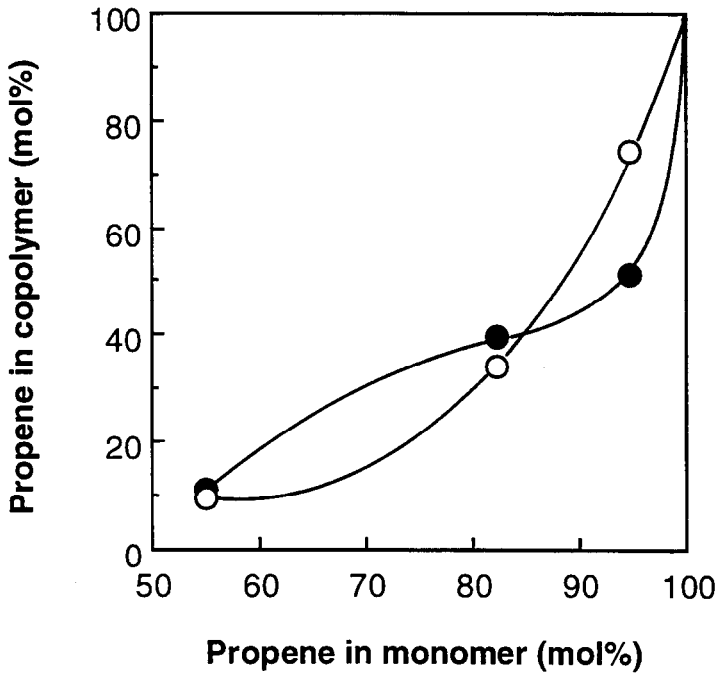

Figure 6-2. Copolymerization diagrams of ethene/propene with metallocene catalysts: (●) Cp_2ZrCl_2; (○) Cp_2HfCl_2.

incorporation of propene was observed with Cp_2ZrCl_2 than with Cp_2HfCl_2 at lower propene in the feed, although the opposite result was observed at 80 mol % of propene in the feed. The reason of this phenomenon is not clear, but reproducibility of the result can be confirmed.

Amounts of polymerized ethene and propene (A_E and A_P) were calculated from the polymer yield and monomer content in the copolymer. The results are summarized in Table 6-2. In the case of copolymerization with Cp_2ZrCl_2, the value of A_E at 20 mol % of propene in the feed was almost twice as high as that of ethene homo-polymerization. The A_E/A_P ratio with Cp_2ZrCl_2 showed the highest value at 80 mol % of propene in the feed (51.7 mol % of propene in the copolymer). In the case of copolymerization with Cp_2HfCl_2, the A_E and A_P values decreased with the increase of propene content. The ratio of A_E to A_P (A_E/A_P) was also decreased with the increase of propene in the feed.

6-3-2. Ethene/Propene Copolymerization with C_2-Symmetrical *ansa*-Metallocene Catalysts

Ethene/propene copolymerization with *rac*-Et(Ind)$_2$MCl$_2$ (M = Zr, Hf) was carried out. The results are summarized in Tables 6-3 and 6-4. The activity in the copolymerization was higher than those in ethene and propene homo-polymerization. Fink *et al.* reported the accelerating effect by α-olefin on the ethene polymerization rate during the ethene/α-olefin copolymerization, and explained this effect by an increase in the concentration of active centers and/or an increase of the rate constant of ethene insertion.[5] This tendency could be explained also by enhancement of the monomer diffusion due to the decrease in crystallinity of the produced polymers.[17] The plots of A_w against propene content of the copolymer with *rac*-Et(Ind)$_2$ZrCl$_2$ and *rac*-Et(Ind)$_2$HfCl$_2$ are shown in Figure 6-3. In the case of using *rac*-Et(Ind)$_2$ZrCl$_2$, the molecular size of obtained polymers decreased with the increase of propene content. On the other hand, the minimum molecular size of copolymer was obtained at 55 mol % of propene content with *rac*-Et(Ind)$_2$HfCl$_2$. Copolymerization diagrams with *rac*-Et(Ind)$_2$MCl$_2$ are shown in Figure 6-4. *rac*-Et(Ind)$_2$HfCl$_2$ was able to incorporate more propene than the zirconocene analog, and this tendency was the same with the results of

ethene/1-butene copolymerization reported by Kaminsky *et al.*[18] The maximum A_E value was observed at 20 mol % of propene in the feed both in *rac*-Et(Ind)$_2$ZrCl$_2$ and *rac*-Et(Ind)$_2$HfCl$_2$ catalysts. While, the A_P value decreased with increase of propene in the feed. The values of A_E/A_P with *rac*-Et(Ind)$_2$ZrCl$_2$ were from 4 to 5 regardless of propene ratio in the feed. In the case of *rac*-Et(Ind)$_2$HfCl$_2$, the values of A_E/A_P decreased remarkably at high molar ratio of propene in the feed.

Table 6-3. Results of ethene/propene (EP) copolymerization with *rac*-Et(Ind)$_2$MCl$_2$–MAO

Run	M	Cat.[a] (μmol)	P in feed (mol %)	P in medium[b] (mol %)	t^c (min)	Yield (g)	Activity (kg EP/ molM·h)	P in polymer[d] (mol %)	A_w[e] (Å)	M_w/M_n[e]
11	Zr	2.4	0	0	60	16.7	7000	0	12700	3.0
12		2.4	20	54.9	60	29.1	12200	21.8	3160	2.2
13		1.9	50	82.3	60	21.2	11100	48.5	1990	2.0
14		4.3	75	92.6	60	45.2	10500	75.5	1570	2.0
15		6.2	90	97.3	30	32.6	10500	88.4	1340	2.0
16		6.5	95	98.8	60	54.0	8400	95.4	1410	2.0
17		7.1	100	100	60	63.6	8900	100	935	2.3
18	Hf	4.4	0	0	60	5.9	1400	0	56400	2.9
19		5.1	20	54.9	40	12.8	3700	24.9	12400	2.3
20		4.8	50	82.3	60	14.8	3100	55.2	7190	2.1
21		5.5	75	92.6	60	14.1	2500	77.4	7810	2.3
22		5.9	90	97.3	60	15.2	2600	92.8	9740	2.2
23		6.5	95	98.8	60	15.8	2400	96.8	11100	2.1
24		5.5	100	100	60	11.7	2100	100	10200	1.9

[a] Amount of catalyst. [b] Determined by gas-chromatography. [c] Polymerization time. [d] Determined by ^{13}C NMR spectroscopy. [e] Determined by GPC.

Table 6-4. Monomer sequence distributions of poly(ethene-*co*-propene) and copolymerization profiles with *rac*-Et(Ind)$_2$MCl$_2$

Run	[PP] %	[EP]+ [PE] %	[EE] %	[PPP] %	[PPE]+ [EPP] %	[PEP] %	[EPE] %	[PEE]+ [EEP] %	[EEE] %	r_E[a]	r_P[b]	$r_E \cdot r_P$	A_E[c] ($\times 10^{-4}$)	A_P[d] ($\times 10^{-4}$)	A_E/A_P
11			100						100				424	---	
12	1.7	40.2	58.1	---	3.4	5.3	17.9	29.3	44.1	3.52	0.0695	0.24	677	155	4.37
13	20.8	55.4	23.8	11.1	17.1	14.6	19.8	24.8	12.6	4.00	0.376	0.64	515	104	4.93
14	56.3	38.5	5.2	40.2	26.2	16.3	8.1	7.9	1.3	3.38	0.234	0.79	365	89.9	4.06
15	78.5	20.2	1.3	73.8	15.2	7.9	1.9	1.2	---	4.71	0.212	1.00	372	77.3	4.81
16	91.0	8.8	0.2	87.4	7.9	4.0	0.5	0.2	---	3.81	0.247	0.73	247	61.0	4.04
17	100			100									---	66.2	
										4.38[e]	0.223[e]				
18			100						100				81.7	---	
19	4.3	41.1	54.5	2.8	8.9	5.9	15.6	27.5	39.3	3.23	0.172	0.56	280	20.0	14.0
20	29.9	50.5	19.6	20.2	21.0	13.7	14.5	20.6	10.1	3.61	0.255	0.92	211	20.8	10.2
21	60.4	34.0	5.6	50.4	21.2	13.5	5.7	7.3	2.0	4.12	0.283	1.17	184	17.1	10.7
22	86.0	13.5	0.5	78.8	12.3	6.8	1.1	1.0	---	2.71	0.348	0.94	55.9	19.6	2.85
23	93.6	6.4	---	94.5	1.8	3.0	0.2	0.5	---	---	0.349	---	49.9	18.0	2.49
24	100			100									---	15.7	
										3.97[e]	0.324[e]				

[a] $r_E = 2[EE]/([EP] \cdot X)$: $X = [M_E]/[M_P]$ ($[M_E]$, $[M_P]$ = concentration of ethene and propene (mol/L), respectively). [b] $r_P = 2[PP] \cdot X/[EP]$.
[c] A_E = mol of polymerized ethene/mol M·h $[M_E]$. [d] A_P = mol of polymerized propene/mol M·h $[M_P]$. [e] Calculated from Fineman–Ross plot.

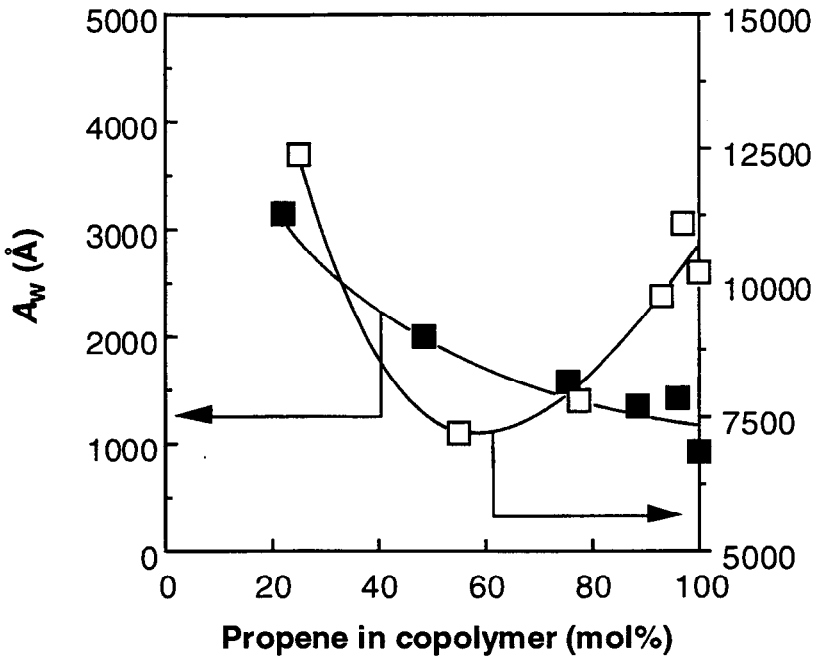

Figure 6-3. Weight-average molecular size (A_w) in dependence on the propene content in EP-copolymer obtained with metallocene catalysts:
(■) *rac*-Et(Ind)$_2$ZrCl$_2$; (□) *rac*-Et(Ind)$_2$HfCl$_2$.

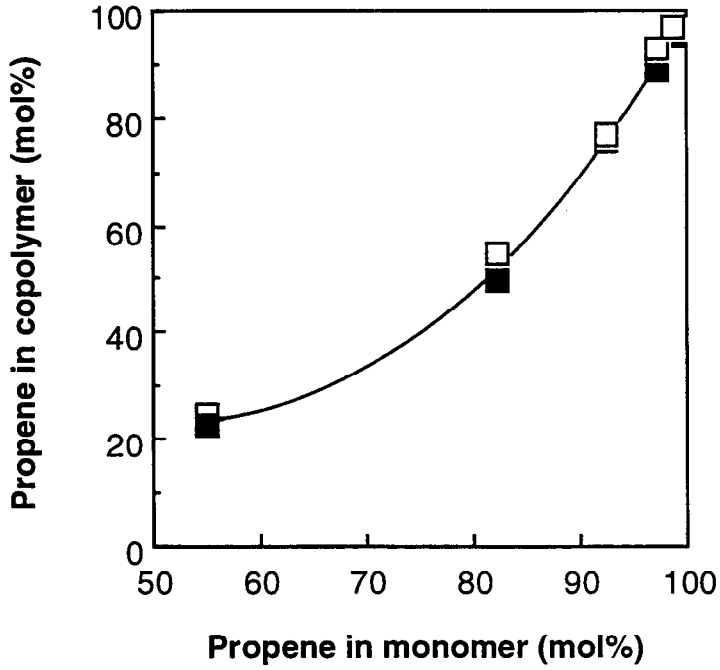

Figure 6-4. Copolymerization diagrams of ethene/propene with metallocene catalysts:
(■) *rac*-Et(Ind)$_2$ZrCl$_2$; (□) *rac*-Et(Ind)$_2$HfCl$_2$.

The copolymerization results with dimethylsilyl-bridged analog, *rac*-$Me_2Si(Ind)_2MCl_2$ (M = Zr, Hf), are shown in Tables 6-5 and 6-6. The tendency of polymerization activity was almost equal to that of *rac*-$Et(Ind)_2MCl_2$. The plots of A_w against propene content of the copolymer with *rac*-$Me_2Si(Ind)_2ZrCl_2$ and *rac*-$Me_2Si(Ind)_2HfCl_2$ are shown in Figure 6-5. The minimum molecular size of copolymer was obtained at 53 mol % of propene content with *rac*-$Me_2Si(Ind)_2HfCl_2$. In the copolymerization with *rac*-$Me_2Si(Ind)_2ZrCl_2$, such the profile of molecular size could not be found clearly. Copolymerization diagrams with *rac*-$Me_2Si(Ind)_2ZrCl_2$ and *rac*-$Me_2Si(Ind)_2HfCl_2$ catalysts are shown in Figure 6-6. The incorporation of propene was almost independent of the metallocene used.

The values of A_E and A_P were also calculated. The dependence of the values on propene in the feed showed almost the same tendency in the case of copolymerization with *rac*-$Et(Ind)_2MCl_2$.

Table 6-5. Results of ethene/propene (EP) copolymerization with *rac*-$Me_2Si(Ind)_2MCl_2$–MAO

Run	M	Cat.[a] (μmol)	P in feed (mol %)	P in medium[b] (mol %)	t^c (min)	Yield (g)	Activity (kg EP/ molM·h)	P in polymer[d] (mol %)	A_w[e] (Å)	M_w/M_n[e]
25	Zr	3.1	0	0	10	6.7	12900	0	46300	4.3
26		3.6	20	54.9	30	22.3	12500	26.6	3830	2.2
27		4.0	50	82.3	60	57.5	14300	55.2	1660	2.1
28		5.1	80	94.7	60	56.6	11000	77.7	1500	2.0
29		4.9	100	100	60	35.0	7100	100	1640	2.0
30	Hf	5.8	0	0	60	3.9	674	0	31200	2.4
31		4.5	20	54.9	60	8.6	1920	26.5	9310	2.3
32		9.0	50	82.3	60	12.1	1350	53.4	4960	2.1
33		10.1	80	94.7	60	10.4	1030	80.3	5390	2.2
34		9.9	100	100	60	5.9	597	100	5920	2.1

[a] Amount of catalyst. [b] Determined by gas-chromatography. [c] Polymerization time. [d] Determined by ^{13}C NMR spectroscopy. [e] Determined by GPC.

Table 6-6. Monomer sequence distributions of poly(ethene-*co*-propene) and copolymerization profiles with *rac*-$Me_2Si(Ind)_2MCl_2$

Run	[PP] %	[EP]+ [PE] %	[EE] %	[PPP] %	[PPE]+ [EPP] %	[PEP] %	[EPE] %	[PEE]+ [EEP] %	[EEE] %	r_E[a]	r_P[b]	$r_E \cdot r_P$	A_E[c] ($\times 10^{-4}$)	A_P[d] ($\times 10^{-4}$)	A_E/A_P
25			100						100				790	---	
26	4.3	44.5	51.2	1.0	4.0	6.3	19.4	28.7	40.6	2.80	0.159	0.44	636	189	3.36
27	25.5	59.3	15.2	13.9	18.7	20.4	20.4	19.1	7.7	2.38	0.185	0.44	562	97.0	5.79
28	58.6	38.2	3.1	50.3	22.2	14.8	7.1	4.6	1.0	2.90	0.172	0.50	452	88.5	5.11
29	100			100									---	52.8	
										2.90[e]	0.191[e]				
30			100						100				41.0	---	
31	4.3	41.1	54.6	2.0	7.0	6.2	16.0	27.7	41.1	3.06	0.220	0.67	98.2	29.1	3.37
32	29.9	50.5	19.6	17.6	20.8	15.1	15.3	20.4	10.8	3.34	0.211	0.70	55.0	13.6	4.05
33	60.4	34.0	5.6	59.2	19.7	11.6	4.1	4.2	1.2	3.84	0.220	0.77	36.9	8.40	4.39
34	100			100									---	4.41	
										3.00[e]	0.201[e]				

[a] $r_E = 2[EE]/([EP]X)$: $X = [M_E]/[M_P]$ ($[M_E]$, $[M_P]$ = concentration of ethene and propene (mol/L), respectively). [b] $r_P = 2[PP]X/[EP]$.

[c] A_E = mol of polymerized ethene/mol M·h $[M_E]$. [d] A_P = mol of polymerized propene/mol M·h $[M_P]$. [e] Calculated from Fineman–Ross plot.

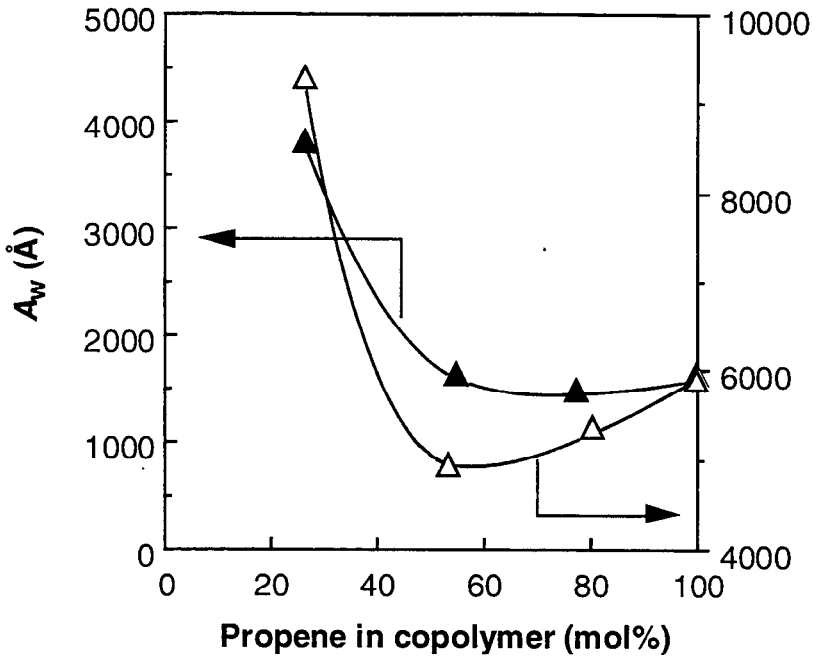

Figure 6-5. Weight-average molecular size (A_w) in dependence on the propene content in EP-copolymer obtained with metallocene catalysts:
(▲) *rac*-$Me_2Si(Ind)_2ZrCl_2$; (△) *rac*-$Me_2Si(Ind)_2HfCl_2$.

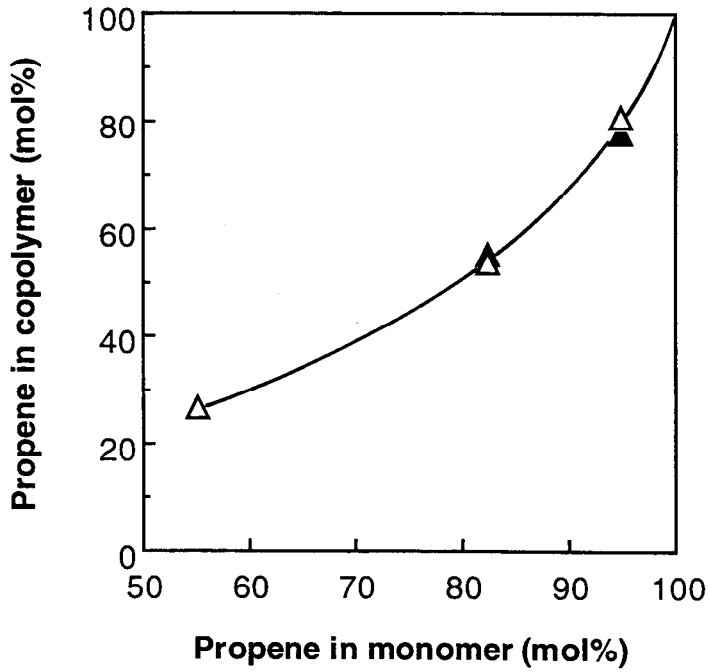

Figure 6-6. Copolymerization diagrams of ethene/propene with metallocene catalysts:
(▲) *rac*-$Me_2Si(Ind)_2ZrCl_2$; (△) *rac*-$Me_2Si(Ind)_2HfCl_2$.

The ethene/propene copolymerization was carried out also with *rac*-$Me_2Si(H_4Ind)_2ZrCl_2$ for a reference. The results are summarized in Table 6-7. The lowest value of A_w, as shown in the copolymerization with *ansa*-hafnocene catalysts, could not be observed in the experiments.

Table 6-7. Results of ethene/propene (EP) copolymerization with *rac*-$Me_2Si(H_4Ind)_2ZrCl_2$–MAO

Run	Cat.[a] (μmol)	P in feed (mol %)	P in medium[b] (mol %)	t[c] (min)	Yield (g)	Activity (kg EP/ molM·h)	P in polymer[d] (mol %)	A_w[e] (Å)	M_w/M_n[e]
35	1.1	0	0	60	4.0	3670	0	44900	2.6
36	3.9	20	54.9	60	20.2	5130	25.8	4430	2.9
37	3.9	50	82.3	60	41.5	10500	57.2	1210	2.5
38	3.9	70	91.1	60	42.7	10800	71.4	886	2.3
39	4.8	80	94.7	60	37.2	7700	79.8	798	2.2
40	5.3	90	97.3	60	34.5	6600	89.4	525	2.2
41	3.9	100	100	60	25.8	6600	100	596	2.1

[a] Amount of catalyst. [b] Determined by gas-chromatography. [c] Polymerization time. [d] Determined by ^{13}C NMR spectroscopy. [e] Determined by GPC.

6-3-3. Chain End Structures of Ethene/Propene Copolymer

Unsaturated end groups (terminated end groups) of obtained copolymers were determined by ^{13}C NMR spectroscopy according to the previous reports.[9,10] The end groups of high molecular size copolymers (A_w is more than 1000 Å) could not be determined under the analysis conditions applied. Four terminated-end groups in ethene/propene copolymer can be considered as shown in Scheme 6-1.[9]

The chain end structures of three samples could be assigned. The results are summarized in Table 6-8. $[PP]_t$ and $[EP]_t$ (as shown in Scheme 6-1 (2) and (4)) were detected in the copolymers with Cp_2ZrCl_2, while only $[PP]_t$ was detected in the case of using *rac*-$Me_2Si(H_4Ind)_2ZrCl_2$. The chain end groups of $[EE]_t$ and $[PE]_t$ could not be observed in these copolymers. The results indicate that the chain transfer reaction should occur at the propene

(1) –E–E terminated chain end: $[EE]_t$

(3) –P–E terminated chain end: $[PE]_t$

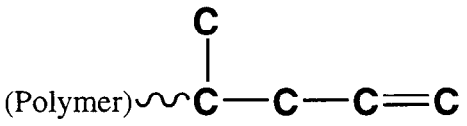

(2) –E–P terminated chain end: $[EP]_t$

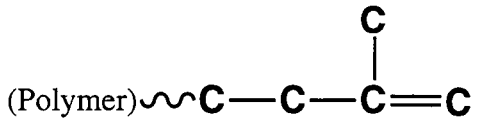

(4) –P–P terminated chain end: $[PP]_t$

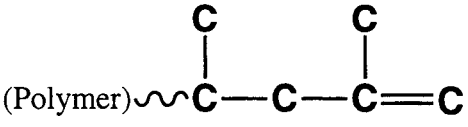

Scheme 6-1. Terminated-end groups of ethene/propene copolymer.

(a)

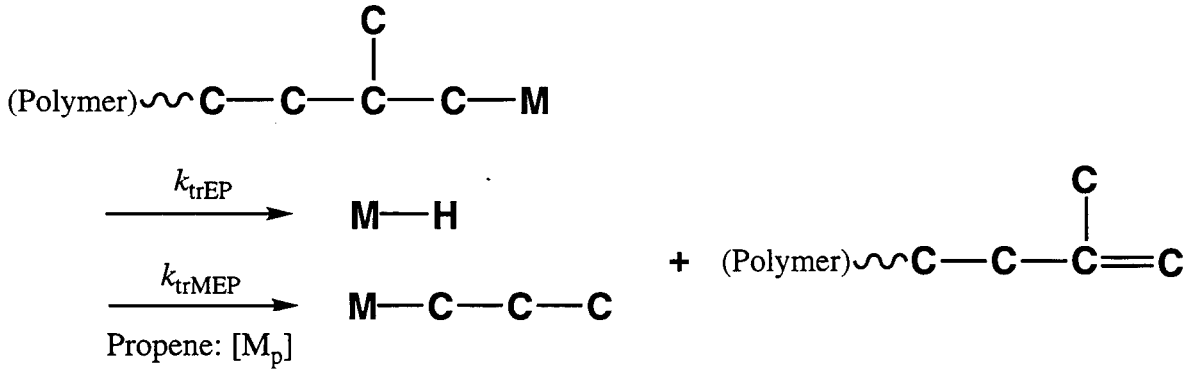

(b)

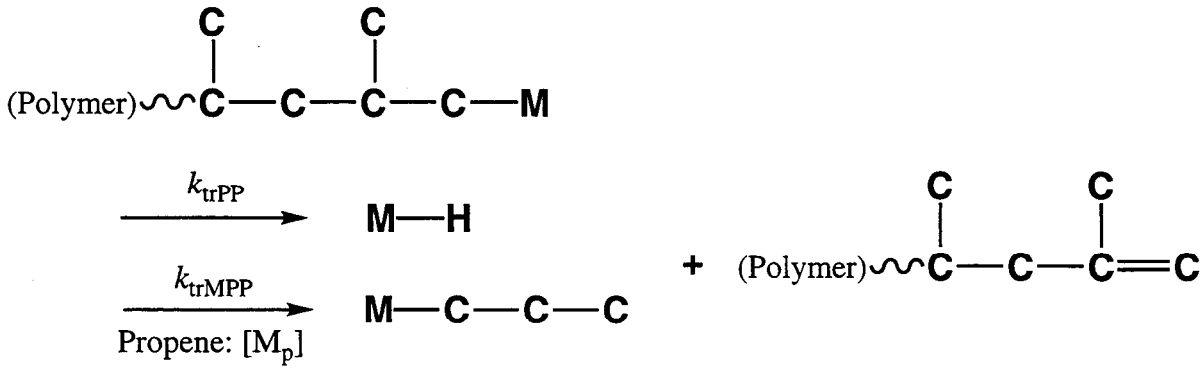

Scheme 6-2. Propene inserted states and chain transfer reactions in ethene/propene copolymerization: (a) E–P–M state; (b) P–P–M state; M = Zr or Hf.

inserted state as described in Scheme 6-2. Assuming that [EP] is equal to [PE] in main chain of the copolymer, where [EP] is ethene–propene sequence derived from a ethene insertion followed by a propene insertion and [PE] is propene–ethene sequence derived from a propene insertion followed by a ethene insertion, the [EP] can be determined as [EP] = 1/2([EP] + [PE]). The [PP]/[EP] values are also shown in Table 6-8. These values are smaller than the values of $[PP]_t/[EP]_t$. It seems reasonable to suppose that chain transfer reaction occurs more frequent at the P–P–Zr state (Scheme 6-2 (b)) than the E–P–Zr state (Scheme 6-2 (a)) in the ethene/propene copolymerizations with Cp_2ZrCl_2 and *rac*-$Me_2Si(H_4Ind)_2ZrCl_2$.

Table 6-8. Chain end structures of poly(ethene-*co*-propene) obtained with Cp_2ZrCl_2 and *rac*-$Me_2Si(H_4Ind)_2ZrCl_2$

Run	Catalyst	[P][a] (mol %)	$[PP]_t$[b] (mol %)	$[EP]_t$[c] (mol %)	$[PP]_t/[EP]_t$	[PP]/[EP][d]
3	Cp_2ZrCl_2	40.4	44.4	55.6	0.80	0.34
4		51.7	59.6	40.4	1.48	0.65
38	*rac*-$Me_2Si(H_4Ind)_2ZrCl_2$	71.4	100	0		2.30

[a] Propene content in the copolymer. [b] Mol% of –P–P terminated end groups. [c] Mol % of –E–P terminated end groups. [d] Molar ratio of P–P sequence to E–P sequence ([EP] = ([EP] + [PE])/2) in the main chain of the copolymer.

The chain end structures of ethene/propene copolymers give important information about chain transfer reaction. However the molecular weights of the copolymers obtained with hafnocene catalysts were too high to analyze the structures. Assuming that chain transfer reaction occurs more frequently at the E–P–M state than at the P–P–M state (M = Hf) in the ethene/propene copolymerization with *ansa*-hafnocene catalysts, the minimum molecular size of resulting copolymer can be explained at about 50 mol % of propene content in the copolymer. The monomer sequence distributions are almost random in the ethene/propene copolymers prepared by *ansa*-hafnocene catalysts, and the copolymer has the highest [EP] content of about 25 mol % at 50 mol % of propene content. If the chain transfer reaction by β-hydrogen elimination is predominant, the copolymer could have minimum molecular size when the chain transfer rate of k_{trEP}[EP] at E–P–M state is larger than that of k_{trPP}[PP] at P–P–M state, where

k_{trEP} and k_{trPP} are, respectively, rate constants of chain transfer by β-hydrogen elimination at E–P–M state and P–P–M state. The same result could be obtained in the case of chain transfer reaction to propene monomer is the main reaction, when the chain transfer rate of $k_{trMEP}[EP][M_p]^a$ at E–P–M state is larger than $k_{trMPP}[PP][M_p]^a$ at P–P–M state, where k_{trMEP}, k_{trMPP}, $[M_p]$, and a are, respectively, rate constant of chain transfer to propene monomer at E–P–M state and P–P–M state, concentration of propene monomer and reaction order.

6-4. Summary

Ethene/propene copolymerization was conducted with various metallocene catalysts combined with MAO. In the case of using non-bridged metallocene catalysts (Cp_2MCl_2: M = Zr, Hf) and C_2-symmetrical *ansa*-zirconocene catalysts (*rac*-$Et(Ind)_2ZrCl_2$, *rac*-$Me_2Si(Ind)_2ZrCl_2$), the molecular size of the resultant copolymers decreased with the increase of propene content. Although, the copolymer prepared by *ansa*-hafnocene catalysts (*rac*-$Et(Ind)_2HfCl_2$, *rac*-$Me_2Si(Ind)_2HfCl_2$) showed the minimum molecular size at about 50 mol % of propene content. The best explanation for this unexpected phenomenon should be found in the chain transfer reaction of the copolymerization. The chain end structures of the copolymers obtained with zirconocene catalysts suggest that comonomer sequence at the propagation chain end affects the chain transfer reaction. However the structures could not be detected by ^{13}C NMR spectroscopy due to the high molecular size of the copolymers obtained with hafnocene catalysts.

References

(1) Kaminsky, W.; Miri, M. *J. Polym. Sci., Polym. Chem. Ed.* **1985**, *23*, 2151.

(2) Kaminsky, W.; Schlobohm, M. *Makromol. Chem., Macromol. Symp.* **1986**, *4*, 103.

(3) Zambelli, A.; Grassi, A. *Makromol. Chem., Rapid Commun.* **1991**, *12*, 523.

(4) Uozumi, T.; Soga, K. *Makromol. Chem.* **1992**, *193*, 823.

(5) Herfert, N.; Montag, P.; Fink, G. *Makromol. Chem.* **1993**, *194*, 3167.

(6) Chien, J. C. W.; He, D. *J. Polym. Sci., Part A: Polym. Chem.* **1991**, *29*, 1585.

(7) Lehtinen, C.; Löfgren, B. *Eur. Polym. J.* **1997**, *33*, 115.

(8) Sugano, T.; Endo, J.; Takahama, T. In *Science and Technology in Catalysis 1994* ; Kodansha Ltd.: Tokyo, 1995; p 371.

(9) Randall, J. C.; Rucker, S. P. *Macromolecules* **1994**, *27*, 2120.

(10) Shiono, T.; Uozumi, T.; Soga, K. *Kobunshi ronbunsyu* **1994**, *51*, 663.

(11) Chien, J. C. W.; He, D *J. Polym. Sci., Part A: Polym. Chem.* **1991**, *29*, 1595.

(12) Herfert, N.; Fink, G. *Makromol. Chem.* **1992**, *193*, 1359.

(13) Koivumäki, J.; Seppälä, J. V. *Polym. Bull.* **1993**, *31*, 441.

(14) Koivumäki, J.; Seppälä, J. V. *Eur. Polym. J.* **1994**, *30*, 1111.

(15) Tsai, W. M.; Chien, J. C. W. *J. Polym. Sci., Part A: Polym. Chem.* **1994**, *32*, 157.

(16) Galimberti, M.; Martini, E.; Piemontesi, F.; Sartori, F.; Camurati, I.; Resconi, L; Albizzati, E. *Makromol. Chem., Macromol. Symp.* **1995**, *89*, 259.

(17) Soga, K.; Ohgizawa, M.; Shiono, T.; Lee, D. H. *Macromolecules* **1991**, *24*, 1699.

(18) Heiland, K.; Kaminsky, W. *Makromol. Chem.* **1992**, *193*, 601.

Chapter 7

Copolymerization of Propene and Nonconjugated Diene with Zirconocene Catalysts

7-1. Introduction

In comparison to conventional heterogeneous Ziegler–Natta catalysts, metallocene catalysts are suitable for homo- and copolymerization of cycloolefins and diolefins. Polyolefins with cyclic groups are excellent materials with high glass transition temperature and high transparency. The properties of these polyolefins can be widely controlled by designing the structures of cyclic groups. From such a point of view, much effort has been focused on copolymerizations and terpolymerizations of olefins with cycloolefins by metallocene catalysts, especially on ethene/cycloolefin copolymers and ethene/propene/cycloolefin terpolymers.[1] Copolymerizations of propene with cycloolefins and dienes with metallocene catalysts have been also conducted.[2] Kaminsky *et al.* and Köller *et al.* investigated the copolymerization of propene and cyclopentene.[1b,2a] Moreover, Henschke *et al.* carried out the copolymerization of propene and norbornene with an isospecific metallocene catalyst and synthesized the polyolefin with high glass transition temperature.[2b]

A disadvantage in homo- and copolymerization of cycloolefins is low productivity, which restricts the synthesis of polyolefins with cyclic groups. Recently, a new method to synthesize the cycloolefin polymers, namely, cyclopolymerization of diolefins, was reported. Waymouth *et al.* performed detailed investigations on the cyclopolymerization of nonconjugated dienes, in particular 1,5-hexadiene, with metallocene catalysts.[3] They succeeded in the synthesis of optically active poly(methylene-1,3-cyclopentane) by enantioselective cyclopolymerization of 1,5-hexadiene with optically active zirconocenes.[4]

Marques *et al.* and Luft *et al.* conducted the ethene/1,5-hexadiene copolymerization with metallocene catalysts.[5] Mülhaupt *et al.* investigated ethene/1,5-hexadiene copolymerization and ethene/styrene/1,5-hexadiene terpolymerization with CGC (constrained geometry catalyst).[6] Copolymerizations of propene and nonconjugated dienes with stereospecific metallocene catalysts seem to be useful method to synthesize polypropene with cyclic groups and to study the mechanism of stereoselectivity in the insertion and cyclization of dienes.

In this chapter, the author reported propene/1,5-hexadiene and propene/1,7-octadiene copolymerizations with stereospecific metallocene catalysts of *rac*-$Me_2Si(Ind)_2ZrCl_2$ and

$Ph_2C(Cp)(Flu)ZrCl_2$. Furthermore, microstructures of the resulting copolymers were studied in detail to confirm the mechanism of propene/nonconjugated diene copolymerization.

7-2. Experimental Part

Materials

Zirconocene complexes, *rac*-$Me_2Si(Ind)_2ZrCl_2$ and $Ph_2C(Cp)(Flu)ZrCl_2$, were purchased from Witco Co., Ltd., and Boulder Science Co., Ltd., respectively, and used without further purification. MAO was donated from Tosoh Akzo Co., Ltd., and used without further purification. Propene (from Mitsubishi Petrochemical Co., Ltd.) was purified by passing it through columns of NaOH, P_2O_5, and molecular sieves 3A. 1,5-Hexadiene, 1,7-octadiene and toluene were commercially obtained and dried with CaH_2.

Copolymerizations of Propene and Nonconjugated Dienes

Copolymerizations of propene and dienes (1,5-hexadiene, 1,7-octadiene) were conducted in a 300 mL glass reactor equipped with a magnetic stirrer. Toluene and a diene (toluene + diene = 190 mL) were added to the reactor. Propene was introduced into the reactor at 40 °C under 1 atm until the solvent was saturated with propene. The amount of dissolved propene was monitored by a gas flow meter to determine the propene concentration in the reaction medium. Toluene solution of MAO (6 mmol of [Al] in 10 mL of solution) and a metallocene catalyst were premixed in a 100 mL glass flask at 25 °C for 5 min. Polymerization was started by introducing the premixed catalyst solution into the reactor. Polymerization was terminated by adding a small amount of methanol. The reaction medium was filtered to remove the catalyst residues. The resultant polymer was obtained by evaporation of filtrate and dried in vacuo at 60 °C for 6 h.

Analytical Procedure

M_n and MWD (M_w/M_n) of the produced polymers were measured at 140 °C by means of GPC (Waters 150C) using *o*-dichlorobenzene as a solvent and calibrated with standard

polystyrene samples. ^{1}H NMR, ^{13}C NMR, and distortionless enhancement by polarization transfer (DEPT) spectra were recorded at 130 °C using a JEOL EX-400 NMR spectrometer in the pulse Fourier transfer (FT) mode. Polymers were dissolved in 1,1,2,2-tetrachloroethane-d_2 (2 wt % for ^{1}H NMR and up to 10 wt % for ^{13}C NMR and DEPT). In the ^{1}H NMR measurements, the pulse angle was 45 °, and 50–100 scans were accumulated in 7 s of pulse repetition. In the ^{13}C NMR measurements, the pulse angle was 45 °, and 1000–1500 scans were accumulated in 5.4 s of pulse repetition. In the DEPT measurements, the pulse angle was 135 °, and 1000–1500 scans were accumulated in 5.4 s of pulse repetition. DSC measurements were made on a Seiko DSC-220 (Seiko Instruments Inc., Tokyo) at a heating rate of 10 °C/min after previous heating to 200 °C and cooling to –50 °C by 10 °C/min.

7-3. Results and Discussion

7-3-1. Copolymerization of Propene and 1,5-Hexadiene.

Copolymerization of propene and 1,5-hexadiene was conducted at 40 °C with the isospecific zirconocene, *rac*-$Me_2Si(Ind)_2ZrCl_2$, and the syndiospecific zirconocene, $Ph_2C(Cp)(Flu)ZrCl_2$. The results are summarized in Tables 7-1 and 7-2. The rate of polymerization (R_p) decreased with an increase of 1,5-hexadiene in the monomer in both systems. The molecular weight of copolymer obtained with $Ph_2C(Cp)(Flu)ZrCl_2$ decreased with the increase of 1,5-hexadiene in the monomer, besides, no clear tendency was found in the case of using *rac*-$Me_2Si(Ind)_2ZrCl_2$.

1,5-Hexadiene content in the copolymers was determined by ^{1}H NMR spectroscopy according to the literature.[7] Copolymerization diagrams of propene/1,5-hexadiene with *rac*-$Me_2Si(Ind)_2ZrCl_2$ and $Ph_2C(Cp)(Flu)ZrCl_2$ are shown in Figure 7-1. A consistently higher incorporation of 1,5-hexadiene was observed with $Ph_2C(Cp)(Flu)ZrCl_2$ than with *rac*-$Me_2Si(Ind)_2ZrCl_2$. This tendency is in good agreement with the results of propene/1-hexene copolymerization, which was conducted with specific catalysts by Soga *et al.*[8]

^{13}C NMR and DEPT (distortionless enhancement by polarization transfer) (135 °) spectra of the copolymer obtained with *rac*-$Me_2Si(Ind)_2ZrCl_2$ in run 5 are shown in Figure 7-2, (a) and

Table 7-1. Results of propene/1,5-hexadiene (HD) copolymerization with *rac*-$Me_2Si(Ind)_2ZrCl_2$–MAO[a]

Run	HD in monomer (mol %)	t[b] (min)	Yield (g)	R_p[c]	HD in polymer[d] (mol %)	Conversion of HD (%)	T_m[e] (℃)	T_g[f] (℃)	M_n[g] (×10^{-4})	M_w/M_n[g]
1	0	30	8.7	8700	0		141.9	-18.7	1.9	2.6
2	6.9	30	6.5	6500	3.1	55.4	116.8	-9.6	2.1	2.6
3	12.9	30	4.2	4200	4.9	27.9	99.9	-8.4	2.0	3.0
4	27.5	30	2.3	2300	15.6	17.7		-6.9	1.9	2.9
5	43.2	60	4.3	2000	26.4	25.6		-3.1	2.6	3.9
6	61.1	60	1.7	860	43.3	7.4		-1.0	1.9	3.1
7	81.3	60	1.2	600	64.8	2.7		1.0	2.9	3.0
8[h]	100	30	8.4	8400	100	60.7		24.6		

[a] Polymerization conditions: Zr = 2.0 μmol, molar ratio of (MAO)Al/Zr = 3000, 1,5-hexadiene + toluene = 200 mL, propene = 1 atm, polymerization temperature = 40 ℃. [b] Polymerization time. [c] Rate of polymerization (kg polymer/mol Zr·h). [d] Determined by ^{13}C NMR spectroscopy. [e] Melting temperature. [f] Glass transition temperature. [g] Determined by GPC using polystyrene standards. [h] 1,5-Hexadiene (20 mL) + toluene (180 mL).

Table 7-2. Results of propene/1,5-hexadiene (HD) copolymerization with $Ph_2C(Cp)(Flu)ZrCl_2$–MAO[a]

Run	HD in monomer (mol %)	t[b] (min)	Yield (g)	R_p[c]	HD in polymer[d] (mol %)	Conversion of HD (%)	T_m[e] (℃)	T_g[f] (℃)	M_n[g] (×10^{-4})	M_w/M_n[g]
9	0	60	4.0	2000	0		125.6 115.6	-2.0	13.6	2.7
10	6.9	30	1.1	1100	5.8	17.0	107.4 91.6	-3.3	8.2	2.7
11	12.9	30	0.83	830	11.3	11.9		-2.2	5.8	2.6
12	27.5	60	1.2	580	25.5	13.9		-1.2	4.2	2.8
13	43.2	60	1.0	500	33.8	7.2		1.8	3.5	2.6
14	61.1	60	0.90	450	50.3	4.3		-1.9	1.7	2.8
15	81.3	60	0.40	200	72.5	1.0		5.2	2.2	2.0
16[h]	100	60	0.41	210	100	3.0		1.8	1.8	3.3

[a] Polymerization conditions: Zr = 2.0 μmol, molar ratio of (MAO)Al/Zr = 3000, 1,5-hexadiene + toluene = 200 mL, propene = 1 atm, polymerization temperature = 40 ℃. [b] Polymerization time. [c] Rate of polymerization (kg polymer/mol Zr·h). [d] Determined by ^{13}C NMR spectroscopy. [e] Melting temperature. [f] Glass transition temperature. [g] Determined by GPC using polystyrene standards. [h] 1,5-Hexadiene (20 mL) + toluene (180 mL).

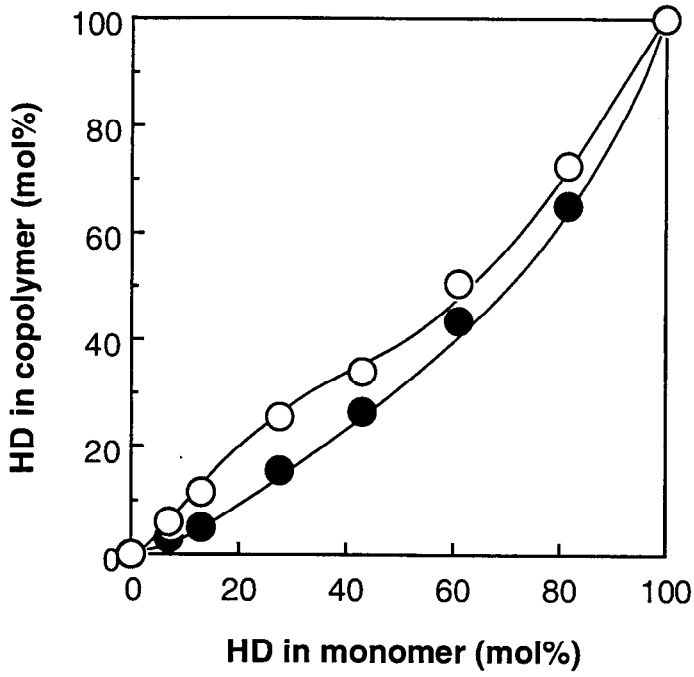

Figure 7-1. Copolymerization diagrams of propene/1,5-hexadiene with *rac*-$Me_2Si(Ind)_2ZrCl_2$ (●) and $Ph_2C(Cp)(Flu)ZrCl_2$ (○).

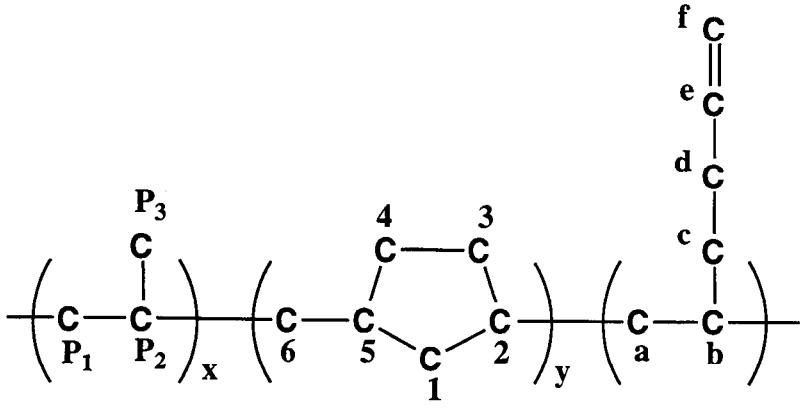

Scheme 7-1. Propene/1,5-hexadiene copolymer.

(b), respectively. Scheme 7-1 shows the corresponding structures of propene/1,5-hexadiene copolymer. The resonances of 20.0–22.2 (P_3), 28.9, 30.2, 31.4 (P_2), 45.1 (P_1 of Pr–MCP sequence), and 46.6 (P_1 of Pr-Pr sequence) ppm, (where Pr = propene and MCP = methylene-1,3-cyclopentane), are assigned to propene units in the copolymer. The resonances at 32.4–33.0 (*cis*-3,4), 33.6–34.2 (*trans*-3,4), 37.0, 38.4, 39.8 (2,5), 40.4 (*trans*-1), 41.7 (*cis*-1), 44.3 (6 of MCP-MCP sequence), and 45.1 (6 of Pr-MCP sequence) ppm are assignable to

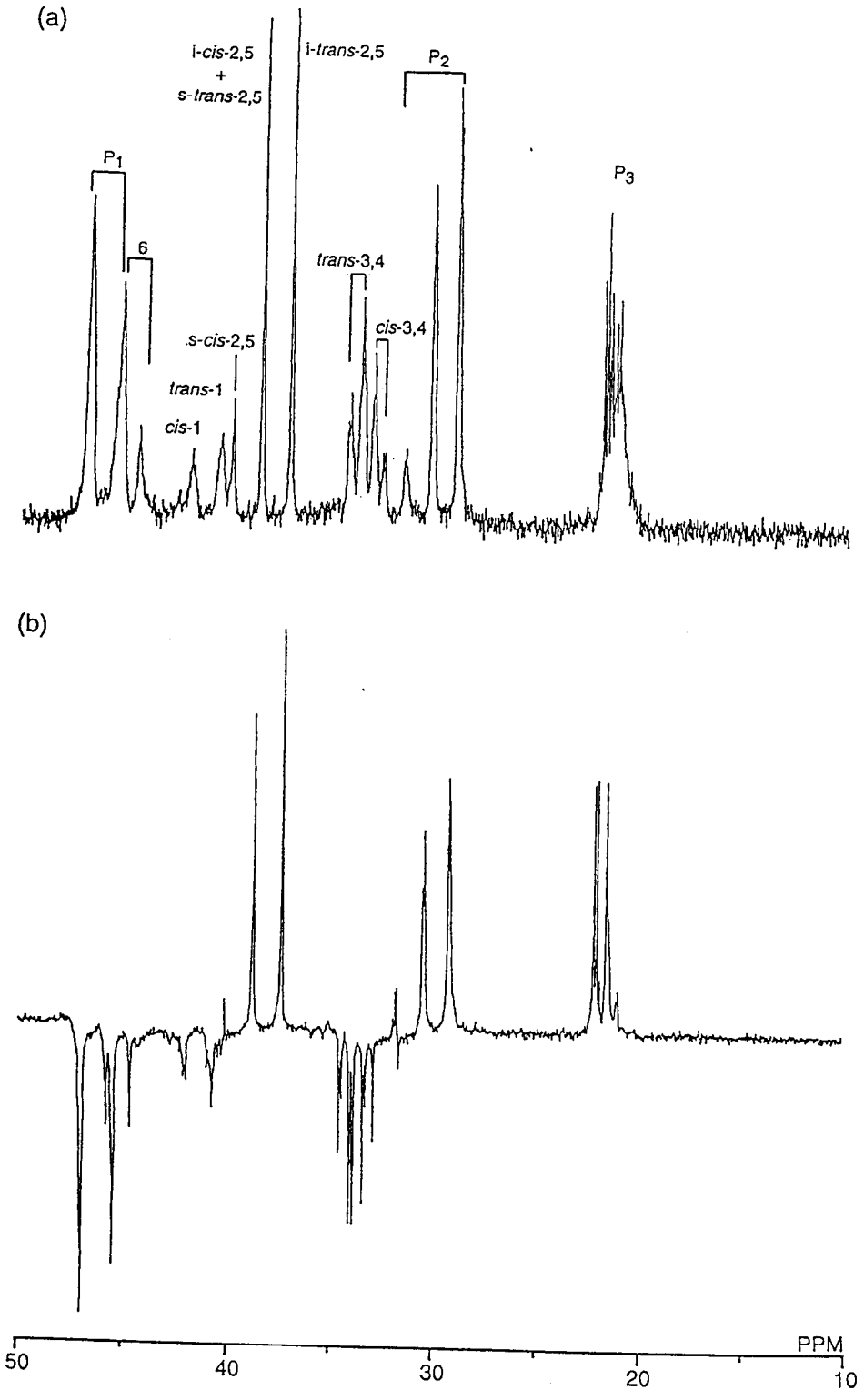

Figure 7-2. ^{13}C NMR spectrum (a) and DEPT spectrum (b) of propene/1,5-hexadiene copolymer obtained with *rac*-$Me_2Si(Ind)_2ZrCl_2$ (run 5).

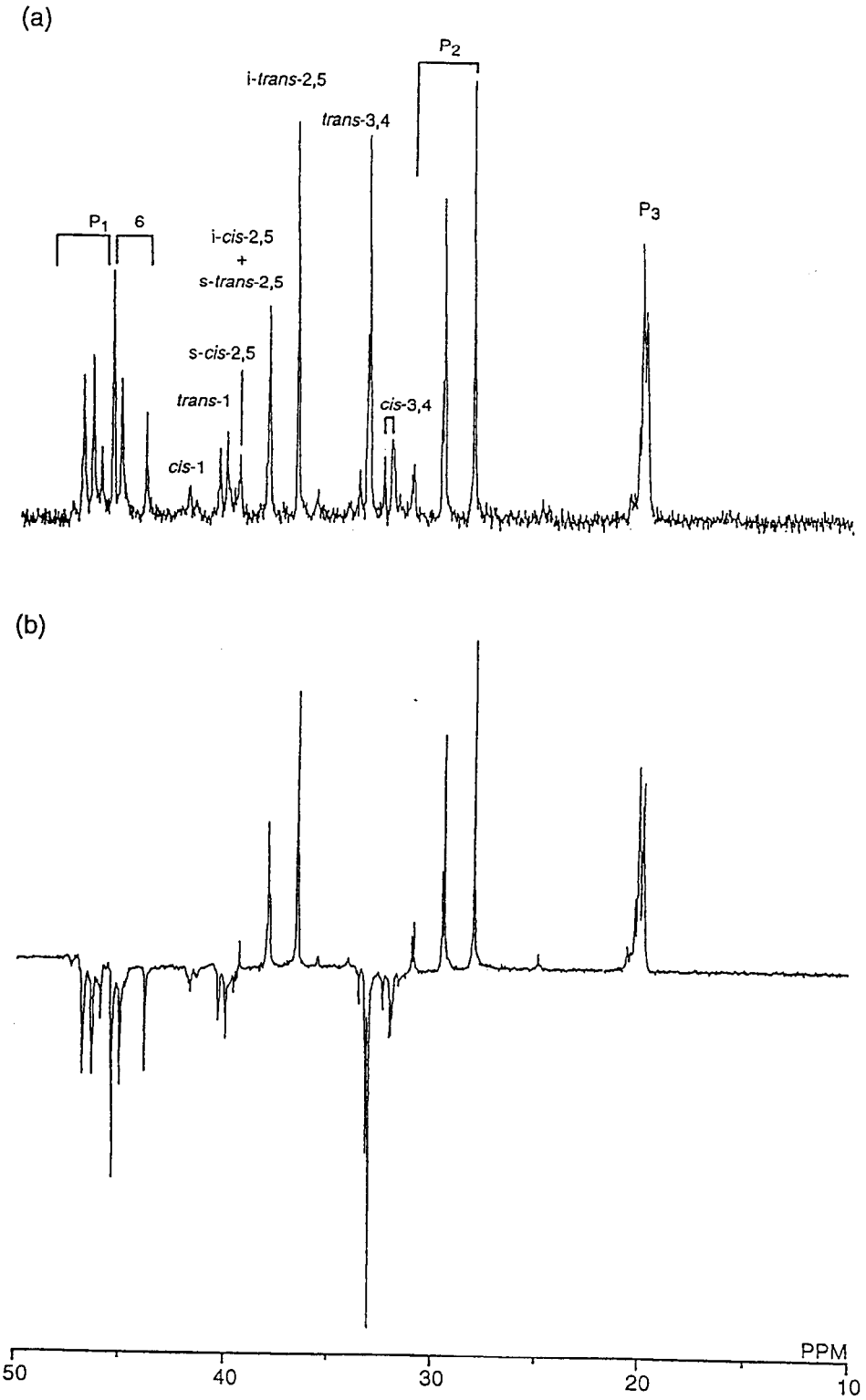

Figure 7-3. ^{13}C NMR spectrum (a) and DEPT spectrum (b) of propene/1,5-hexadiene copolymer obtained with $Ph_2C(Cp)(Flu)ZrCl_2$ (run 13).

cyclic units of MCP derived from the intramolecular cyclization of 1,5-hexadiene.[9] ^{13}C NMR and DEPT (135 °) spectra of the copolymer obtained with $Ph_2C(Cp)(Flu)ZrCl_2$ in run 13 are shown in Figure 7-3, (a) and (b), respectively. The resonances can be assigned according to the method described above.

To characterize the microstructures of propene/1,5-hexadiene copolymers more precisely, ^{13}C NMR spectra of the copolymers with different 1,5-hexadiene contents were investigated. The microstructures of propene/1,5-hexadiene copolymer obtained with *rac*-$Me_2Si(Ind)_2ZrCl_2$ and $Ph_2C(Cp)(Flu)ZrCl_2$ are summarized in Tables 7-3 and 7-4, respectively. The average [*cis*]/[*trans*] molar ratios of MCP units in these copolymers are 35.8/64.2 with *rac*-$Me_2Si(Ind)_2ZrCl_2$ and 31.7/68.3 with $Ph_2C(Cp)(Flu)ZrCl_2$. Waymouth *et al.* reported the effect of metallocene structures on the diastereoselectivity (selectivity of *cis*-cyclization or *trans*-cyclization) in the 1,5-hexadiene polymerization with various zirconocene catalysts.[4d] They concluded that diastereoselectivity in cyclopolymerization of 1,5-hexadiene was affected by the bulkiness of ligand and bite angle associated with the zirconocene catalyst precursors rather than by the symmetry of the zirconocene precursors. Moreover, Cavallo *et al.* carried out conformational calculations about the diastereoselectivity and reported a good agreement with the polymerization results.[3d] The results of propene/1,5-hexadiene copolymerization with *rac*-$Me_2Si(Ind)_2ZrCl_2$ (C_2-symmetrical) and $Ph_2C(Cp)(Flu)ZrCl_2$ (C_s-symmetrical) described above agree with their studies.

Conformational structures of isolated MCP units give important information about the enantioselectivity of propene and 1,5-hexadiene insertion mechanism. Figures 7-4 and 7-5 show ^{13}C NMR spectra of the copolymers with low 1,5-hexadiene content prepared by *rac*-$Me_2Si(Ind)_2ZrCl_2$ (run 3) and $Ph_2C(Cp)(Flu)ZrCl_2$ (run 11), respectively. In these figures, the absence of a resonance at around 44.3 ppm, which is observed when the cyclic 1,5-hexadiene units are adjacent to one another, indicates that all the 1,5-hexadiene units are separated by propene units in the copolymers. No resonance is observed at 31.4 ppm in either Figures 7-4 or 7-5, and the resonances at 28.9 and 30.2 could be assigned to the P_2 carbons of underlined propene units as Pr–<u>Pr</u>–Pr and Pr–<u>Pr</u>–MCP sequence, respectively. The resonances at 37.0, 38.4, and 39.8 ppm, which are observed in Figures 7-2 and 7-3, are

Table 7-3. Microstructures of 1,5-hexadiene (HD) units in poly(propene-*co*-HD) obtained with *rac*-$Me_2Si(Ind)_2ZrCl_2$–MAO

Run	Propene (mol/L)	HD (mol/L)	*cis*[a] (%)	*trans*[a] (%)	Isolated-*cis*		Isolated-*trans*		[C][c] (%)	Δ[C][d] (%)
					m[b] (%)	r[b] (%)	m[b] (%)	r[b] (%)		
2	0.568	0.042	35.1	65.9	100	0	50	50	95.5	
3	0.567	0.084	35.7	64.3	100	0	50	50	94.7	
4	0.561	0.211	33.6	66.4					94.6	3.7
5	0.553	0.421	35.4	64.6					93.1	4.0
6	0.535	0.842	37.8	62.2					91.7	5.1
7	0.484	2.106	37.7	62.3					88.6	4.2
8	---	0.842	29.5	70.5					96.8	

[a] Determined by ^{13}C NMR spectroscopy. [b] Determined by ^{13}C NMR spectroscopy (see Scheme 7-2). [c] Cyclization selectivity determined by ^{1}H NMR spectroscopy. [d] Δ[C] = (cyclization selectivity in homopolymerization of 1,5-hexadiene) – (cyclization selectivity in copolymerization, [C]).

Table 7-4. Microstructures of 1,5-hexadiene (HD) units in poly(propene-*co*-HD) obtained with $Ph_2C(Cp)(Flu)ZrCl_2$–MAO

Run	Propene (mol/L)	HD (mol/L)	*cis*[a] (%)	*trans*[a] (%)	Isolated-*cis*		Isolated-*trans*		[C][c] (%)	Δ[C][d] (%)
					m[b] (%)	r[b] (%)	m[b] (%)	r[b] (%)		
10	0.568	0.042	31.3	68.7	46	54	7	93	98.8	
11	0.567	0.084	30.6	69.4	46	54	8	92	98.6	
12	0.561	0.211	31.4	68.6					98.2	0.2
13	0.553	0.421	31.3	68.7					98.1	–0.1
14	0.535	0.842	32.0	68.0					96.3	0.6
15	0.484	2.106	33.7	66.3					93.8	–0.1
16	---	0.842	32.5	67.5					96.9	

[a] Determined by ^{13}C NMR spectroscopy. [b] Determined by ^{13}C NMR spectroscopy (see Scheme 7-2). [c] Cyclization selectivity determined by ^{1}H NMR spectroscopy. [d] Δ[C] = (cyclization selectivity in homopolymerization of 1,5-hexadiene) – (cyclization selectivity in copolymerization, [C]).

assignable to i-*trans*, i-*cis* + s-*trans*, and s-*cis* of 2,5 carbons (i = isolation, s = sequence) in the MCP units. There are three resonances at 33.0, 33.4, and 34.2 ppm derived from 3,4 carbons of MCP units in Figure 7-4, while, there are four resonances derived from the corresponding carbons at 32.4, 32.8, 33.5, and 34.0 ppm in Figure 7-5.[9]

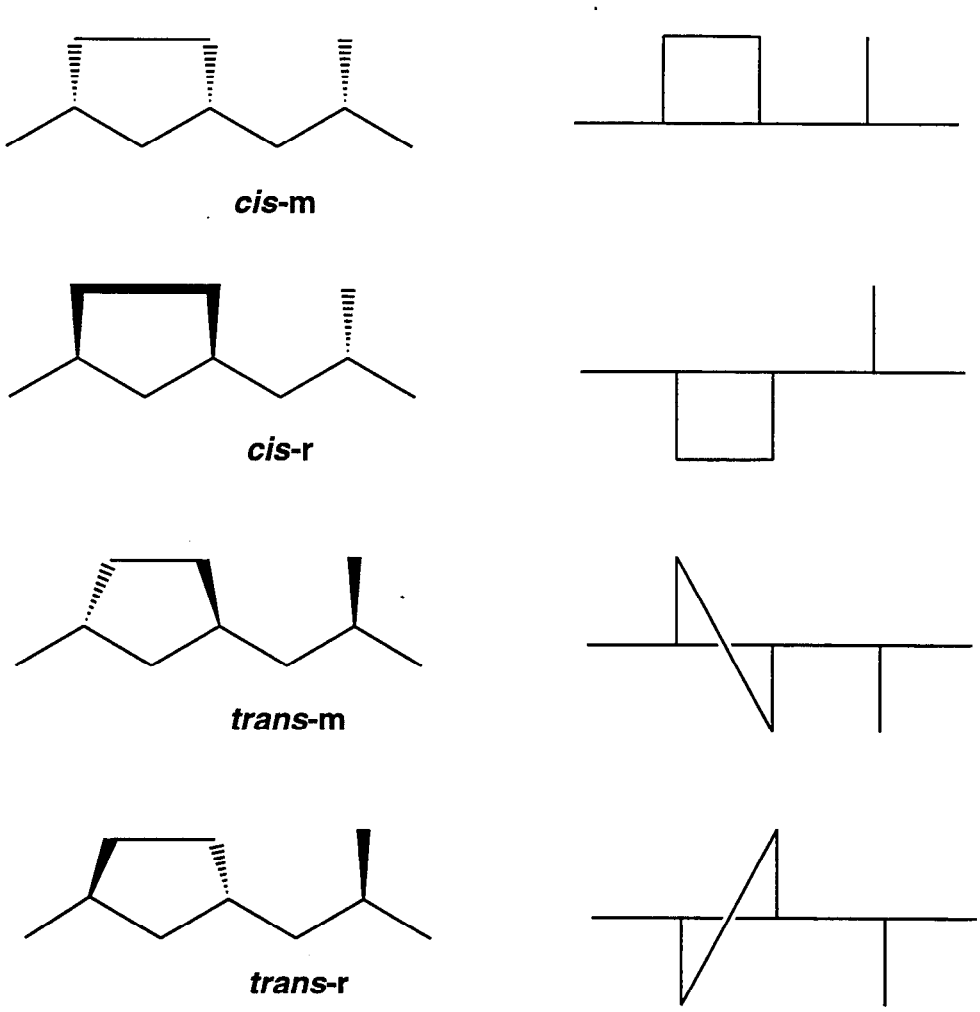

Scheme 7-2. Stereoregulations of mehylene-1,3-cylopentane (MCP) units next to propene units.

The author defines stereoregulations of 3,4 carbons in the isolated MCP units next to propene units as *cis*-m, *cis*-r, *trans*-m, and *trans*-r as shown in Scheme 7-2. Assuming that the enantiomorphic-site control of propene insertion and 1,2-insertion of 1,5-hexadiene proceeds with *rac*-$Me_2Si(Ind)_2ZrCl_2$ as shown in Scheme 7-3 (a) (*si* insertion of (*S*,*S*)-*rac*-$Me_2Si(Ind)_2ZrCl_2$ was applied), *cis*-m, *trans*-m, and *trans*-r can be formed with the same

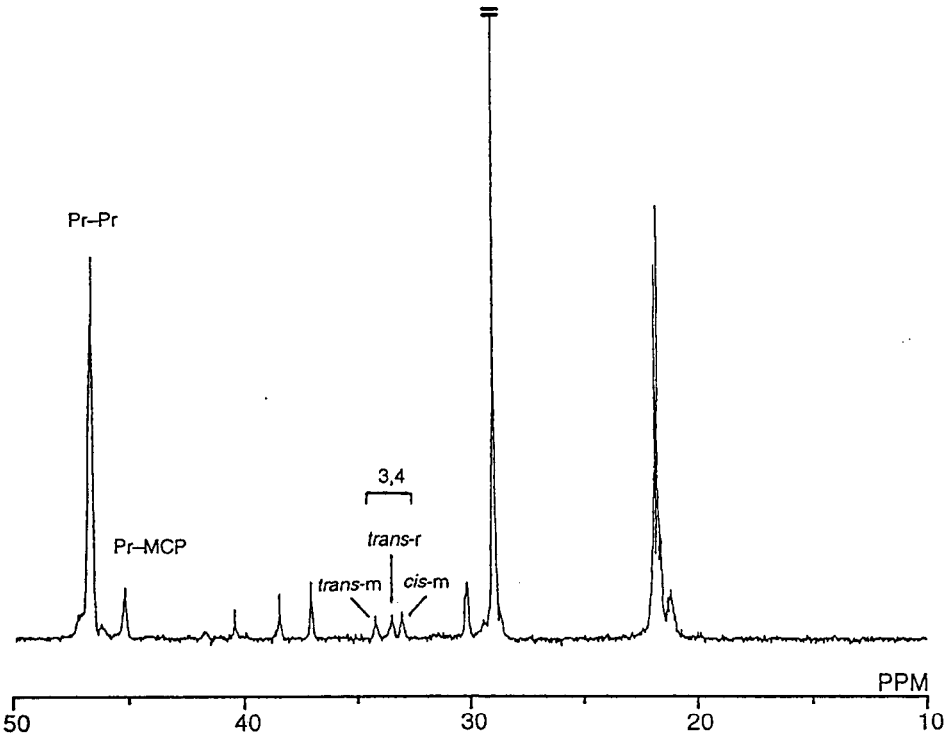

Figure 7-4. ^{13}C NMR spectrum of propene/1,5-hexadiene copolymer obtained with *rac*-$Me_2Si(Ind)_2ZrCl_2$ (run 3).

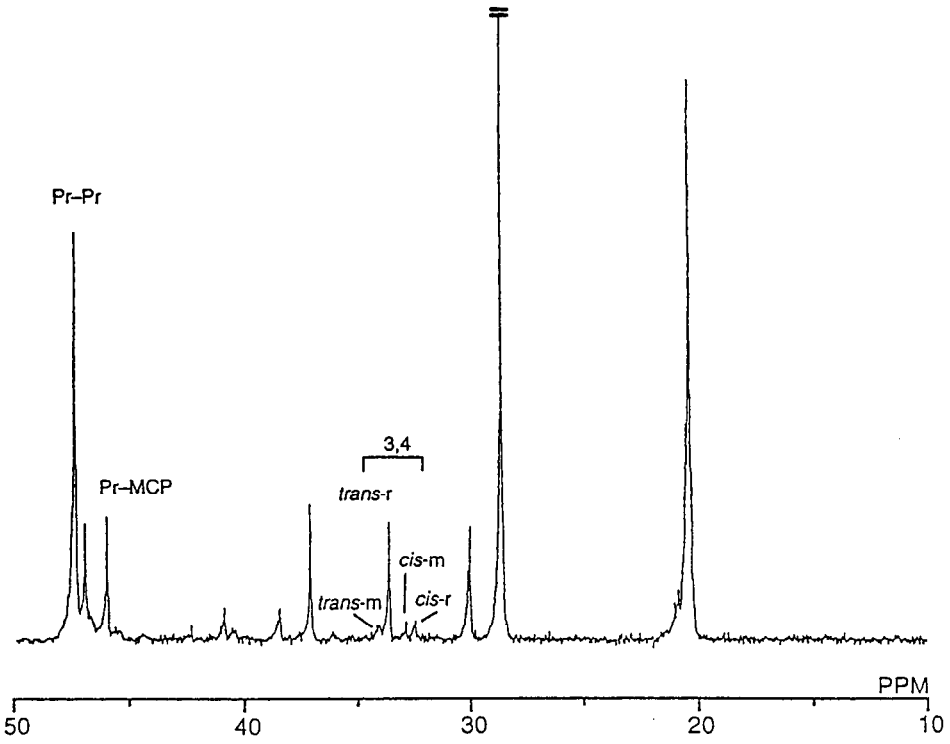

Figure 7-5. ^{13}C NMR spectrum of propene/1,5-hexadiene copolymer obtained with $Ph_2C(Cp)(Flu)ZrCl_2$ (run 11).

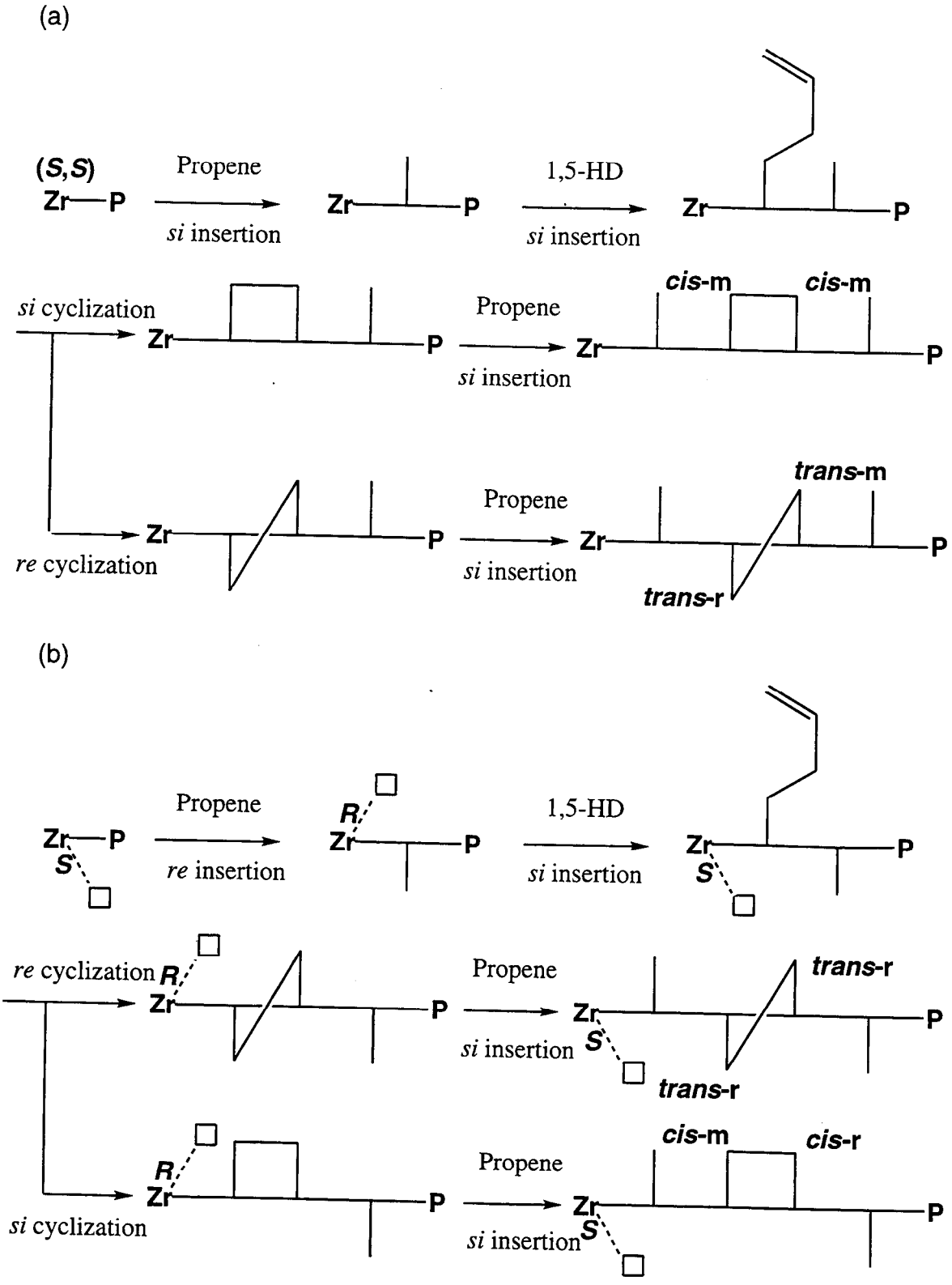

Scheme 7-3. Cyclization mechanisms of 1,5-hexadiene in propene/1,5-hexadiene copolymerization with *rac*-$Me_2Si(Ind)_2ZrCl_2$ (a) and $Ph_2C(Cp)(Flu)ZrCl_2$ (b).

intensity of *trans*-m and *trans*-r. In the same way, the copolymerization with $Ph_2C(Cp)(Flu)ZrCl_2$ proceeds syndiospecifically as shown in Scheme 7-3 (b), *cis*-m and *cis*-r units can be formed together with *trans*-r unit.

Judging from the chemical shifts and intensities of resonances in Figures 7-4 and 7-5, the resonances of 32.4, 32.8–33.0, 33.4–33.5 and 34.0–34.2 were assigned to isolated-3,4 carbons of *cis*-r, *cis*-m, *trans*-r, and *trans*-m units, respectively. In the case of using isospecific *rac*-$Me_2Si(Ind)_2ZrCl_2$, all of *cis* units are m type, and the molar ratio of *trans*-m to *trans*-r is almost 1 as shown in Figure 7-4. These results indicate that the enantiomorphic-site control of propene insertion and 1,2-insertion of 1,5-hexadiene proceeded as shown in Scheme 7-3 (a) with *rac*-$Me_2Si(Ind)_2ZrCl_2$. If the propene insertion and 1,2-insertion of 1,5-hexadiene are perfectly controlled through the syndiospecific polymerization with $Ph_2C(Cp)(Flu)ZrCl_2$, no *trans*-m unit should be observed, and ratio of *cis*-m to *cis*-r should be 1 in the copolymer (Scheme 7-3 (b)). The molar ratio of [*cis*-m]/[*cis*-r] is 46/54 and [*trans*-m]/[*trans*-r] is 8/92 in the copolymer obtained with $Ph_2C(Cp)(Flu)ZrCl_2$ as shown in Figure 7-5. The [r] dyad in the syndiotactic polypropene with $Ph_2C(Cp)(Flu)ZrCl_2$ (run 9) is 98%. The author can suggest two mechanisms for the less stereoselectivity of 3,4 carbons in the isolated MCP units in the copolymer. One is that a propene insertion after the MCP units is less enantioselective in the copolymerization with $Ph_2C(Cp)(Flu)ZrCl_2$. The other is the chain migration of propagating chain end at MCP units to the another vacant site of $Ph_2C(Cp)(Flu)ZrCl_2$ without a propene insertion.

The effect of 1,5-hexadiene concentration on cyclization selectivity was discussed. Figure 7-6 shows the relationship between the cyclization selectivity ([C] = mole percent of cyclic units in the incorporated 1,5-hexadiene) and the 1,5-hexadiene concentration in the monomer. The results of 1,5-hexadiene homopolymerization with *rac*-$Me_2Si(Ind)_2ZrCl_2$ and $Ph_2C(Cp)(Flu)ZrCl_2$ are plotted for references.[10] The cyclization selectivity decreased with an increase of the 1,5-hexadiene concentration in both 1,5-hexadiene homopolymerization and propene/1,5-hexadiene copolymerization. It is quite reasonable that insertion of another 1,5-hexadiene monomer is preferred to the cyclization of the 1,2-inserted unit under the high 1,5-hexadiene concentration. Mülhaupt *et al.* reported the same phenomenon in the 1,5-hexadiene

polymerization with CGC.[6] Δ[C] values, which are summarized in Tables 7-3 and 7-4, mean the differences of cyclization selectivity between homopolymerization[10] and copolymerization at the same 1,5-hexadiene concentration in the monomer. No difference in the cyclization selectivity was observed between homopolymerization and copolymerization with $Ph_2C(Cp)(Flu)ZrCl_2$. On the other hand, the cyclization selectivities in the copolymerization with *rac*-$Me_2Si(Ind)_2ZrCl_2$ is lower than those in homopolymerization (Δ[C] = 3.7–5.1 mol %). This result indicates that propene insertion could disturb the cyclization of the 1,2-inserted 1,5-hexadiene unit in the copolymerization with *rac*-$Me_2Si(Ind)_2ZrCl_2$.

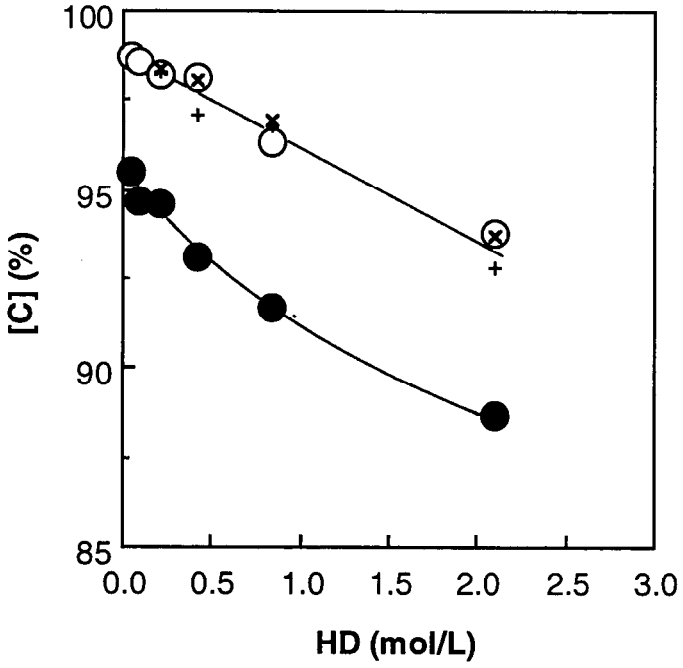

Figure 7-6. Plots of [C] (mole percent of cyclic units) against 1,5-hexadiene concentration of the propene/1,5-hexadiene copolymerization (and 1,5-hexadiene homopolymerization) : copolymerization (●) and homopolymerization (+) with *rac*-$Me_2Si(Ind)_2ZrCl_2$; copolymerization (○) and homopolymerization (×) with $Ph_2C(Cp)(Flu)ZrCl_2$.

7-3-2. Copolymerization of Propene and 1,7-Octadiene

Copolymerization of propene and 1,7-octadiene was conducted with *rac*-$Me_2Si(Ind)_2ZrCl_2$ and $Ph_2C(Cp)(Flu)ZrCl_2$ at 40 °C. The results are summarized in Tables 7-5 and 7-6, respectively. The rate of polymerization (R_p) and the molecular weight of resulting copolymer decreased with an increase of 1,7-octadiene concentration in the monomer. Copolymerization

Table 7-5. Results of propene/1,7-octadiene (OD) copolymerization with *rac*-$Me_2Si(Ind)_2ZrCl_2$–MAO[a]

Run	OD in monomer (mol %)	t[b] (min)	Yield (g)	R_p[c]	OD in polymer[d] (mol%)	Conversion of OD (%)	T_m[e] (℃)	T_g[f] (℃)	M_n[g] (×10^{-4})	M_w/M_n[g]
17	5.6	30	2.1	2100	3.6	25.1	108.6	–5.0	1.9	2.7
18	10.6	30	0.93	930	6.7	9.9	84.9	–8.4	1.6	2.6
19	23.0	60	0.81	410	16.8	7.5		–2.1	1.1	2.5
20	37.4	120	0.68	170	25.0	4.3		2.8	0.93	2.5
21	54.7	120	0.47	120	38.4	2.0		5.0	0.68	2.4
22	75.7	180	0.16	27	60.6	0.3		20.5	0.69	2.3
23[h]	100	180	0.34	57	100	2.3		34.3	0.68	2.5

[a] Conditions: Zr = 2.0 μmol, molar ratio of (MAO)Al/Zr = 3000, 1,7-octadiene + toluene = 200 mL, propene = 1 atm, polymerization temperature = 40 ℃. [b] Polymerization time. [c] Rate of polymerization (kg polymer/mol Zr·h). [d] Determined by ^{1}H NMR spectroscopy. [e] Melting temperature. [f] Glass transition temperature. [g] Determined by GPC using polystyrene standards. [h] 1,7-Octadiene (20 mL) + toluene (180 mL).

Table 7-6. Results of propene/1,7-octadiene (OD) copolymerization with $Ph_2C(Cp)(Flu)ZrCl_2$–MAO[a]

Run	OD in monomer (mol %)	t[b] (min)	Yield (g)	R_p[c]	OD in polymer[d] (mol%)	Conversion of OD (%)	T_g[e] (℃)	M_n[f] (×10^{-4})	M_w/M_n[f]
24	5.6	30	0.50	500	4.7	7.7	1.0	5.4	2.9
25	10.6	60	0.45	230	10.0	6.8	7.9	3.4	3.2
26	23.0	60	0.29	140	20.5	3.1	13.4	1.8	3.1
27	37.4	120	0.31	77	35.9	2.5	8.9	1.5	2.4
28	54.7	120	0.17	43	46.0	0.8	–5.2	1.4	2.3
29	75.7	360	0.08	13	74.8	0.2		1.2	2.6
30[g]	100	360	0.10	8.3	100	0.7	2.2	0.75	2.4

[a] Conditions: Zr = 2.0 μmol, molar ratio of (MAO)Al/Zr = 3000, 1,7-octadiene + toluene = 200 mL, propene = 1 atm, polymerization temperature = 40 ℃. [b] Polymerization time. [c] Rate of polymerization (kg polymer/mol Zr·h). [d] Determined by ^{1}H NMR spectroscopy. [e] Glass transition temperature. [f] Determined by GPC using polystyrene standards. [g] 1,7-Octadiene (20 mL) + toluene (180 mL).

diagrams of propene/1,7-octadiene with *rac*-$Me_2Si(Ind)_2ZrCl_2$ and $Ph_2C(Cp)(Flu)ZrCl_2$ are shown in Figure 7-7, which indicates that $Ph_2C(Cp)(Flu)ZrCl_2$ could incorporate more 1,7-octadiene than *rac*-$Me_2Si(Ind)_2ZrCl_2$.

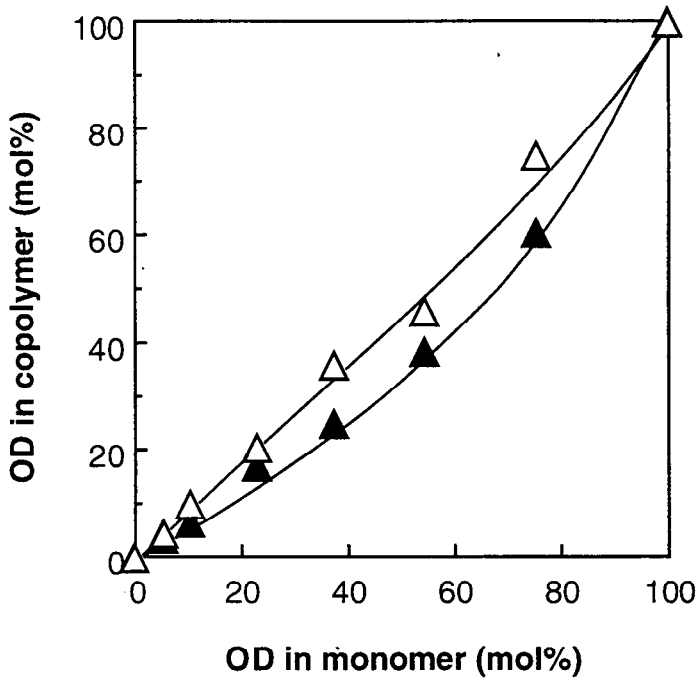

Figure 7-7. Copolymerization diagrams of propene/1,7-octadiene with *rac*-$Me_2Si(Ind)_2ZrCl_2$ (▲) and $Ph_2C(Cp)(Flu)ZrCl_2$ (△).

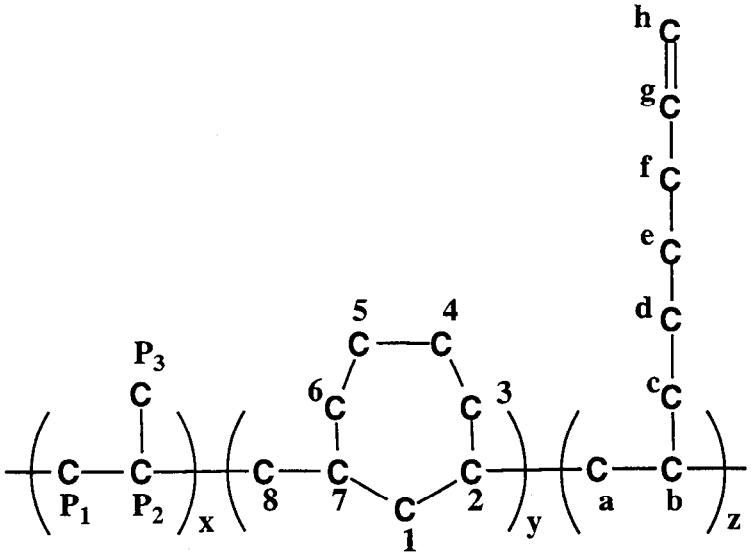

Scheme 7-4. Propene/1,7-octadiene copolymer.

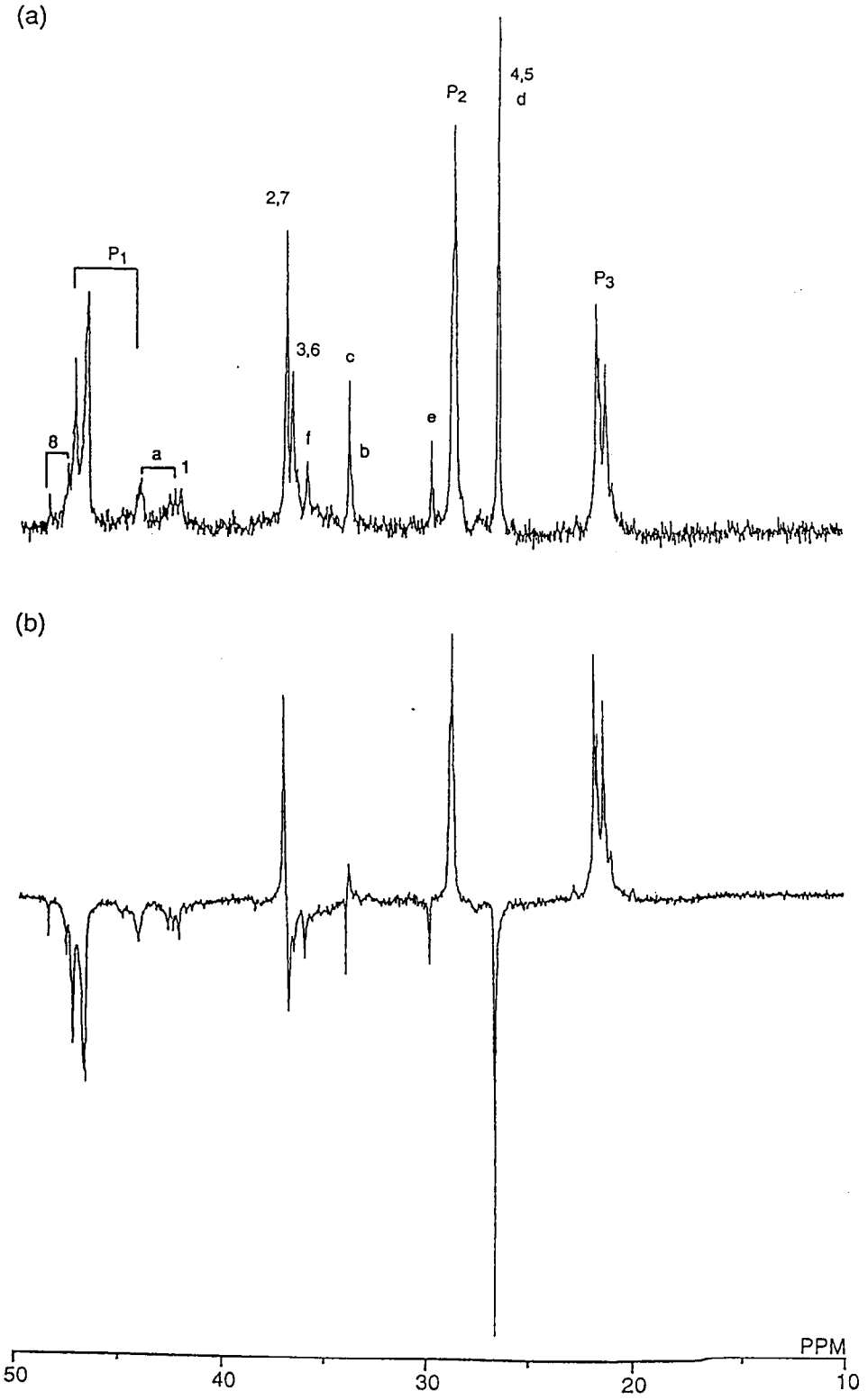

Figure 7-8. ^{13}C NMR spectrum (a) and DEPT spectrum (b) of propene/1,7-octadiene copolymer obtained with *rac*-$Me_2Si(Ind)_2ZrCl_2$ (run 20).

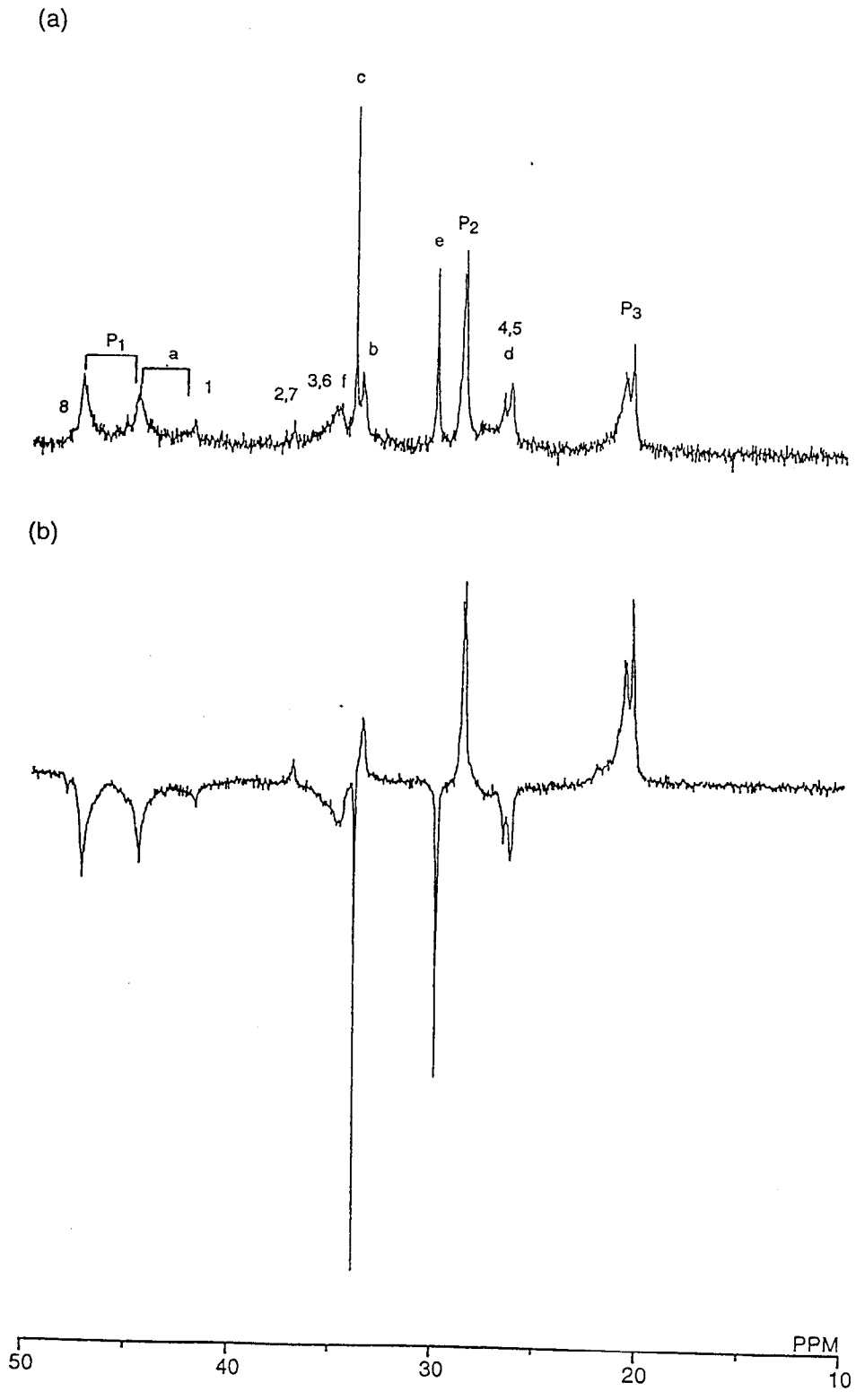

Figure 7-9. ^{13}C NMR spectrum (a) and DEPT spectrum (b) of propene/1,7-octadiene copolymer obtained with $Ph_2C(Cp)(Flu)ZrCl_2$ (run 27).

^{13}C NMR and DEPT (135 °) spectra of copolymers obtained with *rac*-$Me_2Si(Ind)_2ZrCl_2$ in run 20 are shown in Figure 7-8, (a) and (b), respectively. Scheme 7-4 illustrates plausible structures of the copolymer and nomenclature of each carbon. The resonances of 21.0–22.1, 28.8, 44.1, and 46.5–47.5 ppm are assigned to P_3, P_2, and P_1 carbons of propene units in the copolymer. The resonances at 26.7 (4,5), 36.8 (3,6), 37.1 (2,7), 42.2 (1), 47.4–47.6 (8), and 48.6 (8) ppm are assignable to the cyclic units of methylene–cycloheptane as shown in Scheme 7-4. Furthermore, the resonances of 26.7 (d), 30.0 (e), 33.9 (b), 34.0 (c), 36.0 (f), 42.4–42.6, 44.1 (a), 114.5 (g), and 139.5 (h) ppm are assigned to 1,2-addition units of 1,7-octadiene without cyclization.[11] ^{13}C NMR and DEPT (135 °) spectra of copolymer obtained with $Ph_2C(Cp)(Flu)ZrCl_2$ in run 27 are shown in Figure 7-9, (a) and (b), respectively. The resonances can be assigned according to the assignments in the copolymer obtained with *rac*-$Me_2Si(Ind)_2ZrCl_2$.

The effect of 1,7-octadiene concentration on the cyclization selectivity was discussed. The microstructures of 1,7-octadiene units, which were determined by ^1H NMR spectroscopy, are summarized in Tables 7-7 and 7-8. The existence of vinylene groups can be confirmed in the copolymers obtained with *rac*-$Me_2Si(Ind)_2ZrCl_2$, and this structure can be explained by the hydrogen elimination after a 2,1-addition of 1,7-octadiene, whose mechanism was observed in the polymerization of 1,7-octadiene with a vanadium-based catalyst.[7] The internal double bond in olefin polymerization could be formed through a chain transfer mechanism, which was suggested in propene polymerization with zirconocene catalyst: Zr–CH=CHR (R = side chain of olefin) formed by vinylic C–H activation of olefin gives internal olefins by following monomer insertion.[12] Figure 7-10 shows plots of cyclization selectivity ([C] = mole percent of cyclic units in the incorporated 1,7-octadiene) against the 1,7-octadiene concentration in the monomer. The data of 1,7-octadiene homopolymerization with *rac*-$Me_2Si(Ind)_2ZrCl_2$ and $Ph_2C(Cp)(Flu)ZrCl_2$ are plotted for references.[13] Cyclization selectivity decreased with the increase of 1,7-octadiene concentration in both 1,7-octadiene homopolymerization and propene/1,7-octadiene copolymerization. *rac*-$Me_2Si(Ind)_2ZrCl_2$ gave the poly(propene-*co*-1,7-octadiene)s with higher cyclization selectivity than that with $Ph_2C(Cp)(Flu)ZrCl_2$. This difference could be explained by conformational models in the transition state of as shown in

Table 7-7. Microstructures of 1,7-octadiene (OD) units in poly(propene-*co*-OD) obtained with *rac*-$Me_2Si(Ind)_2ZrCl_2$–MAO

Run	Propene (mol/L)	OD (mol/L)	Vinyl[a] (%)	Vinylene[a] (%)	[C][b] (%)	Δ[C][c] (%)
17	0.572	0.034	nd[d]	nd[d]	100.0	
18	0.569	0.068	13.7	2.6	83.7	
19	0.568	0.169	17.9	4.6	77.5	18.9
20	0.566	0.339	23.2	3.9	72.9	22.0
21	0.562	0.677	27.1	2.6	70.3	14.2
22	0.549	1.692	35.8	1.5	62.7	12.3

[a] Determined by ^{1}H NMR spectroscopy. [b] Cyclization selectivity. [c] Δ[C] = (cyclizatrion selectivity in homopolymerization of 1,7-octadiene) – (cyclization selectivity in copolymerization, [C]). [d] Not detectable by ^{1}H NMR spectroscopy due to the low 1,7-octadiene content.

Table 7-8. Microstructures of 1,7-octadiene (OD) units in poly(propene-*co*-OD) obtained with $Ph_2C(Cp)(Flu)ZrCl_2$–MAO

Run	Propene (mol/L)	OD (mol/L)	Vinyl[a] (%)	Vinylene[a] (%)	[C][b] (%)	Δ[C][c] (%)
24	0.572	0.034	30.0	0.3	69.7	
25	0.569	0.068	32.4	1.0	66.7	
26	0.568	0.169	40.3	0.8	58.9	31.0
27	0.566	0.339	45.2	0.9	53.9	23.9
28	0.562	0.677	54.8	0.9	44.3	13.9
29	0.549	1.692	63.2	0.4	36.4	12.5

[a] Determined by ^{1}H NMR spectroscopy. [b] Cyclization selectivity. [c] Δ[C] = (cyclizatrion selectivity in homopolymerization of 1,7-octadiene) – (cyclization selectivity in copolymerization, [C]).

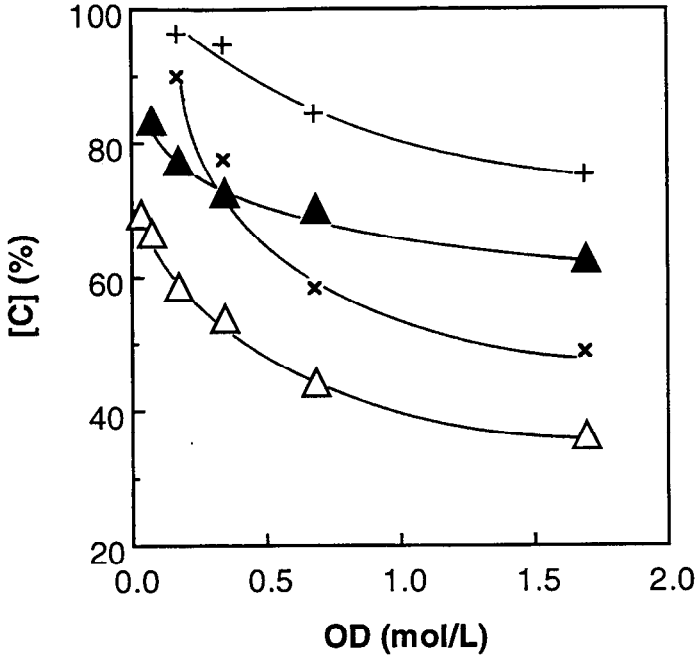

Figure 7-10. Plots of [C] (mole percent of cyclic units) against 1,7-octadiene concentration of thepropene/1,7-octadiene copolymerization (and 1,7-octadiene homopolymerization) : copolymerization (▲) and homopolymerization (+) with *rac*-$Me_2Si(Ind)_2ZrCl_2$; copolymerization (△) and homopolymerization (×) with $Ph_2C(Cp)(Flu)ZrCl_2$.

Scheme 7-5. Assuming that both the initial insertion and following cyclization are enantiofacially selected, homofacial cyclization (*cis*-cyclization from *re* insertion followed by *re* cyclization or *si* insertion followed by *si* cyclization) with *rac*-$Me_2Si(Ind)_2ZrCl_2$ and heterofacial cyclization (*trans*-cyclization from *re* insertion followed by *si* cyclization or *si* insertion followed by *re* cyclization) with $Ph_2C(Cp)(Flu)ZrCl_2$ could proceed preferentially. The heterofacial cyclization with $Ph_2C(Cp)(Flu)ZrCl_2$ hardly occurs because of the steric hindrance of the fluorenyl ligand, and the insertion of another monomer could be preferable to cyclization.

Δ[C] values, which are summarized in Tables 7-7 and 7-8, mean the differences of cyclization selectivity between homopolymerization[13] and copolymerization at the same 1,7-octadiene concentration. The cyclization selectivity in the copolymerization is lower than that in the homopolymerization regardless of the catalysts. The values of Δ[C] in 1,7-octadiene polymerization were larger than those in the 1,5-hexadiene polymerization. These results indicate that propene insertion could occur frequently before the cyclization of the 1,2-inserted 1,7-octadiene at the propagating chain end. The value of Δ[C] in 1,7-octadiene polymerization

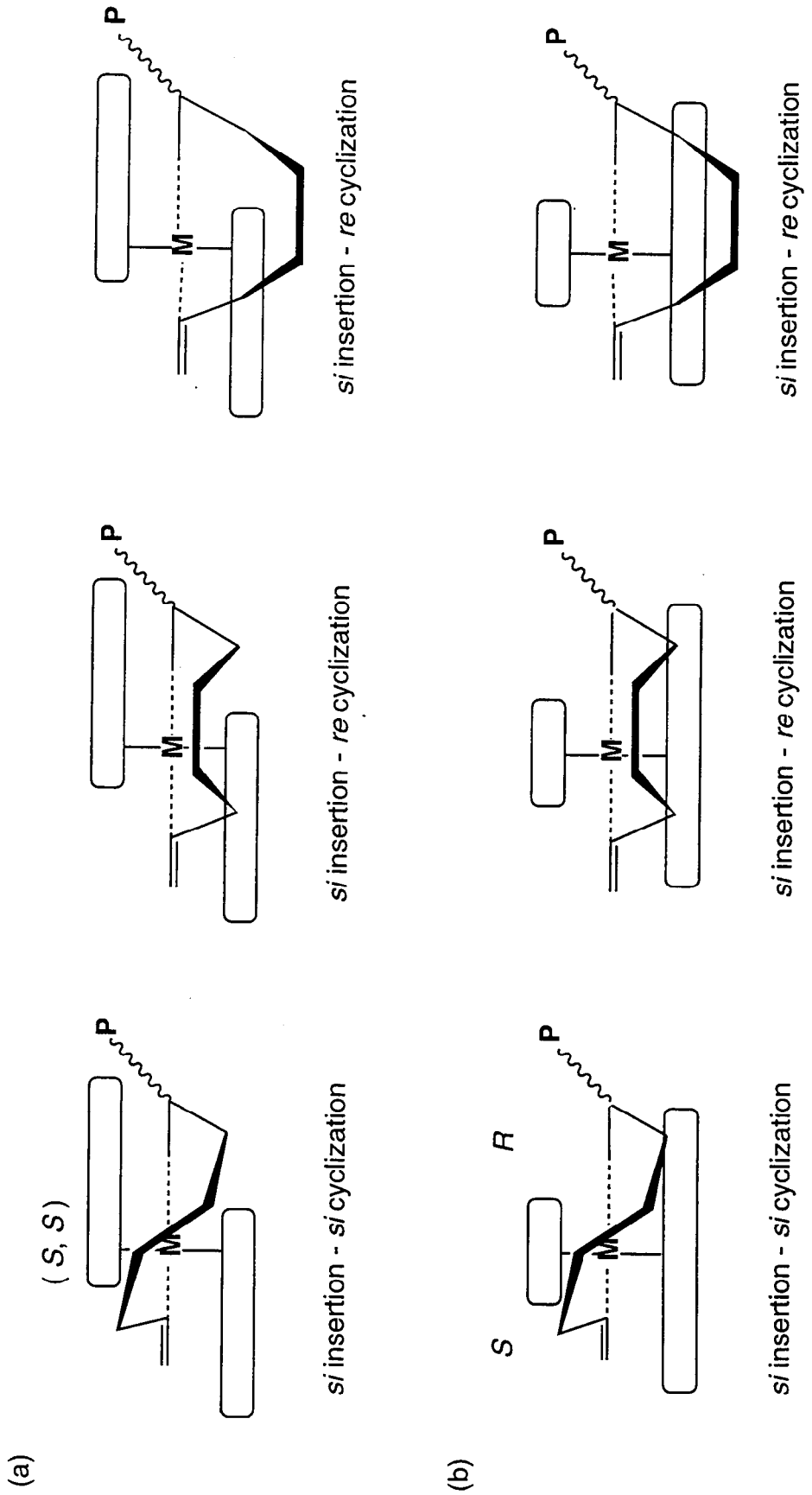

Scheme 7-5. Conformational models in transition state of 1,7-octadiene cyclization with *rac*-$Me_2Si(Ind)_2ZrCl_2$ (a) and $Ph_2C(Cp)(Flu)ZrCl_2$ (b): M = Zr, P = polymer chain.

was almost the same between these two catalysts at the same monomer concentration. This result suggests that the rate constants of propene insertion to the propagating chain ends with 1,2-inserted 1,7-octadiene are not so different between these catalysts.

7-3-3. Copolymerization Parameters

In copolymerization of propene with nonconjugated diene, propagation and cyclization reactions can be described by the following seven equations on condition that the propagation obey the first order Markovian process and the cyclization does the Bernoullian process:[14]

	Rate of reaction	
$M_p^* + M_p \xrightarrow{k_{pp}} M_p^*$	$k_{pp}[M_p^*][M_p]$	(1)
$M_p^* + M_d \xrightarrow{k_{pd}} M_d^*$	$2k_{pd}[M_p^*][M_d]$	(2)
$M_d^* + M_p \xrightarrow{k_{dp}} M_p^*$	$k_{dp}[M_d^*][M_p]$	(3)
$M_d^* + M_d \xrightarrow{k_{dd}} M_d^*$	$2k_{dd}[M_d^*][M_d]$	(4)
$M_d^* \xrightarrow{k_c} M_c^*$	$k_c[M_d^*]$	(5)
$M_c^* + M_p \xrightarrow{k_{cp}} M_p^*$	$k_{cp}[M_c^*][M_p]$	(6)
$M_c^* + M_d \xrightarrow{k_{cd}} M_d^*$	$2k_{cd}[M_c^*][M_d]$	(7)

where M_p^*, M_d^*, and M_c^* are the active centers with last propene, 1,2-inserted diene, and cyclized diene inserted units, $[M_p]$ and $[M_d]$ are concentrations of propene and diene monomer, k_{pp}, k_{pd}, k_{dp}, k_{dd} k_c, k_{cp}, and k_{cd} are rate constants of propene insertion after a propene insertion, diene insertion after a propene insertion, propene insertion after a 1,2-inserted diene, diene insertion after a 1,2-inserted diene, cyclization at a 1,2-inserted diene, propene insertion after a cyclized diene and diene insertion after a cyclized diene, respectively. The ratio of polymerized propene monomer ($d[M_p]$) to polymerized diene monomer ($d[M_d]$) and the cyclized

diene unit in the copolymer ($d[M_c]$) can be expressed by the equations (8) and (9) from the equations (1), (2), (3), (4), (6), and (7):

$$d[M_p]/d[M_d] = (k_{pp}[M_p^*][M_p] + k_{dp}[M_d^*][M_p] + k_{cp}[M_c^*][M_p]) \\ /(2k_{dd}[M_d^*][M_d] + 2k_{pd}[M_p^*][M_d\} + 2k_{cd}[M_c^*][M_d]) \quad (8)$$

$$d[M_p]/d[M_c] = (k_{pp}[M_p^*][M_p] + k_{dp}[M_d^*][M_p] + k_{cp}[M_c^*][M_p])/k_c[M_d^*] \quad (9)$$

Similarly, the ratio of polymerized diene monomer ($d[M_d]$) to the amount of cyclized units in the copolymer ($d[M_c]$) can be expressed by the equation (10) from the equations (2), (4), (5), and (7):

$$d[M_d]/d[M_c] = (2k_{dd}[M_d^*][M_d] + 2k_{pd}[M_p^*][M_d] + 2k_{cd}[M_c^*][M_d])/k_c[M_d^*] \quad (10)$$

Assuming the steady-state conditions, the following three equations can be formed:

$$k_{dp}[M_d^*][M_p] + k_{cp}[M_c^*][M_p] = 2k_{pd}[M_p^*][M_d] \quad (11)$$

$$2k_{pd}[M_p^*][M_d] + 2k_{cd}[M_c^*][M_d] = k_{dp}[M_d^*][M_p] + k_c[M_d^*] \quad (12)$$

$$k_c[M_d^*] = k_{cp}[M_c^*][M_p] + 2k_{cd}[M_c^*][M_d] \quad (13)$$

The equations (14)–(16) were derived from equations (8)–(13).

$$d[M_d]/d[M_p] = 2[M_d]/[M_p] \cdot \{[M_p] + 2r_d[M_d] + K_c'\} / \\ \{2[Md] + r_p[M_p] + K_c'(2[M_d] + r_p[M_p]) / (2r_c[M_d] + [M_p])\} \quad (14)$$

$$d[M_p]/d[M_c] = [M_p] \cdot (1 + r_p[M_p]/2[M_d]) \cdot \{1/K_c' + 1/(2r_c[M_d] + [M_p])\} \quad (15)$$

$$d[M_d]/d[M_c] = 1 + 2[M_d]/K_c + [M_p]/K_c' \quad (16)$$

where $r_p = k_{pp}/k_{pd}$, $r_d = k_{dd}/k_{dp}$, $r_c = k_{cd}/k_{cp}$, $K_c = k_c/k_{dd}$, and $K_c' = k_c/k_{dp} = K_c r_d$.
The equations (14)–(16) could be further developed to equations (17) and (18).

$$2[M_d]/(f_d - 1) = r_c - 1/r_d \cdot \{[M_p]/(f_d - 1)\} \quad (17)$$

$$r_p = f_p/F^2 \cdot K_c'(r_c + F) / \{K_c' + 2[M_d](r_c + F)\} - 1/F \quad (18)$$

where $f_p = d[M_p]/d[M_c]$, $f_d = d[M_d]/d[M_c]$, and $F = [M_p]/2[M_d]$, respectively.

The values of r_d were calculated from the equation (17), and the r_p and r_c values were determined from the equation (18). The data of copolymerization, whose conversion was less than 10% (less than 20% in the case of propene/1,5-hexadiene copolymerization with *rac*-$Me_2Si(Ind)_2ZrCl_2$), was applied to these equations. The values of copolymerization parameters are summarized in Table 7-9. These values agree to the copolymerization behavior as described above.

Table 7-9. Copolymerization parameters of propene/nonconjugated diene with zirconocene catalysts

Catalyst	Diene[a]	r_p	r_d	r_c
rac-$Me_2Si(Ind)_2ZrCl_2$	HD	3.84	0.38	0.18
$Ph_2C(Cp)(Flu)ZrCl_2$		2.28	0.71	0.27
rac-$Me_2Si(Ind)_2ZrCl_2$	OD	3.16	0.45	0.14
$Ph_2C(Cp)(Flu)ZrCl_2$		2.26	0.66	0.24

[a] HD = 1,5-hexadiene, OD = 1,7-octadiene.

7-4. Summary

Copolymers of propene and nonconjugated diene with stereospecific metallocene catalysts give important information on the cyclization reaction of incorporated dienes. The microstructures of propene/1,5-hexadiene copolymers proved clearly that 1,2-insertion of 1,5-hexadiene with isospecific and syndiospecific metallocene catalysts proceeded in enantiomorphic-site control. On the other hand, diastereoselectivity of the cyclization reaction was independent of chirality of the stereospecificity of metallocene catalysts. Propene insertion disturbed the cyclization of 1,2-inserted 1,5-hexadiene in the copolymerization with *rac*-$Me_2Si(Ind)_2ZrCl_2$.

In propene/1,7-octadiene copolymerization, although the stereoselectivity of incorporated 1,7-octadiene could not be determined by ^{13}C NMR spectroscopy, there were some interesting results about the cyclization selectivity of 1,7-octadiene. The higher cyclization selectivity was observed in the copolymerization with *rac*-$Me_2Si(Ind)_2ZrCl_2$ than with $Ph_2C(Cp)(Flu)ZrCl_2$. This result was opposite to that in the propene/1,5-hexadiene copolymerization; higher cyclization selectivity was observed with $Ph_2C(Cp)(Flu)ZrCl_2$. The author considered the conformation of the transition state in the cyclization, and suggested the possibility of enantioselective cyclization of the 1-hexenyl side chain by chiral catalytic sites. Propene insertion could occur frequently before the cyclization at a 1,2-inserted 1,7-octadiene at the propagating chain end in the copolymerization with both *rac*-$Me_2Si(Ind)_2ZrCl_2$ and $Ph_2C(Cp)(Flu)ZrCl_2$.

Copolymerization of propene and nonconjugated diene involving intramolecular cyclization with stereospecific metallocene catalysts could be one of the useful methods to synthesize the stereoregular polypropene with cyclic group. The decrease in polymerization activity was not so drastic compared to that of propene/cycloolefin copolymerization. The cyclization selectivity, namely, content of cyclic groups and pendent vinyl groups, could be controlled by the diene concentration in the monomer. In addition, the remained vinyl side chains could be transferred to functional groups or used for cross-linking reaction.

References and Notes

(1) (a) Kaminsky, W.; Spiehl, R. *Makromol. Chem.* **1989**, *190*, 515. (b) Kaminsky, W.; Bark, A.; Arndt, M. *Makromol. Chem., Macromol. Symp.* **1991**, *47*, 83. (c) Chien, J. C. W.; He, D. *J. Polym. Sci., Part A: Polym. Chem.* **1991**, *29*, 1609. (d) Kaminsky, W.; Bark, A.; Steiger, R. *J. Mol. Catal.* **1992**, *74*, 109. (e) Kaminsky, W.; Noll, A. *Polym. Bull. (Berlin)* **1993**, *31*, 175. (f) Chien, J. C. W.; Xu, B. *Makromol. Chem., Rapid Commun.* **1993**, *14*, 109. (g) Herfert, N.; Montag, P.; Fink, G. *Makromol. Chem.* **1993**, *194*, 3167. (h) Yu, Z.; Marques, M.; Rausch, M. D.; Chien, J. C. W. *J. Polym. Sci., Part A: Polym. Chem.* **1995**, *33*, 2795. (i) Bergström, C. H.; Seppälä, J. V. *J. Appl. Polym. Sci.* **1997**, *63*, 1063. (j) Bergström, C. H.; Väänänen, T. L. J.; Seppälä, J. V. *J. Appl. Polym. Sci.* **1997**, *63*, 1071. (k) Malmberg, A.; Löfgren, B. *J. Appl. Polym. Sci.* **1997**, *66*, 35. (l) Wang, Q.; Weng, J.; Fan, Z.; Feng, L. *Macromol. Rapid Commun.* **1997**, *18*, 1101. (m) Chien, J. C. W.; Yu, Z.; Marques, M. M.; Flores, J. C.; Rausch, M. D. *J. Polym. Sci., Part A: Polym. Chem.* **1998**, *36*, 319. (n) Bergström, C. H.; Starck, P. G.; Seppälä, J. V. *J. Appl. Polym. Sci.* **1998**, *67*, 385. (o) Rische, T.; Waddon, A. J.; Dickinson, L. C.; MacKnight, W. J. *Macromolecules* **1998**, *31*, 1871.

(2) (a) Arnold, M.; Henschke, O.; Köller, F. *J. Macromol. Sci. Pure Appl. Chem.* **1996**, *A33* (Suppl. 3–4), 219. (b) Henschke, O.; Köller, F.; Arnold, M. *Macromol. Rapid Commun.* **1997**, *18*, 617.

(3) (a) Resconi, L.; Waymouth, R. M. *J. Am. Chem. Soc.* **1990**, *112*, 4953. (b) Mogstad, A.; Waymouth, R. M. *Macromolecules* **1992**, *25*, 2282. (c) Kesti, M. R.; Waymouth, R. M. *J. Am. Chem. Soc.* **1992**, *114*, 3565. (d) Cavallo, L.; Guerra, G.; Corradini, P.; Resconi, L.; Waymouth, R. M. *Macromolecules* **1993**, *26*, 260.

(4) (a) Coates, G. W.; Waymouth, R. M. *J. Am. Chem. Soc.* **1991**, *113*, 6270. (b) Coates, G. W.; Waymouth, R. M. *J. Mol. Catal.* **1992**, *76*, 189. (c) Coates, G. W.; Waymouth, R. M. *J. Am. Chem. Soc.* **1993**, *115*, 91. (d) Miller, S. A.; Waymouth, R. M. In *Ziegler Catalysts*; Fink, G., Mülhaupt, R., Brintzinger, H. H., Eds.; Springer-Verlag: Berlin, 1995; p 441.

(5) (a) Coutinho, F. M. B.; Marques, M. F. V. *Polim. Cienc. Technol.* **1993**, *3*(1), 20. (b) Bergemann, C.; Cropp, R.; Luft, G. *J. Mol. Catal. A: Chem.* **1997**, *116*, 323.

(6) Sernetz, F. G.; Mülhaupt, R.; Waymouth, R. M. *Polym. Bull.* **1997**, *38*, 141.

(7) Doi, Y.; Tokuhiro, N.; Soga, K. *Makromol. Chem.* **1989**, *190*, 643.

(8) Uozumi, T.; Soga, K. *Makromol. Chem.* **1992**, *193*, 823.

(9) The resonances in the ^{13}C NMR spectra of poly(propene-*co*-1,5-hexadiene)s were assigned as described below. The author can recognize from the chemical shifts of polypropenes that the resonances at 20–22.2, 28.9 (with *rac*-$Me_2Si(Ind)_2ZrCl_2$), 28.6 (with $Ph_2C(Cp)(Flu)ZrCl_2$), and 46.6 ppm were derived from P_3, P_2 (m), P_2 (r), and P_1

of the homo-sequential units, respectively. Moreover, from the chemical shifts of poly(MCP) homopolymer, the resonances of 32.4, 33.4, 38.4, 39.8, 40.4, 41.7 and 44.3 ppm were assigned to *cis*-3,4, *trans*-3,4, *trans*-2,5, *cis*-2,5, *trans*-1, *cis*-1, and 6 in the homosequential units, respectively.[3,4,10] The primary, secondary and tertiary carbons could be distinguished by the DEPT spectra of the copolymers. In the ^{13}C NMR spectra of copolymers with low content of HD, the resonances at 30.2 and 45.1 ppm were observed and assignable to P_2 and CH_2 (P_1 and 6) of Pr–MCP sequences. Besides, the resonances of 32.4, 32.8–33.0, 33.4–33.5, and 34.0–34.2 ppm were assigned to isolated-3,4 of *cis*-r, *cis*-m, *trans*-r, and *trans*-m, respectively, as described in the Results and Discussion. The resonances of tertiary carbon 37.0 and 38.4 ppm were observed at almost the same intensity of isolated *trans*-3,4 and *cis*-3,4, and the author assigned those resonances to isolated *trans*-2,5 and *cis*-2,5, respectively. In the ^{13}C spectra of the copolymers with high content of HD, the resonances of 31.4 ppm from tertiary carbon was found and assigned to the P_2 of the MCP–Pr–MCP sequence.

(10) Homopolymerization of 1,5-hexadiene with *rac*-$Me_2Si(Ind)_2ZrCl_2$ and $Ph_2C(Cp)(Flu)ZrCl_2$ was carried out under the same conditions of propene/1,5-hexadiene copolymerization (without propene) in the half scale.

(11) The resonances in the ^{13}C NMR spectra of poly(propene-*co*-1,7-octadiene)s were assigned form the chemical shifts of polypropene, poly(1,7-octadiene) with and without an intramolecular cyclization.[7,13]

(12) Resconi, L.; Piemontesi, F.; Camurati, I.; Balboni, D.; Sironi, A.; Moret, M.; Rychlicki, H.; Zeigler, R. *Organometallics* **1996**, *15*, 5046.

(13) Homopolymerization of 1,7-octadiene with *rac*-$Me_2Si(Ind)_2ZrCl_2$ and $Ph_2C(Cp)(Flu)ZrCl_2$ was carried out under the same conditions of propene/1,7-octadiene copolymerization (without propene) in the half scale.

(14) (a) Smets, G.; Deval, N.; House, P. *J. Polym. Sci., Part A* **1964**, *2*, 4835. (b) Matsumoto, A.; Oiwa, M. *J. Polym. Sci., Part A-1* **1971**, *9*, 3607. (c) Matsumoto, A.; Aso, T.; Tanaka, S.; Oiwa, M. *J. Polym. Sci., Polym. Chem. Ed.* **1973**, *11*, 2357. (d) Matsumoto, A.; Kitagami, J.; Oiwa, M. *J. Polym. Sci., Polym. Chem. Ed.* **1973**, *11*, 2365.

Chapter 8

Crystalline Structures of Syndiotactic Poly(propene-*co*-olefin)s

8-1. Introduction

Syndiotactic polypropene can be prepared at a very low polymerization temperature of –78°C with conventional Ziegler–Natta catalyst, such as tris(2-methyl-1,3-butanedionato)vanadium–$AlEt_2Cl$ catalyst system.[1] The polymer obtained is, however, a relatively low molecular weight and poor stereoregularity. Therefore, the properties of highly syndiotactic polypropene has not so far been examined in detail. In the last few years, development in metallocene catalysts, particularly by Ewen and coworkers, has enable us to synthesize highly syndiotactic polypropene with *i*Pr(Cp)(Flu)$ZrCl_2$ in good yield at ambient polymerization temperature.[2] The highly syndiotactic polypropene shows good stiffness, impact strength, and heat resistance. It also has a good transparency because of a small size of spherulite and low crystallinity in comparison with isotactic one. After the finding for the synthesis of highly syndiotactic polypropene, a number of studies have been made on the crystalline structure, morphology, and properties of this polymer.

Three types of unit cells were reported for helical $(t_2g_2)_2$ conformation of the syndiotactic polypropene differing in packing manner of the polymer chain.[3–6] Crystallization conditions (crystallization temperature and time and so on) affect the crystallization behavior, crystalline structure, and morphology of syndiotactic polypropene. The effect of the crystallization temperature has been studied on melting behavior of the syndiotactic polypropene by DSC.[7–15] When the crystallization was conducted at low temperature, a double melting peak was observed in DSC patterns. The first melting peak (low-melting peak) showed a clear dependence on the crystallization temperature. Furthermore, the effect of crystallization conditions on the crystalline structures has been investigated by wide-angle X-ray diffraction (WAXD), small-angle X-ray scattering (SAXS), electron diffraction (ED), and solid state ^{13}C NMR spectroscopy.[7–27] Ordinary WAXD pattern of syndiotactic polypropene shows three major diffraction peaks at 2θ = 12.1, 15.9, and 20.6 ° derived from (200), (010), and (220, 121) reflection planes, respectively.[5,9–19,21,23,26,27] When an isothermal crystallization was conducted at higher temperature (more than 120 °C), the reflection peak at 2θ = 18.8 ° was observed, and assigned to the reflection from (211) planes. Polarizing microscope,

transmission electron micrograph (TEM), and atomic force microscopy (AFM) were applied to observe the effect of crystallization conditions on the crystalline morphology.[8,9,20,22,28–31]

Some reports have been presented about syndiotactic propene-based copolymers prepared by the syndiospecific metallocene catalyst.[32–36] Kressler *et al.* prepared syndiotactic poly(propene-*co*-1-octene) and studied properties and structures of the copolymer.[34,35] De Rosa *et al.* synthesized syndiotactic propene-based copolymers with a small amount of ethene and 1-butene, and conducted the structural characterization of melt-crystallized samples obtained through melting at 200 °C and successive rapid cooling to room temperature.[36] However the analysis of syndiotactic poly(propene-*co*-olefin)s is still much less complete than that of the syndiotactic polypropene.

In this chapter, the author examined structures and properties of several poly(propene-*co*-olefin)s (olefin = ethene, 1-butene, 1-pentene, 1-hexene, 4-methyl-1-pentene) prepared by a syndiospecific metallocene catalyst, and found the peculiar crystalline structure of syndiotactic poly(propene-*co*-1-butene). Furthermore, isothermal crystallization of syndiotactic poly(propene-*co*-olefin)s was conducted and effect of the crystallization temperature on the crystallization behavior and crystalline structure of the copolymers was studied.

8-2. Experimental Part

Materials

*i*Pr(Cp)(Flu)$ZrCl_2$ was synthesized according to the literature.[2] MAO was purchased from Tosoh Akzo Co., Ltd. and used without further purification. 1-Pentene, 1-hexene, and 4-methyl-1-pentene were commercially obtained and dried over molecular sieves 3A.

Copolymerization of propene with ethene was carried out in an agitated 1 L autoclave at 25 °C. Gaseous mixture of propene and ethene was fed to the autoclave containing 300 mL of toluene and the pressure was kept at 8 kg/cm^{2}G. Toluene (10 mL), MAO and the catalyst (1.5 μmol) were mixed in a 100 mL glass flask at 25 °C for 5 min in advance. The molar ratio of (MAO)Al/Zr was adjusted to 1000. The polymerization was started by adding the catalyst solution to the autoclave. The temperature and the monomer gas pressure were kept constant

during the polymerization. After one hour, the polymerization was terminated by adding isobutyl alcohol. The polymer obtained was dissolved in xylene at 130 °C and catalyst residues were removed by filtration at 130 °C. The polymer was precipitated by pouring the solution into large excess of methanol and dried in vacuo at 60 °C for 4 h.

Copolymerizations of propene with other α-olefins were carried out in a 1 L autoclave. Measured amounts of a α-olefin and liquid propene were introduced to the autoclave. Further experiments were conducted with the same procedures as described in the copolymerization of propene with ethene.

Characterization of copolymers

^{13}C NMR spectra of polymers were measured at 67.8 MHz in *o*-dichlorobenzene at 135 °C with a JEOL EX-270 spectrometer. M_w and MWD (M_w/M_n) of the polymers were determined by GPC (Waters 150CV) at 140 °C using *o*-dichlorobenzene as a solvent. DSC measurements were made by a Perkin-Elmer DSC-VII under the following condition. A sample (10 mg) in an aluminum pan was kept at 220 °C in an atmosphere of nitrogen for 5 min, cooled at a rate of 3 °C/min to the room temperature. The sample pan was kept at 23 °C for a week. The sample was analyzed by heating at a rate of 10 °C/min from the room temperature to 220 °C, and the temperature at a maximum peak of the endothermic curve obtained was designated as a melting point. A sample for measurements of X-ray diffraction was gradually crystallized from 230 °C to room temperature for about 12 h and kept at 23 °C for a week. The WAXD patterns were acquired on an automatic Rigaku-RU200B diffractometer in the transmission mode using CuKα radiation.

Isothermal crystallization and characterization of the copolymers

A sample (*ca.* 5 mg) in an aluminum pan was kept at 180 °C for 15 min and then quenched to the crystallization temperature (T_c) in oil bath. DSC measurements of isothermally crystallized samples were made on a Seiko DSC-220 under the heating at a rate of 10 °C/min from room temperature to 200 °C. WAXD patterns of copolymers were also acquired on an automatic Rigaku-RU200B diffractometer in the transmission mode using CuKα radiation.

Kinetic study of isothermal crystallization

Depolarized light intensity (DLI) technique was used to follow crystallization behavior of the copolymers.[37] Isothermal crystallization was carried out with a Kotaki MK-701 by measuring the intensity of depolarized light passing through the specimens during the isothermal treatment. A thin film of the polymer (about 100 μm) was fused between glass cover slips in the furnace at 230 °C for 5 min and then rapidly transferred to the crystallization bath, maintained at a selected temperature in the range of 80–120 °C, until the crystallization should be completed.

8-3. Results and Discussion

8-3-1. Properties and Crystalline Structures of Syndiotactic Poly(propene-*co*-olefin)s

Five kinds of syndiotactic poly(propene-*co*-olefin)s (olefin = ethene, 1-butene, 1-pentene, 1-hexene, and 4-methyl-1-pentene) were examined by GPC, DSC, and WAXD. The structures and properties of polymers obtained are summarized in Table 8-1. Molecular weight of each copolymer decreased with the increase of comonomer content. However, the M_w/M_n values of the copolymers were kept within 1.8–2.2

Figure 8-1 shows a relationship between T_m and comonomer content in the copolymers. The copolymers, other than poly(propene-*co*-1-butene), showed steep melting point depression with the increase of olefin content. On the contrary, poly(propene-*co*-1-butene) showed small depression and, furthermore, had melting point in a whole range of 1-butene content.

The crystallinity of the copolymers was determined from the WAXD pattern according to the method described in a previous paper.[7] The relationship between crystallinity and comonomer content is shown in Figure 8-2. Similar to the profile of melting temperature, poly(propene-*co*-1-butene) exhibited lower decrease of crystallinity than other copolymers and kept crystalline structure in a whole range of 1-butene content. In the case of other poly(propene-*co*-olefin)s, copolymers had no more crystalline structure more than 20 mol % of comonomer content.

Table 8-1. Structures and properties of poly(propene-*co*-olefin)s prepared by *i*Pr(Cp)(Flu)$ZrCl_2$–MAO[a]

Sample	Comonomer	(mol %)[b]	M_w[c] ($\times10^{-4}$)	M_w/M_n	T_m[d] (℃)	X_c[e] (%)	Axial length (Å)[f]	
							a axis	*b* axis
a	—	0	41.6	2.1	147.1	38.1	14.42	5.59
b-1	ethene	3.1	17.1	2.2	123.9	26.1	14.42	5.56
b-2		7.2	14.5	2.0	98.8	18.2	14.36	5.55
b-3		11.2	9.9	2.2	79.4	15.6	14.42	5.24
c-1	1-butene	2.1			139.4			
c-2		6.6	38.2	1.9	124.7	29.8	14.60	5.54
c-3		11.5			112.4			
c-4		19.1	30.8	2.0	94.5	25.2	14.86	5.62
c-5		33.7			72.1			
c-6		67.8	17.4	2.2	50.0	17.1	16.34	5.65
c-7		100	11.9	2.2	45.1	24.5	16.90	5.78
d-1	1-pentene	3.9			114.4			
d-2		5.1	38.6	2.0	108.4	21.4	14.52	5.57
d-3		15.1	32.9	2.0	65.0	10.9	14.64	5.61
d-4		21.1	29.9	1.8				
d-5		100	14.1	2.1	37.3			
e-1	1-hexene	2.8			120.6			
e-2		5.6	40.2	2.0	101.2	17.3	14.56	5.57
e-3		12.7	36.8	2.3	81.5	10.1	14.62	5.55
e-4		21.7	26.0	1.8				
f-1	4-MPT-1[g]	2.4			126.5			
f-2		4.2	36.5	1.9	113.4	21.9	14.56	5.57
f-3		7.4	30.2	2.0	82.7	13.1	14.54	5.59
f-4		17.5	24.1	1.8				
f-5		100	7.8	2.3				

[a] Polymerization conditions: see experimental section. [b] Comonomer content in copolymers by ^{13}C NMR spectroscopy. [c] Determined by GPC using polystyrene standards. [d] Melting temperature obtained from gradually crystallized sample at the condition described in experimental section. [e] X_c denotes the polymer crystallinity, which was determined by WAXD. [f] Calculated from (200) and (010) reflections of WAXD. [g] 4-methyl-1-pentene.

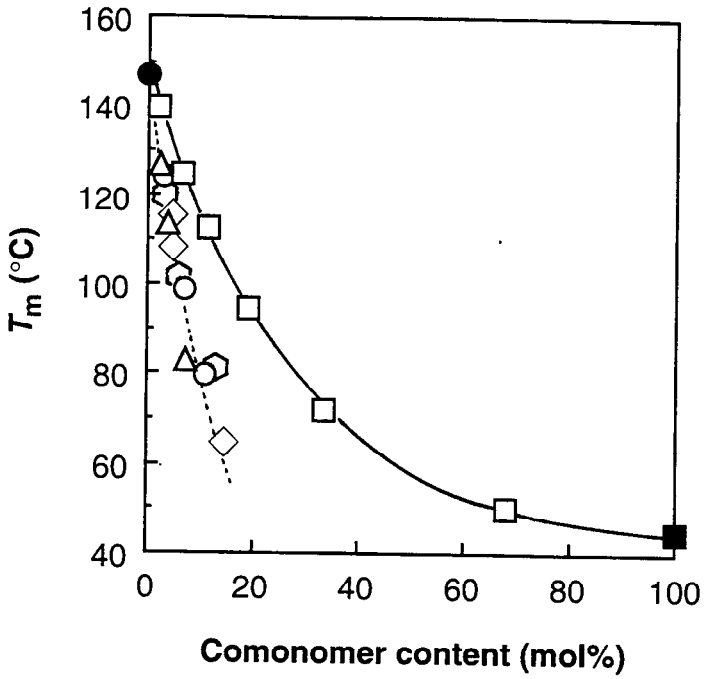

Figure 8-1. Plots of T_m against comonomer content of syndiotactic poly(propene-*co*-olefin)s: olefin = (○) ethene; (□) 1-butene; (◇) 1-pentene; (⬡) 1-hexene; (△) 4-methyl-1-pentene; (●) syndiotactic polypropene; (■) syndiotactic poly(1-butene).

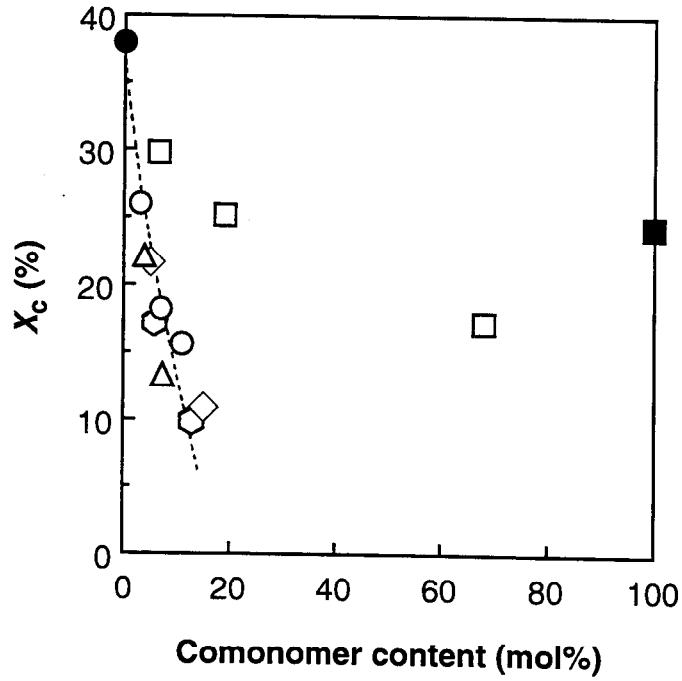

Figure 8-2. Plots of crystallinity against comonomer content of syndiotactic poly(propene-*co*-olefin)s:olefin = (○) ethene; (□) 1-butene; (◇) 1-pentene; (⬡) 1-hexene; (△) 4-methyl-1-pentene; (●) syndiotactic polypropene; (■) syndiotactic poly(1-butene).

The crystalline structure of the copolymers were examined in detail by WAXD to understand the peculiarity of poly(propene-*co*-1-butene) mentioned above.

Three unit cells were proposed for syndiotactic polypropene. The first one is the *C*-centered orthorhombic unit cell (space group $C222_1$, Cell I). The second one contains two chain segments in an orthorhombic cell (space group $Pca2_1$, Cell II). The third one involves the doubling of the cell along the *b* axis and corresponding to an *Ibca* space group (Cell III).

The *a* axial length of the unit cell and the *b* axial length were calculated from the (200) reflections and the (010) reflections, respectively.[3,38,39] The data obtained are summarized in Table 8-1. The copolymers, besides poly(propene-*co*-1-butene), exhibited no significant change in the length of *a* and *b* axes. In contrast, as shown in Figures 8-3 (a) and (b), *a* axis of poly(propene-*co*-1-butene) expanded linearly with the increase of 1-butene content, however, the *b* axis showed a little change. Isotactic poly(propene-*co*-1-butene) prepared by isospecific Ziegler–Natta catalysts is known to have also crystallinity in a whole range of 1-butene content, but the axial length changes drastically where 1-butene content is more than 45 mol %.[40]

Both syndiotactic polypropene and poly(1-butene) have (t_2g_2) conformation in these crystals.[41,42] The continuous melting point depression (Figure 8-1) and linear expansion in the length of *a* axis (Figure 8-3 (a)) from syndiotactic polypropene to syndiotactic poly(1-butene) indicated the isomorphism in the crystalline structures of syndiotactic poly(propene-*co*-1-butene). The projections along the *c* axis are shown in Figure 8-4 (a). Syndiotactic polypropene has three kinds of the unit cells different in the packing manner of left (L-) and right (R-) helicals of the polymer chains. When 1-butene units enter into the unit cells, ethyl groups of 1-butene units should be directed along with *a* axis in any unit cells as shown Figure 8-4 (b). As a result, 1-butene units lead to the expansion of the *a* axis, whereas they will give a slight effect on the *b* axis.

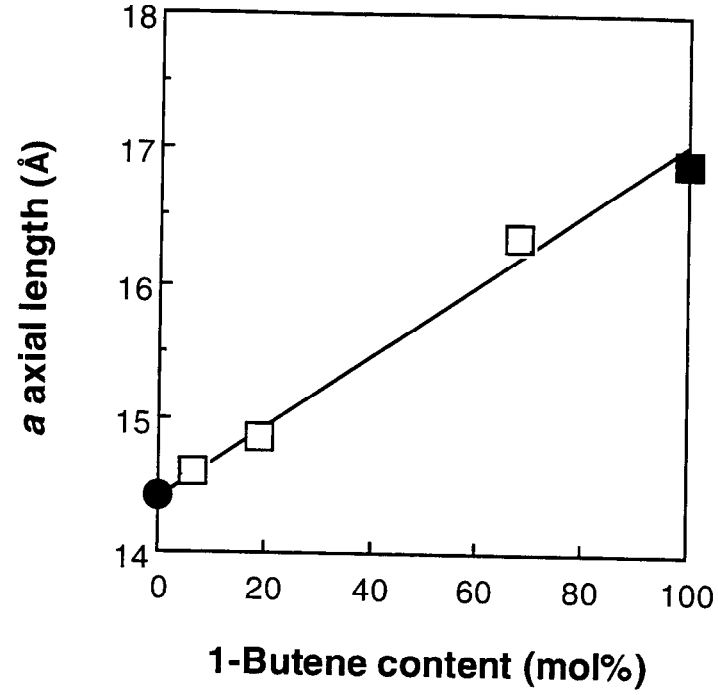

Figure 8-3(a). *a* axial length of the unit cell of syndiotactic poly(propene-*co*-1-butene): (□) propene/1-butene; (●) syndiotactic polypropene; (■) syndiotactic poly(1-butene).

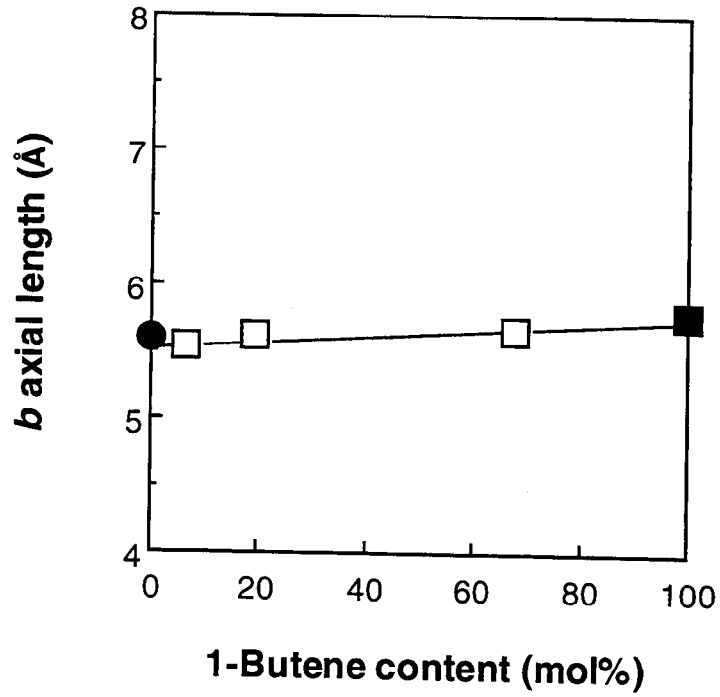

Figure 8-3(b). *b* axial length of the unit cell of syndiotactic poly(propene-*co*-1-butene): (□) propene/1-butene; (●) syndiotactic polypropene; (■) syndiotactic poly(1-butene).

(a)

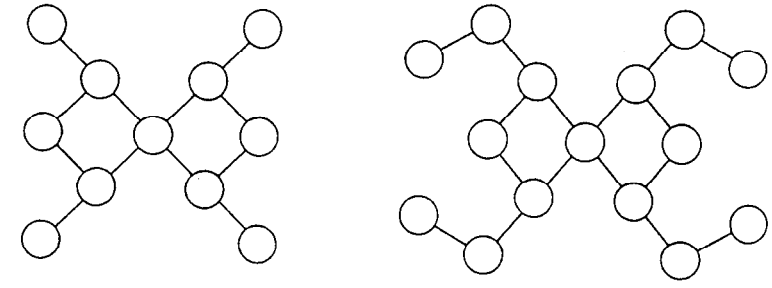

syndiotactic polypropylene

syndiotactic poly(1-butene)

(b)

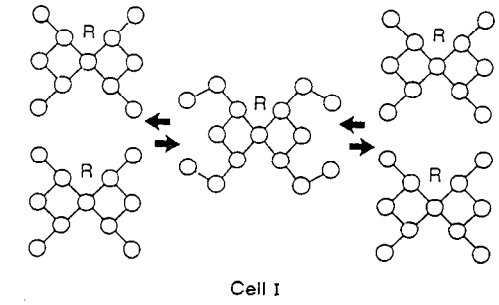

Cell I

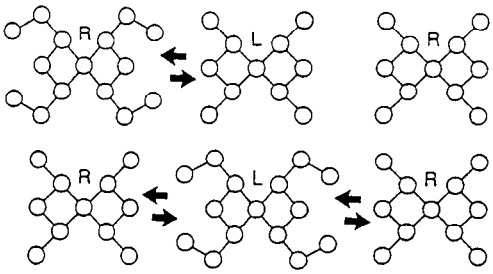

Cell II

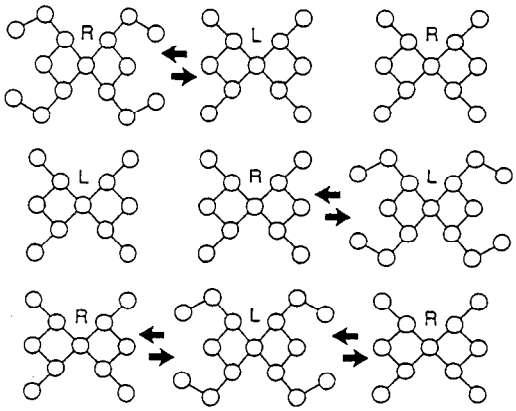

Cell III

Figure 8-4. (a) Molecular-axis projections of syndiotactic polypropene and syndiotactic poly (1-butene) in the crystal. (b) Plausible unit cells for the stable $(t_2g_2)_2$ form of syndiotactic poly (propene-*co*-1-butene): Right- and left-handed helical molecules are identified by R and L.

8-3-2. Isothermal Crystallization of Syndiotactic Poly(propene-*co*-olefin)s

Isothermal crystallization of the syndiotactic poly(propene-*co*-olefin)s with low comonomer content was conducted. The melting behavior and the melting temperature of isothermal crystallized polymers were investigated by DSC at a heating rate of 10 °C/min. The DSC melting curves of typical copolymers (ethene, 1-butene, and 1-hexene copolymers) are shown in Figure 8-5, (a)–(f). Double melting peak or single melting peak with a shoulder was observed in the DSC patterns of the copolymers with low comonomer content when the crystallization was conducted at comparatively low T_c. While a single peak appears in the copolymers crystallized at high T_c (Figure 8-5, (a), (c), and (e)). These phenomena were also observed in the isothermally crystallized syndiotactic polypropene.[7–15] The double melting peak can be explained by the reason that the sample melts at a temperature varying with the crystallization conditions (first peak), recrystallizes from the melt and completely melts (second peak). The second peak almost disappears in the copolymer whose comonomer content is more than *ca.* 5 mol % (Figure 8-5 (b), (d), and (f)). This result indicates that the recrystallization during the melting can not occur due to the slow recrystallization rate at a heating rate 10 °C/min in the copolymers with high comonomer content. The similar tendency was reported in syndiotactic poly(propene-*co*-1-octene) by Kressler *et al.*[35]

Equilibrium melting point (T_m^0) was determined by Hoffman-Week's plot. The first melting peak in the DSC melting curves was applied for T_m at the T_c. The results are summarized in Table 8-2. Heat of fusion per mole of repeating unit of copolymers (ΔH_u) was determined by Flory's equation represented as follows:[43]

$$1/T_m^0(\mathrm{C}) - 1/T_m^0(\mathrm{H}) = -(R/\Delta H_u)\ln N_{pr}$$

where T_m^0(C), T_m^0(H), and N_{pr} are equilibrium melting temperature of copolymer, equilibrium melting temperature of syndiotactic polypropene, and molar fraction of propene units in a copolymer, respectively. The $1/T_m^0$ is plotted against $-\ln N_{pr}$ in Figure 8-6. The ΔH_u values

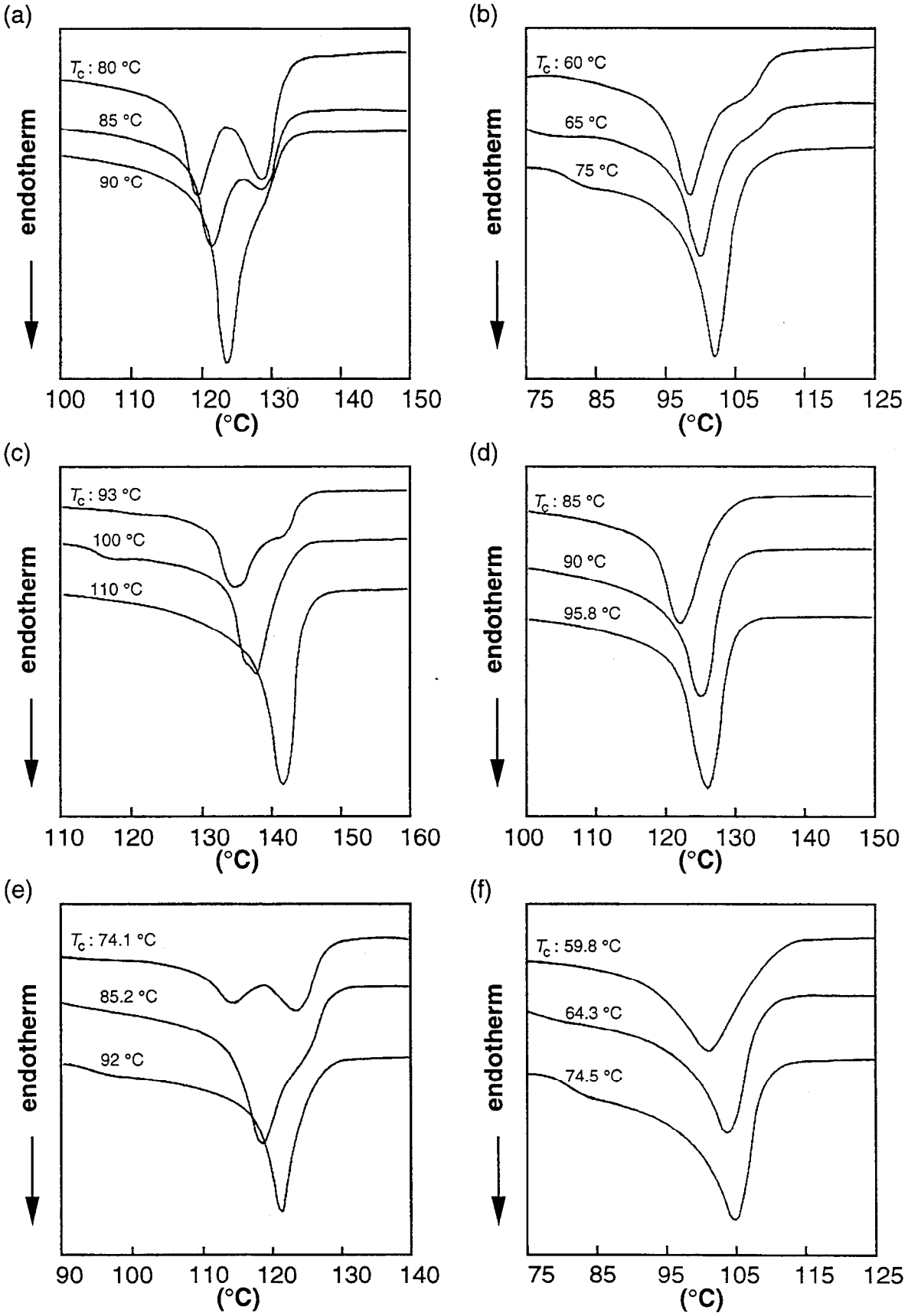

Figure 8-5. DSC melting curves of syndiotactic poly(propene-*co*-olefin)s: olefin = (a) ethene (sample b-1), (b) ethene (sample b-2), (c) 1-butene (sample c-1), (d) 1-butene (sample c-2), (e) 1-hexene (sample d-1), (f) 1-hexene (sample e-2).

Table 8-2. Kinetic parameters for isothermal crystallization of syndiotactic polypropene and syndiotactic poly(propene-*co*-olefin)s

Sample	T_m^{0} [a] (℃)	T_c [b] (℃)	ΔT [c]	$t_{1/2}$ [d] (s)	n [e]	n [f]	K_n [g] (s^{-1})
a	166.7	80	86.7	11	2.30	2.55	2.79×10^{-3}
		90	76.7	14	2.12		2.58×10^{-3}
		100	66.7	30	2.79		5.24×10^{-5}
		110	56.7	85	2.78		3.00×10^{-6}
		120	46.7	298	2.76		1.03×10^{-7}
b-1	143.5	80	63.5	36	2.11	2.38	3.61×10^{-4}
		90	53.5	91	2.70		3.56×10^{-6}
		100	43.5	294	2.34		1.16×10^{-6}
b-2	117.8	80	37.8	1072	2.54	2.54	1.39×10^{-8}
c-1	158.0	80	78.0	13	2.38	2.31	1.55×10^{-3}
		90	68.0	22	2.15		9.01×10^{-4}
		100	58.0	60	2.58		1.79×10^{-5}
		110	48.0	192	2.14		9.01×10^{-6}
c-2	144.4	80	64.4	45	2.48	2.58	5.51×10^{-5}
		90	54.4	97	2.52		6.83×10^{-6}
		100	44.4	432	2.74		4.16×10^{-8}
c-3	132.0	80	52.0	82	2.10	2.23	6.63×10^{-5}
		90	42.0	479	2.35		3.48×10^{-7}
d-1	132.2	80	52.2	91	2.16	2.16	4.07×10^{-5}
		90	42.2	384	2.15		1.93×10^{-6}
d-2	122.7	80	42.7	475	2.45	2.45	1.92×10^{-7}
e-1	140.2	80	60.2	88	2.48	2.50	1.05×10^{-5}
		90	50.2	208	2.51		1.05×10^{-6}
e-2	117.2	80	37.2	1152	2.02	2.02	4.54×10^{-7}
f-1	142.4	80	62.4	37	2.24	2.52	2.13×10^{-4}
		90	52.4	79	2.57		9.20×10^{-6}
		100	42.4	246	2.75		1.84×10^{-7}
f-2	131.5	80	51.5	203	2.08	2.20	1.10×10^{-5}
		90	41.5	470	2.31		4.66×10^{-7}

[a] Equilibrium melting temperature. [b] Crystallization temperature. [c] $T_m^{0} - T_c$ (K). [d] Half time of crystallization. [e] Avrami exponent. [f] Average of Avrami exponent. [g] Kinetic constant.

of copolymers can be determined by the slope of the plots, and 5.2 kJ/mol for 1-butene copolymer and 1.9 kJ/mol for the other copolymers are obtained.

Crystallization kinetics was studied on the basis of the T_m^0. Half time of crystallization ($t_{1/2}$) was determined from the relative DLI technique at various T_cs. The $t_{1/2}$ values of copolymers are summarized in Table 8-2 and the plots of $t_{1/2}$ against degree of supercooling ($\Delta T = T_m^0 - T_c$) are shown in Figure 8-7. The $t_{1/2}$ markedly increased at ΔT less than 55 K. The plots of $t_{1/2}$ against ΔT were located on almost the same curved line.

Isothermal crystallization behavior of polymers can be analyzed by means of the Avrami equation:[44–47]

$$(1 - X_t) = \exp(-K_n t^n) \qquad (1)$$

where X_t is the weight fraction of crystallizable polymer crystallized at time t, K_n is kinetic rate constant, and n is Avrami exponent, respectively. The equation (1) can be written as:

$$\log[-\log(1 - X_t)] = n \log t + \log(K_n/2.3) \qquad (2)$$

By plotting the quantity $\log[-\log(1 - X_t)]$ against $\log t$, it is possible to determine value of the Avrami exponent (n) from the slope of the plots. The Avrami plots of typical syndiotactic poly(propene-*co*-olefin)s (olefin = ethene, 1-butene) are shown in Figure 8-8, (a) and (b), and the Avrami exponents are summarized in Table 8-2. The value of Avrami exponent of copolymers ranged from 2.0 to 2.8 for the primary crystallization. The transition of crystallization process

from primary to secondary crystallization process was observed at $X_t = 0.7$–0.8 in any copolymers. Balbontin *et al.* and Cheng *et al.* measured the Avrami exponent of syndiotactic polypropene with various molecular weights and syndiotacticities, and reported the values of the Avrami exponent, $n = 1.8$–3.9 and 1.9–3.0, respectively ($n = 2.6$ was obtained in this

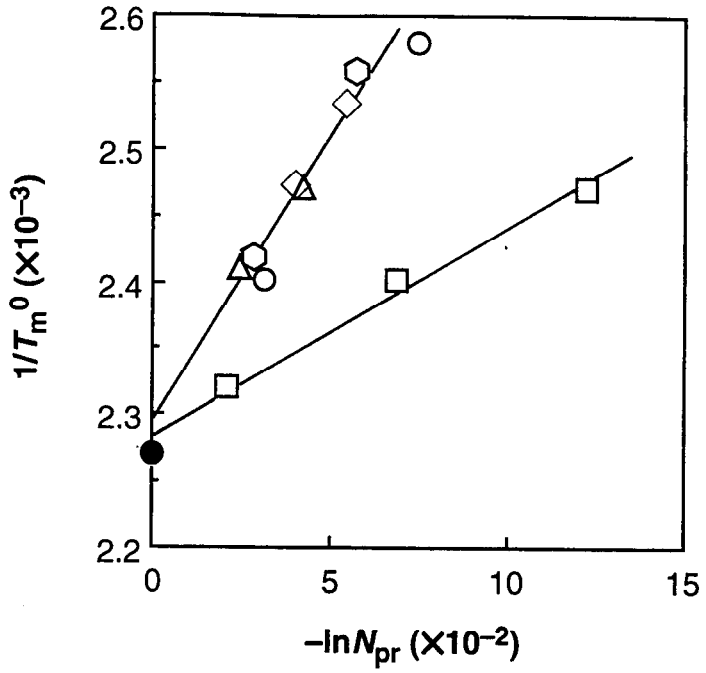

Figure 8-6. Plots of $1/T_m^0$ against $-\ln N_{pr}$ of syndiotactic poly(propene-*co*-olefin)s according to the Flory's equation: olefin = (○) ethene; (□) 1-butene; (◇) 1-pentene; (⬡) 1-hexene; (△) 4-methyl-1-pentene; (●) syndiotactic polypropene.

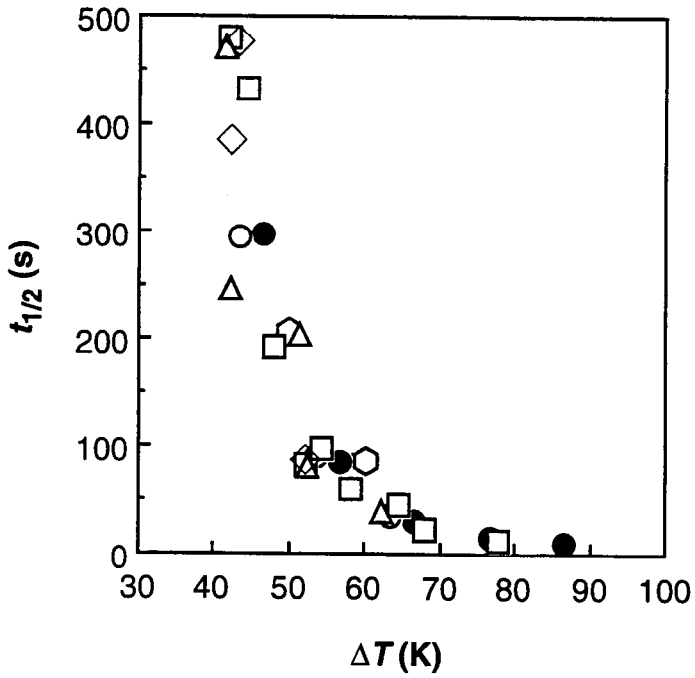

Figure 8-7. Plots of $t_{1/2}$ against ΔT of syndiotactic poly(propene-*co*-olefin)s: olefin = (○) ethene; (□) 1-butene; (◇) 1-pentene; (⬡) 1-hexene; (△) 4-methyl-1-pentene; (●) syndiotactic polypropene.

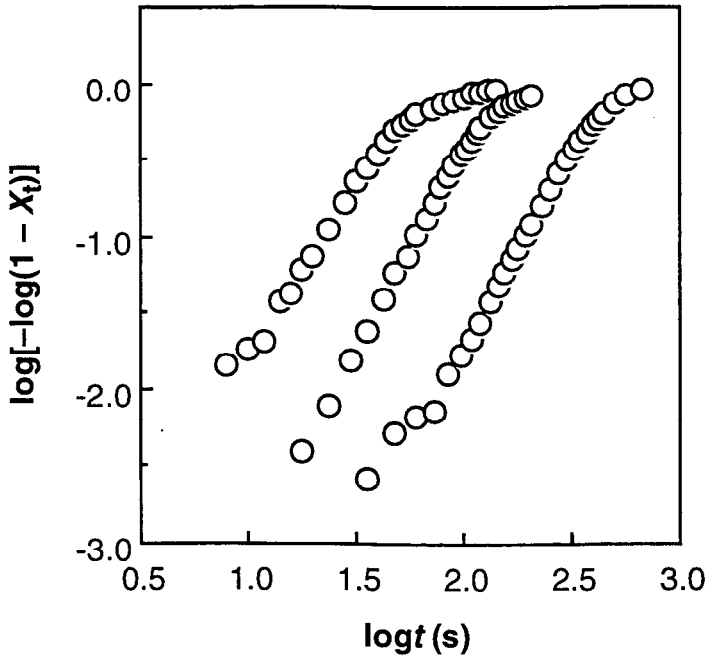

Figure 8-8(a). Plots of log[–log(1 – X_t)] against logt of syndiotactic poly(propene-*co*-ethene)(sample b-1).

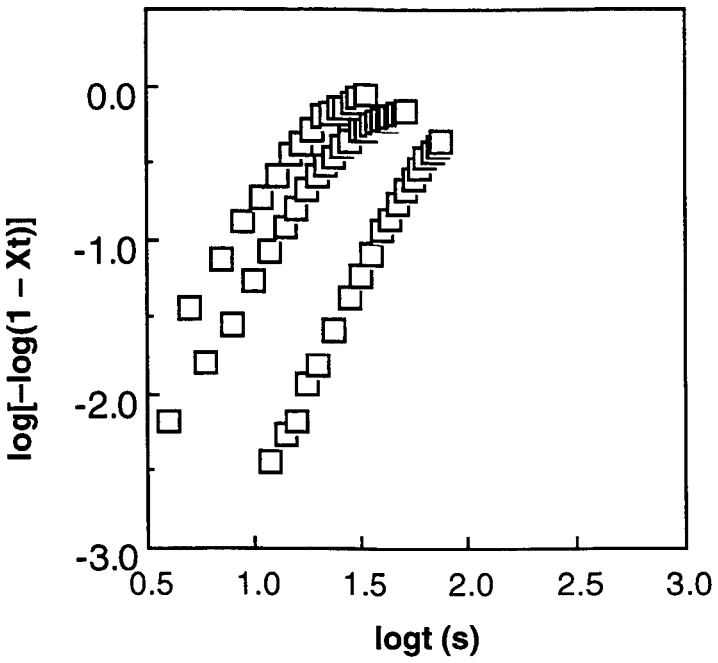

Figure 8-8(b). Plots of log[–log(1 – X_t)] against logt of syndiotactic poly(propene-*co*-1-butene) (sample c-1).

experiment).[11,48] Three-dimensional crystal growth of syndiotactic polypropene was implied by the Avrami exponent in the previous report. Lovinger *et al.* described a transition between three-dimensional (spherulitic) and two-dimensional (axialitic, rectangular single crystal) structures in thin melt crystallized films with the increase of T_c.[4,6] Cheng *et al.* studied morphology of syndiotactic polypropene in the crystallization process by polarized light microscopy observations, and indicated that a heterogeneous nucleation was the main process in the crystallization.[11,28] The Avrami exponents of syndiotactic poly(propene-*co*-olefin)s were within the limits of previously reported values. It seems reasonable to suppose that the crystallization behavior (nucleation and growth) of syndiotactic poly(propene-*co*-olefin)s is almost the same with that of syndiotactic polypropene.

Rate constant (K_n) was calculated from $t_{1/2}$ using following relation:

$$K_n = \ln 2/t_{1/2}^n \qquad (3)$$

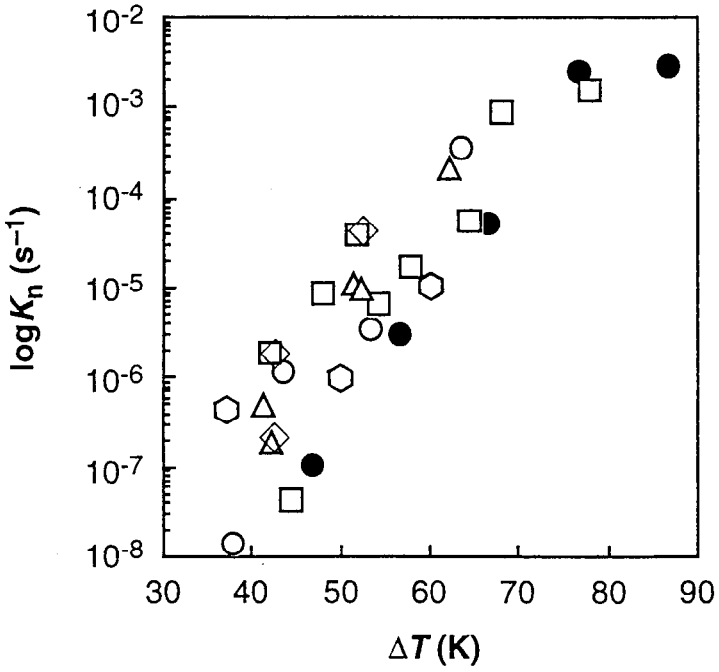

Figure 8-9. Plots of K_n against ΔT of syndiotactic poly(propene-*co*-olefin)s: olefin = (○) ethene; (□) 1-butene; (◇) 1-pentene; (⬡) 1-hexene; (△) 4-methyl-1-pentene; (●) syndiotactic polypropene.

The K_n values are summarized in Table 8-2 and plotted against ΔT in Figure 8-9. Clear effect of the comonomer on the K_n values could not be found in the plots.

Judging from the results, the crystallization behavior of copolymers depends on not the kind of comonomer but the ΔT.

Crystalline structure of isothermally crystallized syndiotactic poly(propene-*co*-olefin)s was studied by WAXD. The crystalline structures of the copolymers are summarized in Table 8-3. The WAXD patterns of syndiotactic polypropene and typical copolymers (ethene, 1-butene, and 1-hexene copolymers) are shown in Figure 8-10, (a)–(e). The characteristic peak at $2\theta = 18.8$ ° derived from (211) could be observed in the syndiotactic polypropene isothermally crystallized at $\Delta T = 57$ and 47 K ($T_c = 110$ and 120 °C) (Figure 8-10 (a)). This reflection is derived from the Cell III. The weak peak at almost the same position was observed in the poly(propene-*co*-1-butene) with low content of 1-butene (sample c-1) isothermally crystallized at $\Delta T = 48$ K ($T_c = 110$ °C) (Figure 8-10 (c)). This result indicates that this copolymer (sample c-1) can compose the crystalline structure of Cell III. On the other hand, the peak derived from (211) could not be observed in the WAXD patterns of other copolymers regardless of ΔT. The WAXD patters of these copolymers were similar to the pattern of Cell II in the syndiotactic polypropene.[10] This result suggests that these copolymers have the crystalline structures based on the unit Cell II of the syndiotactic polypropene.

In comparison of the WAXD patters of copolymers, broadening of peak at $2\theta = 17$–18 ° could be found in the ethene, 1-hexene copolymers (Figure 8-10, (b) and (e)), while sharp peaks at $2\theta = 15.9$ ° derived from (010) reflection were found in the 1-butene copolymers (Figure 8-10, (c) and (d)). Lovinger *et al.* observed the peak at about $2\theta = 17$ ° derived from (110) and (201) reflections in the syndiotactic polypropene with Cell II.[5] Zannetti *et al.* calculated WAXD pattern of the Cell II, and reported that the peak at $2\theta = 17$ ° was observed in both calculated and observed WAXD patterns.[10] These results suggest that the crystalline structure of poly(propene-*co*-1-butene) is slightly different from the Cell II as shown in other

Table 8-3. Crystalline structures of isothermally crystallized syndiotactic poly(propene-*co*-olefin)s

Sample	T_c[a] (℃)	ΔT[b]	X_c[c] (%)	Axial length (Å)[d]		I_{200}/I_{010}[e]
				a axis	*b* axis	
a	90	76.7	24.5	14.62	5.58	1.6
	100	66.7	25.9	14.56	5.58	1.9
	110	56.7	26.7	14.56	11.20, 5.60	1.9
	120	46.7	34.4	14.36	11.12, 5.56	1.7
	130	36.7	26.7	14.52	5.57	1.9
b-1	70	73.5	23.1	14.56	5.56	1.0
	80	63.5	23.1	14.62	5.58	1.3
	90	53.5	23.8	14.58	5.59	1.3
	100	43.5	25.5	14.50	5.56	1.5
c-1	80	78.0	24.6	14.66	5.60	1.4
	90	68.0	24.8	14.56	5.56	1.6
	100	58.0	27.4	14.60	5.56	2.0
	110	48.0	30.5	14.56	5.57	2.0
	120	38.0	27.3	14.64	5.60	1.9
c-2	70	74.4	22.9	14.76	5.60	1.0
	80	64.4	23.5	14.76	5.60	1.1
	90	54.4	23.8	14.66	5.58	1.6
	100	44.4	26.4	14.72	5.59	1.9
e-1	70	70.2	20.1	14.60	5.57	1.0
	80	60.2	20.6	14.64	5.57	1.2
	90	50.2	22.0	14.60	5.57	1.5
	100	40.2	22.1	14.64	5.58	1.8

[a] Crystallization temperature. [b] $T_m^0 - T_c$. [c] Polymer crystallinity determined by WAXD. [d] Caluculated from the (200) and (010) or (020) reflections of WAXD. [e] Intensity ratio of (200) reflection to (010) reflection determined by WAXD.

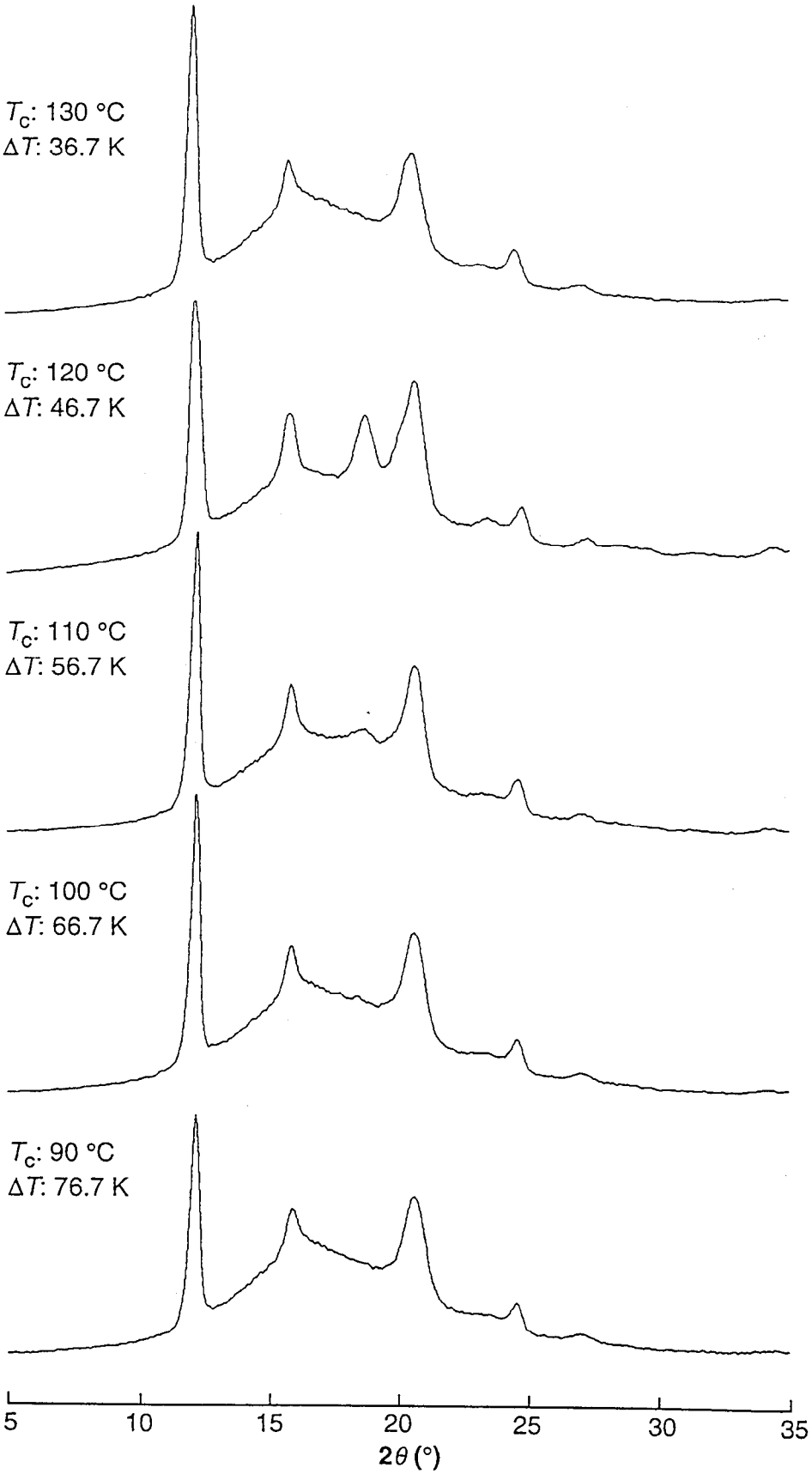

Figure 8-10(a). WAXD patterns of isothermally crystallized syndiotactic polypropene (sample a).

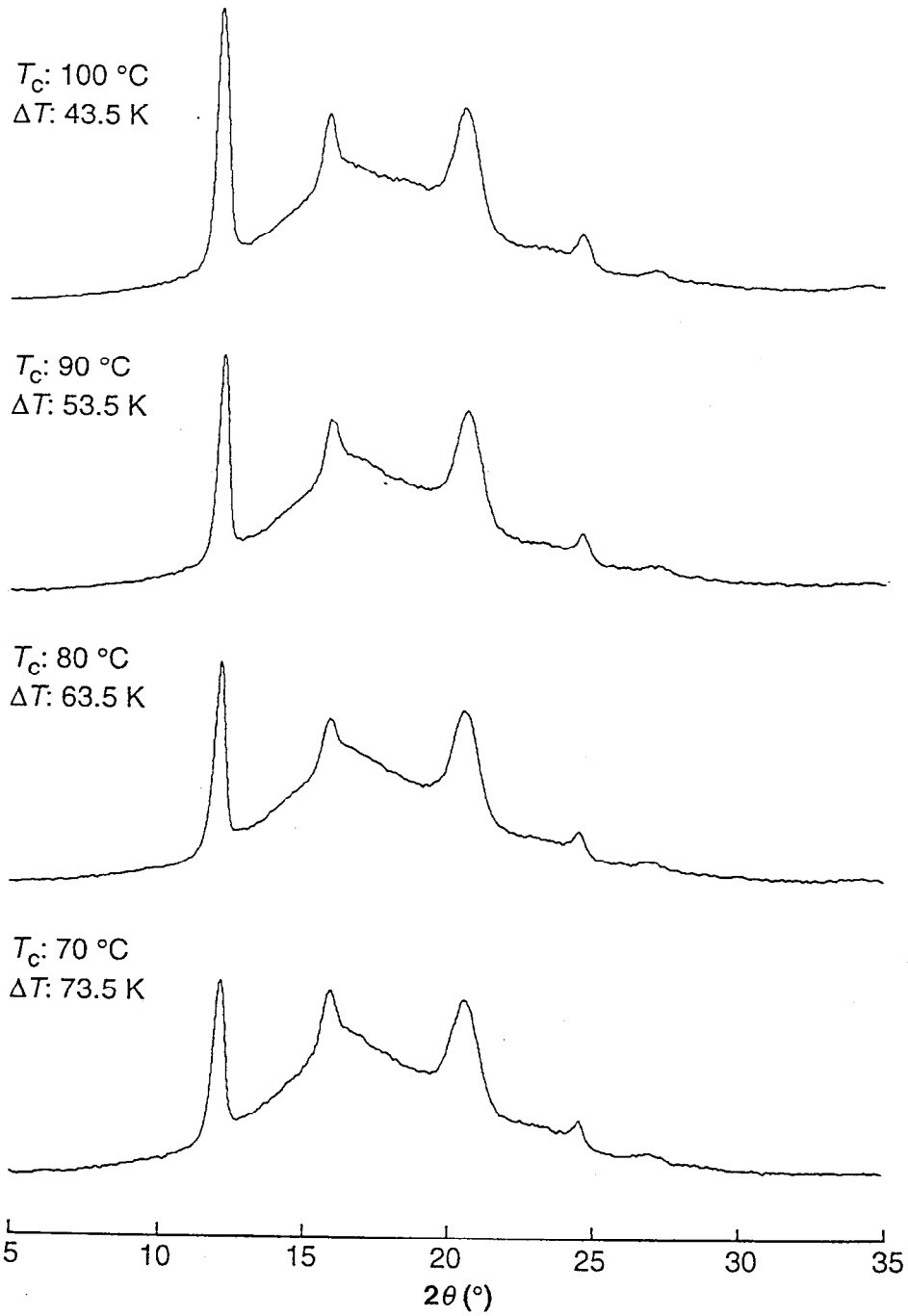

Figure 8-10(b). WAXD patterns of isothermally crystallized syndiotactic poly(propene-*co*-ethene) (sample b-1).

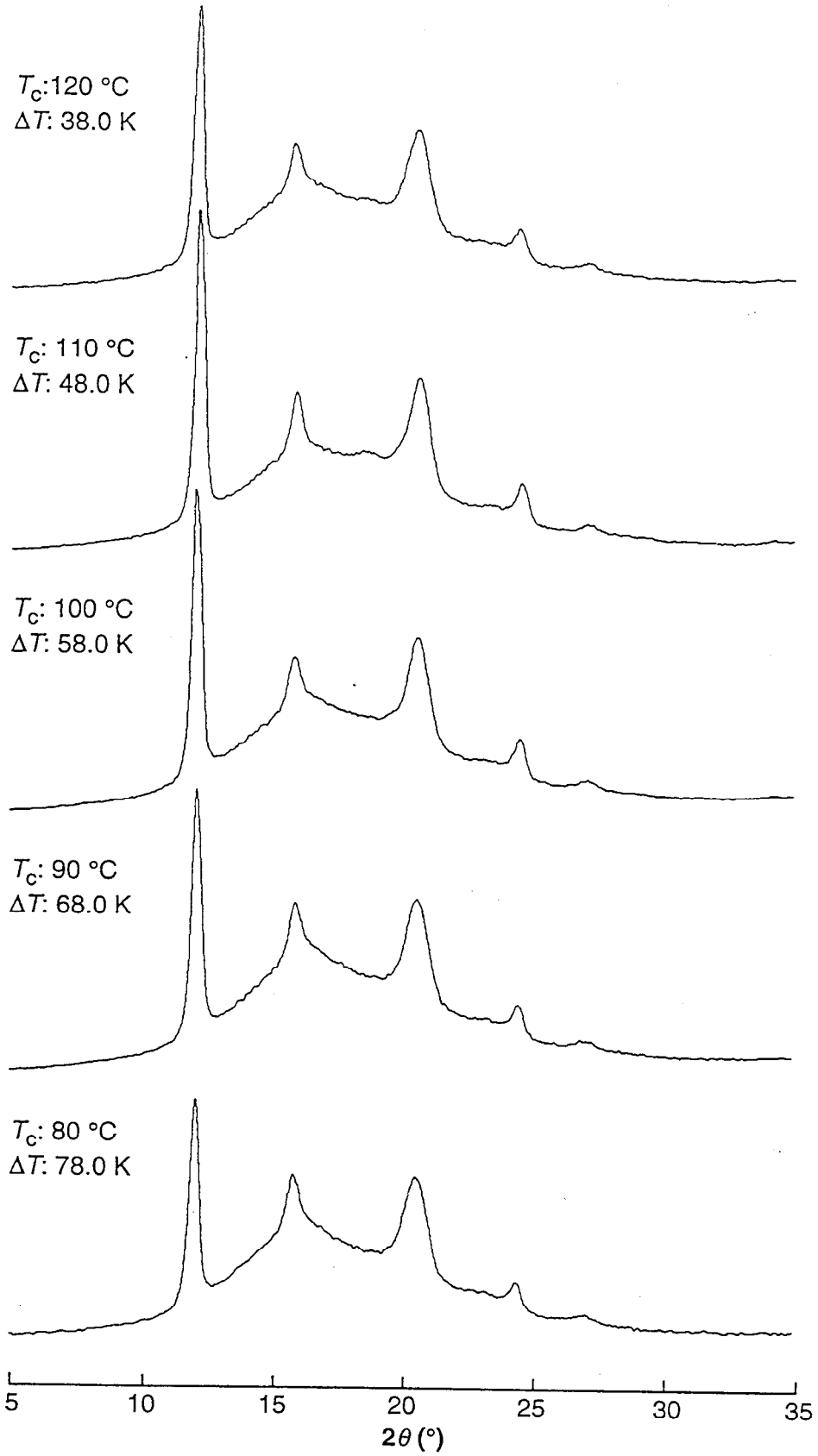

Figure 8-10(c). WAXD patterns of isothermally crystallized syndiotactic poly(propene-*co*-1-butene) (sample c-1).

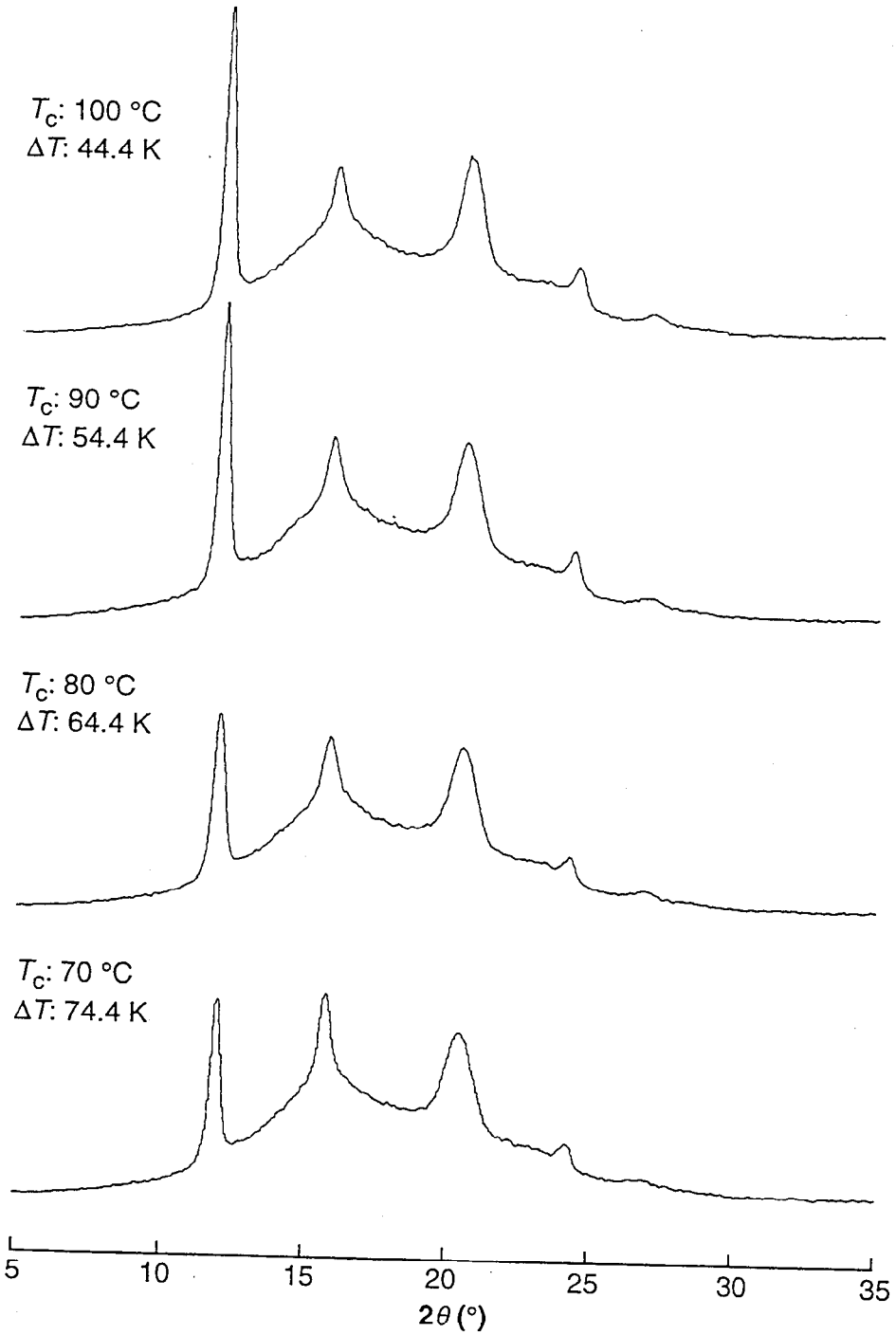

Figure 8-10(d). WAXD patterns of isothermally crystallized syndiotactic poly(propene-*co*-1-butene) (sample c-2).

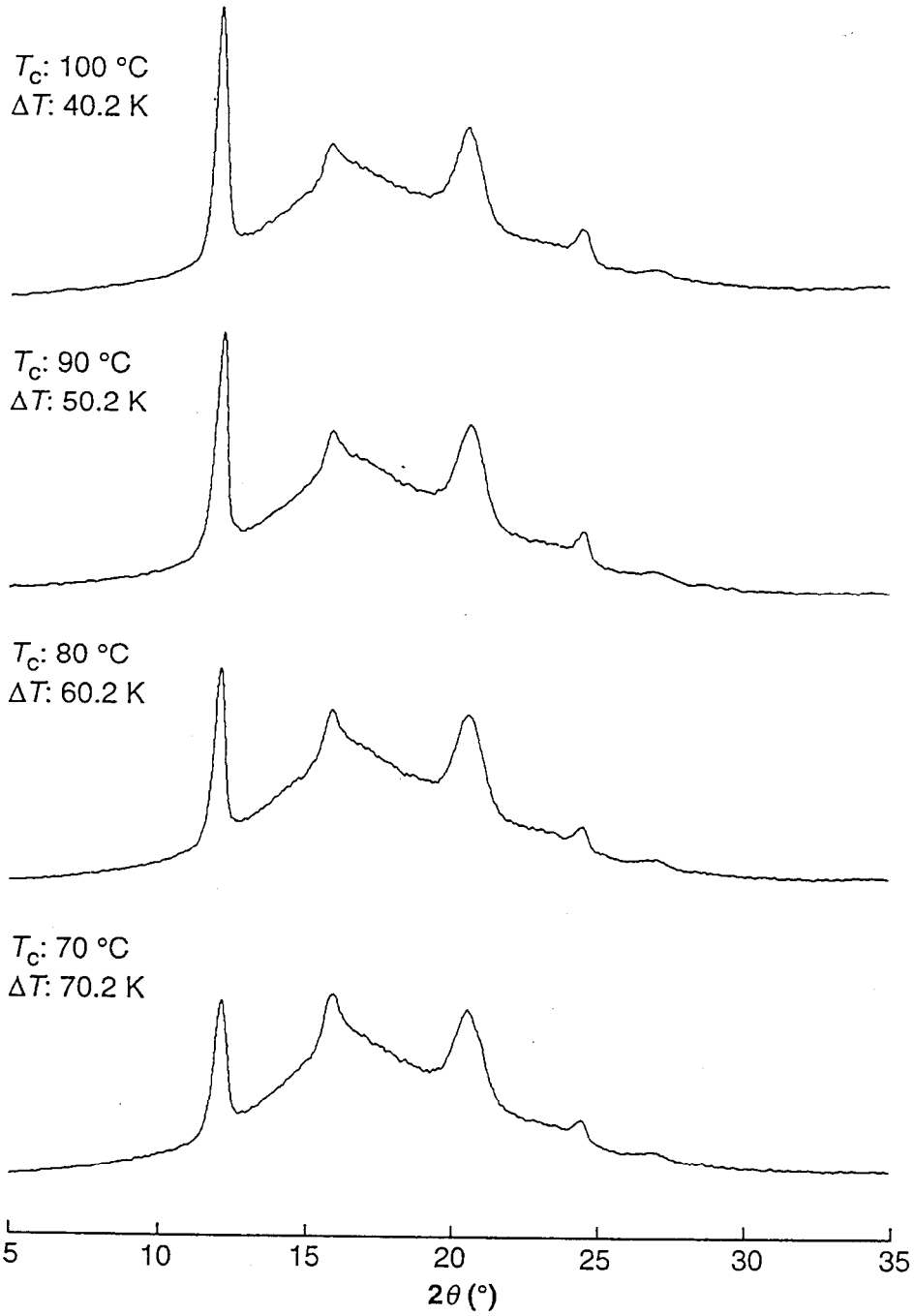

Figure 8-10(e). WAXD patterns of isothermally crystallized syndiotactic poly(propene-*co*-1-hexene) (sample d-1).

copolymers. This difference could cause the peculiar properties of poly(propene-*co*-1-butene).

Intensity ratios of (200) to (010) (I_{200}/I_{010}) are plotted against ΔT in Figure 8-11. The I_{200}/I_{010} values of copolymers (except sample c-1) increased linearly with the decrease of the ΔT due to the increase of the I_{200}. While syndiotactic polypropene and poly(propene-*co*-1-butene) (sample c-1) showed the maximum I_{200}/I_{010} value at about ΔT = 60 and 55 K, respectively. This difference should be caused by the crystalline structure of Cell III in the syndiotactic polypropene and poly(propene-*co*-1-butene) (sample c-1).

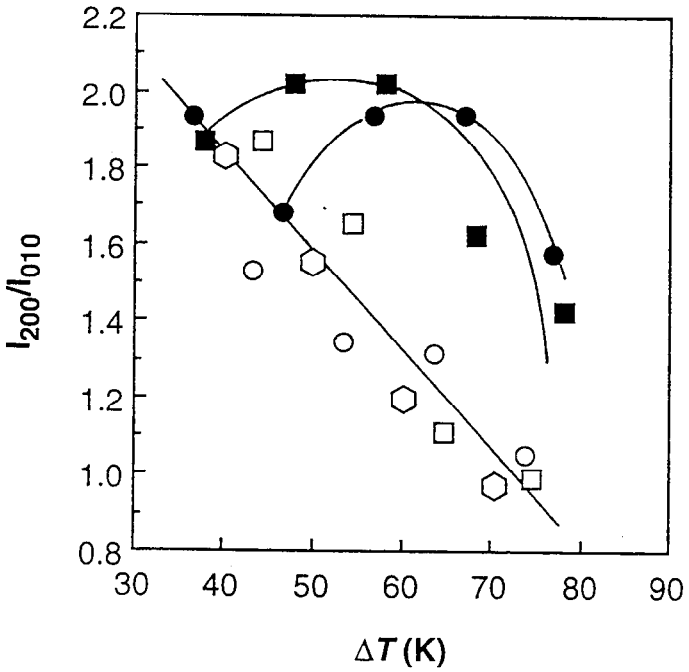

Figure 8-11. Plots of I_{200}/I_{010} against ΔT of syndiotactic poly(propene-*co*-olefin)s: (○) propene/ethene (sample b-1); (■) propene/1-butene (sample c-1); (□) propene/1-butene (sample c-2); (⬡) propene/1-hexene (sample d-1); (●) syndiotactic polypropene (sample a).

8-4. Summary

Structures and properties of various syndiotactic poly(propene-*co*-olefin)s were studied, and peculiar crystalline structure was observed in poly(propene-*co*-1-butene). The 1-butene copolymer showed smaller melting point depression with an increase of comonomer content than other copolymers, and had melting point in a whole range of 1-butene content. Furthermore, the expansion of *a* axis of poly(propene-*co*-1-butene) was observed with the increase of 1-butene content. These results indicate the isomorphism of this copolymer.

The kind of comonomer in the syndiotactic poly(propene-*co*-olefin)s did not affect to the behavior of isothermal crystallization. Avrami exponent (n) of the copolymers ranged from 2.0 to 2.8. These values were almost the same with that of syndiotactic polypropene. The $t_{1/2}$ and K_n depended on the ΔT value in any copolymers. WAXD patter of poly(propene-*co*-1-butene) showed the sharper peak of (010) reflection than other copolymers. The WAXD patters of all the copolymers except poly(propene-*co*-1-butene) indicated the crystalline structure of Cell II, while poly(propene-*co*-1-butene) with low 1-butene content showed the peak of (211) reflection derived from Cell III.

References

(1) Natta, G.; Pasquon, I.; Corradini, P.; Zambelli, A. *J. Am. Chem. Soc.* **1962**, *84*, 1488.

(2) Ewen, J. A.; Jones, R. L.; Razavi, A.; Ferrara, J. D.; *J. Am. Chem. Soc.* **1988**, *110*, 6255.

(3) Corradini, P.; Natta, G.; Ganis, P.; Temussi, P. A. *J. Polym. Sci., Part C: Polym. Symp.* **1967**, *16*, 2477.

(4) Lotz, B.; Lovinger, A. J.; Cais, R. E. *Macromolecules* **1988**, *21*, 2375.

(5) Lovinger, A. J.; Lotz, B.; Davis, D. D. *Polymer* **1990**, *31*, 2253.

(6) Lovinger, A. J.; Davis, D. D.; Lotz, B. *Macromolecules* **1991**, *24*, 552.

(7) Haftka, S.; Könnecke, K. *J. Macromol. Sci., Phys.* **1991**, *B30*(4), 319.

(8) Galambos, A., Wolkowicz, M., Zeigler, R. *ACS Symp. Ser., Catal. Polym. Synth.* **1992**, *496*, 104.

(9) Lovinger, A. J.; Lotz, B.; Davis, D. D.; Schumacher, M. *Macromolecules* **1994**, *27*, 6603.

(10) Marigo, A.; Marega, C.; Zannetti, R. *Macromol. Rapid Commun.* **1994**, *15*, 225.

(11) Rodriguez-Arnold, J.; Zhang, A.; Cheng, S. Z. D.; Lovinger, A. J.; Hsieh, E. T.; Chu, P.; Johnson, T. W.; Honnell, K. G.; Geerts, R. G.; Palackal, S. J.; Hawley, G. R.; Welch, M. B. *Polymer* **1994**, *35*, 1884.

(12) Auriemma, F.; Lewis, R. H.; Spiess, H. W.; De Rosa, C. *Macromol. Chem. Phys.* **1995**, *196*, 4011.

(13) Loos, J.; Buhk, M.; Petermann, J.; Zoumis, K.; Kaminsky, W. *Polymer* **1996**, *37*, 387.

(14) Schmidtke, A. J.; Strobl, G.; Thurn-Albrecht, T. *Macromolecules* **1997**, *30*, 5804.

(15) De Rosa, C.; Auriemma, F.; Vint, V.; Galimberti, M. *Macromolecules* **1998**, *31*, 6206.

(16) Lovinger, A. J.; Lotz, B.; Davis, D. D.; Padden, F. J., Jr. *Macromolecules* **1993**, *26*, 3494.

(17) De Rosa, C.; Corradini, P. *Macromolecules* **1993**, *26*, 5711.

(18) Asanuma, T.; Nakanishi, S.; Shiomura, T.; Kanaya, T. *Sen-i Gakkaishi*, **1993**, *49*, 260.

(19) Sozzani, P.; Simonutti, R.; Galimberti, M. *Macromolecules* **1993**, *26*, 5782.

(20) Stocker, W.; Schumacher, M.; Graff, S.; Long, J.; Wittmann, J. C.; Lovinger, A. J.; Lotz, B. *Macromolecules* **1994**, *27*, 6948.

(21) Auriemma, F.; Born, R.; Spiess, H. W.; De Rosa, C.; Corradini, P. *Macromolecules* **1995**, *28*, 6902.

(22) Thomann, R.; Wang, C.; Kressler, J.; Jüngling, S.; Mülhaupt, R. *Polymer* **1995**, *36*, 3795.

(23) De Rosa, C.; Auriemma, F.; Corradini, P. *Macromolecules* **1996**, *29*, 7452.

(24) Asakura, T.; Aoki, A.; Date, T.; Demura, M.; Asanuma, T. *Polym. J.* **1996**, *28*, 24.

(25) Loos, J.; Schauwienold, A. M.; Yan, S.; Petermann, J.; Kaminsky, W. *Polym. Bull.* **1997**, *38*, 185.

(26) De Rosa, C.; Auriemma, F.; Vinti, V. *Macromolecules* **1997**, *30*, 4137.

(27) Lovinger, A. J.; Lotz, B. *J. Polym. Sci., Part B: Polym. Phys.* **1997**, *35*, 2523.

(28) Rodriguez-Arnold, J.; Bu, Z.; Cheng, S. Z. D.; Hsieh, E. T.; Johnson, T. W.; Geerts, R. G.; Palackal, S. J.; Hawley, G. R.; Welch, M. B. *Polymer* **1994**, *35*, 5194.

(29) Nakaoki, T.; Hayashi, H.; Kitamura, R. *Polymer* **1990**, *21*, 4833.

(30) Tsukruk, V. V.; Reneker, D. H. *Macromolecules* **1995**, *28*, 1370.

(31) Bu, Z.; Yoon, Y.; Ho, R. M.; Zhou, W.; Jangchud, I.; Eby, R. K.; Cheng, S. Z. D.; Hsieh, E. T.; Johnson, T. W.; Geerts, R. G.; Palackal, S. J.; Hawley, G. R.; Welch, M. B. *Macromolecules* **1996**, *29*, 6575.

(32) Uozumi, T.; Soga, K. *Makromol. Chem.* **1992**, *193*, 823.

(33) Jüngling, S.; Mülhaupt, R.; Fischer, D.; Langhauser, F. *Angew. Makromol. Chem.* **1995**, *229*, 93.

(34) Thomann, R.; Kressler, J.; Mülhaupt, R. *Macromol. Chem. Phys.* **1997**, *198*, 1271.

(35) Thomann, R.; Kressler, J.; Mülhaupt, R. *Polymer* **1998**, *39*, 1907.

(36) De Rosa, C.; Auriemma, F.; Vinti, V.; Grassi, A.; Galimberti, M. *Polymer* **1998**, *39*, 6219.

(37) (a) Magill, J. H. *Polymer* **1961**, *2*, 221. (b) Magill, J. H. *Polymer* **1962**, *3*, 35. (c) Magill, J. H. *Polymer* **1962**, *3*, 655..

(38) Natta, G.; Pasquon, I.; Corradini, P.; Pegoraro, M.; Zambelli, A. *A. Rend. Accad. Naz. Lincei* **1960**, *28*, 539.

(39) Natta, G.; Corradini, P.; Ganis, P. *Makromol. Chem.* **1960**, *39*, 238.

(40) Cavallo, P.; Martuscelli, E.; Pracella, M. *Polymer* **1977**, *18*, 42.

(41) De Rosa, C.; Venditto, V.; Guerra, G.; Pirozzi, B.; Corradini, P. *Macromolecules* **1991**, *24*, 5645.

(42) De Rosa, C.; Venditto, V.; Guerra, G.; Corradini, P. *Macromol. Chem.* **1992**, *193*, 1351.

(43) Flory, P. J. *Trans. Faraday Soc.* **1955**, *390*, 51.

(44) (a) Avrami, M. *J. Chem. Phys.* **1939**, *7*, 1103. (b) Avrami, M. *J. Chem. Phys.* **1940**, *8*, 212. (c) Avrami, M. *J. Chem. Phys.* **1941**, *9*, 177.

(45) Evans, U. R. *Trans. Faraday Soc.* **1945**, *41*, 365.

(46) Mandelkern, L. In *Crystallization of Polymer*; McGraw-Hill: New York, 1964.

(47) Khanna, Y. P.; Taylor, T. J. *Polym. Eng. Sci.* **1988**, *28*, 1042.

(48) Balbontin, G.; Dainelli, D.; Galimberti, M.; Paqanetto, G. *Makromol. Chem.* **1992**, *193*, 693.

Chapter 9

Summary

This thesis consists of general introduction and the seven experimental chapters, each of which is summarized as follows.

Chapter 1 General Introduction

The previous studies concerning group 4 metallocene catalysts for olefin polymerizations, stereospecific polymerization of α-olefins with metallocene catalyst and development of cocatalysts were summarized. Cocatalyst for metallocene catalyst plays important role in the olefin polymerization, and a great deal of effort has been made on development of cocatalysts. What seems to be lacking, however, is the detailed study of correlation between metallocene catalysts and cocatalysts for catalytic performance. From such a view point, this work has been aimed at understanding the effect of cocatalyst on olefin polymerization, especially ethene and propene polymerization.

In addition, copolymerizations of olefins with metallocene catalysts were briefly reviewed. In comparison to conventional Ziegler–Natta catalysts, higher incorporation of higher α-olefin and cycloolefin is one of the important features of metallocene catalysts. In this work, several propene-based copolymers were synthesized by metallocene catalysts and structures of copolymers were investigated.

Chapter 2 Effect of Cocatalysts on Ethene Polymerization with Zirconocene Catalysts

Ethene polymerization was carried out with *rac*-$Me_2Si(Ind)_2ZrCl_2$ using MAO as a cocatalyst in toluene. A clear bimodal MWD was observed in the polyethene obtained. The low molecular weight fraction of the polyethenes were produced at initial stage of the polymerization. The MWD of polyethene was independent of the molar ratio of (MAO)Al/Zr and the [Zr] concentration. The high molecular weight fraction disappeared, however, when the polymerization was performed either at a low temperature or using dry MAO. Addition of $AlMe_3$ to the MAO caused to increase of the low molecular weight fraction at the initial stage of

polymerization. The low molecular weight fraction was also increased when the polymerization was conducted in the mixture of toluene and CH_2Cl_2 as a solvent. From these results, the formation of active species in ethene polymerization was discussed.

Polymerization of ethene was conducted with Cp_2ZrCl_2 and *rac*-$Me_2Si(Ind)_2ZrCl_2$ using AlR_3 (R = Me, Et, *i*Bu)/$Ph_3CB(C_6F_5)_4$ or $B(C_6F_5)_3$. In the case of polymerization with Cp_2ZrCl_2–AlR_3/$Ph_3CB(C_6F_5)_4$ system, induction time to reach the maximum R_p was observed. Especially, it took about 30 min to show the polymerization activity with Cp_2ZrCl_2–$AlEt_3$/$Ph_3CB(C_6F_5)_4$ system. When $B(C_6F_5)_3$ was used for cation-forming reagent, no activity was shown with $AlEt_3$ while high activity was observed with Al*i*Bu_3. On the other hand, in the polymerization with *rac*-$Me_2Si(Ind)_2ZrCl_2$ and $Ph_3CB(C_6F_5)_4$ as a cation-forming reagent, high activity was observed with both $AlEt_3$ and Al*i*Bu_3. When $B(C_6F_5)_3$ was used instead of $Ph_3CB(C_6F_5)_4$, very low activity was observed with $AlEt_3$, whereas high activity was appeared with Al*i*Bu_3. The maximum rate of polymerization (R_p) was found at the initial time of polymerization following rapid drop of R_p using Al*i*Bu_3/$B(C_6F_5)_3$ as a cocatalyst. Mechanisms in formation of active species were discussed on the basis of activity and rate-time profile of the polymerization.

Chapter 3 Effect of Cocatalysts on α-Olefin Polymerization with Zirconocene Catalysts

Propene, 1-butene, and 1-hexene polymerization were conducted the mixtures of *rac*- , *meso*-$Me_2Si(2,3,5\text{-}Me_3Cp)_2ZrCl_2$ and *rac*-, *meso*-$Me_2Si(2\text{-}MeInd)_2ZrCl_2$ combined with MAO or AlR_3 (R = Et, *i*Bu)/$Ph_3CB(C_6F_5)_4$ as cocatalysts. The activity ratios of *rac*-isomer to *meso*-isomer, $R_p(rac)/R_p(meso)$, changed with the combined cocatalysts.

In the polymerization with $Me_2Si(2,3,5\text{-}Me_3Cp)_2ZrCl_2$, higher $R_p(rac)/R_p(meso)$ values were observed using MAO than using AlR_3/$Ph_3CB(C_6F_5)_4$ as cocatalysts in any kinds of α-olefin polymerizations. The values of $R_p(rac)/R_p(meso)$ with each cocatalyst were almost the same regardless of α-olefins.

The same polymerizations were investigated with the mixture of *rac*-, *meso*-$Me_2Si(2\text{-}MeInd)_2ZrCl_2$. The polymerization profile of propene was determined from the rate of overall propene consumption and fraction of isotactic and atactic polymers which were sampled during the polymerization. The value of $R_p(rac)/R_p(meso)$ in propene and 1-butene polymerizations decreased in the following order with the combined cocatalysts: $AlEt_3/Ph_3CB(C_6F_5)_4$ > $Al\textit{i}Bu_3/Ph_3CB(C_6F_5)_4$ > MAO. In the case of 1-hexene polymerization, considerably high $R_p(rac)/R_p(meso)$ values were obtained regardless of cocatalysts used. The result indicated the steric hindrance of the active sites in *meso*-$Me_2Si(2\text{-}MeInd)_2ZrCl_2$ for 1-hexene coordination.

Chapter 4 Chain Transfer Reaction by Trialkylaluminum in Stereospecific Polymerization of Propene with Zirconocene Catalysts

Stereospecific polymerization of propene was carried out with isospecific *rac*-$Et(Ind)_2ZrCl_2$, *rac*-$Me_2Si(Ind)_2ZrCl_2$, and syndiospecific *i*$Pr(Cp)(Flu)ZrCl_2$ combined with AlR_3 (R = Et, *i*Bu)/$Ph_3CB(C_6F_5)_4$. In the isospecific polymerization with *rac*-$Et(Ind)_2ZrCl_2$ and *rac*-$Me_2Si(Ind)_2ZrCl_2$, the molecular weight of polypropenes decreased with an increase in the molar ratio of $AlEt_3$/Zr, whereas, an effect of $Al\textit{i}Bu_3$ concentration on molecular weight was not observed. The chain end groups of resulting polypropenes were studied by ^{13}C NMR spectroscopy and an increase in the molar ratio of Et end groups (derived from chain transfer to $AlEt_3$) to *n*Pr end groups (derived from β-hydrogen transfer) was observed with the increase in the molar ratio of $AlEt_3$/Zr. On the other hand, the chain transfer reactions not only by $AlEt_3$ but $Al\textit{i}Bu_3$ were detected in syndiospecific polymerization with *i*$Pr(Cp)(Flu)ZrCl_2$. The molar ratio of alkyl (R) end groups (derived from chain transfer to AlR_3) to *n*Pr end groups was higher in the polypropene obtained with $AlEt_3$ than that obtained with $Al\textit{i}Bu_3$. The ratios of k_{trA} to k_p (k_{trA} = rate constant of chain transfer to AlR_3, k_p = rate constant of propagation) were determined by kinetic study.

Chapter 5 Effect of Cocatalysts on Microstructures of Polypropene Obtained with Zirconocene Catalysts

Polypropenes were prepared by aspecific, isospecific, and syndiospecific zirconocene catalysts combined with MAO or AlR_3 (R = Et, *i*Bu)/$Ph_3CB(C_6F_5)_4$ as cocatalysts. The microstructures of the polypropenes were studied by ^{13}C NMR spectroscopy. Effect of cocatalysts on the stereospecificity of atactic polypropenes was not observed with any zirconocene catalysts. Clear difference of isospecificity and regioselectivity of isotactic polypropenes prepared by C_2-symmetrical zirconocene catalysts could not be observed using any cocatalysts. On the other hand, the [rrrr] pentad fraction of syndiotactic polypropene prepared by *i*Pr(Cp)(Flu)$ZrCl_2$ with MAO was found to be higher than with $AlR_3/Ph_3CB(C_6F_5)_4$. The stereoirregular fraction of [rmmr] was almost the same in any syndiotactic polypropenes, but the [rmrr] fraction was higher in the polypropenes obtained with $AlR_3/Ph_3CB(C_6F_5)_4$. The frequent migration of propagating polymer chain to the vacant site was suggested in syndiospecific polymerization with *i*Pr(Cp)(Flu)$ZrCl_2$ using AlR_3 (R = Et, *i*Bu)/$Ph_3CB(C_6F_5)_4$ as cocatalysts.

Chapter 6 Molecular Size of Poly(ethene-*co*-propene) Obtained with Zirconocene and Hafnocene Catalysts

Copolymerization of ethene with propene was carried out with Cp_2MCl_2, *rac*-Et(Ind)$_2MCl_2$, and *rac*-$Me_2Si(Ind)_2MCl_2$ (M = Zr, Hf) using MAO as a cocatalyst. Molecular size of the copolymer decreased with an increase of propene content in the copolymerization with zirconocene and non-bridged hafnocene catalysts. On the other hand, the minimum molecular size of poly(ethene-*co*-propene) was obtained at about 50 mol % of propene content in the copolymer with *ansa*-hafnocene catalysts (*rac*-Et(Ind)$_2HfCl_2$ and *rac*-$Me_2Si(Ind)_2HfCl_2$). The polymerization activity was decreased with the increase of propene feed ratio with non-bridged aspecific metallocene catalysts (Cp_2MCl_2), while the rate enhancement effect was observed in the copolymerization with isospecific metallocene catalysts. The profile of molecular size was

discussed based on the chain propagation, chain transfer reaction in the copolymerization, and chain end structures of the copolymers obtained.

Chapter 7 Copolymerization of Propene and Nonconjugated Diene with Zirconocene Catalysts

Copolymerizations of propene with 1,5-hexadiene and 1,7-octadiene were carried out with isospecific *rac*-$Me_2Si(Ind)_2ZrCl_2$ and syndiospecific $Ph_2C(Cp)(Flu)ZrCl_2$ combined with MAO. Cycloaddition of nonconjugated dienes with intramolecular cyclization proceeded in the copolymerizations.

In the copolymerization of propene with 1,5-hexadiene, stereoselectivity in the cycloaddition of 1,5-hexadiene was investigated based on the structures of isolated methylene-1,3-cyclopentane units. It was found that 1,5-hexadiene was inserted stereospecifically by enantiomorphic-site control with both catalysts. The diastereoselectivity in cyclization step of 1,2-inserted 1,5-hexadiene was, however, independent of stereospecificity of the catalysts. It was suggested that a propene insertion after the cycloaddition of 1,5-hexadiene was less enantioselctive in the copolymerization with $Ph_2C(Cp)(Flu)ZrCl_2$. Decrease of cyclization selectivity was observed with an increase of 1,5-hexadiene concentration. The cyclization selectivity in copolymerization was smaller than that in 1,5-hexadiene homopolymerization with *rac*-$Me_2Si(Ind)_2ZrCl_2$ at the same 1,5-hexadiene concentration due to the obstruction of cyclization by propene insertion.

In the copolymerization of propene with 1,7-octadiene, the cyclization selectivity of 1,7-octadiene was smaller than that of the copolymerization with 1,5-hexadiene. The cyclization selectivity of poly(propene-*co*-1,7-octadiene) obtained with $Ph_2C(Cp)(Flu)ZrCl_2$ was lower than that with *rac*-$Me_2Si(Ind)_2ZrCl_2$. The difference of the cyclization selectivity with catalysts used was discussed by the conformational models in the transition state of cyclization. Smaller cyclization selectivity was observed in the copolymerization in comparison to that in 1,7-octadiene homopolymerization with both catalysts, and this tendency made it clear that propene insertion could disturb the cyclization of the 1,2-inserted 1,7-octadiene. The

monomer reactivity ratios were calculated on the basis of the copolymer composition equations involving the intramolecular cyclization reaction.

Chapter 8 Crystalline Structures of Syndiotactic Poly(propene-*co*-olefin)s

Five kinds of syndiotactic poly(propene-*co*-olefin)s (olefin = ethene, 1-butene, 1-pentene, 1-hexene, and 4-methyl-1-pentene) were prepared by *i*Pr(Cp)(Flu)$ZrCl_2$–MAO. Structures and properties of those copolymers were examined by ^{13}C NMR, GPC, DSC, and X-ray diffraction analyses. T_m of the copolymers, except poly(propene-*co*-1-butene), showed a drastic depression with an increase of comonomer content. On the contrary, poly(propene-*co*-1-butene) showed a small depression of T_m with an increase of 1-butene and, furthermore, had T_m in the whole range of 1-butene content.

Crystalline structure of syndiotactic poly(propene-*co*-1-butene) was studied by wide angle X-ray diffractometry, and the *a* axis of the copolymer expanded linearly with an increase of 1-butene content while the *b* axis showed little change. Plausible unit cells for the syndiotactic poly(propene-*co*-1-butene) in the crystal were proposed.

Isothermal crystallization behavior of the syndiotactic poly(propene-*co*-olefin)s was examined by depolarized light intensity technique. It was found that kind of comonomer did not affect the crystallization behavior. The crystalline structures of isothemally crystallized copolymers were studied by WAXD, and structures of Cell II were suggested in all the copolymers except poly(propene-*co*-1-butene) with low 1-butene content.

List of Publications

Chapter 2

Molecular weight and molecular weight distribution of polyethene obtained with *rac*-$Me_2Si(Ind)_2ZrCl_2$/methylaluminoxane

N. Naga, K. Mizunuma

Macromol. Chem. Phys. **1998**, *199*, 113.

Profiles of ethylene polymerization with zirconocene–trialkylaluminum/borane compound

N. Naga, T. Shiono, T. Ikeda

submitted to *J. Mol. Catal.*

Chapter 3

Effect of co-catalyst system on α-olefin polymerization with *rac*- and *meso*-[dimethylsilylenebis(2,3,5-trimethyl-cyclopentadienyl)]zirconium dichloride

N. Naga, K. Mizunuma

Macromol. Rapid Commun. **1997**, *18*, 581.

Polymerization behavior of α-olefins with *rac*- and *meso*- type *ansa*-metallocene catalysts: Effects of cocatalyst and metallocene ligand

N. Naga, T. Shiono, T. Ikeda

Macromol. Chem. Phys. in press

Chapter 4

Chain transfer reaction by trialkylaluminum (AlR_3) in the stereospecific polymerization of propylene with metallocene–AlR_3/$Ph_3CB(C_6F_5)_4$

N. Naga, K. Mizunuma

Polymer **1998**, *39*, 5059.

Chapter 5

Stereochemical control in propylene polymerization with non-bridged metallocene dichloride/methylaluminoxane

N. Naga, K. Mizunuma,

Polymer **1998**, *39*, 2703.

Chapter 6

Study of molecular size in ethylene-propene copolymerization with zirconocene and hafnocene catalysts

N. Naga, Y. Ohbayashi, K. Mizunuma

Macromol. Rapid Commun. **1997**, *18*, 837.

Chapter 7

Copolymerization of propene and nonconjugated diene involving intramolecular cyclization with metallocene/methylaluminoxane

N. Naga, T. Shiono, T. Ikeda

Macromolecules in press

Cyclopolymerization of 1,7-octadiene with metallocene/methylaluminoxane

N. Naga, T. Shiono, T. Ikeda,

Macromol. Chem. Phys. in press

Chapter 8

Properties and crystalline structures of syndiotactic poly(propylene-*co*-1-butene)

N. Naga, K. Mizunuma, H. Sadatoshi, M. Kakugo

Macromolecules **1997**, *30*, 2197.

Isothermal crystallization of syndiotactic poly(propylene-*co*-olefin)s

N. Naga, K. Mizunuma, H. Sadatoshi, M. Kakugo

submitted to *Polymer*

Other publications not described in this thesis

I. Original Papers

(1) Synthesis of recyclable polyolefins from α,ω-dihydroxypolybutadiene using condensation and hydrogenation reactions

T. Shiono, N. Naga, K. Soga

Makromol. Chem., Rapid Commun. **1991**, *12*, 387.

(2) Synthesis of α,ω-divinylpolyethylene-like polymers from *cis*-1,4-polybutadiene using partial hydrogenation and metathesis degradation with ethylene
T. Shiono, N. Naga, K. Soga
Makromol. Chem., Rapid Commun. **1993**, *14*, 323.

(3) 部分水素化シス-1,4-ポリブタジエンのエチレンによるメタセシス分解
塩野　毅, 永　直文, 曽我　和雄
高分子論文集, **1993**, *50*, 873.

(4) Synthesis of titanium(IV) complexes that contain the bis(silylamide) ligand of the type $[1,8\text{-}C_{10}H_6(NR)_2]_2^-$, and alkene polymerization catalyzed by $[1,8\text{-}C_{10}H_6(NR)_2]TiCl_2$-cocatalyst system
K. Nomura, N. Naga, K. Takaoki, A. Imai
J. Mol. Catal. A **1998**, *130*, L209.

(5) Synthesis of various non-bridged titanium(IV) cyclopentadienyl-aryloxy complexes of the type $CpTi(OAr)X_2$, and their use in catalysis of alkene polymerization. - Important roles of substituents on both aryloxy and cyclopentadienyl groups
K. Nomura, N. Naga, M. Miki, K. Yanagi, A. Imai
Organometallics **1998**, *17*, 2152.

(6) Olefin polymerization by cyclopentadienyl-aryloxy titanium(IV) complexes–cocatalyst system
K. Nomura, N. Naga, M. Miki, K. Yanagi
Macromolecules **1998**, *31*, 7588.

(7) Ethylene homopolymerization and ethylene/1-butene copolymerization catalyzed by $[1,8\text{-}C_{10}H_6(NR)_2]TiCl_2$–cocatalyst system
K. Nomura, N. Naga, K. Takaoki
Macromolecules **1998**, *31*, 8009.

II. Review Articles

(1) 分解性ポリオレフィンーそのモデルとリサイクル使用の可能性ー
曽我　和雄，塩野　毅，永　直文
化学と工業　**1992**, 第４５巻，第８号，1405.

(2) 分解・再利用型ポリオレフィンの開発を夢みて
曽我　和雄，塩野　毅，永　直文
ファインケミカル　**1993**, *22*, No. 4, 5.

(3) ニッケル及びパラジウム錯体触媒によるオレフィン重合
野村　琴広，永　直文，触媒技術の動向と展望１９９７，触媒学会，p 56.

Acknowledgments

I would like to express my sincere gratitude to Associate Professor Takeshi Shiono for his constant guidance and helpful discussion throughout the duration of this work. This work could never have been continued without his guidance.

I wish to express my grateful appreciation to Professor Tomiki Ikeda for his helpful advice and discussion.

I gratefully acknowledge to Professor Kazuo Soga for his helpful support and discussion.

I would like to express my deep gratitude to Dr. Akihiko Kanazawa for his helpful comment and discussion.

I would like to express my sincere thanks to Dr. Toshiya Uozumi for his considerable supports and encouragement.

I am indebted to Associate Professor Kotohiro Nomura for his helpful support and discussion.

Grateful acknowledgment is made to Senior Research Associate Kooji Mizunuma, Senior Research Associate Hajime Sadatoshi, Senior Research Associate Tatusya Miyatake, Research Associate Makoto Satoh, Mr. Kenichiro Yada, Mr. Yoshiaki Ohbayashi, Mr. Kazuo Takaoki at Petrochemicals Research Laboratory, Sumitomo Chemical Co., Ltd., and President Masahiro Kakugo at Sumika Plastech Co., Ltd. for their constant support.

I am grateful to Chisso Co., Ltd., Tosoh Akzo Co., Ltd., Asahi Glass Co., Ltd. and Mitsubishi Chemical Co., Ltd. (Japan Polychem Corporation) for their kind cooperation.

Finally, I would like to express my sincere thanks to all members of Ikeda-Shiono laboratory for their experimental assistance and encouragement, and also, my sincere thanks to the members and graduates of Professor Soga's laboratory.

1999

Naofumi Naga